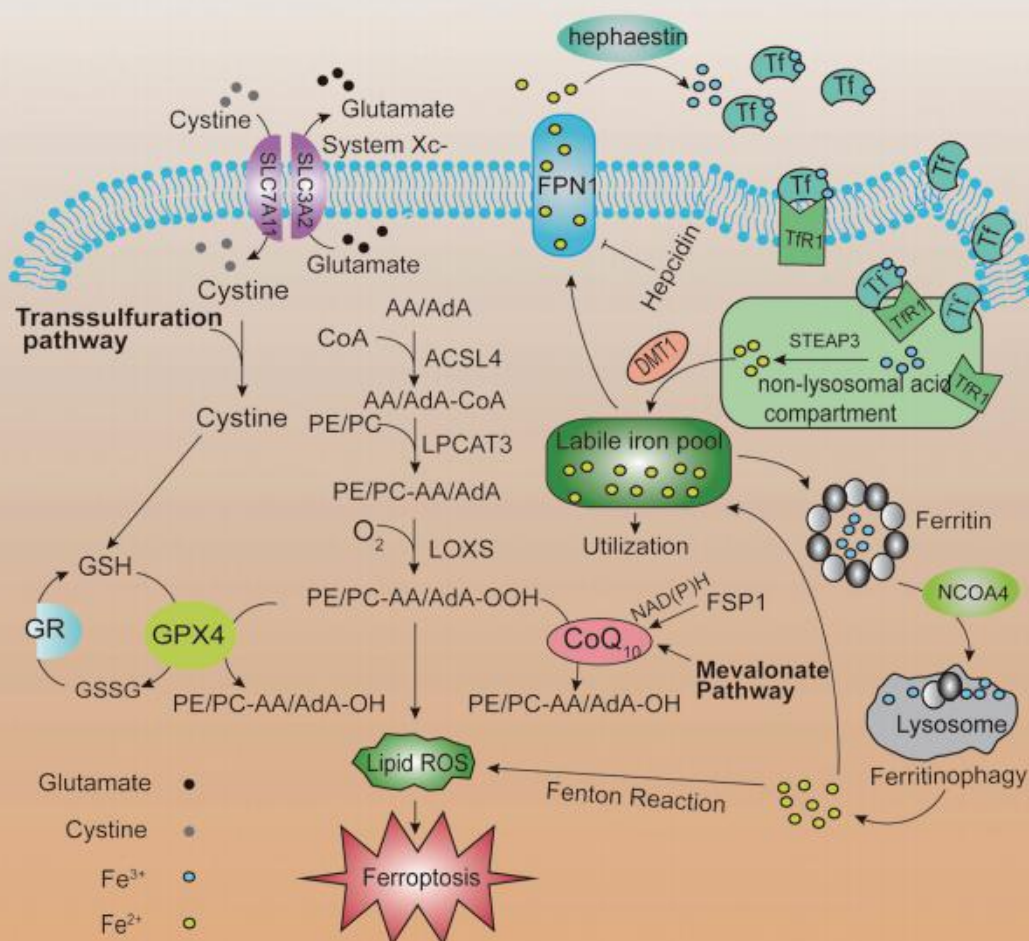


# Journal of Exploratory Research in Pharmacology

**2023** Volume 8 Issue 3  
July / August / September



## Ferroptosis: Opportunities and Challenges in Cancer

page 243

## Editors-in-Chief

**Prof. Ramón Cacabelos**

EuroEspes Biomedical Research Center,  
Corunna, Spain

Continental University Medical School,  
Huancayo, Peru

**Prof. Ben J. Gu**

The Florey Institute of Neuroscience & Mental  
Health, Parkville, Australia

## Managing Editor

**Lisa Li Chen**

Wuhan, China

## Technical Editor

**Huili Zhang**

Wuhan, China

## Contact Information

### Editorial Office

**Managing Editor:** Lisa Li Chen

**Telephone:** +1-409-420-2868

**E-mail:** jerp@xiahepublishing.com

**Postal Address:** 14090 Southwest Freeway,  
Suite 300, Sugar Land,  
Texas, 77478, USA

### Publisher

Xia & He Publishing Inc.

**Website:** www.xiahepublishing.com

**E-mail:** service@xiahepublishing.com

**Postal Address:** 14090 Southwest Freeway,  
Suite 300, Sugar Land, Texas,  
77478, USA

**Current Issue: Volume 8, Issue 3**

Publication date: September 25, 2023

## Aims and Scope

*Journal of Exploratory Research in Pharmacology (JERP)* publishes original innovative exploratory research articles, state-of-the-art reviews, editorials, short communications that focus on novel findings and the most recent advances in basic and clinical pharmacology, covering topics from drug research, drug development, clinical trials and application. Topics included, but not limited to the following areas will be considered for publication in JERP: drug composition and properties; synthesis and design of drugs and potential drugs; molecular/cellular and organ/system mechanisms; signal transduction/cellular communications/interactions; toxicology; chemical biology; molecular/biomarker diagnostics; therapeutics; medical applications; interventional (phases I-IV) clinical trials; observational (post-marketing) clinical studies on investigational new drugs; pharmacogenetics; pharmacoeugenetics; pharmacokinetics; pharmacodynamics; molecular pharmacology; transgenic models.

## Indexing & Archiving

*JERP* is now included in Dimensions, Directory of Research Journals Indexing (DRJI), Google Scholar, Index Copernicus, Naver Academic, Publons, ResearchGate, Road, ScienceGate, Scilit, Semantic Scholar.

## Open Access

*JERP* adopts open access publishing model, and all articles are distributed under the terms of the CC BY-NC 4.0 license (<http://creativecommons.org/licenses/by-nc/4.0/>). Under this license, anyone may copy, distribute, or reuse these articles for non-commercial purposes, provided the original work is properly cited. Manuscripts submitted for publication in an open access journal are subject to the same rigorous peer-review and quality control as in scholarly subscription journals.

## Disclaimer

All articles published in Xia & He journals represent the views and opinions of their authors, and not the views, opinions, or policies of the publisher, except where explicitly indicated. Xia & He Publishing shall not be held responsible for the use of views and opinions expressed in the articles; use of any information in the articles shall not be considered an endorsement by Xia & He Publishing of the products advertised.

## Links

Journal Home: <https://www.xiahepublishing.com/journal/jerp>

Editorial Board: <https://www.xiahepublishing.com/journal/jerp/editors>

Archive: <https://www.xiahepublishing.com/journal/jerp/archive>

Instructions for Authors: <https://www.xiahepublishing.com/journal/jerp/instruction>

Online Submission System: <https://mc03.manuscriptcentral.com/jerp>

## Editorial Board

# JERP

### Associate Editors

**Xin-Sheng Gu**

Hubei University of Medicine  
Shiyan, China

**Igor Tsigelny**

Department of Neurosciences, University of California, San Diego  
La Jolla, USA

**Massimo Tusconi**

Section of Psychiatry, Department of Medical Sciences and Public Health, University of Cagliari  
Cagliari, Italy

### Editorial Board Members

**Nisar Ahmad**

Sialkot, Pakistan

**Sarfuddin Azmi**

Riyadh, Saudi Arabia

**Ebru Basaran**

Eskisehir, Turkey

**Monica Butnariu**

Timișoara, Romania

**Kishore B. Challagundla**

Omaha, USA

**Jamshidkhan Chamani**

Mashhad, Iran

**Yong Chen**

Nanchang, China

**Hongwei Cheng**

Xiamen, China

**Meltem Cetin**

Erzurum, Turkey

**Janaina Fernandes**

Rio de Janeiro, Brazil

**Nianqiao Gong**

Wuhan, China

**Simona Gurzu**

Targu-Mures, Romania

**Georges Doumet Helou**

Los Angeles, USA

**Tahereh Hosseinabadi**

Tehran, Iran

**Zhen-peng Huang**

Xi'an, China

**Peter Illes**

Leipzig, Germany

**Fahad Said Khan**

Rawalakot, Pakistan

**Fahim Ullah Khan**

Peshawar, Pakistan

**Sunil Kumar**

Farrukhabad, India

**Dohyun Ignacio Lee**

Cheongju, South Korea

**Xiao-Hong Li**

Michigan, USA

**Xin Li**

Changsha, China

**Xin Li**

Shanghai, China

**Charis Liapi**

Athens, Greece

**Linsheng Liu**

Suzhou, China

**Yu Liu**

Ningbo, China

**Zhao-Ying Liu**

Changsha, China

**Ali Noman**

Faisalabad, Pakistan

**Cyprian Ogbonna Onyeji**

Ile-Ife, Nigeria

**Min-Hua Peng**

Shenzhen, China

**Hakim Rahmoune**

Setif, Algeria

**Senthilkumar Rajagopal**

Bangalore, India

**Rahimnejad**

Babol, Iran

**Reza Rastmanesh**

Maryland, USA

**Celestino Sardu**

Naples, Italy

**Seung-Yong Seong**

Seoul, South Korea

**Muhammad Shahid**

Peshawar, Pakistan

**Rohit Sharma**

Varanasi, India

**Rajesh Kumar Singh**

Jalandhar, India

**Bing Sun**

Washington, D.C., USA

**Daniel Tagoe**

Burlington, USA

**Srijayaprakash Babu Uppada**

Omaha, USA

**Suzana Uzun**

Zagreb, Croatia

**Weidong Wang**

Oklahoma, USA

**Yang Wang**

Guangzhou, China

**Karol Wróblewski**

Rzeszów, Poland

**J. Ruth Wu-Wong**

Libertyville, USA

**Tony Kwong-Fai Wong**

Hong Kong, China

**Baoming Wu**

Hefei, China

**Wen-Rui Xie**

Guangzhou, China

**Shao-hua Xie**

Stockholm, Sweden

**Chuanming Xu**

Nanchang, China

**Fan Yang**

Luoyang, China

**Jianshe Yang**

Shenzhen, China

## Editorial Board Members

**Wenqing Yang**

Shanghai, China

**Shi-Jun Yue**

Xianyang, China

**Xiaobin Zeng**

Shenzhen, China

**Jinwei Zhang**

Exeter, UK

**Lingmin Zhang**

Guangzhou, China

**Wei Zhao**

Hong Kong, China

**Hai-Jing Zhong**

Guangzhou, China



# JOURNAL OF EXPLORATORY RESEARCH IN PHARMACOLOGY

## CONTENTS

2023 8(3):181–265

### Editorial

#### Reducing the Risks of Nuclear War—the Role of Health Professionals

Kamran Abbasi, Parveen Ali, Virginia Barbour, Kirsten Bibbins-Domingo, Marcel GM Olde Rikkert, Andy Haines, Ira Helfand, Richard Horton, Bob Mash, Arun Mitra, Carlos Monteiro, Elena N. Naumova, Eric J. Rubin, Tilman Ruff, Peush Sahni, James Tumwine, Paul Yonga and Chris Zielinski . . . . . 181

### Original Articles

#### Clinical Analysis of the Association Between Chinese Medicine Syndromes and Risk Factors for Hypertension

Zhen Zhao, Pei-Zhong Liu, Peng-Chong Du, Chao-Yang Zheng, Da-Wei Wang, Jian Xu, Rong-Yuan Yang and Qing Liu . . . . . 184

#### Determination of Brain Distribution of Amino Acid Neurotransmitters in Pigs and Rats by HPLC-UV

Si-Yu Meng, Mo-Huan Tang, Xue-Jiao Zhao and Zhao-Ying Liu . . . . . 192

### Review Articles

#### Non-human Primate Models of Alzheimer's Disease

Yihan Li and Ben J. Gu. . . . . 199

#### Brief Insight on Nanovesicular Liposomes as Drug-delivery Carriers for Medical Applications

Madhavi Pravinkumar Chudasma, Sakshi Alpeshkumar Shah, Mohammad Hamran Nasiruddin Qureshi, Nirav Shah, Devarshi Shah, Riddhi Trivedi and Viral Hareshkumar Shah . . . . . 222

#### Flavin-containing Monooxygenases in the Brain and their Involvement in Neurodegeneration and Aging

Boyu Li and Zhuoling An. . . . . 237

#### Ferroptosis: Opportunities and Challenges in Cancer

Ying-Jie Jia, Yu Zhang, Xu-Bin Ma, Yang Wang, Ying-Qi Tian, Peng-Xing He and Yi-Chao Xu . . . . . 242

#### Nanotechnology-based Therapeutic Strategies for Dry Eye Disease

Anil K. Philip. . . . . 253

### Case Report

#### New Topical Treatment for Psoriasis: A Case Report

Jose Miguel Ingelmo Calvo, José Ruiz Cobo and Mohamed Farouk Allam . . . . . 263



## Editorial

# Reducing the Risks of Nuclear War—the Role of Health Professionals



Kamran Abbasi<sup>1</sup>, Parveen Ali<sup>2</sup> , Virginia Barbour<sup>3</sup> , Kirsten Bibbins-Domingo<sup>4</sup> , Marcel GM Olde Rikkert<sup>5</sup> , Andy Haines<sup>6</sup> , Ira Helfand<sup>7</sup>, Richard Horton<sup>8</sup> , Bob Mash<sup>9</sup> , Arun Mitra<sup>10</sup>, Carlos Monteiro<sup>11</sup> , Elena N. Naumova<sup>12</sup> , Eric J. Rubin<sup>13</sup> , Tilman Ruff<sup>14</sup> , Peush Sahni<sup>15</sup> , James Tumwine<sup>16</sup> , Paul Yonga<sup>17</sup> and Chris Zielinski<sup>18,19,20\*</sup>

<sup>1</sup>Editor-in-Chief, *British Medical Journal*; <sup>2</sup>Editor-in-Chief, *International Nursing Review*; <sup>3</sup>Editor-in-Chief, *Medical Journal of Australia*; <sup>4</sup>Editor-in-Chief, *JAMA*; <sup>5</sup>Editor-in-Chief, *Dutch Journal of Medicine*; <sup>6</sup>London School of Hygiene and Tropical Medicine; <sup>7</sup>Past President, *International Physicians for the Prevention of Nuclear War*; <sup>8</sup>Editor-in-Chief, *The Lancet*; <sup>9</sup>Editor-in-Chief, *African Journal of Primary Health Care & Family Medicine*; <sup>10</sup>Past President, *International Physicians for the Prevention of Nuclear War*; <sup>11</sup>Editor-in-Chief, *Revista de Saúde Pública*; <sup>12</sup>Editor-in-Chief, *Journal of Public Health Policy*; <sup>13</sup>Editor-in-Chief, *New England Journal of Medicine*; <sup>14</sup>Past President, *International Physicians for the Prevention of Nuclear War*; <sup>15</sup>Editor-in-Chief, *National Medical Journal of India*; <sup>16</sup>Editor-in-Chief, *African Health Sciences*; <sup>17</sup>Editor-in-Chief, *East African Medical Journal*; <sup>18</sup>Centre for Global Health, University of Winchester, UK; <sup>19</sup>World Association of Medical Editors; <sup>20</sup>International Physicians for the Prevention of Nuclear War

Received: July 18, 2023 | Revised: July 30, 2023 | Accepted: July 31, 2023 | Published online: August 07, 2023

In January, 2023, the Science and Security Board of the Bulletin of the Atomic Scientists moved the hands of the Doomsday Clock forward to 90 s before midnight, reflecting the growing risk of nuclear war.<sup>1</sup> In August, 2022, the UN Secretary-General António Guterres warned that the world is now in “a time of nuclear danger not seen since the height of the Cold War.”<sup>2</sup> The danger has been underlined by growing tensions between many nuclear armed states.<sup>1,3</sup> As editors of health and medical journals worldwide, we call on health professionals to alert the public and our leaders to this major danger to public health and the essential life support systems of the planet—and urge action to prevent it.

Current nuclear arms control and non-proliferation efforts are inadequate to protect the world’s population against the threat of nuclear war by design, error, or miscalculation. The Treaty on the Non-Proliferation of Nuclear Weapons (NPT) commits each of the 190 participating nations” to pursue negotiations in good faith on effective measures relating to cessation of the nuclear arms race at an early date and to nuclear disarmament, and on a treaty on general and complete disarmament under strict and effective international control”.<sup>4</sup> Progress has been disappointingly slow and the most recent NPT review conference in 2022 ended without an agreed statement.<sup>5</sup> There are many examples of near disasters that have exposed the risks of depending on nuclear deterrence for the indefinite future.<sup>6</sup> Modernisation of nuclear arsenals could increase risks: for example, hypersonic missiles decrease the time

available to distinguish between an attack and a false alarm, increasing the likelihood of rapid escalation.

Any use of nuclear weapons would be catastrophic for humanity. Even a “limited” nuclear war involving only 250 of the 13 000 nuclear weapons in the world could kill 120 million people outright and cause global climate disruption leading to a nuclear famine, putting 2 billion people at risk.<sup>7,8</sup> A large-scale nuclear war between the USA and Russia could kill 200 million people or more in the near term, and potentially cause a global “nuclear winter” that could kill 5–6 billion people, threatening the survival of humanity.<sup>7,8</sup> Once a nuclear weapon is detonated, escalation to all-out nuclear war could occur rapidly. The prevention of any use of nuclear weapons is therefore an urgent public health priority and fundamental steps must also be taken to address the root cause of the problem—by abolishing nuclear weapons.

The health community has had a crucial role in efforts to reduce the risk of nuclear war and must continue to do so in the future.<sup>9</sup> In the 1980s the efforts of health professionals, led by the International Physicians for the Prevention of Nuclear War (IPPNW), helped to end the Cold War arms race by educating policy makers and the public on both sides of the Iron Curtain about the medical consequences of nuclear war. This was recognised when the 1985 Nobel Peace Prize was awarded to the IPPNW (<http://www.ippnw.org>).<sup>10</sup>

In 2007, the IPPNW launched the International Campaign to Abolish Nuclear Weapons, which grew into a global civil society campaign with hundreds of partner organisations. A pathway to nuclear abolition was created with the adoption of the Treaty on the Prohibition of Nuclear Weapons in 2017, for which the International Campaign to Abolish Nuclear Weapons was awarded the 2017 Nobel Peace Prize. International medical organisations, including the International Committee of the Red Cross, the IPPNW, the World Medical Association, the World Federation of Public Health Associations, and the International Council of Nurses, had key roles in the process leading up to the negotiations, and in the

**Abbreviations:** IPPNW, International Physicians for the Prevention of Nuclear War; NPT, Non-Proliferation of Nuclear Weapons.

\***Correspondence to:** Chris Zielinski, International Physicians for the Prevention of Nuclear War. ORCID: <https://orcid.org/0000-0001-6596-698X>. E-mail: [CZielinski@ippnw.org](mailto:CZielinski@ippnw.org)

**How to cite this article:** Abbasi K, Ali P, Barbour V, Bibbins-Domingo K, Rikkert MGMO, Haines A, et al. Reducing the Risks of Nuclear War—the Role of Health Professionals. *J Explor Res Pharmacol* 2023;8(3):181–183. doi: 10.14218/JERP.2023.00000A.



negotiations themselves, presenting the scientific evidence about the catastrophic health and environmental consequences of nuclear weapons and nuclear war. They continued this important collaboration during the First Meeting of the States Parties to the Treaty on the Prohibition of Nuclear Weapons, which currently has 92 signatories, including 68 member states.<sup>11</sup>

We now call on health professional associations to inform their members worldwide about the threat to human survival and to join with the IPPNW to support efforts to reduce the near-term risks of nuclear war, including three immediate steps on the part of nuclear-armed states and their allies: first, adopt a no first use policy;<sup>12</sup> second, take their nuclear weapons off hair-trigger alert; and, third, urge all states involved in current conflicts to pledge publicly and unequivocally that they will not use nuclear weapons in these conflicts. We further ask them to work for a definitive end to the nuclear threat by supporting the urgent commencement of negotiations among the nuclear-armed states for a verifiable, time-bound agreement to eliminate their nuclear weapons in accordance with commitments in the NPT, opening the way for all nations to join the Treaty on the Prohibition of Nuclear Weapons.

The danger is great and growing. The nuclear armed states must eliminate their nuclear arsenals before they eliminate us. The health community played a decisive part during the Cold War and more recently in the development of the Treaty on the Prohibition of Nuclear Weapons. We must take up this challenge again as an urgent priority, working with renewed energy to reduce the risks of nuclear war and to eliminate nuclear weapons.

### Acknowledgments

None.

### Funding

Respective authors were paid by their employers. Chris Zielinski's time was funded by International Physicians for the Prevention of Nuclear War.

### Conflict of interest

KB-D is a full-time employee of the American Medical Association, working as the Editor-in-Chief of JAMA and the JAMA Network. AH is principal investigator of the Pathfinder Initiative 2020–2025, co-investigator of Sustainable Healthy Food Systems research programme 2017–2023, and co-investigator of Complex Urban Systems for Sustainability and Health 2017–2023, all funded by the Wellcome Trust, with additional funding from the Oak Foundation for the Pathfinder Initiative, and he reports royalties from Cambridge University Press for the coauthored book *Planetary Health*; consultancy fees paid to his institution from the Wellcome Trust for his role as Senior Advisor on Climate Change and Health in 2021; travel/meeting support from WHO and Human Frontiers Science Program; and he is a member of the Cool Roofs trial steering committee Nouna Research Centre, Burkina Faso/University of Heidelberg, is Co-chair of the International Advisory Committee, NIHR Clean-Air (Africa) Global Health Research Unit, is a member of the Independent Advisory Group, Collaboration for the Establishment of an African Population Cohort Consortium, and he was Co-chair of the InterAcademy Partnership, Climate Change and Health Working Group 2019–2022 and Co-chair of the Academy of Medical Sciences/Royal Society working group on “A healthy future—tackling climate change mitigation and human health together” 2020–2021

(all unpaid). IH reports honoraria for several speaking engagements, all donated to Back from the Brink, the International Physicians for the Prevention of Nuclear War, or Physicians for Social Responsibility; travel/ meeting support for Nobel Peace Laureates' Summit, the World Federation of Public Health Associations World Congress, and the UN Human Rights Commission Youth Summit; and he is a member of the steering committee of Back from the Brink and the International Steering Group of the International Campaign to Abolish Nuclear Weapons, a Board member of the International Physicians for the Prevention of Nuclear War and Physicians for Social Responsibility, and a Trustee of the Phillips Exeter Academy (all unpaid). MGMOR reports research grants from the Dutch Research Council, NOW (grant number COMPL.21COV.001) and from the Netherlands Organisation for Health Research ZonMw (grant number 09120012010063) and he is Chair of the Dutch guideline committee on cognitive impairments and dementia. TR reports a contract with the Institute for Energy and Environmental Research (USA) for papers addressing the health and environmental consequences of nuclear testing in multiple locations, including Australia, French Polynesia, central Pacific, and China; honorarium from The Choisun Ilbo media group in South Korea for a lecture on nuclear weapons in 2022 and for nuclear weapons presentations from Hyogo Medical Practitioners Association (Japan), Peace Boat (Japan), and the University of Sydney; he was an expert witness on radiation and health for Environmental Justice Australia acting for Mine-Free Glenaladale regarding proposed Fingerboards Mineral Sands Mine to the Victorian Government Fingerboards Inquiry and Advisory Committee; he is a member of RV3 Rotavirus Vaccine Development Scientific Advisory Board, Murdoch Children's Research Institute/ Royal Children's Hospital; he is a member of the Committee of International Campaign to Abolish Nuclear Weapons Australia; he is a member of the Internet Peace Prize Award Committee (Sunfull Foundation, South Korea); he was a member of the Victorian International Humanitarian Law Advisory Committee, Australian Red Cross; he is a Board member of the Initiative for Peacebuilding, Faculty of Arts, University of Melbourne; he is an At-large Board member of the International Physicians for the Prevention of Nuclear War; he was Co-president of the International Physicians for the Prevention of Nuclear War 2012–23; and he is Honorary Principal Fellow, Melbourne School of Population and Global Health, University of Melbourne. PY reports grants from Atea Pharmaceuticals; honoraria for lectures, presentations, and educational events from bioMérieux and Pfizer Pharmaceuticals; fees for participation on an advisory board from Pfizer Pharmaceuticals; and he is a member of the Antimicrobial Stewardship Study Group Executive Committee (2022–2024) and the Clinical Practice Guideline Panel on Vaccinations in Immunocompromised hosts for the European Society of Clinical Microbiology and Infectious Diseases. CZ reports consulting fees for his role as senior adviser on the international journals project from the International Physicians for the Prevention of Nuclear War. All the other authors declare no competing interests.

### Author contributions

Ira Helfand and Andy Haines developed the idea of the editorial and led drafting along with Chris Zielinski. All other authors contributed significantly to the editorial content.

### References

- [1] Science and Security Board, Bulletin of the Atomic Scientists. A time

- of unprecedented danger: it is 90 seconds to midnight. 2023 Doomsday Clock Statement. Jan 24, 2023. Available from: <https://thebulletin.org/doomsday-clock/current-time/>. Accessed June 1, 2023.
- [2] UN. 2022. Future Generations Counting on Our Commitment to Step Back from Abyss, Lift Cloud of Nuclear Annihilation for Good, Secretary-General Tells Review Conference, Press Release Aug 1, 2022 SG/SM/21394. Available from: <https://press.un.org/en/2022/sgsm21394.doc.htm>. Accessed 10 July 2023.
  - [3] Tollefson J. Is nuclear war more likely after Russia's suspension of the New START treaty? *Nature* 2023;615(7952):386. doi:10.1038/d41586-023-00679-w, PMID:36882544.
  - [4] UN. 2005 Review Conference of the Parties to the Treaty on the Non-Proliferation of Nuclear Weapons (NPT). May 2–27, 2005. Available from: <https://www.un.org/en/conf/npt/2005/npttreaty.html>. Accessed June 2, 2023.
  - [5] Mukhatzhanova G. 10th NPT Review Conference: why it was doomed and how it almost succeeded. Arms Control Association. October, 2022. Available from: <https://www.armscontrol.org/act/2022-10/features/10th-npt-review-conference-why-doomed-almost-succeeded>. Accessed June 2, 2023.
  - [6] Lewis P, Williams H, Pelopidas B, Aghlani S. Too close for comfort, cases of near nuclear use and options for policy. Chatham House Report. April, 2014. Available from: <https://www.chathamhouse.org/2014/04/too-close-comfort-cases-near-nuclear-use-and-options-policy>. Accessed June 1, 2023.
  - [7] Bivens M. Nuclear famine. IPPNW. August, 2022. Available from: <https://www.ippnw.org/wp-content/uploads/2022/09/ENGLISH-Nuclear-Famine-Report-Final-bleed-marks.pdf>. Accessed June 1, 2023.
  - [8] Xia L, Robock A, Scherrer K, Harrison CS, Bodirsky BL, Weindl I, *et al*. Global food insecurity and famine from reduced crop, marine fishery and livestock production due to climate disruption from nuclear war soot injection. *Nat Food* 2022;3(8):586–596. doi:10.1038/s43016-022-00573-0, PMID:37118594.
  - [9] Helfand I, Lewis P, Haines A. Reducing the risks of nuclear war to humanity. *Lancet* 2022;399(10330):1097–1098. doi:10.1016/S0140-6736(22)00422-6, PMID:35255264.
  - [10] Nobel Prize Outreach AB. International Physicians for the Prevention of Nuclear War—facts. 1985. Available from: <https://www.nobelprize.org/prizes/peace/1985/physicians/facts/>. Accessed June 1, 2023.
  - [11] UN Office for Disarmament Affairs. Treaties Database. Treaty on the Prohibition of Nuclear Weapons, status of the Treaty. 2023. Available from: <https://treaties.unoda.org/t/tpnw>. Accessed June 1, 2023.
  - [12] Center for Arms Control and Non-Proliferation. No first use: frequently asked questions. 2023. Available from: <https://armscontrolcenter.org/issues/no-first-use/no-first-use-frequently-asked-questions/>. Accessed June 2, 2023.





## Original Article

# Clinical Analysis of the Association Between Chinese Medicine Syndromes and Risk Factors for Hypertension



Zhen Zhao<sup>1#</sup>, Pei-Zhong Liu<sup>1#</sup>, Peng-Chong Du<sup>2</sup>, Chao-Yang Zheng<sup>3</sup>, Da-Wei Wang<sup>4</sup>, Jian Xu<sup>3</sup>, Rong-Yuan Yang<sup>1\*</sup> and Qing Liu<sup>1\*</sup>

<sup>1</sup>Guangdong Provincial Hospital of Chinese Medicine-Zhuhai Hospital, The 2nd Clinical School of Medicine, Guangzhou University of Chinese Medicine, Zhuhai, China; <sup>2</sup>Clinic of Baijiao Town of Doumen District, Zhuhai, China; <sup>3</sup>Guangdong Provincial Hospital of Chinese Medicine-HEMC Hospital, Guangzhou, China; <sup>4</sup>The First Affiliated Hospital of Guangzhou University of Traditional Chinese Medicine, Guangzhou, China

Received: October 11, 2022 | Revised: November 07, 2022 | Accepted: December 03, 2022 | Published online: January 29, 2023

## Abstract

**Background and objectives:** The application of Chinese medicine in clinic is based on the classical theory of traditional Chinese medicine (TCM) syndrome differentiation, which remains not fully understood. This study aims to explore and interpret the associations between TCM syndromes and multiple clinical risk factors of hypertension.

**Methods:** A total of 203 patients with hypertension were retrospectively studied. After the regression analysis of confounding factors for different types of hypertension, the potential association between TCM syndrome and risk factors were analyzed.

**Results:** The comorbidity of left ventricular hypertrophy was probably an independent risk factor for different types of hypertension. The correlation analysis indicated that the disease course was positively correlated with the syndrome differentiation degree (Spearman's coefficient = 0.185,  $p < 0.05$ ) and blood stasis syndrome (Spearman's coefficient = 0.291,  $p < 0.05$ ). The hypertension risk group was positively correlated with the blood stasis syndrome (Spearman's coefficient = 0.207,  $p < 0.05$ ). Age was positively correlated with the blood stasis syndrome (Spearman's coefficient = 0.231,  $p < 0.05$ ) and qi-deficiency syndrome (Spearman's coefficient = 0.187,  $p < 0.05$ ), but was negatively correlated with the liver-yang hyperactivity syndrome (Spearman's coefficient = -0.167,  $p < 0.05$ ).

**Conclusions:** There are correlations between TCM syndromes and the clinical risk factors of hypertension. These findings may help to interpret the TCM syndrome differentiation theory.

## Introduction

Hypertension is the leading cause of cardiovascular disease and premature death worldwide, and the incidence of hypertension in

patients continues to increase.<sup>1,2</sup> The most appropriate antihypertensive drug should be selected, according to the actual situation of the patient, which is in line with the overall concept of traditional Chinese medicine (TCM) syndrome differentiation.<sup>3,4</sup> However, the TCM syndrome remains not fully understood.

TCM has a history of more than two-thousand years in China, and is increasingly being welcomed by a number of developed countries, such as Australia and the United States. Hypertension can be categorized as headache or dizziness in TCM. The treatments for headache or dizziness are guided by the TCM syndrome differentiation based on the factors of qi, blood stasis, yang, yin, phlegm and others. These dialectical diagnoses and treatments reflect the individualization of TCM syndromes for hypertension for a certain relationship with clinical risk factors, such as age, disease course, hypertension grade, blood homocysteine, coagulation parameters, risk stratification of hypertension and others,<sup>5–7</sup> and are consistent with the individual modern medicated selection of antihypertensive drugs.<sup>8</sup>

**Keywords:** Hypertension; Traditional Chinese medicine syndrome; Correlation analysis; Risk factors; Retrospective study.

**Abbreviations:** BMI, body mass index; BNP, brain natriuretic peptide; CHD, coronary heart disease; Cr, creatinine; HCY, homocysteine; INR, international normalized ratio; LDL, low density lipoprotein cholesterol; TCM, traditional Chinese medicine.

**\*Correspondence to:** Rong-Yuan Yang and Qing Liu, Guangdong Provincial Hospital of Chinese Medicine-Zhuhai Hospital, The 2nd Clinical School of Medicine, Guangzhou University of Chinese Medicine, Zhuhai 519015, China. ORCID: <https://orcid.org/0000-0002-8792-8017> (RYY); <https://orcid.org/0000-0002-2199-2999> (QL). Tel: +86 020-81887233 (RYY); +86 13631223512 (QL), Fax: +86 020-81882533 (RYY); +86 0756-3325088 (QL), E-mail: yangrongyuan@163.com (RYY); 851757626@qq.com (QL)

<sup>#</sup>These authors contributed equally to this work.

**How to cite this article:** Zhao Z, Liu PZ, Du PC, Zheng CY, Wang DW, Xu J, et al. Clinical Analysis of the Association Between Chinese Medicine Syndromes and Risk Factors for Hypertension. *J Explor Res Pharmacol* 2023;8(3):184–191. doi: 10.14218/JERP.2022.00071.

The present study aimed to explore and interpret the potential associations between TCM syndromes and multiple clinical risk factors of hypertension. The present retrospective study revealed the correlations between TCM syndromes and the clinical risk factors of hypertension, which can help to interpret the process of classifying and distinguishing TCM syndromes with common clinical risk factors, and individually guide the clinical medication. These present findings may help bridge the gap between Chinese medicine and Western medicine.

## Methods

### *Study design and ethics approval*

A retrospective study was conducted in the Department of Cardiology, Guangdong Provincial Hospital of Chinese Medicine. All TCM diagnostic information, demographic characteristics and clinical data of hypertensive patients, who were screened based on the inclusion and exclusion criteria for the present study, were collected. The present study was approved by Ethics Committee of Guangdong Provincial Hospital of Chinese Medicine (No. ZE2019-079-01).

### *Inclusion and exclusion criteria for the participants*

According to the Guidelines for the Prevention and Treatment of Hypertension in China<sup>9</sup> and the latest guidelines,<sup>10,11</sup> patients with a systolic blood pressure of  $\geq 140$  mmHg and/or a diastolic blood pressure of  $\geq 90$  mmHg in the resting non-medication state for three times within three days were diagnosed with hypertension. Hypertension was classified as level 1, 2 and 3, based on the level of blood pressure. All patients were local residents of Guangzhou. Patients diagnosed with hypertension, but had normal blood pressure, were excluded. Furthermore, pregnant or lactating women were excluded. All hypertensive patients who met the above inclusion criteria were included for the present study.

### *TCM syndrome definition, risk factors and bias elimination*

According to the Diagnostics of TCM edited by Tietao Deng,<sup>12</sup> the four TCM syndromes were defined, as follows:

1. Qi deficiency syndrome was defined as a syndrome with shortage of qi, and disinclination to talk, lassitude, dizziness, spontaneous sweating, worse when active and weak pulse;
2. Blood stasis syndrome was defined as a syndrome with stabbing pain, pain with fixed locations, lump, hemorrhage, cyanotic lips, tongue and nails, and rough pulse;
3. Phlegm-dampness syndrome was defined as a syndrome with cough and vomiting or spitting sputum, chest distress, nausea, lumps, greasy tongue coating and slippery pulse, or a syndrome with edema, retention of urine, and enlarged tongue with white slippery coating;
4. Liver-yang hyperactivity syndrome was defined as a syndrome with vertigo and tinnitus, headache, red face, irritability, palpitation and forgetfulness, insomnia and dreams, lumbar and knee soreness, heavy head and decreased foot sensation, red tongue with slight coating, and strong pulse string.

Since TCM syndrome differentiation is mainly based on symptoms, this would easily lead to measurement bias. In order to reduce the measurement bias, the syndrome differentiations for hypertension were completed by two attending physicians, who are Chinese medicine practitioners, based on the above-mentioned criteria, and according to the recorded case data. If there were disagreements in the syndrome differentiation for hypertension, a

chief physician would carry out the syndrome differentiation for hypertension.

The patient demographics, such as age, gender and clinical data, as well as the course of hypertension, grade of hypertension, risk stratification of hypertension, and diagnosis of comorbidities, were obtained. The highest blood pressure in the previous measurements and the blood pressure measured during the hospitalization were recorded, and the highest values were used for grading. The cardiovascular risks were stratified by risk factor, target organ damage and complication. According to the Chinese Guidelines for the Prevention and Treatment of Hypertension, the risk stratification was assessed based on the following: hypertension (grades 1–3), age  $>55$  years old (male) or  $>65$  years old (female), smoking, impaired glucose tolerance (two-hour postprandial blood glucose of 7.8–11.0 mmol/L) and/or fasting blood glucose (6.1–6.9 mmol/L), dyslipidemia (total cholesterol of  $\geq 5.7$  mmol/L [220 mg/dl], low-density lipoprotein cholesterol of  $>3.3$  mmol/L [130 mg/dl], or high-density lipoprotein cholesterol of  $<1.0$  mmol/L [40 mg/dl]), family history of early onset of cardiovascular disease (first-degree relative age of onset of  $<55$  years old [male] or  $<65$  years old [female]), abdominal obesity (waist circumference of  $\geq 90$  cm [male] or  $\geq 85$  cm [female], or obese (body mass index of  $\geq 28$  kg/m<sup>2</sup>), and blood homocysteine (HCY) increase of more than 10  $\mu$ mol/L. Homocysteine was collected after admission. In order to avoid errors between the research data and original clinical data, two researchers recorded the data obtained from the database.

### *Statistical analysis*

A database was established for the present study, and all statistical analyses of the data were conducted using the SPSS statistical software (version 21.0). Demographic data were statistically analyzed using descriptive analysis. Quantitative data were expressed as mean $\pm$ standard deviation (SD), and categorical data were expressed in composition ratio. The relationship between TCM syndromes and potentially related clinical biochemistry indexes for different types of hypertension was analyzed by multivariable regression. The potential correlation among quantitative values was analyzed by Pearson's bivariate correlation after the normality test using the Kolmogorov-Smirnov method, and the counting data was analyzed by Spearman's bivariate correlation. A correlation coefficient of  $>0$  was considered a positive correlation, while correlation coefficient of  $<0$  was considered a negative correlation. A  $p$ -value of  $<0.05$  was considered statistically significant.

## Results

### *Characteristics of patients with hypertension*

A total of 203 hypertensive patients were enrolled for the present study. The demographic and clinical data are presented in Table 1. These patients included 89 male and 114 female patients, with an average age of  $67.84 \pm 12.45$  years old. The average age of women was  $68.38 \pm 10.82$  years old, with a minimum age of 39 years old and a maximum age of 92 years old. The average age of men was  $67.15 \pm 14.30$  years old, with a minimum age of 22 years old and a maximum age of 91 years old.

The disease course is detailed in Table 2. That is, 103 of 203 hypertensive patients had a disease course of 0–5 years, accounting for 50.74% of all patients, 65 patients had a disease course of 6–10 years, accounting for 32.02% of all patients, 24 patients had a disease course of 11–20 years, accounting for 11.82% of all patients, and 11 patients had a disease course of  $>20$  years, accounting for

**Table 1. Gender and age composition for the 203 hypertensive patients**

	Number (n)	Minimum age (years)	Maximum age (years)	Mean age	Standard deviation
Male	89	22	91	67.15	14.30
Female	114	39	92	68.38	10.82
Total	203	22	92	67.84	12.45

5.42% of all patients.

The severity of hypertension for this population is presented in Table 2. That is, 18 patients had hypertension grade 1, accounting for 8.87% of all patients, 65 patients had hypertension grade 2, accounting for 32.02% of all patients, and 120 patients had hypertension grade 3, accounting for 59.11% of all patients.

The stratification of various risk factors and the target organ damage revealed the following: 172 patients were assigned to the very high-risk group, which had the largest proportion (84.73%); one patient was assigned to the low-risk group, which had the smallest proportion (0.49%); 12 patients were assigned to the intermediate risk group, accounting for 5.91% of all patients; 18 patients were assigned to the high-risk group, accounting for 8.87%

of all patients (Table 2).

Furthermore, 107 patients developed heart failure or coronary heart disease (CHD), 65 patients had diabetes mellitus, and 36 patients had impaired glucose tolerance. In addition, 111 patients developed cerebrovascular disease, 86 patients had high homocysteine, and one patient had single or multiple conditions (Table 2).

#### ***Distribution of TCM syndromes for hypertension***

There were a total of 469 patients: 156 (33.26%) patients had qi-deficiency syndrome, 180 (38.38%) patients had phlegm-dampness syndrome, 108 (23.03%) patients had blood stasis syndrome, and 25 (5.23%) patients had liver-yang hyperactivity syndrome (Table 3).

**Table 2. Characteristics of the 203 hypertension patients**

Variable	Number (n)	Proportion (%)
Disease course (years)		
0–5	103	50.74
6–10	65	32.02
11–20	24	11.82
>20	11	5.42
Total	203	100.00
Hypertension grade		
Grade 1	18	8.87
Grade 2	65	32.02
Grade 3	120	59.11
Total	203	100.00
Risk stratification		
Low risk	1	0.49
Intermediate risk	12	5.91
High risk	18	8.87
Very high risk	172	84.73
Total	203	100.00
Combined disease		
Left ventricular hypertrophy	93	45.81
Heart failure or coronary heart disease	107	26.42
Diabetes	65	16.05
Abnormal glucose tolerance	36	8.89
Cerebrovascular disease	111	27.41
Hyperhomocysteinemia	86	21.23
Total	405	100.00

**Table 3. Distribution of TCM syndromes in hypertension patients**

TCM syndromes	Frequency (n)	Proportion (%)
Qi-deficiency syndrome	156	33.26
Phlegm-dampness syndrome	180	38.38
Blood stasis syndrome	108	23.03
Liver-yang hyperactivity syndrome	25	5.33
Total	469	100.00

TCM, traditional Chinese medicine.

**Multivariable regression for hypertension, TCM syndromes and biochemistry indexes**

The univariate and multivariable regression analysis for hypertension classification indicated that age, days of hospitalization, years of hypertension, family history, and the comorbidities of left ventricular hypertrophy, cerebrovascular disease and heart disease are associated with the development of hypertension, and that the comorbidities of left ventricular hypertrophy is an independent risk factor for hypertension in this population (Table 4).

The further multivariable regression analysis revealed that abnormal HbA1c levels are associated with the qi-deficiency type of hypertension, but there was no significant association of biochemistry with the other TCM syndromes (Supplementary Tables 1–2).

**The correlation between TCM syndromes and risk factors of hypertension**

The correlation between the disease course and TCM syndromes

was determined by Spearman's correlation analysis. The Spearman's correlation coefficient between the disease course and complexity of the TCM syndromes was 0.185, indicating a positive correlation ( $p < 0.05$ ). Furthermore, the Spearman's correlation coefficient between the disease course and blood stasis syndrome was 0.291, indicating a positive correlation ( $p < 0.05$ ) (Fig. 1 and Table 5).

The further Spearman's analysis revealed that age is positively correlated with blood stasis syndrome (Spearman's correlation coefficient = 0.231,  $p < 0.05$ ) or qi-deficiency syndrome (Spearman's correlation coefficient = 0.187,  $p < 0.05$ ), but not with phlegm-dampness syndrome (Spearman's correlation coefficient =  $-0.018$ ,  $p > 0.05$ ) in this population. In addition, there was a negative correlation between age and liver-yang hyperactivity syndrome (Spearman's correlation coefficient =  $-0.167$ ,  $p < 0.05$ ) (Fig. 2 and Table 6).

However, the correlation analysis revealed that there was no statistically significant difference between the blood pressure grade and TCM syndrome. Furthermore, there was no significant difference in the correlation between the hypertension risk group, and qi-deficiency syndrome (Spearman's correlation coefficient = 0.066,  $p > 0.05$ ) and phlegm-dampness syndrome (Spearman's correlation coefficient =  $-0.021$ ,  $p > 0.05$ ), suggesting that the correlation between the hypertension risk group, and qi-deficiency syndrome or phlegm-dampness syndrome cannot be considered. Next, the correlation between the hypertension risk group and blood stasis syndrome (Spearman's correlation coefficient = 0.207,  $p < 0.05$ ) was statistically significant, indicating that there may be a positive correlation between the hypertension risk group and blood stasis syndrome. Furthermore, the correlation between the hypertension risk group and liver-yang hyperactivity syndrome

**Table 4. Multivariable regression for hypertension classification and the related confounding**

Variable	Model fitting standard value	$\chi^2$	$p$
Age	185.006	184.856	0.000*
Gender	0.206	0.056	0.972
Hospitalization days	218.719	218.569	0.000*
Hypertension years	531.453	531.303	0.000*
Smoking	3.702	3.552	0.169
Family history	11.565	11.415	0.003*
Impaired sugar tolerance	0.181	0.031	0.985
Abnormal blood lipid	0.684	0.534	0.766
Left ventricular hypertrophy	107.580	107.430	0.000*
Impaired renal function	0.419	0.268	0.874
Cerebrovascular disease	105.585	105.435	0.000*
Heart disease	133.383	133.233	0.000*
Peripheral vascular disease	1.376	1.226	0.996
Diabetes	3.934	3.784	0.151
Qi-deficiency syndrome	1.428	1.278	0.528
Phlegm-dampness syndrome	3.315	3.164	0.206
Hyperactivity of liver-yang	3.969	3.819	0.148
Complexity of syndrome	0.261	0.110	1.000

Note: \* $p < 0.05$  indicates that the difference is statistically significant.

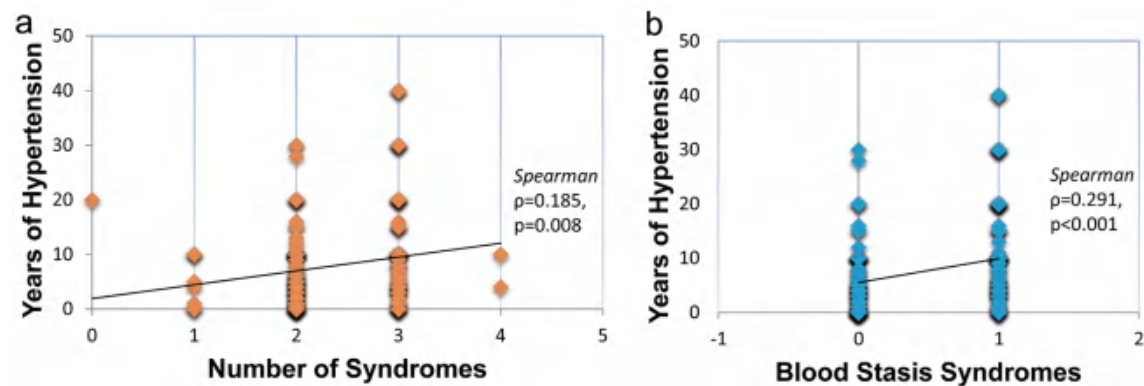


Fig. 1. Correlations between the disease course and complexity of TCM syndromes or blood stasis syndrome. (a) Correlations between the disease course and complexity of TCM syndromes. (b) Correlations between the disease course and blood stasis syndrome. TCM, traditional Chinese medicine.

Table 5. The correlation between the disease course, and complexity of syndrome differentiation or blood stasis syndrome in hypertension patients

Variable		Syndrome differentiation	Blood stasis syndrome
Disease course	Spearman's correlation coefficient	0.185	0.291
	<i>p</i>	0.008*	0.000*

Note: \*the difference was statistically significant.

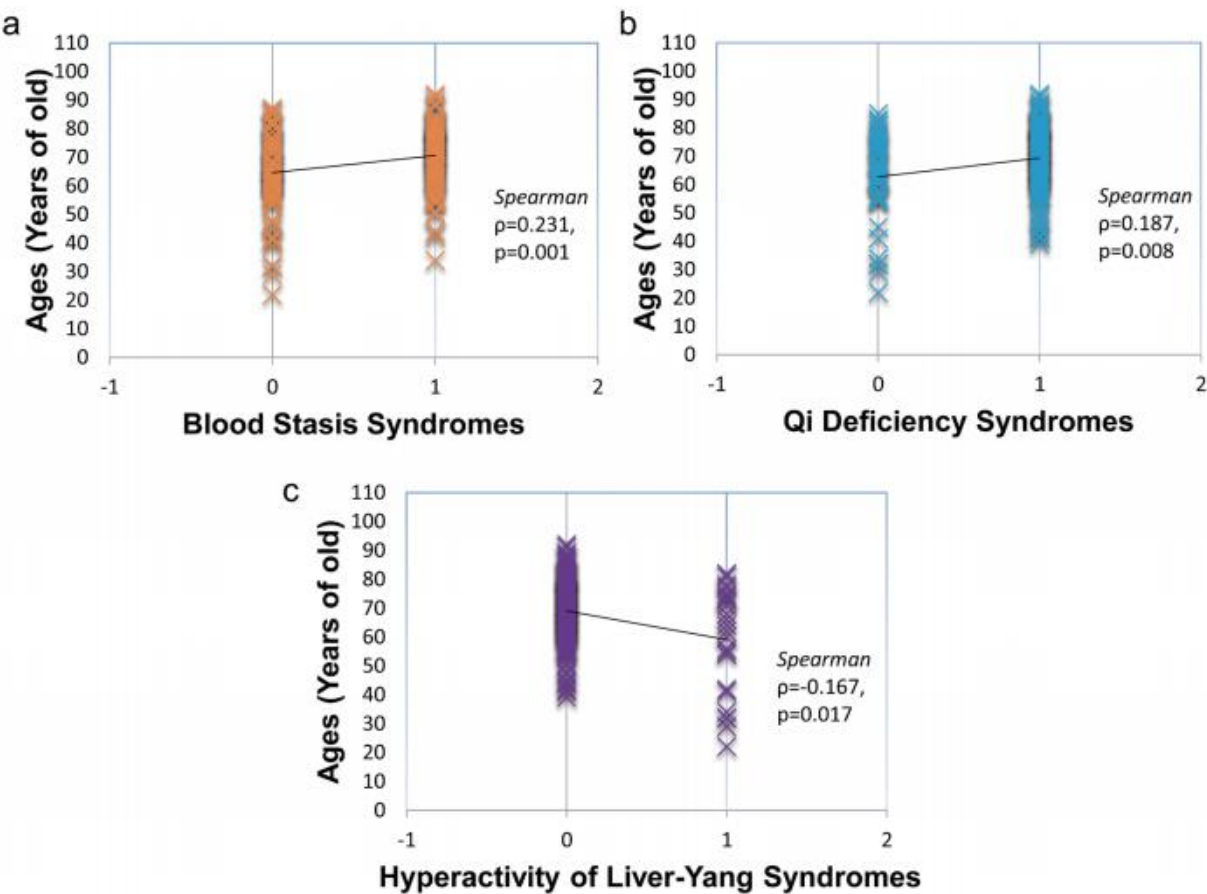


Fig. 2. Correlations between age and TCM syndromes in hypertension. (a) Correlations between age and blood stasis syndrome. (b) Correlations between age and Qi deficiency syndrome. (c) Correlations between age and hyperactivity of Liver-Yang syndrome. TCM, traditional Chinese medicine.



**Table 6. The correlation between syndrome differentiation and various variables in hypertensive patients**

Variable		Blood stasis syndrome	Qi-deficiency syndrome	Phlegm-dampness syndrome	Liver-yang hyperactivity syndrome
Hypertension grading	Spearman's correlation coefficient	0.061	0.013	0.057	-0.031
	<i>p</i>	0.387	0.856	0.419	0.664
Hypertension risk grouping	Spearman's correlation coefficient	0.207	0.066	-0.021	-0.135
	<i>p</i>	0.003*	0.347	0.764	0.55 (one-tailed test, 0.028*)
Age	Spearman's correlation coefficient	0.231	0.187	-0.018	-0.167
	<i>p</i>	0.001*	0.008*	0.804	0.017*
Combined with diabetes	Spearman's correlation coefficient	0.030	0.101	-0.021	-0.129
	<i>p</i>	0.671	0.150	0.764	0.067 (one-tailed test, 0.034*)
Combined heart disease	Spearman's correlation coefficient	0.160	0.252	0.004	-0.216
	<i>p</i>	0.023*	0.000*	0.957	0.002*

Note: \**p* < 0.05 indicates that the difference was statistically significant. Heart disease refers to heart failure or coronary heart disease.

(Spearman's correlation coefficient = -0.135, one-tailed test, *p* < 0.05) suggested a possible negative correlation.

## Discussion

### *The correlation between TCM syndromes and the hypertension grade*

The data indicated that there was no significant correlation between the different types of TCM syndromes and hypertension grade in hypertension patients. The reason for this may be because the present study used the method of splitting complex syndromes into several single syndromes to determine the correlation between each single syndrome and the blood pressure grade. In contrast, previous studies were conducted through cluster analysis, and the single syndrome type and blood pressure grade were not analyzed, which may lead to different conclusions.<sup>8</sup>

The stratification of higher hypertension risk factors revealed that more risk factors existed in hypertensive patients.<sup>13</sup> The correlation between different TCM syndromes and hypertension risk factors indicated that the higher the risk stratification of hypertension, the greater the probability for blood stasis syndrome, and the smaller the probability for liver-yang hyperactivity syndrome in this population. It can be inferred that the liver-yang hyperactivity syndrome mostly occurred in the early stage of hypertension, which is consistent with the reports of other studies,<sup>3</sup> and that TCM for the treatment of hypertension in patients with the liver-yang hyperactivity syndrome can effectively reduce blood pressure.<sup>14</sup>

### *The correlation between TCM syndromes and disease course of hypertension*

The present study revealed that the disease course for hypertension was positively correlated with the complexity of the syndrome differentiation. That is, the longer the disease course, the more complicated the syndrome differentiation. The type of syndrome differentiation is a complex of multiple single syndromes. This may be correlated to the old age of hypertensive patients in the selected sample, and the combination of other geriatric diseases. The development of hypertension would easily damage the target organs, such as the heart,<sup>15,16</sup> brain,<sup>17,18</sup> kidney and eyes, and various co-

morbidities would interact with each other,<sup>19</sup> thereby increasing the complexity of syndrome differentiation after the change in disease course.

Furthermore, the present study revealed that there is positive correlation between the disease course and blood stasis syndrome. That is, the longer the disease course of hypertension, the more probable the blood stasis syndrome. This coincides with the TCM theory that there would probably be stasis in most chronic diseases. Based on this observation, it can be noted that hypertension is a risk factor for CHD, and that a long-term disease course of hypertension would more easily lead to CHD.<sup>20</sup> In terms of treatment, the existing evidence revealed that the application of TCM, which has the property of promoting blood circulation and removing blood stasis, can effectively treat hypertension and its complications.<sup>21-24</sup>

### *The correlation between TCM syndromes and age in patients with hypertension*

The present study revealed that older patients have a higher chance to develop blood stasis syndrome and qi-deficiency syndrome. Furthermore, the older the patient, the smaller the probability of occurrence of liver-yang hyperactivity syndrome. Similarly, studies have revealed that qi-deficiency is the basic pathogenesis and common syndrome of hypertension in the elderly. Hypertensive patients become weaker as they become older, which is consistent with the results of the present study. Furthermore, as age increases, the disease course of hypertension would become longer. Thus, it can be concluded that the longer the disease course of hypertension, the greater the probability for blood stasis syndrome, and the more complicated the syndrome differentiation.

### *The correlation between TCM syndromes and plasma homocysteine in hypertension*

Studies have revealed that homocysteine is one of the risk factors for cardiovascular and cerebrovascular diseases in the Chinese population.<sup>25-27</sup> However, the present study revealed that there was no correlation between the individual syndrome of hypertensive patients and plasma homocysteine levels. This may be correlated to the small sample size of the study, or the small proportion of hyperhomocysteinemia patients. Another reason may be that the

present study was performed based on a single syndrome, instead of complex syndrome differentiations for hypertension. Further investigations are needed to confirm the relationship between the homocysteine level and TCM syndromes for hypertension.

The present data indicates that the syndromes for hypertension were differentially distributed in the distinct ages of patients. In the elderly, the most common syndromes for hypertension were blood stasis syndrome and qi-deficiency syndrome, while liver-yang hyperactivity syndrome mostly occurred in young patients. The complexity of TCM syndromes, particularly blood stasis syndrome, would accumulate as the disease course of hypertension is prolonged. The present data is consistent to some reports on the different distributions of TCM syndromes in hypertension patients.<sup>3,28</sup> Thus, the syndrome differentiation and treatment of TCM should be carried out based on the age of the patient and duration of the disease course (years), in order to help in the administration of Chinese medication after individual treatment.

### Future directions

Future studies would focus in illustrating the underlying mechanisms and determining why these TCM syndromes were correlated with hypertension risk factors, thereby providing evidences to understand Chinese medicine theories.

### Conclusions

Overall, the present study revealed that the distribution of TCM syndromes in patients with hypertension, from more to less is, as follows: qi-deficiency syndrome, phlegm-dampness syndrome, blood stasis syndrome and liver-yang hyperactivity syndrome. The univariate and multivariable regression for the confounding of the hypertension classification revealed that the comorbidity of left ventricular hypertrophy was probably an independent risk factor for hypertension classification. The correlation analysis revealed that the disease course is positively correlated with the complexity of the TCM syndrome or blood stasis syndrome, and that age is positively correlated with blood stasis syndrome or qi-deficiency syndrome, while age is negatively correlated with liver-yang hyperactivity syndrome.

Compared to several studies that discussed the correlation between Chinese medicine syndromes and hypertension, the present study selected elderly patients with a mean age of >65 years old, in order to determine the relationship between the geriatric disease, and TCM syndrome differentiation and treatment. The present retrospective study revealed the relationship between TCM syndromes and the clinical risk factors of hypertension. This would be helpful in interpreting the process for classifying and distinguishing TCM syndromes with common clinical risk factors, which may provide guidance for individual clinical medications, helping to bridge the gap between Eastern and Western medicine, to some extent.

### Acknowledgments

None.

### Funding

The study was supported by the National Natural Science Foundation of China (No. 8227427, to QL), the Guangdong Medical

Science and Technology Research Fund Project (No. B2020155, to QL), the Guangdong Provincial Bureau of Traditional Chinese Medicine Fund Project (No. 20221360, to QL), the Zhuhai Medical Science and Technology Research Fund Project (No. ZH-24013310210002PWC, to QL), the Special Funding for TCM Science and Technology Research of Guangdong Provincial Hospital of Chinese Medicine (No. YN2020QN10, to QL), and the Municipal School (College) Joint Funding Project of Guangzhou Science and Technology Bureau (No. SL2023A03J00081, to QL).

### Conflict of interest

The authors declare that there are no competing interests.

### Author contributions

The study was designed by QL. The initial search, data analysis and manuscript writing were performed by ZZ. The critical comments and typesetting correction on the final version were made by QL and RY. The manuscript was finalized by QL. All authors have critically read and revised the manuscript.

### Ethical statement

The study was approved by the Ethics Committee of Guangdong Provincial Hospital of Chinese Medicine (No. ZE2019-079-01). The individual informed consent for this retrospective study was waived.

### Data sharing statement

The technical appendix, statistical code, and dataset are available from the corresponding author on reasonable request (E-mail: 851757626@qq.com).

### References

- [1] Zhou B, Perel P, Mensah GA, Ezzati M. Global epidemiology, health burden and effective interventions for elevated blood pressure and hypertension. *Nat Rev Cardiol* 2021;18(11):785–802. doi:10.1038/s41569-021-00559-8, PMID:34050340.
- [2] Mills KT, Stefanescu A, He J. The global epidemiology of hypertension. *Nat Rev Nephrol* 2020;16(4):223–237. doi:10.1038/s41581-019-0244-2, PMID:32024986.
- [3] Wang J, Xiong X, Liu W. Traditional chinese medicine syndromes for essential hypertension: a literature analysis of 13,272 patients. *Evid Based Complement Alternat Med* 2014;2014:418206. doi:10.1155/2014/418206, PMID:24660016.
- [4] Chen SL, Liu XY, Xu WM, Mei WY, Chen XL. Clinical study of western medicine combined with Chinese medicine based on syndrome differentiation in the patients with polarized hypertension. *Chin J Integr Med* 2012;18(10):746–751. doi:10.1007/s11655-012-1231-7, PMID:22965699.
- [5] Moran A, Gu D, Zhao D, Coxson P, Wang YC, Chen CS, *et al*. Future cardiovascular disease in china: markov model and risk factor scenario projections from the coronary heart disease policy model-china. *Circ Cardiovasc Qual Outcomes* 2010;3(3):243–252. doi:10.1161/CIRCOUTCOMES.109.910711, PMID:20442213.
- [6] Shenoy V, Mehendale V, Prabhu K, Shetty R, Rao P. Correlation of serum homocysteine levels with the severity of coronary artery disease. *Indian J Clin Biochem* 2014;29(3):339–344. doi:10.1007/s12291-013-0373-5, PMID:24966483.
- [7] Leng Y, Li H, Bai Y, Ge Q, Yao G. Effect of traditional Chinese medicine on intra-abdominal hypertension and abdominal compart-

- ment syndrome: A systematic review and Meta-analysis. *J Crit Care* 2016;34:24–29. doi:10.1016/j.jccr.2016.03.021, PMID:27288604.
- [8] Wu A, Zhang D, Gao Y, Lou L, Zhu H, Chai L, *et al*. The Correlation between High-Sensitivity C-Reactive Protein, Matrix Metalloproteinase 9, and Traditional Chinese Medicine Syndrome in Patients with Hypertension. *Evid Based Complement Alternat Med* 2013;2013:780937. doi:10.1155/2013/780937, PMID:23606891.
- [9] Yin R, Yin L, Li L, Silva-Nash J, Tan J, Pan Z, *et al*. Hypertension in China: burdens, guidelines and policy responses: a state-of-the-art review. *J Hum Hypertens* 2022;36(2):126–134. doi:10.1038/s41371-021-00570-z, PMID:34215840.
- [10] Unger T, Borghi C, Charchar F, Khan NA, Poulter NR, Prabhakaran D, *et al*. 2020 International Society of Hypertension global hypertension practice guidelines. *J Hypertens* 2020;38(6):982–1004. doi:10.1097/HJH.0000000000002453, PMID:32371787.
- [11] Li G, Hu R, Zhang X. The impact of the 2020 International Society of Hypertension global hypertension practice guidelines on the prevention and control of hypertension in China. *Hypertens Res* 2021;44(8):1040–1041. doi:10.1038/s41440-021-00649-7, PMID:33824488.
- [12] Tietao D. *Diagnostics of traditional Chinese medicine*. Shanghai: Shanghai Science and Technology Publishing House; 2006.
- [13] Carey RM, Whelton PK. 2017 ACC/AHA Hypertension Guideline Writing Committee. Prevention, Detection, Evaluation, and Management of High Blood Pressure in Adults: Synopsis of the 2017 American College of Cardiology/American Heart Association Hypertension Guideline. *Ann Intern Med* 2018;168(5):351–358. doi:10.7326/M17-3203, PMID:29357392.
- [14] Wang J, Feng B, Yang X, Liu W, Liu Y, Zhang Y, *et al*. Tianma gouteng yin as adjunctive treatment for essential hypertension: a systematic review of randomized controlled trials. *Evid Based Complement Alternat Med* 2013;2013:706125. doi:10.1155/2013/706125, PMID:23710230.
- [15] Niaz S, Latif J, Hussain S. Serum resistin: A possible link between inflammation, hypertension and coronary artery disease. *Pak J Med Sci* 2019;35(3):641–646. doi:10.12669/pjms.35.3.274, PMID:31258568.
- [16] Liu HH, Cao YX, Sun D, Jin JL, Zhang HW, Guo YL, *et al*. High-sensitivity C-reactive protein and hypertension: combined effects on coronary severity and cardiovascular outcomes. *Hypertens Res* 2019;42(11):1783–1793. doi:10.1038/s41440-019-0293-8, PMID:31235846.
- [17] Sharp SJ, Aarsland D, Day S, Sørnesyn H, Ballard C, Alzheimer's Society Vascular Dementia Systematic Review Group. Hypertension is a potential risk factor for vascular dementia: systematic review. *Int J Geriatr Psychiatry* 2011;26(7):661–669. doi:10.1002/gps.2572, PMID:21495075.
- [18] Sierra C. Essential hypertension, cerebral white matter pathology and ischemic stroke. *Curr Med Chem* 2014;21(19):2156–2164. doi:10.2174/0929867321666131227155140, PMID:24372222.
- [19] Düzova A, Karabay Bayazit A, Canpolat N, Niemirska A, Kaplan Bulut I, Azukaitis K, *et al*. Isolated nocturnal and isolated daytime hypertension associate with altered cardiovascular morphology and function in children with chronic kidney disease: findings from the Cardiovascular Comorbidity in Children with Chronic Kidney Disease study. *J Hypertens* 2019;37(11):2247–2255. doi:10.1097/HJH.0000000000002160, PMID:31205198.
- [20] Gaudieri V, Acampa W, Rozza F, Nappi C, Zampella E, Assante R, *et al*. Coronary vascular function in patients with resistant hypertension and normal myocardial perfusion: a propensity score analysis. *Eur Heart J Cardiovasc Imaging* 2019;20(8):949–958. doi:10.1093/ehjci/jez025, PMID:30768182.
- [21] Wu L, Gao Y, Zhang S, Fang Z. The Effects of Breviscapine Injection on Hypertension in Hypertension-Induced Renal Damage Patients: A Systematic Review and a Meta-Analysis. *Front Pharmacol* 2019;10:118. doi:10.3389/fphar.2019.00118, PMID:30846938.
- [22] Wei H, Xiao Y, Tong Y, Chen Y, Luo X, Wang Y, *et al*. Therapeutic effect of angelica and its compound formulas for hypertension and the complications: Evidence mapping. *Phytomedicine* 2019;59:152767. doi:10.1016/j.phymed.2018.11.027, PMID:31100657.
- [23] Yang X, Yang G, Li W, Zhang Y, Wang J. Therapeutic Effect of Ilex hainanensis Merr. Extract on Essential Hypertension: A Systematic Review and Meta-Analysis of Randomized Controlled Trials. *Front Pharmacol* 2018;9:424. doi:10.3389/fphar.2018.00424, PMID:29867454.
- [24] Owoicho Orgah J, Wang M, Yang X, Wang Z, Wang D, Zhang Q, *et al*. Danhong Injection Protects Against Hypertension-Induced Renal Injury Via Down-Regulation of Myoglobin Expression in Spontaneously Hypertensive Rats. *Kidney Blood Press Res* 2018;43(1):12–24. doi:10.1159/000486735, PMID:29393225.
- [25] Yuan X, Wang T, Gao J, Wang Y, Chen Y, Kaliannan K, *et al*. Associations of homocysteine status and homocysteine metabolism enzyme polymorphisms with hypertension and dyslipidemia in a Chinese hypertensive population. *Clin Exp Hypertens* 2020;42(1):52–60. doi:10.1080/10641963.2019.1571599, PMID:30786773.
- [26] Yang B, Fan S, Zhi X, He J, Ma P, Yu L, *et al*. Interactions of homocysteine and conventional predisposing factors on hypertension in Chinese adults. *J Clin Hypertens (Greenwich)* 2017;19(11):1162–1170. doi:10.1111/jch.13075, PMID:28942612.
- [27] Fan YL, Zhan R, Dong YF, Huang L, Ji XX, Lu P, *et al*. Significant interaction of hypertension and homocysteine on neurological severity in first-ever ischemic stroke patients. *J Am Soc Hypertens* 2018;12(7):534–541. doi:10.1016/j.jash.2018.03.011, PMID:29678422.
- [28] Wang J, Xiong X, Yang X. Is it a new approach for treating senile hypertension with kidney-tonifying chinese herbal formula? A systematic review of randomized controlled trials. *Evid Based Complement Alternat Med* 2014;2014:473038. doi:10.1155/2014/473038, PMID:24693323.



## Original Article

# Determination of Brain Distribution of Amino Acid Neurotransmitters in Pigs and Rats by HPLC-UV



Si-Yu Meng<sup>1,2#</sup>, Mo-Huan Tang<sup>1,2#</sup>, Xue-Jiao Zhao<sup>1,2#</sup> and Zhao-Ying Liu<sup>1,2\*</sup>

<sup>1</sup>College of Veterinary Medicine, Hunan Agricultural University, Changsha, China; <sup>2</sup>Hunan Engineering Technology Research Center of Veterinary Drugs, Hunan Agricultural University, Changsha, China

Received: April 06, 2023 | Revised: May 30, 2023 | Accepted: June 07, 2023 | Published online: July 13, 2023

## Abstract

**Background and objectives:** Amino acid neurotransmitters are closely correlated to the neurological function of the brain, and the imbalance of amino acid neurotransmitters can lead to a variety of neurological diseases. Therefore, the development of a simple method to detect five neurotransmitters (aspartate, glutamate, glycine, taurine,  $\gamma$ -aminobutyric) in the brain is urgently needed.

**Methods:** The sample was initially treated and derived, and analyzed using liquid chromatography. In the range of 0.300–100.000 mol/L, the linear relationship was good, and the correlation coefficient was  $\geq 0.999$ . Furthermore, the intra-day accuracy of this method was 1.48–13.85%, and the inter-day accuracy was 2.13–12.61%. Moreover, the limit of detection (LOD, signal-to-noise ratio 3 [S/N = 3]) was 0.15–0.20 mol/L, and the limit of quantitation (LOQ, S/N = 10) was 0.30–0.55 mol/L. This approach was used to compare the content of amino acids in the brain of pigs and rats.

**Results:** The data revealed that most of the amino acid neurotransmitters were higher in the five brain tissues obtained from pigs, when compared to those obtained from rats. Aspartate and taurine had the greatest concentrations in brain tissues obtained from pigs and rats, respectively (except the cerebellum).

**Conclusions:** It can be concluded that there are differences in the content of neurotransmitters in brain regions among animals. The development of this method would support the detection of neurotransmitters in the brain.

## Introduction

Amino acid neurotransmitters is a common substance to transmit nerve information, and plays an extremely vital role in nerve organization, particularly in terms of neural functions of the brain.<sup>1</sup> There are two types of amino acid neurotransmitters: excitatory and inhibitory. Excitatory neurotransmitters include aspartate (Asp) and glutamate (Glu), while inhibitory neurotransmitters include glycine (Gly), taurine (Tau), and  $\gamma$ -aminobutyric (GABA).

These five amino acid neurotransmitters are involved in the functions of the nervous system. For instance, the excessive activation of Glu receptors would result in central nervous system disorders.<sup>2</sup> Variations in the amount of Asp generated and released in neuronal terminals would have an impact on the functional functions of the brain, including cognition, memory, intellect and emotion.<sup>3</sup> The lack of GABA can manifest itself in different ways, such as anxiety and panic.<sup>4</sup> Tau has a promising therapeutic potential in the central nervous system, where it protects against toxicity and damage induced by the functions of the nervous system. Furthermore, Tau may also help to treat a number of neurological conditions, including epilepsy, stroke, and neurodegenerative illnesses.<sup>5</sup> Gly not only improves sleep quality and prevents neurological disorders, such as epilepsy, depression and pain,<sup>6</sup> but is also critical for regulating hippocampal excitation and inhibiting balance.<sup>7</sup> Therefore, it is critical to quantitatively detect amino acid neurotransmitters in multiple brain regions, and determine how amino acid neurotransmitters change during various physiological and pathological processes.

With the advancement of techniques for examining amino ac-

**Keywords:** HPLC-UV; Aspartate; Glutamate; Glycine; Taurine;  $\gamma$ -aminobutyric.

**Abbreviations:** ASP, aspartate; GABA,  $\gamma$ -aminobutyric; GLU, glutamate; GLY, glycine; HPLC, high-performance liquid chromatography; LOD, limit of detection; LOQ, limit of quantitation; S/N, signal-to-noise ratio; TAU, taurine.

**\*Correspondence to:** Zhao-Ying Liu, College of Veterinary Medicine, Hunan Agricultural University, Furong District, Changsha 410128, Hunan, China. ORCID: <https://orcid.org/0000-0002-9050-2287>. Tel: 86+15111179464, E-mail: [liu\\_zhaoying@hunau.edu.cn](mailto:liu_zhaoying@hunau.edu.cn)

**#**Contributed equally to this work.

**How to cite this article:** Meng SY, Tang MH, Zhao XJ, Liu ZY. Determination of Brain Distribution of Amino Acid Neurotransmitters in Pigs and Rats by HPLC-UV. *J Explor Res Pharmacol* 2023;8(3):192–198. doi: 10.14218/JERP.2023.00029.



ids, an increasing number of detection methods have been applied to detect amino acid neurotransmitters in various sample types. At present, amino acid neurotransmitters test samples include the cerebrospinal fluid, blood and urine, and the high-performance liquid chromatography (HPLC)-Triple time-of-flight (TOF) method is used.<sup>8</sup> This approach is highly sensitive, but the disadvantage is its complex operation. In addition, previous studies have tested amino acids obtained from the hippocampus of the brain of rats using gas chromatography-mass spectrometry (GC-MS),<sup>9</sup> but other areas of the brain were not tested. Furthermore, the liquid chromatography-tandem mass spectrometry (LC-MS/MS) approach has been employed to detect brain amino acid content,<sup>10</sup> but the high cost of equipment and maintenance has made this method less accessible. These shortcomings highlight the need to establish a simple and cost-effective detection method. Therefore, the present study developed a liquid phase pre-column derivation-based method to address this need.

Since most amino acids are not ultraviolet (UV) absorbent, derivations must be performed to quantitatively measure the amino acid content before using the liquid phase. The common derivative reagents include phenyl isothiocyanate (PITC), FOMC-Cl, 6-aminoquinolyl-N-hydroxysuccinimidyl carbamate (AQC), and ortho-phthalaldehyde (OPA). However, these reagents have various disadvantages. For example, FOMC-Cl itself and its decomposition product, FOMC-OH, induces fluorescence, which affects the separation efficiency,<sup>11</sup> OPA derivatives are unstable, and require immediate analysis after derivatization,<sup>12</sup> and the presence of PITC in a sample would shorten the life of the column. A sensitive derivatization reagent that works well with amino acids is 4-fluoro-7-nitrobenzofurazan (NBD-F),<sup>13</sup> and this also applies for partial proteins<sup>14</sup> and drug concentration in plasma.<sup>15</sup> Pre-column derivation using 4-Fluoro-7-nitrobenzofurazan (NBD-F) can lead to several benefits, including gentle reaction conditions, consistent byproducts, and rapid assay time.<sup>16</sup>

As a result, HPLC was developed for the determination of amino acid neurotransmitters in the brain using the NBD-F derived reagent. This has been successfully used to compare the amino acid neurotransmitter content in the brain of pigs and rats. This technique has been proven to be straightforward and useful for estimating the amount of amino acid neurotransmitters.

## Methods and materials

### Instruments and reagents

The liquid chromatography system comprised of the following: a rapid-resolution binary pump, an SPD-20A UV detector, a SIL-20A auto-sampler (with a 600  $\mu$ L injection loop), and a CBM-20A system controller; 1/100,000 electronic balance (ATX224 Shimadzu production Institute); acidity meter (Shanghai Mettler-Toledo Instrument Co., Ltd.); high-speed frozen centrifuge (Eppendorf, Germany); ultrapure water system (Millipore, Bedford, MA, USA).

The Asp, Glu, Gly, Tau and GABA were purchased from Beijing Solarbio Science & Technology Co., Ltd. The NBD-F was purchased from Shanghai McLean Biochemical Technology Co., Ltd. The HPLC grade acetonitrile and methanol were purchased from Merck (USA). The HPLC grade phosphoric acid was purchased from Comeo Chemical Reagent Co., Ltd. The analytical grade potassium tetraborate was purchased from Shanghai Jingchun Biochemical Technology Co., Ltd. All of the substances were obtained from Chinese Pharmaceutical Chemical Reagent

Co., Ltd., including the sodium dihydrogen phosphate and disodium hydrogen phosphate of analytical quality. The Milli-Q ultrapure water system was used to create ultrapure water.

### Experimental animals

Laboratory animals: The Hunan Agricultural University Ethics Committee authorized the use of animals for the research (No. 2020-43). Twelve male Sprague-Dawley rats (weighing 180-240 g) were obtained from SJA Laboratory Animal Co., Ltd. The blank pig brain tissue samples were obtained from Hunan New Wufeng Co., Ltd. (Liuyang, China). The Chinese Guidelines for the Care and Use of Laboratory Animals were followed in the present study. The investigators will continue to follow these guidelines in future experiments.

### Standard solution

Standard reserve solution: accurate weighing of dissolved Glu, Asp, Gly, Tau and GABA in water. The first two formulations were 10 mmol/L, and the last three formulations were 100 mmol/L. Then, these were stored at  $-20^{\circ}\text{C}$ . Five kinds of standard amino acids were prepared into 1 mmol/L of mixed standard working solution, with 100 mmol/L and 10 mmol/L, respectively, and stored at  $4^{\circ}\text{C}$ .

Derivative reagent: the NBD-F was accurately weighed and prepared into a reserve solution at a concentration of 0.1 mol/L, and this was kept away from light at  $-20^{\circ}\text{C}$  until analysis.

Potassium tetraborate solution: the potassium tetraborate was accurately weighed and dissolved in water, and the amount was fixed to 100 mL. Using a calibrated pH meter, the pH of the solution was adjusted to  $9.5 \pm 0.1$ . Then, 40 Hz of ultrasound was applied for 10 minutes, and this was stored at  $4^{\circ}\text{C}$  through a membrane.

### Sample collection and pretreatment

#### Sample preservation

The hippocampus, cortex, striatum, brainstem and cerebellum were quickly removed from the skull of the pigs and rats, and separated from the ice plate. Before use, the separated brain tissues were kept at  $-80^{\circ}\text{C}$ . After accurate weighing, normal saline was added to homogenize at a mass-volume ratio of 1:1. Then, the homogenate was centrifuged at 12,000 rpm for 10 minutes at  $4^{\circ}\text{C}$  to separate the supernatant, and this was transferred and purified using an organic membrane filter with a pore size of 0.22  $\mu\text{m}$ .

#### Sample pretreatment

The mixed amino acid solution or sample supernatant (100  $\mu\text{L}$ ), potassium tetraborate solution (350  $\mu\text{L}$ ), and NBD-F working solution (50  $\mu\text{L}$ ) were mixed in 1.5 mL light-proof centrifuge tubes, and allowed to react in a heated constant temperature mixer at  $60^{\circ}\text{C}$  for 10 minutes.

### Chromatographic conditions

The analytes were separated in the ChromCore C18 column (150 $\times$ 4.6 mm, 5  $\mu\text{m}$ ) using the FLC automatic 2-D liquid chromatography coupling instrument. Mobile phase A was methanol, and mobile phase C was the phosphate buffer (0.02 mol/L, including 0.2 mmol/L of sodium dihydrogen phosphate and 0.2 mmol/L of sodium disodium phosphate, pH 6.0). Then, a 0.22  $\mu\text{m}$  water system filter membrane was used to filter the mobile phase. The injection volume was 20  $\mu\text{L}$ , the column temperature was  $45^{\circ}\text{C}$ , the wavelength was 472 nm, and the mobile phase flow rate was 1.0 mL/min.



### Method of validation

Five standard amino acids were selected, and these were detected from the hippocampus samples obtained from pigs. Then, the limit of detection (LOD), limit of quantitation (LOQ), linearity, precision, and accuracy were determined to confirm the dependability of the method. Next, after the five standard amino acids were selected, these were detected from the hippocampus samples obtained from pigs. Then, the standard curve was drawn using the concentration and peak area of Asp, Glu, Gly, Tau, and GABA in milli-q water. Three concentrations (QCH, QCM and QCL) of quality control samples were prepared ( $n = 6$ ). The precision and accuracy were measured within six days, within days, and between days using the QC samples of the same concentration. The detection limit was set at a signal-to-noise ratio (S/N) of 3, and the quantitative limit was set at a S/N of 10.

### Statistical analysis

GraphPad Prism 8.0.1 was used to conduct the multivariate ANOVA analysis on the experimental results, and the findings of the experiment were presented in mean  $\pm$  standard deviation. The difference was considered to be significant when  $p < 0.05$ , while this was considered to be highly significant when  $p < 0.01$ .

## Results and discussion

### Enhancing separation conditions

#### Liquid chromatographic conditions

Gradient-free elution was used for the present study. Following the previous experiments, the isometric elution of 25% methanol buffer salt, 15% methanol buffer salt, and 5% methanol buffer salt for 25 minutes was determined. Due to the strong retention of GABA on this column, and in order to enable GABA to be eluted smoothly without affecting the normal peak emission of Asp and Glu, 12% methanol buffer salt was selected as the flow stage. In addition, the impact of pH (6.0, 6.5 and 6.8) in the buffer salt mobile phase on the target peak was determined, and the pH was detected to be 6.0. Therefore, the ChromCore C18 column was selected, and this was eluted for 18 minutes in 12% methanol buffer salt. Thus, the five neurotransmitter amino acids were completely separated in the ChromCore C18 column, and the peak shape was good. However, after the addition of the biological matrix, there were other unknown peaks that were not completely eluted. In order to prevent the normal injection of the next needle to be affected, the investigators decided to extend the isometric elution to 25 minutes. The results indicated that the five amino acid neurotransmitters totally separated after 25 minutes at pH 6.0, and the isometric elution with 12% methanol buffer salt after 18 minutes was determined.

Based on the previous experiments, three derivative systems were compared, and the best concentration and derivative solution of NBD-F under the best derivative environment were obtained. The following were investigated: the mixed derivative system that consisted of the sample + potassium tetraborate + NBD-F solution, the mixed derivative system that consisted of the sample + potassium tetraborate + NBD-F and methanol, and the mixed derivative system that consisted of the sample + potassium tetraborate + NBD-F + acetonitrile. In addition, the NBD-F solution of 10, 50 and 100 mmol/L under the conditions of the three mixed derivative systems were investigated. It was revealed that the 10 mmol/L NBD-F solution had the best peak

shape and separation, without acetonitrile and methanol.

### pH, temperature and time

In the present experiment, after studying and analyzing the derivatization conditions of amino acids, it was revealed that the pH of the derivative reagents, temperature, and reaction heating time affects the sensitivity of the detection method. Therefore, the pH of the reaction medium was investigated. The effect of various pH levels (8.5, 9.0, 9.5 and 10.0) on the peak area of the derivative product of amino acid was investigated. It was revealed that the derivative yield of potassium tetraborate with pH 9.5 was the highest.

Based on this information, the effects of several derivatization temperatures (30, 45, 60 and 75°C) and time ranges (1–20 minutes) on the peak area of the derivatives were determined. It was found that the reaction time of heating for 10 minutes at 60°C can make the derivatization reaction complete, and allowed for more ideal peak areas and separations to be obtained.

### Chromatography and detection

The chromatographic conditions in the experimental study were used to determine the selectivity of the five amino acid neurotransmitters, and draw the chromatogram for the five brain areas in pigs and rats (Fig. 1). Within the chosen experimental parameters, the retention time of the symmetrical resolution of the analyte in its vicinity was not disturbed by the additional substances. Furthermore, the five kinds of amino acid neurotransmitters were entirely separated in 18 minutes. As shown in Figure 1b, the peak emergence time of Asp, Glu, Gly, Tau and GABA in the chromatogram was 2.44, 3.29, 8.09, 10.01 and 16.20 minutes, respectively. As shown in Figure 1c, the peak emergence time for Asp, Glu, Gly, Tau and GABA in pigs in the chromatogram was 2.42, 3.38, 7.96, 9.88 and 17.29 minutes, respectively.

### Linearity, detection and quantitative limits, precision and accuracy

The linear relationships of the five standard amino acid neurotransmitters were determined within the range of seven different concentrations (0.300–100.0  $\mu\text{mol/L}$ ). The regression equations for the correction curves, peak area relative standard deviations (RSDs), detection limits, and quantitation limits are presented in Table 1. The results revealed that the strong linear relationship among the five amino acids is good, with correlation coefficients totaling higher than 0.999.

Precision and accuracy were assessed by measuring the RSD of the five amino acid neurotransmitters in the hippocampus of pigs within and between six days (Table 1). The concentration of the amino acid neurotransmitters was 0.15–0.20  $\mu\text{mol/L}$  and 0.30–0.55  $\mu\text{mol/L}$ , respectively.

According to the experimental results, the LOD value of Asp, Glu, Gly, Tau and GABA was 0.15, 0.15, 0.20, 0.20 and 0.20  $\mu\text{mol/L}$ , respectively. Although the sensitivity of this method was not high, this satisfies the basic quantification, and provides a new method for the detection of amino acids in the brain.

### Results of the method application

The method has been successfully applied in two animal substrates (rats and pigs). The outcomes are presented in Figure 2. The blank contents of the five amino acid neurotransmitters in the five brain regions (hippocampus, cortex, striatum, cerebellum and brainstem) were respectively measured in rats and pigs.

The findings revealed that the method of determining the con-

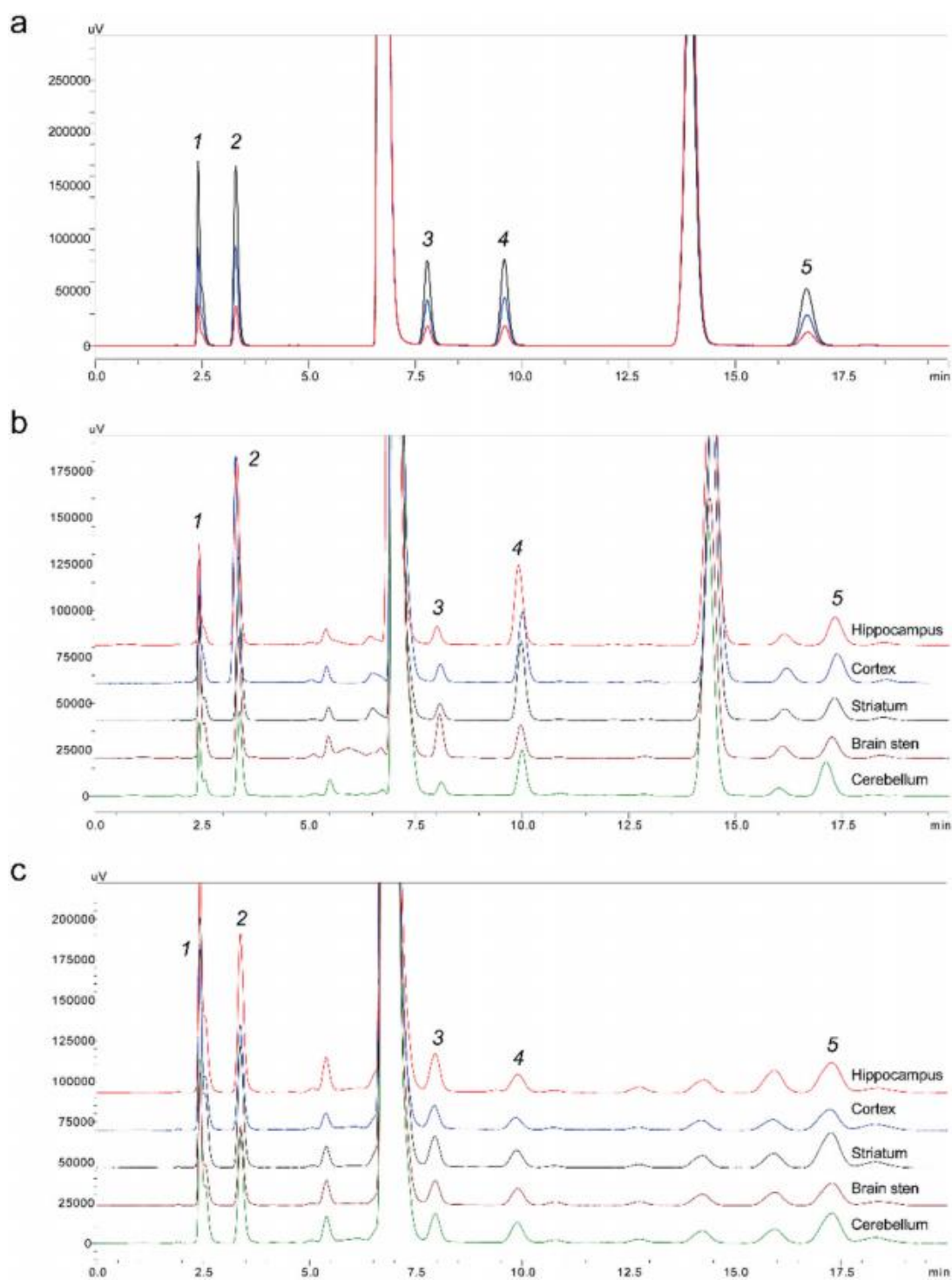


**Fig. 1. High-performance liquid chromatography: (1) Asp, (2) Glu, (3) Gly, (4) Tau, and (5) GABA.** (a) Standard solution for the five amino acids; (b) Specimens obtained from the rat brain regions; (c) Specimens obtained from the pig brain regions.

centration of amino acid neurotransmitters in rats and pigs has strong selectivity, because the peak area and resolution of the amino acid targets in the five separate brain areas of rats and pigs were good. In the pig samples, the content of Asp was the highest in the different brain regions. Furthermore, the results revealed that the

amino acid neurotransmitters in the brain of rats were generally lower, when compared to those in the brain of pigs. However, the amount of Tau in the brain of rats was higher, when compared to that in the brain of pigs. These results show that for the amino acid neurotransmitters in both pigs and rats, Asp, Glu, Gly and GABA

Table 1. Linearity, detection limit, quantitative limit, precision and accuracy of the pig hippocampal samples

Compound	Regression equation	r <sup>2</sup>	QC, n = 6	RSD (%)		Accuracy (%)		LOD (μmol/L)	LOQ (μmol/L)
				Intra-day	Inter-day	Intra-day	Inter-day		
Asp	y = 24.15x + 4,953.5	0.9999	QCH	1.48	2.13	88.98	88.14	0.15	0.3
			QCM	2.40	5.47	87.66	94.46		
			QCL	7.72	5.94	91.91	85.91		
Glu	y = 27.708x + 6869.8	0.9993	QCH	1.76	2.81	89.01	87.71	0.15	0.3
			QCM	7.74	8.66	110.80	111.98		
			QCL	13.85	12.61	101.73	108.68		
Gly	y = 17.686x + 4,103.2	0.9997	QCH	3.14	3.49	88.72	87.26	0.2	0.5
			QCM	6.14	6.68	87.66	96.94		
			QCL	4.64	3.53	85.99	85.70		
Tau	y = 19.415x + 7,971.5	0.9991	QCH	1.84	2.15	87.44	88.27	0.2	0.5
			QCM	2.94	5.86	89.47	98.89		
			QCL	3.63	4.16	93.19	88.49		
GABA	y = 20.378x + 6,738.8	0.9999	QCH	3.59	2.59	87.95	89.13	0.2	0.55
			QCM	7.13	7.35	88.43	90.14		
			QCL	4.50	3.53	91.97	86.31		

Asp, aspartate; Glu, glutamate; Gly, glycine; Tau, taurine; GABA, γ-aminobutyric; RSD, relative standard deviations; LOD, limit of detection; LOQ, limit of quantitation.

were significantly different in the hippocampus, while Tau was not significantly different. In the cortex, Asp, Glu, Gly and GABA presented with significant differences, while Tau did not present with significant differences. In the striatum, Asp, Gly, Tau and GABA presented with significant differences, but there was no significant difference in Glu. In the cerebellum, there were significant differences between Asp and Gly, and between Glu and GABA, while there was no significant difference in Tau. In the brain stem, Asp,

Glu, Gly and GABA markedly varied, while Tau did not markedly vary. Interestingly, it was observed that the excitatory amino acid neurotransmitters and inhibitory amino acid neurotransmitters balanced with each other in each region of the animal brain, and this was not dominated by any one kind of amino acid neurotransmitter. Animal amino acid neurotransmitters are regulated by two different types of amino acid neurotransmitters, and these maintain the dynamic balance of the body under normal physiology.

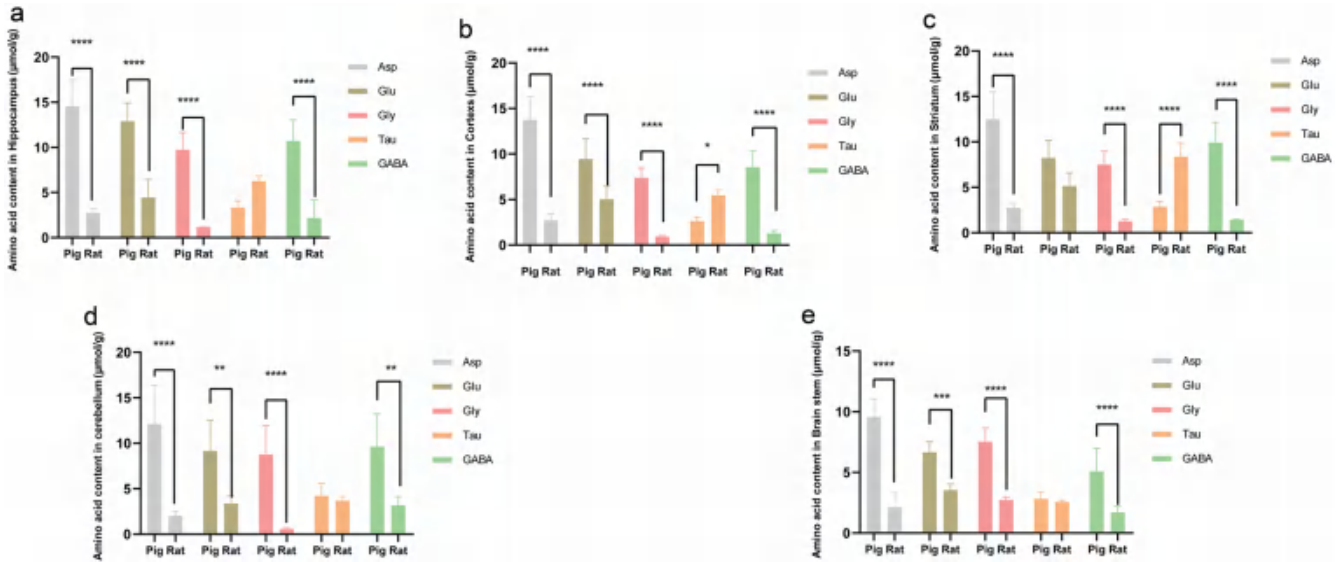


Fig. 2. Comparison of amino acid neurotransmitters in the five different brain regions in pigs and rats: (a) hippocampus, (b) cortex, (c) striatum, (d) cerebellum, and (e) brain stem. Levels of amino acids in the five different brain regions in pigs and rats. The data were expressed as mean ± standard error of the mean (SEM, n = 6). \*p < 0.05, \*\*p < 0.01, \*\*\*\*p < 0.0001, pig vs. rat.

### Comparison of the contents of amino acid neurotransmitters between pigs and rats

Earlier studies on the hippocampus of the brain of rats have revealed that this has the highest concentration of Glu, followed by Asp.<sup>16</sup> However, this result was slightly different from what was revealed in the present study. It was found that the Tau content was the highest in the hippocampus, cortex, striatum and cerebellum, and that the glutamic acid content was the highest in brain stem. The reason for this difference may be due to difference in conditions during processing, such as sample derivation. In previous studies, the highest concentrations of Glu were detected in the hippocampus and cortex of pigs, followed by Asp.<sup>17</sup> This finding differs from the present results, which revealed that the highest concentration was Asp, followed by Glu. It was analyzed that the reason for this difference may be because the sensitivity to different amino acids varied due to different methods. However, the results remained consistent. For example, in the cortex of pigs, except for Glu and Asp, which had the highest content, the ranking of the contents of the other three amino acids in descending order was GABA, Gly and Tau.

### Future directions

A number of studies have revealed that the imbalance of amino acids in the brain is associated with a variety of neurological diseases, such as Alzheimer's disease, anxiety and depression. Based on this, a simple brain amino acid detection method was established, in order to provide technical support for the monitoring of these diseases, hoping to provide help in the prevention of neurodegenerative diseases. Future research would be conducted, and focus will be given on the exploration of the methodology, providing technical support for scientific research in the future.

### Conclusions

The present study offers a quick and low-cost method for identifying amino acid neurotransmitters in brain tissues. This technique has been used to identify amino acid neurotransmitters in five different regions of the brain in pigs and rats. These findings demonstrate the suitability of this approach for identifying amino acid neurotransmitters in animal brain tissues.

### Acknowledgments

None.

### Funding

None.

### Conflict of interest

One of the authors, Dr. Zhao-Ying Liu, has been an editorial board member of *Journal of Exploratory Research in Pharmacology* since February 2023. The authors have no other conflict of interests to declare.

### Author contributions

ZYL and SYM: contributed to study concept and design; MHT and

XJZ: acquisition of the data; SYM and MHT: assay performance and data analysis; MHT: drafting of the manuscript; SYM: critical revision of the manuscript; ZYL: supervision.

### Ethical statement

The Hunan Agricultural University Ethics Committee authorized the use of animals in research (No. 2020-43). The 12 male Sprague-Dawley rats, which weighed 180–240 g, were obtained from SJA Laboratory Animal Co., Ltd. The samples of blank pig brain tissues were obtained from Hunan New Wufeng Co., Ltd. (Liuyang, China). The Chinese Guidelines for the Care and Use of Laboratory Animals were followed in the study.

### Data sharing statement

No additional data are available.

### References

- [1] Kölker S. Metabolism of amino acid neurotransmitters: the synaptic disorder underlying inherited metabolic diseases. *J Inher Metab Dis* 2018;41(6):1055–1063. doi:10.1007/s10545-018-0201-4, PMID:29869166.
- [2] Kwan C, Kang W, Kim E, Belliveau S, Frouni I, Huot P. Metabotropic glutamate receptors in Parkinson's disease. *Int Rev Neurobiol* 2023;168:1–31. doi:10.1016/bs.irn.2022.10.001, PMID:36868628.
- [3] Hou Y, Li X, Dai Z, Wu Z, Bazer FW, Wu G. Analysis of Glutathione in Biological Samples by HPLC Involving Pre-Column Derivatization with o-Phthalaldehyde. *Methods Mol Biol* 2018;1694:105–115. doi:10.1007/978-1-4939-7398-9\_10, PMID:29080160.
- [4] Möhler H. The GABA system in anxiety and depression and its therapeutic potential. *Neuropharmacology* 2012;62(1):42–53. doi:10.1016/j.neuropharm.2011.08.040, PMID:21889518.
- [5] Jakaria M, Azam S, Haque ME, Jo SH, Uddin MS, Kim IS, *et al*. Tau-rine and its analogs in neurological disorders: Focus on therapeutic potential and molecular mechanisms. *Redox Biol* 2019;24:101223. doi:10.1016/j.redox.2019.101223, PMID:31141786.
- [6] Ullah R, Jo MH, Riaz M, Alam SI, Saeed K, Ali W, *et al*. Glycine, the smallest amino acid, confers neuroprotection against D-galactose-induced neurodegeneration and memory impairment by regulating c-Jun N-terminal kinase in the mouse brain. *J Neuroinflammation* 2020;17(1):303. doi:10.1186/s12974-020-01989-w, PMID:33059700.
- [7] Lushnikova I, Maleeva G, Skibo G. Glycine receptors are involved in hippocampal neuronal damage caused by oxygen-glucose deficiency. *Cell Biol Int* 2018;42(10):1423–1431. doi:10.1002/cbin.11034, PMID:30022566.
- [8] Deng S, Scott D, Garg U. Quantification of Five Clinically Important Amino Acids by HPLC-Triple TOF™ 5600 Based on Pre-column Double Derivatization Method. *Methods Mol Biol* 2016;1378:47–53. doi:10.1007/978-1-4939-3182-8\_6, PMID:26602116.
- [9] Wood PL, Khan MA, Moskal JR. Neurochemical analysis of amino acids, polyamines and carboxylic acids: GC-MS quantitation of tB-DMS derivatives using ammonia positive chemical ionization. *J Chromatogr B Analyt Technol Biomed Life Sci* 2006;831(1-2):313–319. doi:10.1016/j.jchromb.2005.12.031, PMID:16406747.
- [10] Wang LS, Zhang MD, Tao X, Zhou YF, Liu XM, Pan RL, *et al*. LC-MS/MS-based quantification of tryptophan metabolites and neurotransmitters in the serum and brain of mice. *J Chromatogr B Analyt Technol Biomed Life Sci* 2019;1112:24–32. doi:10.1016/j.jchromb.2019.02.021, PMID:30836315.
- [11] Wumbei A, Goeteyn L, Lopez E, Houbraeken M, Spanoghe P. Glyphosate in yam from Ghana. *Food Addit Contam Part B Surveill* 2019;12(4):231–235. doi:10.1080/19393210.2019.1609098, PMID:31046629.
- [12] Nuhu F, Gordon A, Sturmey R, Seymour AM, Bhandari S. Measurement of Glutathione as a Tool for Oxidative Stress Studies by High Performance Liquid Chromatography. *Molecules* 2020;25(18):4196.

- doi:10.3390/molecules25184196, PMID:32933160.
- [13] Ferré S, González-Ruiz V, Zangari J, Girel S, Martinou JC, Sardella R, *et al*. Separation and determination of cysteine enantiomers in plasma after derivatization with 4-fluoro-7-nitrobenzofurazan. *J Pharm Biomed Anal* 2022;209:114539. doi:10.1016/j.jpba.2021.114539, PMID:34954468.
- [14] Miyamoto T, Takahashi N, Sekine M, Ogawa T, Hidaka M, Homma H, *et al*. Transition of serine residues to the D-form during the conversion of ovalbumin into heat stable S-ovalbumin. *J Pharm Biomed Anal* 2015;116:145–149. doi:10.1016/j.jpba.2015.04.030, PMID:25982752.
- [15] Ouchi S, Matsumoto K, Okubo M, Yokoyama Y, Kizu J. Development of HPLC with fluorescent detection using NBD-F for the quantification of colistin sulfate in rat plasma and its pharmacokinetic applications. *Biomed Chromatogr* 2018;32(5):e4167. doi:10.1002/bmc.4167, PMID:29235137.
- [16] Wu X, Wang R, Jiang Q, Wang S, Yao Y, Shao L. Determination of amino acid neurotransmitters in rat hippocampi by HPLC-UV using NBD-F as a derivative. *Biomed Chromatogr* 2014;28(4):459–462. doi:10.1002/bmc.3062, PMID:24132719.
- [17] Zhao XJ, Wang N, Zhang MJ, Liu SS, Yu H, Tang MH, *et al*. Simultaneous determination of five amino acid neurotransmitters in rat and porcine blood and brain by two-dimensional liquid chromatography. *J Chromatogr B Analyt Technol Biomed Life Sci* 2021;1163:122507. doi:10.1016/j.jchromb.2020.122507, PMID:33387860.





## Review Article

# Non-human Primate Models of Alzheimer's Disease



Yihan Li<sup>1</sup> and Ben J. Gu<sup>1,2\*</sup>

<sup>1</sup>The Florey Institute, The University of Melbourne, Parkville, Australia; <sup>2</sup>National Clinical Research Centre for Aging and Medicine, Huashan Hospital, Fudan University, Shanghai, China

Received: January 29, 2023 | Revised: March 02, 2023 | Accepted: March 10, 2023 | Published online: April 20, 2023

## Abstract

Alzheimer's disease (AD) is a chronic neurodegenerative disorder characterised by cognitive impairment and numerous pathologies, including  $\beta$ -amyloid ( $A\beta$ ) and Tau proteopathies, altered immune responses, and brain atrophy. Despite hundreds of years of investigations into its underlying pathogenesis, the aetiology of AD is not clearly understood. AD diagnostic criteria are not effective at identifying pre-clinical patients and current AD treatments cannot postpone or reverse disease progression. The development of non-human primate (NHP) models of AD is urgently required due to their close phylogenetic relationship to humans, similar neuroanatomy, comparable genetics, and high complexity of high-order cognitive functions, making them a better model of AD than rodents. We compared and contrasted AD-associated pathological features and behavioural alterations manifested between naturally aged spontaneous and induced NHP models of AD. Induced models of AD can be established using injections of  $A\beta$  oligomers, brain homogenates, neurotoxins, or formaldehyde. In recent decades, both spontaneous and induced NHP models of AD have been used to facilitate the development of neuroimaging tracers and therapeutic treatments, aiding in the translational application of lab discoveries into clinical trials involving human subjects. The establishment of a standardised NHP model of AD is expected by making a guideline concerning NHP species, types and doses of inducers, frequency of injections, and duration of inoculation. Its development can be facilitated by a comprehensive assessment of NHPs, including all AD-associated pathologies and a wide range of behavioural examinations. NHP models of AD have contributed to AD research and their evolution is expected to better recapitulate AD features and present greater translational potential in the near future.

**Keywords:** Rhesus monkey; Cynomolgus monkey; Tree shrews; Squirrel monkeys; Mouse lemurs.

**Abbreviations:** 3R Tau, Tau isoforms with 3 repeats; 4R Tau, Tau isoforms with 4 repeats; AChE, acetylcholinesterase enzyme; AD, Alzheimer's disease; ApoE, apolipoprotein E; ApoJ, apolipoprotein J; APP, amyloid precursor protein;  $A\beta$ , beta-amyloid;  $A\beta$ 1-40,  $A\beta$  ending in residue 40;  $A\beta$ 1-42,  $A\beta$  ending in residue 42;  $A\beta$ ,  $A\beta$  oligomer; BDNF, brain-derived neurotrophic factor; CAA, cerebral amyloid angiopathy; CSF, cerebrospinal fluid; DMT, disease-modifying treatments; DMTS, delayed match to sample; DNMS, delayed nonmatching-to-sample; DR, delayed response; DRST, delayed recognition span task; EEG, electroencephalogram; EOAD, early-onset AD; FA, formaldehyde; GFAP, glial fibrillary acidic protein; GSM,  $\gamma$ -secretase modulators; ICV- $A\beta$ , intracerebroventricular administration of  $A\beta$ ; ICV-STZ, intracerebroventricular injection of STZ; IT- $A\beta$ , intrathecal administration of  $A\beta$ ; LOAD, late-onset AD; M4, the fourth subtype of mAChR; mAb, monoclonal antibodies; mAChR, M1 muscarinic acetylcholine receptor; MAPT, microtubule-associated protein Tau; NFT, neurofibrillary tangles; NHP, non-human primate; NMDA, N-methyl-D aspartate; NT, neuropil threads; PET, positron emission tomography; PHF, paired helical filaments; PSEN1, presenilin 1; PSEN2, presenilin 2; P-Tau, hyperphosphorylated Tau; P-Tau181P, Tau phosphorylated at threonine 181; P-Tau231P, Tau phosphorylated at threonine 231; SNP, single nucleotide polymorphisms; STM, short-term memory; STZ, streptozotocin; t-Tau, total Tau.

\*Correspondence to: Ben J. Gu, The Florey Institute, The University of Melbourne, 30 Royal Parade, Parkville, Victoria 3052, Australia. ORCID: <https://orcid.org/0000-0001-5500-4453>. Tel: +61 3 9035 6317, Fax: +61 3 9035 3100, E-mail: [ben.gu@florey.edu.au](mailto:ben.gu@florey.edu.au)

**How to cite this article:** Li Y, Gu BJ. Non-human Primate Models of Alzheimer's Disease. *J Explor Res Pharmacol* 2023;8(3):199–221. doi: 10.14218/JERP.2023.00006.

## Introduction of Alzheimer's disease (AD)

### Background of AD

AD is a devastating neurodegenerative disorder that constitutes 70–80% of all dementia cases worldwide.<sup>1</sup> It is clinically manifested by deterioration in learning, episodic memory, visuospatial orientation, and executive abilities that eventually deprive patients' capabilities of performing daily activities.<sup>1,2</sup> Pathologically, AD is characterised by brain atrophy at the macroscopic level, and extracellular senile plaques, intracellular neurofibrillary tangles (NFT), and glial cell engagement at the microscopic level.<sup>3</sup> Macroscopically, the brains of AD patients are marked by moderate cortical atrophy and enlarged sulcal spaces in the frontal and temporal cortices, which characterise the final stage of dementia in disease progress, but is not specific to AD.<sup>3</sup> Currently, scientists define the pre-clinical phase of AD as the cellular phase, during which alterations of proteopathies, neurons, and glial cells drive disease progression before the clinical presentation of cognitive impairment and executive deficits.<sup>4,5</sup> Correspondingly, the diagnostic criteria of AD have shifted from the gold-standard post-mortem examination of parenchymal beta-amyloid ( $A\beta$ ) and Tau proteopathies to the current suite of biofluid biomarkers and molecular imaging.<sup>6</sup>

A $\beta$  neuroimaging by positron emission tomography (PET) and cerebrospinal fluid (CSF) measurements of A $\beta$ , total Tau (t-Tau), and hyperphosphorylated Tau (p-Tau) allow an accurate diagnosis of individuals with pre-clinical and prodromal AD.<sup>5</sup> However, the costliness and invasiveness of molecular neuroimaging and CSF measurements limit their application as a population-based screening technique in hospital settings.<sup>6</sup> Since the first identification and classification of AD in the last century, and despite decades of extensive efforts, cost-effective early diagnostic tools, effective disease-modifying treatments (DMT), and a sophisticated understanding of AD pathogenesis, much about AD remains inconclusive.<sup>2</sup> With the ongoing aging of the global population, this devastating chronic disease will impose extensive economical, psychological, and physical burdens on individuals, families, and countries.

### *A $\beta$ -related pathologies*

As first described over 100 years ago, the classical pathological features of AD include extracellular A $\beta$  plaques and intracellular NFTs.<sup>1</sup> A $\beta$  plaques are the aggregated form of A $\beta$  peptides, including A $\beta$  peptides ending in residue 40 (A $\beta$ <sub>1-40</sub>) and ending in residue 42 (A $\beta$ <sub>1-42</sub>), both of which result from the abnormal processing of amyloid precursor protein (APP) by  $\beta$ - and  $\gamma$ -secretases.<sup>3,7</sup>  $\beta$ -secretase cleaves the juxta-membrane domain of APP and generates the ectodomain, after which  $\gamma$ -secretase cleaves multiple sites in the transmembrane domain of APP, leading to the production of carboxy terminal fragments and A $\beta$  peptides, ranging from 38 to 43 residues.<sup>3,7</sup> Among these 4.5kDa A $\beta$  peptides, A $\beta$ <sub>1-42</sub> is the most hydrophobic, fibrillogenic, and amyloidogenic component, which corresponds with its high neurotoxicity in AD.<sup>7</sup> Two types of A $\beta$  plaques have been mainly observed in AD, namely diffuse plaques, and dense core plaques. Diffuse plaques are weakly stained by thioflavin-S and are deprived of activated glial cells or neuritic components, while dense core plaques can be intensely stained by thioflavin-S and Congo red due to the presence of numerous A $\beta$  fibrils.<sup>3</sup> Dense core plaques are usually associated with Tau<sup>+</sup> or dystrophic neurites, which are also known as neuritic plaques.<sup>3</sup> In the peripheral zone of dense core neuritic plaques, some dystrophic neurites contain Tau filaments, suggesting the presence of NFT-bearing neurons in that region.<sup>3</sup> Other types of dystrophic neurites may contain cytoskeletal proteins or may become accumulated by degenerating mitochondria and lysosomal bodies.<sup>3</sup> Considering the complicated molecular and cellular components of A $\beta$  plaques, investigating the mechanism underlying plaque formation, A $\beta$  neurotoxicity, immune activation, neuronal loss, and Tau involvement is critical to advance our understanding of AD pathogenesis and cognitive decline. Beyond the composition of A $\beta$  plaques, A $\beta$  peptides aggregate and propagate in stereotypic patterns in AD, leading to the staging schemes described by Braak and Thal.<sup>8</sup> Thal has improved the three-stage Braak staging into an advanced five-stage scheme: A $\beta$  deposits in neocortex exclusively in phase one; A $\beta$  spreads into the allocortical brain regions in phase two; A $\beta$  further spreads into diencephalic nuclei, the striatum, and the cholinergic nuclei of the basal forebrain in phase three; A $\beta$  further spreads into several brainstem nuclei in phase four; A $\beta$  eventually propagates into the cerebellum in phase five.<sup>8</sup> In human AD, the abnormal production of A $\beta$  and the imbalanced clearance of A $\beta$  results in the aberrant deposition of A $\beta$  plaques in the brains of AD patients, during which Tau pathologies, neuronal swelling, cytoskeletal abnormalities, intracellular organelle dysfunction, and glial activation are engaged. This is extremely challenging to replicate in animal models of AD.

In addition to the brain parenchyma, A $\beta$  peptides are also deposited in the walls of small- to medium-sized blood vessels of the brain, which is known as cerebral amyloid angiopathy (CAA). The walls of leptomeningeal and cortical arteries and occasionally, veins, are predominantly occupied by A $\beta$ <sub>1-40</sub> peptides, while A $\beta$ <sub>1-42</sub> peptides are the main component of neuritic plaques in the parenchyma.<sup>9</sup> Parenchymal A $\beta$  plaques and CAA can both be caused by A $\beta$  peptides with a common origin, suggesting a potential shared mechanism driving both A $\beta$  proteopathies.<sup>9</sup> A $\beta$ <sub>1-42</sub> peptides may first be deposited in the vessel wall, while A $\beta$ <sub>1-40</sub> peptides may subsequently be deposited in the walls along the perivascular drainage pathways, while fibrillogenic neuron-derived A $\beta$ <sub>1-42</sub> peptides are more likely to deposit in the parenchyma to form A $\beta$  plaques.<sup>9</sup> Parenchymal A $\beta$  plaques originate in the neocortex of the brain and subsequently propagate into the allocortex, thalamus, and basal ganglia, but CAA may predominantly affect the posterior lobar brain regions and rarely deposit in the deep grey nuclei, white matter, and brainstem.<sup>9</sup> Additionally, A $\beta$  peptides in the walls of vessels are amalgamated with A $\beta$ -associated proteins, including complement proteins, apolipoprotein E (ApoE), and apolipoprotein J (ApoJ/CLU). As the two major A $\beta$  proteopathies in AD pathophysiology, CAA and parenchymal A $\beta$  plaques may share a common origin of A $\beta$  peptides, metabolism, and clearance mechanisms, while different lengths of A $\beta$  peptides, different A $\beta$ -associated proteins, and different associations with cognitive deficits are noted.

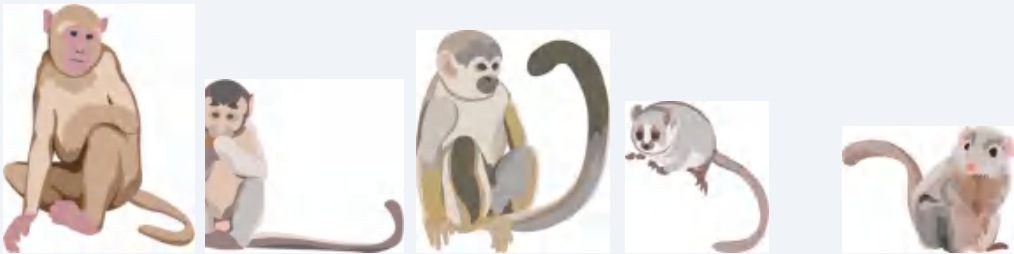
### *Tau-related pathologies*

A solid neuropathological diagnosis of human AD requires the detection of both A $\beta$  plaques and NFTs, the latter of which is more tightly associated with synaptic loss and cognitive impairment.<sup>10</sup> Tau filaments are termed as paired helical filaments (PHF) because they comprise two filaments that twist to form a periodic structure.<sup>3</sup> In AD, PHFs are structured by six isoforms of Tau, including isoforms with 3 repeats (3R Tau) and 4-repeats (4R Tau) in the microtubule binding domain. These isoforms are generated through alternative splicing of the microtubule-associated protein Tau (MAPT) gene (chr17).<sup>3,11</sup> Axonal Tau plays an important role by interacting with tubulin, stabilising microtubule structure, and supporting microtubule-dependent axonal transport.<sup>11</sup> Pathophysiologically, Tau can be hyperphosphorylated with nine phosphates per molecule, resulting in fibrillisation of p-Tau and aggregation into NFTs.<sup>11</sup> These molecular alterations undermine its original abilities to bind and stabilise microtubules in axons, thus resulting in the deposition of intraneuronal lesions, including p-Tau, pre-tangle materials, NFTs in cell bodies, neuropil threads (NT) in neuronal processes, and other materials in neuritic plaques.<sup>12</sup> In the brains of AD patients, the distribution pattern and sequence of Tau lesions have also been categorised in three stages, as described by Braak and colleagues.<sup>12</sup> Abnormal Tau is initially detected in transentorhinal and entorhinal regions, gradually spreading to the limbic allocortex and adjoining neocortex, and eventually propagating to the primary and secondary fields.<sup>12</sup>

### *AD genetics*

AD can be divided into early-onset AD (EOAD) and late-onset AD (LOAD) based on the age of onset. EOAD accounts for less than 1% of total AD cases. It is determined by autosomal dominant mutations in genes encoding APP (*APP*), presenilin 1 (*PSEN1*) and presenilin 2 (*PSEN2*). Mutations in the *APP* gene generally predispose APP to be cleaved by  $\beta$ -secretase, leading to the production of more A $\beta$ <sub>1-42</sub> peptides that aggregate and propagate easily.<sup>13</sup>

**Table 1.** The most widely used NHP in the field of AD

Animal species	Rhesus macaques	Cynomolgus monkeys	Squirrel monkeys	Mouse lemurs	Tree shrews
Classification	Old world monkey	Old world monkey	New world monkey	Prosimian	Non primate
Scheme					
General background					
Scientific name	<i>Macaca mulattas</i>	<i>Macaca fascicularis</i>	<i>Simia sciurea</i>	<i>Microcebus murinus</i>	<i>Tupaia belangeri chinensis</i>
Body length	45–64 cm	40–65 cm	25–35 cm	12–13 cm	26–41 cm
Weight	5–12 kg	9 kg	0.5–1.1 kg	50–120 g	50–270 g
Life span	34–40 years	35 years	15–20 years	8–14 years	8 years
Age considered old	20–25 years old	20 years old	12 years old	5 years old	7 years old
Recruited in references					

NHP, non-human primate; AD, Alzheimer's disease.

Mutations in *PSEN1* and *PSEN2* change the specificity of cleavage sites on APP, preferring to be cleaved at position 42 instead of 40, also resulting in more  $A\beta_{1-42}$  production.<sup>14</sup> Numerous mutations in EOAD genes converge on the same outcome of altered proteolytic APP processing and  $A\beta_{1-42}$  overproduction, which forms the foundation of the A $\beta$ -amyloid theory.<sup>7</sup> LOAD accounts for the remaining 99% of total AD cases, and is currently explained by the imbalanced production and clearance of A $\beta$  in the brain.<sup>1</sup> The risk of an individual developing LOAD is largely determined by common polymorphisms in the *APOE* gene. This gene encodes the glycoprotein ApoE that is ubiquitously expressed in the brain, liver, and myeloid cells, and which plays a role in cholesterol and lipid transportation, neuronal growth, and immunoregulation.<sup>15</sup> The *APOE* gene encodes three isoforms: protective ApoE  $\epsilon$ 2, neutral ApoE  $\epsilon$ 3, and detrimental ApoE  $\epsilon$ 4.<sup>15</sup> Two different amino acids in the three isoforms significantly modify the structure and function of ApoE, resulting in alterations in A $\beta$  clearance, lipid metabolism, glucose metabolism, innate immune responses, and mitochondrial dysfunction.<sup>16</sup> For instance, CAA in capillaries, arterioles, and small arteries are highly associated with ApoE  $\epsilon$ 4, which might be explained by the reduced transendothelial clearance of A $\beta$ -apolipoprotein complexes compared with ApoE  $\epsilon$ 2 and ApoE  $\epsilon$ 3 carriers.<sup>3</sup> The precise mechanism by which *APOE*  $\epsilon$ 4 increases AD risk remains inconclusive, thus further investigation of the *APOE* gene in AD is critical for advancing our understanding of AD.

### Animal models of AD

Despite extensive investigations into AD for over 100 years, the underlying pathophysiological mechanisms remain unknown, the disease aetiology is still insufficiently understood, accurate diagnostic tools cannot be widely applied for population screening, and the DMTs are lacking. In light of these urgent demands in the field, the development and study of reliable animal models of AD becomes essential to enable the study of the pre-clinical and prodromal phase

of AD, which is difficult to access in AD patients.<sup>2</sup> A wide range of species have been assessed in AD-related research and various rodent models of AD have dominated the field in recent decades.<sup>2</sup> Genetic mutations associated with A $\beta$  and Tau processing have provided a solid foundation for generating hundreds of transgenic murine models that have evolved over time to imitate specific features of AD and facilitate the translational application of laboratory discoveries.<sup>17</sup> Rodent models have many advantages, including low financial costs, large sample sizes, easier genetic manipulation, conventional animal care, etc. Unfortunately, rodents are also associated with low translational potential for the development of diagnostic markers and therapeutic treatments due to the reduced complexity of their brain structure and circuitry compared to humans.<sup>2</sup> For instance, APP transgenic mice rarely manifest the Tau hyperphosphorylation and brain atrophy that are found in human AD.<sup>2</sup> Thus, to understand a complicated age-related human disorder, using the brain of a non-human primate (NHP) with a closer phylogenetic relationship to humans, a similar neuroanatomy structure, comparable genetics, similarly complicated neural circuitry, and higher-order cognitive functions is greatly preferred (Table 1).

### Normal aging studies in NHPs

Aging is the single largest risk factor for AD.<sup>1</sup> Although aged NHPs cannot recapitulate the full spectrum of AD, they are ideal models of normal aging, cognitive deterioration, and executive processing impairment. Since the 1970s, numerous studies have reported age-related impairments in cognition in a wide range of animals, particularly NHPs, including short-term memory (STM), learning abilities, and executive functions, which have been similarly documented during aging of human.<sup>18</sup> The Rhesus monkey (*Macaca mulattas*), an old world monkey closely relative to the cynomolgus monkeys, has been predominantly employed in early studies that investigated the association between learning impairment, memory dysfunction, and normal aging in NHPs.<sup>19</sup> Rhesus monkeys have a body length of

45–64 cm, a body weight of 5–12 kg, and a life expectancy of 34–40 years (Table 1).<sup>20</sup> In 1978, Bartus and colleagues used an indirect delayed response (DR) procedure and identified a profound impairment in STM in the aged ( $\geq 18$  years old) compared to younger (3–5 years old) rhesus monkeys.<sup>21</sup> STM is defined as the ability of an individual to temporarily memorise a limited amount of information for a very short interval. Deficits in STM are one of the best characterised alterations in normal aging.<sup>18,22</sup> STM deterioration in rhesus monkeys emerged in early middle age during normal aging, similar to what is observed in humans.<sup>18</sup> They further evaluated monkeys' abilities to learn visual discrimination and reversal problems.<sup>23</sup> The aged rhesus monkeys ( $\geq 18$  years old) constantly demonstrated severe deficiency with reversal problems, but no age-related deterioration in colour and pattern discrimination was observed.<sup>23</sup> Another concept that is closely associated with STM is working memory that temporarily stores, processes, and manipulates STM necessary for complicated cognitive tasks, such as language comprehension, learning, and reasoning.<sup>22</sup> A decline in the working memory of aged primates has been documented in several NHP studies using a neurotoxin-induced model of AD.<sup>24–27</sup>

The seminal studies conducted by Bartus and colleagues failed to identify age-related impairment in recognition memory, but they inspired subsequent studies in this field. In 1987, rhesus monkeys of four different age groups were trained in a delayed nonmatching-to-sample (DNMS) task that examined the subject's ability to recognise a novel object from a familiar object, following a specific delay interval.<sup>18,28</sup> Although their learning abilities were marginally impaired with aging, significant age-related impairment in recognising objects were observed when delay intervals or lists of objects were increased.<sup>28</sup> This study contradicted Bartus' previous results and identified impairment in visual recognition memory during normal aging of NHPs.<sup>28</sup> The DNMS task was also used later on female aged rhesus monkeys (22–26 years old).<sup>29</sup> The aged rhesus monkeys required significantly more training than young monkeys (9–11 years old) to learn basic principles of the task, but their recognition memory was minimally impaired compared with the young, consistent with Bartus' results.<sup>29</sup> Rapp and colleagues then required rhesus monkeys to remember the order of subjects and identified significant age-related deterioration in their task-dependent recognition memory.<sup>29</sup> These findings further suggested different susceptibilities to age-related impairment in different memory functions in NHPs. In 1993, Bachevalier conducted a more comprehensive investigation into memory functions of rhesus monkeys by selecting multiple memory tasks associated with distinct brain areas.<sup>30</sup> This study described widespread behavioural deficits in aged rhesus monkeys, including visuospatial orientation, DR tasks, and object recognition memory (measured using DNMS) in young middle/teen age, middle age, and old age of rhesus monkey, respectively.<sup>30</sup> These memory abilities are associated with different brain regions, illustrating that certain cerebral systems were predisposed to early degenerative neuronal damage.<sup>30</sup> Delayed recognition span tasks (DRST) are another important recognition memory task, in which NHPs are required to recognise a novel stimuli among an increasing array of serially presented stimuli to examine their spatial and colour condition.<sup>31</sup> It was used to assess the recognition memory of eight aged rhesus monkeys (25–27 years old) that presented with recognition memory impairment in both the spatial and colour conditions of the DRST.<sup>31</sup> Visuospatial orientation was also compromised in young middle/teen age in rhesus monkeys compared with other memory deficits.<sup>30</sup> The impairment in recognition memory is not associated with the age-related decline in the length of cholinergic fibres of rhesus

monkeys.<sup>32</sup> Some controversies were observed in these studies, but age-associated abnormalities in recognition memory among aged NHPs are supported by increasing evidence as technology has improved, and sample sizes have increased. During normal aging, NHPs manifest similar symptoms to human AD, particularly cognitive behavioural alterations, suggesting their potential to be used as a model of age-related neurodegenerative disorders.

## Spontaneous NHP models of AD

### *A $\beta$* pathologies in aged NHPs

Aged NHPs demonstrate cognitive deficits that are similarly observed in aged humans, but also spontaneously develop age-associated human AD-resembling pathologies, such as extracellular A $\beta$  plaques, CAA, intracellular p-Tau, dystrophic neurites, and glial activation. All aged NHP species exhibit A $\beta$ -related proteopathies in their cerebellum and vasculature, but differences in the age of onset, burden level, biological composition, and spatial distribution are still observed.<sup>2</sup> In 1985, numerous A $\beta$  plaques in the prefrontal and temporal cortices in six aged rhesus monkeys were identified, the densities of which were significantly associated with age, suggesting a positive association between age and A $\beta$  burden in aged NHPs.<sup>33</sup> Subsequent studies identified similar results in the frontal, temporal, and parietal cortices of aged rhesus monkeys and aged squirrel monkeys, as measured by thioflavin-S and silver staining.<sup>34–36</sup> The total burden level of parenchymal A $\beta$  in the temporal and occipital cortices of aged rhesus monkeys was comparable to those of humans with AD, while the A $\beta_{1-40}$  level may outweigh the A $\beta_{1-42}$  level in aged rhesus monkeys.<sup>37</sup> The highest A $\beta$  plaque densities were noticed in the frontal and temporal cortices, while few A $\beta$  peptides were deposited in the hippocampal formation, highly resembling the A $\beta$  distribution in human AD.<sup>37,38</sup> Another type of old-world monkeys that have been extensively used in this field is the cynomolgus monkey (*Macaca fascicularis*), also known as crab-eating macaques (Table 1).<sup>20</sup> Cynomolgus monkeys have a body length of 40–65 cm, a body weight of up to 9 kg, and a life expectancy of up to 35 years (Table 1).<sup>20</sup> Both diffuse and classical A $\beta$  plaques with dense cores were detected primarily in the temporal cortex of the superior and inferior gyri and amygdala in aged cynomolgus monkeys.<sup>39,40</sup> These A $\beta$  plaques were surrounded by abnormal, swollen neurites in silver-stained sections,<sup>34–36,40</sup> similar to what is reported in human AD.<sup>2</sup> Aged old-world monkeys illustrated similar A $\beta$  plaques in the parenchyma compared to the brains of humans diagnosed with AD. More examinations into the pathologies and behavioural alterations are required to designate them as suitable animal models of AD.

Squirrel monkeys (*Simia sciurea*), a widely used new-world monkey, have a body length of 25–35 cm, a body weight of 0.5–1.1 kg, and life expectancy of 15–20 years (Table 1). The smaller body and shorter life expectancy of aged squirrel monkeys explain the deposition of smaller A $\beta$  plaques in their cerebellum at a relatively younger age ( $\sim 12$  years old) compared with rhesus monkeys ( $\sim 25$  years old).<sup>19,35</sup> Like rhesus monkeys, A $\beta_{1-40}$  is the more abundant peptide in the brains of aged squirrel monkeys, in contrast to human AD.<sup>41,42</sup> C-terminal specific antibodies against A $\beta_{1-40}$  and A $\beta_{1-42}$  were used to evaluate the A $\beta$  burden in the brains of 11 rhesus monkeys (21–31 years) and one 59-year-old chimpanzee.<sup>41</sup> In rhesus monkeys, A $\beta_{1-40}^{+}$  plaques outnumbered A $\beta_{1-42}^{+}$  plaques with a mean ratio of 2.08, which was significantly higher than the ratio of A $\beta_{1-40}$ :A $\beta_{1-42}^{+}$  plaques in human AD (0.37).<sup>41</sup> Similar results were observed in another study using two aged Formosan



rock macaques (*Macaca cyclopis*), which are close relatives to rhesus monkeys.<sup>42</sup> The high A $\beta$ <sub>1-40</sub> burden level in aged NHPs may be caused by different APP processing mechanisms or altered A $\beta$ -ApoE interaction, which favours the production of A $\beta$ <sub>1-40</sub> in aged NHPs.<sup>42</sup> These early studies recognised the age-associated A $\beta$  burden level and widespread distribution in the brains of aged NHPs, which highly resembled human AD despite the distinct levels of A $\beta$ <sub>1-40</sub> and A $\beta$ <sub>1-42</sub>. A wide range of recent studies have all repeated the identification of this classical human AD-resembling A $\beta$  proteopathy in the brains of various NHPs, utilizing more advanced experimental techniques to elucidate the interaction between A $\beta$  plaques, AD genetics, glial activation, and Tau hyperphosphorylation in these spontaneous NHP model of AD.<sup>40,43-52</sup>

The tree shrew is also a small primate used as a NHP model of AD, in particular the Chinese tree shrew (*Tupaia belangeri chinensis*) (Table 1). They have body lengths of 26–41 cm, body weights of 50–270 g, and a life expectancy of 8 years old (Table 1). In one early study, Pawlik and colleagues did not identify A $\beta$  deposits in the neural parenchyma or cerebral vasculature of eight aged tree shrews (7–8 years old).<sup>53</sup> Subsequent studies using anti-A $\beta$ <sub>1-42</sub> antibodies detected A $\beta$  depositions in the cortex, subiculum, basal ganglia, mammillary body, and hypothalamus, accompanied by weak Congo red<sup>+</sup> A $\beta$  plaques in the brains of aged tree shrews.<sup>54</sup>

Another A $\beta$ -related pathology, CAA, may be more consistent than parenchymal A $\beta$  deposits in aged NHPs.<sup>2</sup> Thioflavin-S<sup>+</sup> A $\beta$  plaques in the walls of intracortical and meningeal microvessels of aged rhesus monkeys and aged squirrel monkeys were identified.<sup>34-36</sup> Uno and colleagues conducted a well-powered study using the brains of 81 rhesus monkeys (16–39 years old).<sup>45</sup> Young rhesus monkeys (16–19 years old) did not manifest parenchymal A $\beta$  plaques, while the majority of the aged monkeys (26–39 years old) presented numerous A $\beta$  depositions in their brains.<sup>45</sup> CAA developed simultaneously with parenchymal A $\beta$  plaques after the age of 20 years old, and was detected in 38% of the oldest rhesus monkeys, suggesting a lower frequency of CAA compared with parenchymal A $\beta$  plaques in aged rhesus monkeys.<sup>45</sup> CAA was also observed in other species of aged old-world monkeys.<sup>39,40</sup> In contrast to the relatively low vascular A $\beta$  deposits in aged old-world monkeys, cerebrovascular A $\beta$  is the most abundant form of A $\beta$  proteopathy in squirrel monkeys.<sup>55,56</sup> Three forms of A $\beta$  deposits were identified in nine squirrel monkeys (8–27 years old) from high to low density: dense A $\beta$  deposits to the vascular wall, classical parenchymal A $\beta$  plaques with a dense core, and diffuse A $\beta$  plaques.<sup>55</sup> Among the four aged squirrel monkeys, the ratio of CAA to dense parenchymal A $\beta$  plaques was over 5.<sup>55</sup> Although A $\beta$ <sub>1-42</sub> and A $\beta$ <sub>1-40</sub> were detected in both parenchymal and cerebrovascular plaques, more A $\beta$ <sub>1-40</sub> existed in CAA in the larger arterioles of aged squirrel monkeys.<sup>56</sup> One remarkable difference between humans and squirrel monkeys is the heavy deposition of A $\beta$  in the capillaries, suggesting species-specific predispositions of vulnerable cerebral vasculature to A $\beta$  pathology.

In addition to old and new world monkeys, mouse lemurs (*Microcebus murinus*), a prosimian resembling the earliest primates, have been frequently used to study normal aging of NHPs (Table 1).<sup>2</sup> Mouse lemurs are characterised by a small body length of 12 cm and a tail with a similar length (Table 1).<sup>20,46</sup> They have a small body weight of 50–120 g and a short life expectancy of 8–14 years (Table 1).<sup>20,46</sup> Bons and colleagues first utilised mouse lemurs to study A $\beta$  proteopathies during normal aging of NHPs.<sup>44</sup> They compared eight aged mouse lemurs (8–12 years old) with three young mouse lemurs (1–3 years old), and recognised three forms of A $\beta$  proteopathies in the brains, including round thiofla-

vin-S<sup>+</sup> A $\beta$  plaques, round A $\beta$  plaques with a thioflavin-S<sup>+</sup> dense core, and extensive A $\beta$  deposits in leptomeningeal, cortical arteries and arterioles, and occasionally, capillaries.<sup>44</sup> Only half of the aged mouse lemurs exhibited parenchymal A $\beta$  plaques, whose size resembled those observed in rhesus monkeys and humans. All aged mouse lemurs demonstrated extensive CAA, suggesting a higher frequency of CAA compared with that of human AD.<sup>44</sup> Mestre-Frances and colleagues further investigated the A $\beta$  compositions of CAA in aged NHPs using 30 mouse lemurs (2–13 years old).<sup>57</sup> Intensive deposits of A $\beta$ <sub>1-42</sub> were observed in the cortical arteriole and capillary walls, but A $\beta$ <sub>1-40</sub> deposits were mainly noticed in the tunica media of leptomeningeal vessels, where A $\beta$ <sub>1-42</sub> was weakly detected.<sup>57</sup> This study illustrated a promising NHP model of AD concerning the similarities in A $\beta$  proteopathies compared to human AD, including high parenchymal burden of A $\beta$ <sub>1-42</sub> and high vascular deposition of A $\beta$ <sub>1-40</sub>. Cognitive impairment of the aged mouse lemur is another essential criterion to be assessed. Schmidtke and colleagues recruited 37 aged mouse lemurs (>5 years old) and identified significant associations between cortical A $\beta$  burden level and pretraining success (intraneuronal A $\beta$ ) and discrimination learning (extracellular A $\beta$ ).<sup>51</sup> Even though the accumulation of A $\beta$  in the walls of neocortical vessels were detected, no association between CAA and cognitive decline was found.<sup>51</sup> A $\beta$  proteopathies in the aged mouse lemur were also documented in recent studies, in which the interactions between A $\beta$ , Tau, genetic factors, and immune cells were further elaborated.<sup>43,58</sup>

#### A $\beta$ -associated genetics and proteins in aged NHPs

AD is a complicated disorder determined by both genetic and environmental factors. Both EOAD and LOAD are largely influenced by genetic mutations or single nucleotide polymorphisms (SNP) that result in the overproduction of amyloidogenic A $\beta$ <sub>1-42</sub> and impaired clearance of A $\beta$  peptides. The differences in A $\beta$  proteopathies between aged NHPs and humans with AD inspire another question regarding whether A $\beta$ -associated genetics and proteins are different between humans and NHPs. Full-length cDNA encoding APP<sub>695</sub> of aged cynomolgus monkeys were sequenced, demonstrating 100% sequence homology to human, while two amino acid substitutions were reported in APP<sub>695</sub> of rats and mice.<sup>39</sup> None of the EOAD-associated mutations were found in the lemur APP gene.<sup>46</sup> The common longer isoforms in aged cynomolgus monkeys, APP<sub>751</sub> and APP<sub>770</sub>, demonstrated a few amino acid substitutions compared with human APP.<sup>39</sup> The brain homogenates of humans and monkeys demonstrated a similar profile of membrane-associated, full-length APP, and truncated isoforms of APP, in contrast to the profile of rat and mouse brains, suggesting highly similar proteolytic processing of APP between NHPs and human.<sup>39</sup> APP was also detected in the swollen neurites of classical A $\beta$  plaques but absent in diffuse A $\beta$  plaques in the brain of aged cynomolgus monkeys.<sup>40</sup> In aged rhesus monkeys, APP was detected in swelling neurons and neuritic plaques associated with A $\beta$ .<sup>59</sup> In mouse lemurs, an APP sequence analysis of exon 16 and 17, which encodes for A $\beta$ , illustrated 100% homology with human A $\beta$ , suggesting conserved RNA splicing in mouse lemurs and humans.<sup>58</sup> A $\beta$  and APP were simultaneously detected in A $\beta$  plaques and CAA, while APP itself was further deposited in neurons, astrocytes, and oligodendrocytes.<sup>58</sup> The labelling level of APP was significantly associated with age in mouse lemurs, suggesting a more sophisticated distribution of APP and A $\beta$  proteopathies in aged mouse lemurs.<sup>58</sup> Additionally, the activity of  $\beta$ -secretase (BACE1) was increased with age in both rhesus monkeys and humans, while its expression level remained the same.<sup>60</sup> The genetic



background of the tree shrew has also been investigated and their primary sequences of APP revealed 98% similarity and 97% identity to human APP.<sup>53</sup> A high-quality reference genome of Chinese tree shrews has been recently generated and their expression pattern of A $\beta$  and NFT formation pathway genes resembled that of human brain, with a similar aging-dependent effect.<sup>61,62</sup> Both genetic sequences and distributive patterns of APP and A $\beta$  are highly conserved between multiple species of NHPs and human, making them ideal models of AD with higher genetic homology.

EOAD-associated PSEN1 and PSEN2 have also been investigated in NHPs. The cDNA encoding PSEN1 from mouse lemurs exhibited 95.3% sequence similarity with human PSEN1, which was slightly higher than murine PSEN1.<sup>63</sup> The 2% difference between lemur and mouse PSEN1 showed the conservation of a particular proteolytic processing in both lemur and human.<sup>63</sup> PSEN1 was detected in neurons and neurites in multiple cortical layers, hippocampus, and subcortical structures in aged mouse lemurs.<sup>63</sup> Another study specifically cloned a 1340 bp cDNA fragment encoding PSEN2 from a mouse lemur brain that demonstrated 95.5% homology to human PSEN2 and 93.5% homology to mouse PSEN2.<sup>64</sup> None of the EOAD-associated PSEN1 or PSEN2 mutations in humans corresponded to lemur PSEN1 and PSEN2 amino acid differences.<sup>46</sup> PSEN2 was distributed throughout the lemur brain, including dense signals in the cortical and subcortical structures and cerebral vessels, and light signals in the hippocampal neurons and the dentate gyrus.<sup>64</sup> The co-localisation of PSEN1, PSEN2, and APP was observed, but only age-related increase in PSEN2 expression was noticed in the lemur brain.<sup>63,64</sup> Lemur APP, PSEN1, and PSEN2 showed higher homology to human proteins than those of rats and mice, suggesting a higher degree of conservation between lemurs and humans. Furthermore, the age-related expressions of PSEN1 and PSEN2 were also investigated in the brain of cynomolgus monkeys. PSEN1 was detected in neurons and neuritic plaques in the neocortex and cerebellum of cynomolgus monkeys and PSEN1 levels in the nuclear fraction were significantly elevated with age, indicating age-related PSEN1 accumulation in the endoplasmic reticulum associated with the nuclear membrane.<sup>65</sup> On the contrary, PSEN2 was also detected in large pyramidal neurons and neuritic plaques, but its expression level remained unchanged during aging of cynomolgus monkeys.<sup>66</sup> Recently, PSEN2 mRNA in the Chinese tree shrew has been characterised, demonstrating 97.64% sequence similarity to human PSEN2.<sup>67</sup> Even though the protein structure of PSEN2 indicates similarities to human PSEN2, tree shrew PSEN2 possesses only seven  $\alpha$ -helices, while human PSEN2 contains ten  $\alpha$ -helices.<sup>67</sup> These observations suggest a more important involvement of PSEN1 compared with PSEN2 in disease progression of NHPs, but more studies are needed to elucidate their roles and functions in NHP compared with those of humans.

Beyond EOAD-associated genetics, APOE remains the single largest genetic risk factor for AD in humans. In mouse lemurs, APOE genotyping revealed monomorphisms that possessed the two diagnostic sites that defined the ApoE  $\epsilon$ 4 allele of human, albeit with 9 amino acid substitutions compared with human ApoE.<sup>68</sup> One type of vervet monkey, the *Caribbean vervet*, was also found to be homozygous for the ApoE  $\epsilon$ 4 allele.<sup>69</sup> APOE was heavily deposited in line with A $\beta$  proteopathies, including the parenchymal A $\beta$  plaques and CAA.<sup>68</sup> APOE was further detected in astrocytes of the cortical parenchyma, oligodendrocytes of the corpus callosum, and neurons of multiple cortical lobes, the hippocampus, and the brainstem of the aged mouse lemur.<sup>68</sup> Like mouse lemurs and humans, APOE was detected in diffuse and classical A $\beta$  plaques

and meningeal and cortical vessels in the brains of aged chimpanzees, cynomolgus monkeys, and rhesus monkeys, while old-world monkeys exhibited more neuritic plaques with APOE staining.<sup>40,70</sup> In cynomolgus monkeys, APOE was detected in some astrocytes and mononuclear cells around cortical blood vessels, co-localising with glial fibrillary acidic protein (GFAP) in astrocytes.<sup>40</sup> Additionally, APOE genetics were also studied in aged vervet monkeys (*Chlorocebus aethiops*), illustrating ApoE  $\epsilon$ 4 monomorphism among 30 vervet monkeys.<sup>69</sup> In brief, NHPs are homozygous for ApoE  $\epsilon$ 4 that is highly detrimental in human AD. This interesting discrepancy between NHPs and humans makes it necessary to understand the protective mechanism underlying why these ApoE  $\epsilon$ 4 homozygotes display dense parenchymal and vascular A $\beta$  plaques, but never develop the devastating cognitive decline and behavioural alterations observed in humans diagnosed with AD.

### *Tau pathologies in aged NHPs*

Unlike human AD, NFTs are virtually lacking in the brains of aged NHPs.<sup>2</sup> Only a few old-world monkeys, new-world monkeys, and prosimians illustrated NFTs and dystrophic neurites near neuritic plaques in early studies.<sup>2</sup> In aged rhesus monkeys (30–31 years old) with cerebral A $\beta$  plaques, PHF<sup>+</sup> or Tau<sup>+</sup> NFTs or A $\beta$  plaques were absent in their brains using antiserum while this same antiserum generated intensive signals in the brains of human with AD.<sup>34</sup> In a recent study, the monoclonal antibody (mAb), AT8, against a phosphorylated epitope of human Tau protein detected sparsely scattered p-Tau in the cingulate cortex in the brains of aged old-world monkeys, including Campbell's guenon and Hamadryas baboon.<sup>71</sup> AT8<sup>+</sup> p-Tau was detected in the entorhinal cortex and hippocampus of one 28-year-old rhesus monkey, which was simultaneously confirmed using AT100, PHF-1, and TG-3 antibodies, illustrating a similar distribution pattern to Tauopathy in the brains of human with AD.<sup>71</sup> Meanwhile, another five 28-year-old rhesus monkeys exhibited high A $\beta$  burdens in their prefrontal cortices but no Tau AT8 immunoreactivity, suggesting rare p-Tau immunoreactivity in aged rhesus monkeys around 30 years.<sup>71</sup> Even though rhesus monkeys exhibit human AD-resembling A $\beta$  depositions and glial activation, the low incidence of Tauopathy during their normal aging may restrict their suitability as a NHP model of AD. In 2018, a cohort of rhesus monkeys from young to extreme old age ( $\leq$ 38 years old) illustrated similar qualitative patterns and sequences of Tau and A $\beta$ , highly resembling human AD.<sup>49</sup> P-Tau was initially detected in cell islands, dendritic microtubules, and transporting endosomes of the entorhinal cortex in young rhesus monkeys (7–9 years old) (like Braak stage I).<sup>49</sup> In early aged rhesus monkeys (24–26 years old), AT8 immunoreactivity was mildly detected in the outer layer II of the entorhinal cortex with one case illustrating cognitive impairment (like Braak stage I/II).<sup>49</sup> In aged rhesus monkeys (33–34 years old), AT8 labelling further propagated intensively and widely throughout cell islands of the layer II and occasionally in the deeper entorhinal cortex (like Braak stage III).<sup>49</sup> Surprisingly, mature NFTs were recognised in both layer II and V of the entorhinal cortex in the oldest rhesus monkey (38 years old) (like Braak III/IV).<sup>49</sup> Given the co-existence of parenchymal A $\beta$  plaques, CAA, and intracellular A $\beta$  in endosomes, dendrites, and exons, this study first demonstrated human AD-resembling Tauopathies, especially NFTs, in extremely aged NHPs, although the low incidence was distinct from that of human AD.<sup>49</sup> Subsequently, a cohort of nine female rhesus monkeys (8.3–28.6 years old) demonstrated pyramidal cells labelled with AT8 and pT217 antibodies in the dorsolateral prefrontal cortex, which are currently used in CSF diagnosis of human AD.<sup>72</sup> These pT217<sup>+</sup>

pyramidal cells contained aggregated, filamentous structures that highly resembled NFTs in human AD.<sup>72</sup> While early studies hardly ever detected Tau signals in aged rhesus monkeys, recent studies have demonstrated that rhesus monkeys can naturally develop p-Tau, filamentous structures, and rare NFTs, suggesting a promising NHP model of AD that assist in elucidating the associations between A $\beta$ , p-Tau, and cognitive deficits in AD.

PHF- and Tau-specific antibodies did not detect any NFTs or neuritic plaques in the brains of aged cynomolgus monkeys (19 years old) and aged chimpanzees (59 years old) in early studies.<sup>39,40,70</sup> Of note, very limited numbers of neurons in the lateral putamen region of three aged chimpanzees were slightly labelled with Alz-50 (against p-Tau).<sup>70</sup> In 2010, a cohort of 24 cynomolgus monkeys (6–36 years old) were found to have A $\beta$  plaques in their neocortical and hippocampal regions in middle age, which was associated with age rather than p-Tau accumulation.<sup>47</sup> Intracellular p-Tau was first detected in neurons and oligodendrocytes in the temporal cortex and hippocampus of cynomolgus monkeys in a 19-year-old cynomolgus monkey using 2B11 (against human Tau phosphorylated at amino acid 231).<sup>47</sup> In humans over 20 years of age, 2B11<sup>+</sup> glial cells increased proportionally with age, but 2B11<sup>+</sup> neurons were only detected in a 36-year-old cynomolgus monkey, in which a strong p-Tau signal was occasionally detected in neurons, oligodendrocytes, and dystrophic neurites in its temporal cortex.<sup>47</sup> Interestingly, the number of 2B11<sup>+</sup> neurons in this 30-year-old monkey was smaller than that of the 19-year-old monkey, which might be explained by a specific conformational change of Tau under pathological conditions by an unknown mechanism.<sup>47</sup> Later, another 21 brains of cynomolgus monkeys (7–36 years old) were studied for A $\beta$  and Tau proteopathies.<sup>52</sup> A $\beta$  plaques were detected in eight brains of monkeys at 24 years old, while p-Tau deposits were found in only five brains from monkeys over 30 years old, suggesting a similar sequence of AD-associated lesions to humans with AD.<sup>52</sup> AT8<sup>+</sup> p-Tau lesions were distributed predominantly in oligodendrocyte-like cells throughout the white matter and basal ganglia, which was different from p-Tau patterns in human with AD, mainly in the hippocampus.<sup>52</sup> Only 4R Tau was detected with AT8 immunoreactivity, which was diffuse and granular in the neuronal cytoplasm and dendrites, instead of NFT organisations.<sup>52</sup> In old-world monkeys, the co-existence of A $\beta$  and Tau proteopathies were detected in normal aging, during which human AD-resembling A $\beta$  plaques and CAA were deposited earlier, while human AD-resembling NFTs were rarely detected. The classical amyloid theory states that neurotoxic A $\beta$  peptides induce subsequent Tau phosphorylation, NFT accumulation, glial activation, and neuronal death, as demonstrated by close associations between A $\beta$  and p-Tau lesions in the brains of human with AD. Therefore, at least in old-world monkeys, the accumulation of p-Tau and, occasionally NFTs, merely reflected the age-dependent hyperphosphorylation and aggregation of Tau induced by A $\beta$ .<sup>47</sup>

Tau and p-Tau in mouse lemurs have been well investigated in many studies while NFTs are rarely observed.<sup>68,73</sup> In early studies, Tau deposits in mouse lemurs were morphologically and biochemically different from NFTs observed in humans with AD, similarly to those in old-world monkeys.<sup>74</sup> A well-powered quantitative analysis of Tau recruited 40 mouse lemurs (1–13 years old).<sup>74</sup> By using 961-S28T, Tau accumulations (maybe PHF) were found in the frontal cortex, the occipital cortex, and the parietal and temporal cortices, the prevalence, and densities of which were associated with age in both young and old groups.<sup>74</sup> Quantitatively, aged mouse lemurs ( $\geq 8$  years old) exhibited significantly higher Tau burdens than the young in all neocortical areas, subiculum, and

amygdala, while the entorhinal cortex, subiculum, and amygdala were affected by Tau in the aged group exclusively.<sup>74</sup> In contrast to Tau distribution in mouse lemurs, the frontal cortex usually exhibited low NFT burden, while hippocampal formation was predisposed to Tauopathy in the brains of human with AD.<sup>12</sup> These contradictions suggest a different neuronal vulnerability to Tauopathy in the neocortex of mouse lemurs and humans.<sup>74</sup> More specifically, Tau proteins were modified and aggregated in granules close to the membrane of the neuronal perikaryal and dendrites in the aged mouse lemur.<sup>46</sup> Aggregated p-Tau reactive to PHF antibodies were detected with A $\beta$  and ApoE in neurons and oligodendrocytes in the neocortex and hippocampus, as well as vascular A $\beta$  depositions.<sup>46,68</sup> Co-localisation of p-Tau and PSEN2 was occasionally noticed in some neurons of the frontal, parietal, and occipital cortices.<sup>64</sup> Compared with old-world monkeys and new-world monkeys, mouse lemurs exhibit more consistent Tau, p-Tau, and A $\beta$  depositions during aging, but rarely develop severe PHFs or NFTs.

In addition to rhesus monkeys, cynomolgus monkeys, and mouse lemurs, p-Tau was briefly studied in vervet monkeys, common marmosets, and tree shrews. A cohort of nine middle-aged vervet monkeys (11.2 years old in average) and nine aged vervet monkeys (21.7 years old in average) all exhibited A $\beta$  and Tau proteopathies in their brains.<sup>75</sup> A $\beta$  plaques were detected throughout the cortex in all aged vervets and in one middle-aged vervet, resembling early Braak staging in AD.<sup>75</sup> Intracellular PHF<sup>+</sup> p-Tau was detected in small cells with granular morphology in all monkeys, but NFTs were rarely observed.<sup>75</sup> Interestingly, higher levels of PHF<sup>+</sup> p-Tau was associated with slower gait speed, suggesting poorer integration of complex cognitive and motor processes and potential cognitive deficits.<sup>75</sup> Brain atrophy was associated with both the level of p-Tau in parenchyma and the level of Tau phosphorylated at threonine 181 (p-Tau181P).<sup>75</sup> This study demonstrated widespread A $\beta$  depositions, limited p-Tau aggregation, Tau-associated cognitive decline, and potential brain atrophy during the natural aging of vervet monkeys. Although none of these features meet the severity level observed in human AD, vervet monkeys may be a good NHP model recapitulating most cardinal features of AD. The common marmoset (*Callithrix jacchus*) is becoming an increasingly popular NHP model of AD due to its small body size (10–12 cm), small body weight (80–100 g), multiple births, and short life span (7–17 years).<sup>20</sup> Among male marmosets (1.6–18 years old), p-Tau was detected in their medial temporal areas and parietal cortices, and the level of Tau phosphorylated at threonine 231 (p-Tau231P) was positively associated with age.<sup>76</sup> By using Alz50, early fibrillary aggregation of p-Tau was detected in cytoplasmic compartments of neurons and glia-like cells in adolescent and aged marmosets.<sup>76</sup> Aged marmosets presented fewer active microglia but more dystrophic microglia in the dentate gyrus.<sup>76</sup> Hyperphosphorylation and conformational changes to Tau were exclusively detected in the dystrophic microglia.<sup>76</sup> Although extensive NFTs are not observed in marmosets, they still seem to be a valuable NHP model that demonstrates some features of human AD. Lastly, only one very recent study demonstrated Tau hyperphosphorylation in aged tree shrews, including adult tree shrews (3.8 years old in average) and aged tree shrews (6–7.5 years old).<sup>77</sup> As assessed by AT100, Tau hyperphosphorylation was significantly elevated in the dentate gyrus, the CA3 hippocampal region, and the subcortical structures of aged tree shrews in the absence of NFTs.<sup>77</sup> These aged tree shrews carried a higher number of IBA1<sup>+</sup> active microglia containing ferritin as well as microglia with a dystrophic phenotype.<sup>77</sup> Although not widely studied, tree shrews presented similar parenchymal A $\beta$  plaques, vascular A $\beta$  depositions,

Tau hyperphosphorylation, and microglial activation compared to human AD, indicating its potential suitability as a NHP model for translational research in AD.

### **Brain atrophy/neurodegeneration in aged NHPs**

The brains of naturally aging NHPs resemble human AD in many aspects, but the macroscopic feature of human AD, brain atrophy, is inconsistently observed. Using an optical fractionator technique, a preservation of neurons was observed in the subiculum, entorhinal cortex layer II, CA1, CA2, CA3, hilus, and the dentate gyrus of the hippocampal formation in aged rhesus monkeys.<sup>78,79</sup> In mouse lemurs, 20% of the elderly ( $\geq 5$  years old) demonstrated neurodegeneration.<sup>46</sup> Remarkable brain atrophy was observed in the cortex, corpus callosum, fornix, hippocampus, septum, thalamus, hypothalamus, basal ganglia, brainstem, and cerebellum, accompanied with ventricle dilatation, intensive parenchymal A $\beta$  plaques, and neurons with p-Tau.<sup>43,46</sup> Very recently, the number of neurons in CA1 and CA3 hippocampal subfields of chimpanzees were found to be negatively associated with advanced aging but not with AD pathologies.<sup>80</sup> In vervet monkeys, their cortical grey matter volume and temporal-parietal cortical thickness was negatively associated with age, potentially increasing the risk of cognitive decline.<sup>81</sup> In general, naturally aging NHPs demonstrate human-AD resembling proteopathies, glial activation, but severe brain atrophy and cognitive decline is rarely observed, striking our interest into the protective mechanism preventing severe demented symptoms from occurring.

### **Advantages and disadvantages of spontaneous NHP model of AD**

This chapter has elaborated the past and current findings of human AD-resembling pathologies in aged NHPs, including rhesus monkeys, cynomolgus monkeys, squirrel monkeys, and mouse lemurs (Table 2). Although species-to-species differences do exist, these species of NHPs demonstrate extensive A $\beta$  depositions in parenchyma and cerebral vessels, some degree of Tau and p-Tau depositions in parenchyma, rare intraneuronal accumulation of NFTs, glial cell activation, lemur-restricted brain atrophy, and mild cognitive deficits. Compared with other animal models of AD, naturally aging NHPs display high similarity to human AD because of their close phylogenetic relationship with humans, similar neuroanatomy, comparable genetics, and greater complexity in high-order cognitive functions.<sup>2,19</sup> Therefore, aging NHPs can be regarded as a promising model resembling AD that would improve our understanding of age-related cognitive impairment, disease-causing mechanisms, molecular and cellular interactions, and gene-environment interactions, further facilitating the development of diagnostic techniques and therapeutic innovations. Nevertheless, spontaneous NHP models of AD carry a few major limitations. Firstly, although naturally aging NHPs spontaneously demonstrate A $\beta$  proteopathies, they rarely exhibit AD-like NFTs or brain atrophy, suggesting some difficulty in using aged NHPs to analyse the interaction between A $\beta$ , Tau, and neuronal death. Secondly, cognitive deficits and executive function impairments in aged NHPs are much milder than those in human AD, which may be an obstacle to assess the performance of novel therapeutic treatments. It is interesting to study their protective mechanisms against severe NFTs, brain atrophy, and cognitive decline, while they display severe A $\beta$  proteopathies and ApoE  $\epsilon 4$  homozygosity. Lastly, NHPs usually have a long-life expectancy, compared with rodent models of AD, suggesting a longer inoculation period before AD-resembling symptoms thus adding to already high costs.

These disadvantages limit the broad use of naturally aging NHPs as spontaneous AD models.<sup>20</sup>

### **Induced NHP models of AD**

#### **A $\beta$ oligomer (A $\beta$ o)-induced NHP models of AD**

To overcome the disadvantages of spontaneous NHP models of AD, researchers injected A $\beta$  oligomers or fibrils into the brains of rhesus monkeys and cynomolgus monkeys, to establish an induced NHP model of AD. Synthetic soluble A $\beta$  peptides were first injected into multiple neocortical sites of rhesus monkeys (4–5 years old), but no AD-resembling cellular changes were noticed, although this may be caused by the short inoculation time or the solubility of the A $\beta$ .<sup>82,83</sup> The microinjection of plaque-equivalent A $\beta_{1-40}$  and A $\beta_{1-42}$  fibrils into the cerebral cortex of aged rhesus monkeys (25–28 years) resulted in diffuse A $\beta$  depositions with dense cores, clusters of dystrophic neurites, profound neuronal loss, intensive Tau phosphorylation, and microglia proliferation surrounding the injection sites.<sup>84</sup> These AD-resembling pathological alterations are associated with age as fibrillar A $\beta$  injection into young rhesus monkeys (5 years old) caused milder alterations.<sup>84</sup> In 2010, an induced NHP model of AD was established in middle aged rhesus monkeys (16–17 years old) via intracranial injection of A $\beta_{1-42}$  and thiorphan, which inhibited A $\beta$  clearance.<sup>85</sup> A $\beta_{1-42}$ /thiorphan-treated NHPs exhibited more significant intracellular A $\beta_{1-42}$  accumulation, cholinergic neuronal loss and atrophy, and microglia and astrocyte infiltration into the basal ganglia, cortex, and hippocampus of rhesus monkeys, compared with control monkeys.<sup>85</sup> However, they failed to show working memory deficits in DR tasks, possibly due to a short inoculation time of seven weeks.<sup>85</sup> Very recently, Beckman and colleagues conducted a more comprehensive study. A $\beta$ o was infused into the lateral ventricles of four female rhesus monkeys to compare with another two monkeys injected with scrambled A $\beta$  peptides and three age-matched female controls (11–19 years old).<sup>86</sup> Repeated A $\beta$ o injections resulted in A $\beta$  depositions near the pyramidal neurons in the dorsolateral prefrontal cortex and reductions in spine density in the apical and basal dendrites in A $\beta$ o-treated NHPs exclusively, indicating A $\beta$ o-induced interrupted synaptic integrity.<sup>86</sup> The volume of microglia in A $\beta$ o-treated monkeys were enlarged in the dorsolateral prefrontal cortices, in which active engulfment of synaptic markers by these microglia were noticed.<sup>86</sup> In the dentate gyrus of A $\beta$ o-treated monkeys, an increased number of rounded, amoeboid, and IBA-1<sup>+</sup> microglia were noted, suggesting altered innate immune responses induced by A $\beta$  oligomers.<sup>86</sup> TNF- $\alpha$  levels in cerebrospinal fluid (CSF) were also elevated in A $\beta$ o-treated monkeys that were associated with an increase in microglial activation in the dorsolateral prefrontal cortex, but no there were no detectable changes in Tau phosphorylation and neurofilament light levels.<sup>86</sup> In these studies, both soluble and insoluble A $\beta$ o or fibrils were used to establish the induced NHP models of AD and the administration of insoluble A $\beta$  fibrils is more likely to generate Tau phosphorylation and neuronal atrophy in rhesus monkeys, which better replicates the pathogenesis observed in human AD cases. Only one study examined memory deficits after A $\beta$ o injection and no deterioration in working memory was seen. In future studies, a longer injection period of A $\beta$ o, a longer inoculation period, and more cognitive examinations are expected to validate whether A $\beta$ o-treated rhesus monkeys can be used as an appropriate NHP model of AD.<sup>87</sup>

Unlike the extensive investigations into rhesus monkeys, the investigations into induced models of AD using cynomolgus

Table 2. Spontaneous (naturally aging) and induced NHP models of AD

Model types	Rhesus macaques	Cynomolgus monkeys	Squirrel monkeys	Mouse lemurs	Tree shrews
Spontaneous model					
A $\beta$ plaques	AD-resembling burden level and distribution of A $\beta$ plaques; more A $\beta$ <sub>1-40</sub> than A $\beta$ <sub>1-42</sub>	More A $\beta$ <sub>1-40</sub> than A $\beta$ <sub>1-42</sub> ; smaller A $\beta$ plaques compared with human	More A $\beta$ <sub>1-40</sub> than A $\beta$ <sub>1-42</sub>	More A $\beta$ <sub>1-42</sub> than A $\beta$ <sub>1-40</sub> in A $\beta$ plaques	Inconsistent results
CAA	Lower CAA burden than A $\beta$ plaques		Higher CAA burden than A $\beta$ plaques	Extensive CAA with high A $\beta$ <sub>1-40</sub>	Inconsistent results
Tauopathy	Rare AT8 <sup>+</sup> p-Tau; NFTs in the oldest old	rare AT8 <sup>+</sup> p-Tau in the oldest old	–	Age-associated p-Tau accumulations	Rare p-Tau
Neuronal death	–	–	–	20% of elderly demonstrated brain atrophy	–
Genetics (compared to human)	APOE $\epsilon$ 4 monomorphism	identical APP <sub>695</sub> ; similar APP <sub>751</sub> & APP <sub>700</sub> ; APOE $\epsilon$ 4 monomorphism	–	Identical APP exon 16 & 17; similar PSEN1 & PSEN2; APOE $\epsilon$ 4 monomorphism	Similar APP & PSEN2; APOE $\epsilon$ 4 monomorphism
Induced model					
A $\beta$ o-induced	A $\beta$ , glial activation, p-Tau, memory deficits	A $\beta$ , p-Tau, NFTs, glial activation, brain atrophy	–	–	A $\beta$ , NFTs, brain atrophy, cognitive deficits
AD brain homogenate-induced	–	–	–	A $\beta$ , p-Tau, NFTs, brain atrophy, memory and learning deficits	A $\beta$ , p-Tau
STZ-induced	–	A $\beta$ , p-Tau, glial activation, brain atrophy	–	–	–
FA-induced	Memory decline, A $\beta$ , p-Tau, glial activation, p-Tau	–	–	–	–

AD, Alzheimer's disease; APOE, apolipoprotein E; APOE, apolipoprotein E; APP, amyloid precursor protein; CAA, cerebral amyloid angiopathy; NFT, neurofibrillary tangles; NHP, non-human primate; PSEN1, presenilin 1; PSEN2, presenilin 2.



monkeys only began in the past ten years. A well-known study conducted by Forny-Germano and colleagues injected synthetic A $\beta_{1-42}$  oligomers into the brains of four female cynomolgus monkeys compared with three sham animals.<sup>88</sup> The monkeys were younger than expected to naturally develop AD-resembling pathologies and symptoms.<sup>88</sup> The intracerebroventricular administration of A $\beta$  (ICV-A $\beta$ ) resulted in dense A $\beta$  accumulation in the entorhinal cortex, hippocampus (dentate gyrus), striatum, and amygdala, but little A $\beta$  accumulation in the midbrain or cerebellum.<sup>88</sup> Of note, whether A $\beta$  distribution was caused by the diffusion of solution or the propagation of disease-causing mechanism remains unknown.<sup>89</sup> Tau hyperphosphorylation at serine residue 396, an AD-specific epitope, was also induced in all regions with A $\beta$  accumulation in the brains of ICV-A $\beta$ -treated monkeys. Compared with sham-operated monkeys, Tau phosphorylation in ICV-A $\beta$ -treated monkeys was significantly higher.<sup>88</sup> The detection of high molecular mass p-Tau (>180 kDa) and low molecular mass p-Tau (<20 kDa) suggested Tau aggregates or oligomers, and truncated small Tau fragments in NFTs, respectively.<sup>88</sup> P-Tau, characterised by early phosphorylation markers, was detected in the brains of ICV-A $\beta$ -treated monkeys, as stained using AT100 and CP13 antibodies that recognised Tau phosphorylated at serine residue 212 and threonine residue 214, and at serine residue 202, respectively.<sup>88</sup> NFTs were also investigated using thioflavin-S staining, Alz59, and PHF-1, and their positive signals were detected in the neocortex of ICV-A $\beta$ -treated monkeys, resembling the distribution pattern of Tau tangles in human AD.<sup>88</sup> Regarding glial activation, a higher number of GFAP<sup>+</sup> astrocytes and IBA-1<sup>+</sup> microglia were noted in the frontal cortex, hippocampus, and amygdala of ICV-A $\beta$ -treated monkeys compared with those of sham monkeys.<sup>88</sup> Furthermore, synapse numbers, presynaptic and postsynaptic proteins, and synaptic puncta numbers were all decreased in ICV-A $\beta$ -treated monkeys, compared with controls, while A $\beta$ -induced apoptosis was not observed.<sup>88</sup> In brief, this study successfully demonstrated an ICV-A $\beta$ -induced NHP model of AD that recapitulated cardinal neuropathologies of AD except brain atrophy and behavioural alterations (behavioural alterations were not assessed in this study). The efficiency of this model is remarkable because cynomolgus monkeys only received one A $\beta$  injection every three days for up to 24 days and they were sedated only one week after treatment.<sup>88</sup> If experimenters allowed more time for inoculation, brain atrophy, learning decline, memory deficits, and behavioural alterations may be observed, alerting future studies to investigate NHP in a more comprehensive way. In 2021, a new injection method was proposed: bilateral injection of soluble A $\beta$  into the cerebral parenchyma of seven cynomolgus monkeys (~20 years old).<sup>90</sup> The authors prolonged the injection process into four injections over five months, followed by an eight-month inoculation before examination.<sup>90</sup> Using 6E10, 4G8, silver, thioflavin-S, and Congo Red staining, A $\beta$  plaques were found throughout the grey matter of limbic structures and the association cortex, accompanied by dense cores, in A $\beta$ -treated monkeys.<sup>90</sup> Intracellular NFTs reactive with AT8 and AT100 were also detected in neurons and astrocytes, and their morphological features resembled those observed in human AD, illustrating the co-existence of A $\beta$  and Tau proteopathies exclusively in A $\beta$ -treated monkeys.<sup>90</sup> Astrocytic and microglial activation surrounding A $\beta$  plaques were also noted, in which the inflammasome/caspase-1 signal was also activated and associated with A $\beta$  and Tau lesions.<sup>90</sup> Most importantly, the signals of neurodegeneration and the expressions of necroptotic cell death markers were detected in A $\beta$ -treated monkeys, while the density and intensity of presynaptic markers and the number of

basal forebrain cholinergic neurons were reduced.<sup>90</sup> In this study, the elevation of A $\beta$  dosage, injection period, and inoculation procedures resulted in potential neuronal loss and brain atrophy in A $\beta$ -treated monkeys, in addition to those cardinal AD features previously established in the Forny-Germano study. These two well-designed studies used ICV and intraparenchymal delivery methods of synthetic A $\beta$  and presented comprehensive characterisations of cynomolgus monkeys as the induced-NHP models of AD, including AD proteopathies, innate immune activation, indicative neuronal loss, and potential brain atrophy. They provided novel insights into future studies using increasing dosages, injections, and inoculation times are necessary to visualise Tau pathology and further increase the possibility of observing brain atrophy and behavioural alterations in NHPs.

Both ICV and intrathecal administration of A $\beta$  (IT-A $\beta$ ) into the brains of vervet monkeys has been reported to build an induced vervet model of AD.<sup>91</sup> Vervet monkeys received IT-A $\beta$  1–3 times a week for four weeks and were terminated at 1, 4, or 12 weeks after the last dose.<sup>91</sup> ICV-A $\beta$ -treated vervets exhibited higher levels of p-Tau, but all other AD-related pathologies were not assessed.<sup>91</sup> IT-A $\beta$ -treated vervets also demonstrated more intensive p-Tau signal as granular cytoplasmic staining in the perikaryal, fibres in the hippocampus, the dentate gyrus, the entorhinal cortex, and the subiculum.<sup>91</sup> 6E10<sup>+</sup> diffuse A $\beta$  depositions, IBA-1<sup>+</sup> microglia, and GFAP<sup>+</sup> astrocytes were all increased in IT-A $\beta$ -treated vervets compared with vehicle-treated vervets.<sup>91</sup> Most strikingly, significant reductions in hippocampal volumes were observed in IT-A $\beta$ -treated vervets that were terminated at four weeks after A $\beta$  administration, suggesting an acute, visible brain atrophy that was rarely observed in either spontaneous or induced NHP model of AD.<sup>91</sup> However, this study did not assess the biological components and conformational alterations of proteopathies, the morphological changes or activation of microglia and astrocytes, the pro-inflammatory profile in the vervet brain, and, most importantly, the behavioural alterations after IT-A $\beta$  injections.

In a study of tree shrews, 12 adult males were administered ICV-A $\beta$  (A $\beta_{1-40}$  peptides) and compared against six controls, followed by four-week inoculation period before brain imaging, histochemical examinations, and genetic analyses.<sup>92</sup> As expected, A $\beta$  burden, neuritic plaques, and NFTs were detected exclusively in the brains of ICV-A $\beta$ -treated tree shrews.<sup>92</sup> At four weeks post-injection, the hippocampal areas, the thickness of cells and the size of cells in the CA3 and the dentate gyrus of the ICV-A $\beta$ -treated tree shrews were significantly reduced, compared with untreated tree shrews.<sup>92</sup> The apoptosis assay further revealed an increased number of TUNEL<sup>+</sup> cells in the hippocampus, particularly in the dentate gyrus, of the ICV-A $\beta$ -treated tree shrews exclusively, indicating hippocampal atrophy.<sup>92</sup> ICV-A $\beta$ -treated tree shrews spent more time finding food at four weeks post-injection, reflecting altered hippocampal functions.<sup>92</sup> This study first screened differentially expressed genes between ICV-A $\beta$ -treated and control tree shrews at four weeks post-injection and identified downregulated BCL-2/BCL-XL-associated death promoter, inhibitor of apoptosis protein, and cytochrome C, as well as upregulated tumour necrosis factor receptor 1 in AD pathways.<sup>92</sup> These apoptosis-related gene alterations may explain brain atrophy in ICV-A $\beta$ -treated tree shrews. This study established an ICV-A $\beta$ -induced NHP model of AD that comprehensively examined AD proteopathies, brain atrophy, glial activation, and cognitive functions. The genetic analyses further elucidated the potential underlying mechanisms of brain atrophy. Strong evidence supports the idea that A $\beta$ -induced tree shrews can be a good NHP model of AD, but more sophisticated



examinations of their behavioural alterations are needed.

Collectively, injecting ICV-A $\beta$  and IT-A $\beta$  into the brains of NHPs can be efficient at inducing an NHP model of AD that recapitulates most of the cardinal features of human AD. It is beneficial for the study of A $\beta$ -associated consequences, particularly given the central role of A $\beta$  in AD pathogenesis. However, high doses of A $\beta$ , the precision of the surgery, and extensive inoculation time all make it challenging and expensive to build a stable A $\beta$ -induced NHP model of AD.<sup>20</sup> A significant gap in knowledge shared by most of the current studies is the lack of behavioural assessments due to incomplete study design or short inoculation period before termination that may limit the manifestation of any cognitive changes. Future studies are necessary to prolong the injection period and inoculation period, and allow for the incorporation of behavioural assessments that evaluate the suitability of A $\beta$ -induced NHP model of AD.

### ***Brain homogenate-induced NHP models of AD***

The concept of a NHP model of AD induced by intracerebral injection of affected brain material has also been proposed. A total of 33 marmosets received an intracerebral injection of cerebral homogenates that were sourced from patients diagnosed with AD, other types of dementia, or myocardial infarctions as a control.<sup>93</sup> These marmosets were terminated once they showed neurological signs or survived 4.5–6.5 years if they did not manifest behavioural abnormality.<sup>93</sup> Among the AD brain homogenate-treated marmosets (6–7 years old), widespread A $\beta$  plaques, dystrophic neurites, and CAA were observed, but no NFTs or brain atrophy were detected.<sup>93</sup> Similar results were obtained in later studies, demonstrating that A $\beta$  or other associated factors can initiate and accelerate A $\beta$  deposition in parenchyma and cerebral vessels in marmosets but may not induce Tau pathology, glial activation, or neuronal death.<sup>94,95</sup> Moreover, 12 mouse lemurs were bilaterally inoculated with brain extracts from patients with AD, leading to widespread A $\beta$  and Tau proteopathies after 21-month inoculation period.<sup>96</sup> In AD brain homogenate-treated lemurs, diffuse A $\beta$  plaques, classical A $\beta$  plaques, and CAA were detected throughout the brain, accompanied by Tau proteopathy stained by AT8, AT100, and anti-pS422 antibodies.<sup>96</sup> AT8<sup>+</sup> NFTs or NFT-resembling p-Tau accumulations were localised around the inoculation sites (posterior cingulate cortex) along with the hippocampal and temporal areas.<sup>96</sup> This study successfully observed slight brain atrophy in the posterior cingulate cortex of AD-inoculated lemurs at 0–4 months and 9–15 months post-inoculation.<sup>96</sup> Simultaneously, AD brain homogenate-treated lemurs exhibited impaired learning abilities and impaired long-term memory performance compared with control lemurs, although their motor function remained intact.<sup>96</sup> For the first time in primates, this study demonstrated a comprehensive NHP model of AD that recapitulated major AD-associated proteopathies along with cognitive deficits and brain atrophy, highlighting the importance of long inoculation periods in experimental design. Of note, the severity of NFTs, brain atrophy, and behavioural abnormalities are still milder in AD brain homogenate-treated lemurs compared with humans diagnosed with AD.

### ***Streptozotocin (STZ)-induced NHP models of AD***

STZ is a glucosamine-nitrosourea compound with a molecular weight of 265 Da, which was originally identified as an antibiotic with antimicrobial and antitumour effects.<sup>20,97</sup> The ICV injection of STZ (ICV-STZ) disrupts the phosphorylation of insulin receptors and blocks the insulin signalling pathway, leading to cholinergic impairments in the nervous system and compromised cog-

nition and memory, mimicking the insulin resistant brain state in human AD.<sup>20</sup> ICV-STZ and intraperitoneal injections of STZ can further degrade enzymes responsible for A $\beta$  clearance, promote A $\beta$  and Tau aggregation, glucose hypometabolism, oxidative stresses, and neurodegeneration.<sup>20,97</sup> STZ has been previously injected into transgenic mice to build animal models of AD, suggesting their potential use in inducing NHP models of AD.<sup>97</sup> Two cynomolgus monkeys (3 years old) received ICV-STZ (2 mg/kg) at the cerebellomedullary cistern 3 times on day 1, 7, and 14, and compared with two cynomolgus monkeys receiving normal saline.<sup>98</sup> In the ICV-STZ-treated monkeys, increased sulcal markings were observed using magnetic resonance imaging (MRI) 6 weeks after the first IVC-STZ injection, suggesting immediate diffuse brain atrophy, but these structural changes were resolved at 12 weeks post-injection.<sup>98</sup> [<sup>18</sup>F]-FDG-PET was used to characterise glucose metabolism in this model and revealed glucose hypometabolism in the precuneus, posterior cingulate, and medial temporal areas in ICV-STZ-treated monkeys, which resembled the distributive pattern of glucose hypometabolism in early AD patients.<sup>98</sup> This same group subsequently used the same experimental design to investigate molecular changes induced by ICV-STZ in female cynomolgus monkeys (3 years old). The mRNA expression of insulin-related genes was altered in the anterior part of the cerebrum, frontal cortex, and hippocampus, which resembled these areas of the brain in patients with early AD.<sup>99</sup> Subsequently, ICV-STZ-treated cynomolgus monkeys were used to characterise the profile of 7 APP processing-related genes (ADAM10, ADAM17, BACE1, PSEN2, NCSTN, APH1A, and PSENEN) and five Tau phosphorylation-related genes (CDK5, CDK5R1, CAPN1, AKT1, and GSK3 $\beta$ ).<sup>100</sup> In ICV-STZ-treated monkeys, mRNA levels of ADAM10, ADAM17, PSEN2, PSENEN, NCSTN, and APH1A were significantly upregulated 1.6–2.1 fold in the precuneus and occipital cortex compared with control monkeys, while BACE1 upregulation was only observed in the occipital cortex.<sup>100</sup> Downregulation of ADAM17 and upregulation of PSENEN and NCSTN were observed in the frontal cortex.<sup>100</sup> The Tau-associated genes, CDK5R1, CAPN1, and GSK3 $\beta$  were significantly upregulated in the precuneus and occipital cortex.<sup>100</sup> ICV-STZ treatment generally resulted in higher transcription levels of APP processing and Tau phosphorylation-related genes in the frontal and occipital cortices, except CDK5, indicating that these genes might be simultaneously regulated in specific regions.<sup>100</sup> In a later study, 6 cynomolgus monkeys (5–8 years old) were used to assess ICV-STZ-induced AD-resembling features.<sup>101</sup> Half of the monkeys were administered 4 doses of STZ (2 mg/kg) via the cerebellomedullary cistern on weeks 0, 1, 2, and 28, while the other half of the cohort were injected with artificial CSF.<sup>101</sup> Monkeys were terminated 36 weeks after the first dose of ICV-STZ, which was equivalent to 8 weeks after the final dose of ICV-STZ.<sup>101</sup> ICV-STZ-treated monkeys exhibited prominent A $\beta$  plaques with dense core in the parenchyma of the temporal cortex and dense CAA in microvessels in the insular cortex, while the brains of control monkeys illustrated minimal or no A $\beta$  immunoreactivity, approximately four-fold different as quantified using immunostaining.<sup>101</sup> In the temporal cortex and hippocampus, p-Tau was detected in the neuronal cytoplasm as tangles and straight fragments, accompanied by severe cell loss, atrophy, and morphological alterations.<sup>101</sup> Within the ventricular wall and the periventricular area, densely stained GFAP<sup>+</sup> astrocytic fibres and numerous IBA-1<sup>+</sup> microglia/macrophages with amoeboid morphology were observed in ICV-STZ-treated monkeys, indicating astrogliosis, microglial activation, and inflammatory processes.<sup>101</sup> This study was the first ICV-STZ study that comprehensively assessed

the histology of the brain in these monkeys and demonstrated an induced model that resembled AD. Interestingly, monkeys that received 3 ICV-STZ injections did not display structural changes at week 24, but monkeys that received 4 ICV-STZ injections on week 28 displayed ventricular enlargement and parenchymal atrophy at weeks 30, 32, and 34.<sup>101</sup> The first three doses of ICV-STZ may make the brain more susceptible to cerebral damage and additional doses may be needed to induce remarkable brain atrophy, further illustrating the importance of dose and inoculation time in NHP studies. To date, only one study has comprehensively assessed the microscopic and macroscopic features of ICV-STZ-treated monkeys, and no study has evaluated ICV-STZ-induced cognitive decline and behavioural changes yet. Of note, the surgical procedures used in this method may cause penetration injuries that would affect the general theoretical basis of the model.<sup>20</sup> Considering these limitations, more studies are needed to strengthen the validity of this model.

### Formaldehyde (FA)-induced NHP models of AD

AD is a complicated disorder that is determined by both genetic and environmental risk factors, including air pollution, heat waves, heavy metals, and others. For instance, long-term exposure to environmental lead led to elevated expression of AD-related genes and transcriptional regulators (Sp1), decreased DNA methyltransferase activity, and increased DNA oxidative damage in aged cynomolgus monkey.<sup>102</sup> FA is a highly reactive single-carbon aldehyde that is widely distributed in living organisms (intrinsic FA) and the environment (extrinsic FA).<sup>20,103</sup> Endogenous FA is the by-product of aldehyde metabolism sourced from the oxidation of methanol, histone demethylation, and methylamine deamination.<sup>103</sup> FA has been classified as a carcinogen and teratogen by the World Health Organisation.<sup>20</sup> It is known to damage the balance of neurotransmitters, influence long-term potentiation in the hippocampus, and influence DNA methylation that may eventually lead to memory decline.<sup>20</sup> In AD, patients intrinsically accumulate excessive FA which then induces A $\beta$  aggregation, Tau hyperphosphorylation and fibrillation, neuronal loss, memory impairment, and learning deficits.<sup>103</sup> In Yang *et al*, 4 male rhesus monkeys (3–4 years old) were chronically fed with 3% methanol *ad libitum* and compared with nine control monkeys to study the chronic effects of methanol exposure.<sup>104</sup> After the variable spatial delay response task was performed, two methanol-treated monkeys experienced persistent memory decline that lasted 6 months after the feeding regimen.<sup>104</sup> Meanwhile, approximately 1.25 years into this study, the level of p-Tau in CSF was dramatically higher in methanol-treated monkeys compared with the control monkeys.<sup>104</sup> A $\beta$  plaques and p-Tau were identified in the parietal, temporal, frontal lobes, and the hippocampus of methanol-treated monkeys exclusively.<sup>104</sup> This study investigated the chronic effects of methanol and its FA metabolite in AD, but its results were limited by its small sample size and inconsistent study design for each rhesus monkeys. In the following study, young rhesus monkeys (5–8 years old) were administered with ICV-FA injections over 12 months to study FA-induced effects.<sup>105</sup> ICV-FA-treated monkeys exhibited A $\beta$  plaques, neuritic-like plaques, NFT-like formations, higher level of p-Tau, neuronal loss, and activated astrocytes and microglia in their hippocampus, entorhinal cortex, and prefrontal cortex, compared with controls.<sup>105</sup> Similarly, ICV-FA-treated monkeys illustrated significant spatial working memory impairments.<sup>105</sup> In these two studies of FA-induced NHP models of AD, FA-treated NHPs demonstrated consistent A $\beta$  depositions, Tau hyperphosphorylation, and memory impairment. Nevertheless, the method of methanol feeding

requires modification as methanol itself is associated with side effects that are hard to distinguish based on histological examination and behaviour assessment.<sup>20</sup>

### Advantages and disadvantages of induced NHP models of AD

This chapter has discussed current studies that used ICV-A $\beta$ , IT-A $\beta$ , AD brain homogenate, ICV-STZ, methanol, and ICV-FA to induce NHP models of AD (Table 2). Aged NHPs share great similarities with human, including neuroanatomy, neurophysiology, complicated behaviours, and complex emotions, making them ideal models for human disorders. The application of A $\beta$ , AD brain homogenate, STZ, and FA further fills the gap between naturally ageing NHPs and human with AD by inducing Tau hyperphosphorylation, potential fibrillation of p-Tau, neuronal loss, brain atrophy, cognitive decline, and memory impairment. Most importantly, the injection or feeding of AD-associated inducers allow the emergence of AD-associated pathologies and behaviours at the young adult age in NHPs rather than at the elder age in naturally aged NHPs, which greatly limits financial needs and shortens experimental procedures. Nevertheless, all current modelling methods are associated with limitations. First, the dose, injection period, and inoculation period vary between studies and the procedures have not been standardised. Studying two well-designed A $\beta$ -induced NHP studies, increasing the dosage, prolonging the injection period, and extending the inoculation period up to two years may allow NHPs to develop all AD-resembling pathologies and symptoms, most importantly, brain atrophy and cognitive decline.<sup>88,90</sup> The occurrence of brain atrophy and cognitive decline is hardly observed in spontaneous NHP models of AD, but they are severely affected in patients with AD, suggesting their importance in therapeutic development and validation in AD models. Secondly, the study design of constructing an induced NHP model of AD awaits great improvement. Many studies only included two or three NHPs in the treatment group, so the presentation of AD-resembling pathologies may be a result of chance. A more comprehensive assessments of induced NHPs is encouraged, including the examinations of A $\beta$  plaques, CAA, p-Tau, NFTs, glial activation, inflammatory profile, neuronal death, brain atrophy, and behavioural changes. A more standardised evaluation of NHP models will contribute to better communication between studies, making the ultimate use of time and capital in each study, and leading to more efficient construction of a well-recognised standardised NHP model of AD. In addition, given the incomplete understanding of AD aetiology, all artificially induced models are based on a specific hypothesis of AD, making it hard for one NHP model to fully recapitulate AD pathologies and symptoms.<sup>20</sup> Constructing such models should be one of the main focuses and obstacles in this field. More efforts are expected to improve methodology, increase consistency, and eventually standardise the protocol of induced NHP models of AD.

### Evaluation of NHP models of AD

While spontaneous and induced NHP models of AD are still being developed, the methods and techniques used to assess hallmarks of AD in these models must be standardised simultaneously. Most of the diagnostic techniques used in human AD studies and the behavioural tests used in rodent models of AD have been applied in NHP models of AD to evaluate disease pathology and treatment efficacy. Common clinical examinations include A $\beta$  PET scan, MRI, and electroencephalogram (EEG), while biofluid samples, such as CSF and plasma samples, are mainly used in laboratory tests. Various behavioural and cognitive tests, which are specific to

NHP models of AD, have also been recently developed.

### Brain imaging

A $\beta$  PET scans are broadly used in clinical settings for AD diagnosis and increasingly used in NHP models of AD. The common tracer used in human studies, Pittsburgh Compound B (<sup>11</sup>C-PIB), is not suitable for use in aged rhesus monkeys, squirrel monkeys, or chimpanzees.<sup>106</sup> <sup>18</sup>F-Fluoroazabenzoxazoles (MK-3328), developed by Merck, has shown promising results for rhesus monkeys, which will be discussed in the next chapter.<sup>107</sup> Besides A $\beta$  PET scans, <sup>18</sup>F-ASEM which targets the nicotinic acetylcholine receptor has also been used in a NHP model.<sup>108</sup>

MRIs have also been used in NHP models of AD to evaluate disease progression. Gary and colleagues induced AD-like symptoms in 12 middle-aged mouse lemurs (~3.5 years old) by intracerebral injections of brain extracts from AD patients, followed by an 18-month inoculation and monitoring with a 7.0 Tesla spectrometer.<sup>109</sup> Progressive cerebral atrophy was observed.<sup>109</sup> MRI was also applied in middle-aged and aged vervet monkeys to investigate the associations between brain volumetrics and other AD markers.<sup>75</sup> Smaller MRI volumes in the right prefrontal, left inferior, and left posterior temporal cortex were found to be associated with higher levels of pTau-181 in CSF.<sup>75</sup> Similar age-related brain volume changes in young and old vervet monkeys were also reported using MRI.<sup>81</sup> Additionally, MRI has been used to examine amyloid-related imaging abnormalities, a potentially serious side effect in clinical trials for AD that is closely associated with CAA. Aged squirrel monkeys showed both edematous and hyperintense types of amyloid-related imaging abnormalities, accompanied by reactive astrocytosis, microgliosis, infiltration of systemic inflammatory/immune cells, damage to axons and myelin, and hemosiderin deposition.<sup>110</sup>

### EEG and electromyogram (EMG)

EEG and EMG are common clinical methods for monitoring brain function, but neither has been widely used in NHP models. Gary and colleagues applied EEG and EMG coupling analysis in their mouse lemur model of AD. Briefly, after inoculation with brain extracts from AD patients, slow wave EEG frequencies were observed with a lower delta frequency and a higher theta frequency in the experimental group, compared with the control-inoculated group.<sup>109</sup> New EEG devices designed specifically for rhesus monkeys have also been reported,<sup>111</sup> which could greatly facilitate the studies of NHP models.

### Laboratory tests

Many of the current clinical laboratory diagnostic methods have also been used in studies of NHP models of AD, including the CSF biomarker assay, cell biology examination, and histological staining. Chen and colleagues measured A $\beta$ <sub>1-40</sub>, A $\beta$ <sub>1-42</sub>, t-Tau, and P-Tau181P in 329 vervet monkeys and found similar changes in these biomarkers as in human AD patients.<sup>112</sup> Increased levels of FA in CSF were found in aged rhesus monkeys and the levels were negatively associated with the A $\beta$  burden.<sup>113</sup>

Immunohistochemical staining is broadly used in NHP models of AD. In a study comparing 6-month-old APP/PS1 mice, ~31-year-old rhesus monkeys, and ~86-year-old humans, mitochondrial clusters were found surrounding A $\beta$  plaques in all three species.<sup>114</sup> Larger particles of lipofuscin, a deposit of oxidised lipids and proteins, and greater plaque-associated astrocyte activation were found in the brains of monkeys and human participants. Extensive non-ramified microglia were also noticed.<sup>114</sup> T cell infiltration was found in the white matter of the parenchyma of the

aged monkeys,<sup>115</sup> resembling human AD. Other AD-resembling pathological characteristics, such as A $\beta$  plaques, dendritic spine loss, Tau, p-Tau, and activated astrocytes, were also found in NHP models of AD.<sup>86,109</sup> These data demonstrate similar pathological features shared by both aged NHP and human subjects.

### Behavioural tests

Monkeys have a rich behavioural repertoire that lends themselves as suitable for translational studies of human cognition.<sup>18</sup> Many behavioural tests have also been developed in NHP models.

### Cognitive and learning tests

#### A computerised visuospatial learning task

After a stimulus is presented to a monkey, the computer screen becomes blank. Following a 2-s delay, three objects are presented. The monkey is expected to choose the original object. Usually 20 trials/session are presented over 20 consecutive sessions.<sup>116</sup>

#### Manual delayed match to position task

A test of working memory capacity in a Wisconsin General Testing Apparatus.<sup>29,85,117</sup> It assesses monkeys' ability to correctly identify the location of a food reward that they previously saw hidden, following various delays.<sup>115,118</sup>

#### DNMS task

A benchmark task of learning and recognition memory that measures a monkeys' ability to distinguish between a recently presented object and a novel object following a delay period of 10 s. Once this is learned, additional tests of recognition memory will be performed after delays of 2 mins and 10 mins. Outputs of the acquisition phase, 2-min delay phase, and 10-min delay phase are used as measurements of learning and recognition memory.<sup>115,119-121</sup>

#### Computerised delayed match to sample (DMTS) task

This task begins with a pre-training session known as "shaping procedures" followed by a DMTS trial. In the previous apparatus, colour choice selections are made by pressing clear push keys with light emitting diodes located behind them. The current apparatus is equipped with touch-sensitive computer monitors that presents the colour choices automatically.<sup>118</sup>

#### Circular platform test

Spatial performance is assessed in a circular platform apparatus, which is a modified version of the Barnes maze, specifically adapted for mouse lemurs.<sup>122,123</sup>

#### Visual discrimination test (mouse lemurs)

The cognition of mouse lemurs is evaluated in an apparatus adapted from the Lashley jumping stand apparatus, a vertical cage made of plywood walls, except for the front panel, which is a one-way mirror allowing observation. Two discrimination tasks are performed, a learning task and a long-term memory task. These tests involve a succession of visual discrimination tasks, during which the mouse lemur must jump from a heightened central platform to one of two lateral boards.<sup>109</sup> One of the boards allows access to a reinforcing chamber containing a positive reward (the possibility of reaching a safe nestbox for a 2-min rest).<sup>109</sup>

#### Touchscreen-based cognitive testing

Mouse lemurs are trained individually in customised, sound-attenuated Bussey-Saksida Touchscreen Chambers.<sup>124</sup> Lemurs receive



one training session per day. Each session lasts for a maximum duration of 30 (pre-training sessions) or 60 (sessions during actual cognitive testing) mins or until 30 trials have been completed by the respective subject. All lemurs are naïve to the touchscreen setup and must undertake a pre-training procedure before they begin the actual cognitive task. The pre-training procedure consists of five different stages (PT 1 to PT 5), during which the lemurs procedurally learn to interact with random, pictorial pre-training stimuli presented in one of two possible response windows on the touchscreen for a reward. The actual cognitive test, a pairwise discrimination/pairwise discrimination reversal, includes two fundamentally different stages: an initial, visual PD acquisition stage followed by a PDR procedure.<sup>51,124</sup>

#### T-maze

This test is designed based on earlier studies in rats and macaques and is scaled for the relative size of NHPs. Each monkey is introduced into the maze in a series of stages. Following pre-training, monkeys are trained on the spatial DNMS tasks. The monkey is only rewarded if it enters the correct choice arm. This learning phase continues for four trials/day, five days/week, until the animal achieves a criterion of 36 correct responses in 40 consecutive trials.<sup>125</sup>

#### DRST Object and Spatial

This tests monkeys' working memory capacities by requiring them to identify a new stimulus among an increasing array of serially presented, familiar stimuli using spatial and subsequent nonspatial (objects) stimuli. The span of correct responses across trials is a measurement of working memory.<sup>115,119</sup>

#### Conceptual set shifting task

This tests monkeys' executive function by requiring them to learn rules that are not explicitly learned. It resembles the Wisconsin Card Sorting Task: once a task is learned, the "rule" is switched, so that monkeys must shift to learn a new rule. The errors monkeys make, specifically the perseverative errors made after set shifting, is the measurement of executive function.<sup>115</sup>

#### Spatial reversal learning

A stimulus tray with three identical, equally spaced wells is used. The correct response is to displace the plaque on the positive side and obtain the food reward. The outcome measure is the total number of trials required for three sequential reversals.<sup>119,126</sup>

#### Inhibitory control of behaviour (squirrel monkeys)

The apparatus is a clear Plexiglas box with one open side baited with a treat. The box is locked into place on a horizontal tray secured to a tripod placed in front of each monkey's cage. After initial training, the box opening is oriented towards different directions, the direction of each reach attempt and the hand used on successful retrievals are recorded.<sup>127</sup>

#### Motor function assays

##### Motor function assay

NHPs are placed on a platform. Distance travelled and movement speed are quantified for each NHP using a commercially available video-tracking system in accordance with the published procedures.<sup>128,129</sup>

##### Accelerating rotarod task (mouse lemurs)

Mouse lemurs are placed on a 5-cm-diameter rotating cylinder

turning at 20 rotations per minute (rpm). The rod then accelerates steadily up to 40 rpm until the end of the test, which is reached when the animal falls or grips onto the rod during at least three consecutive turns without stabilising its balance. Latency to fall off or grip the rod is recorded for each trial. Mouse lemurs will take five consecutive trials, and the best result is recorded with the values expressed in seconds.<sup>109</sup>

##### Gait speed (usual walking speed)

The time a NHP takes to traverse a minimum of three feet at a normal pace without provocation is recorded as its usual walking speed via stopwatch. The measurements of usual walking speed are conducted during the day (07:00–16:00 hours) over the course of a month before necropsy. A minimum of five valid instances are used to calculate the mean speed.<sup>75,130</sup>

#### Applications of NHP models of AD:

##### PET imaging and tracer validation

Although the gold-standard diagnosis of AD is the post-mortem examination of A $\beta$  and Tau proteopathies, the field is currently evolving the diagnostic criteria into a suite of neuroimaging and fluid biomarkers to identify pre-clinical and prodromal patients with biomarker positivity before the onset of dementia symptoms. CSF measurements of A $\beta$  and Tau, and PET imaging of A $\beta$  burden are currently the most advanced and accurate diagnostic tools that are restricted in research settings and clinical trials. To further improve the diagnostic accuracy and sensitivity, developing various neuroimaging techniques and identifying AD-specific radiopharmaceuticals that allow the non-invasive appraisal of A $\beta$  or Tau lesions are encouraged.<sup>2</sup> Given the similarity of neuroanatomy, genetics, and protein homology between NHPs and humans, NHPs can make great contributions to the pre-clinical evolution of AD-associated radiopharmaceuticals regarding safe evaluation, kinetics mimicking, selectivity, and specificity assessments.<sup>2</sup> Four [<sup>18</sup>F]Fluoroazabenzoxazoles PET tracers, including [<sup>18</sup>F]MK-3328, [<sup>18</sup>F]AD-269, [<sup>18</sup>F]AD-278, and [<sup>18</sup>F]AD-265, were evaluated for their *in vitro* binding to human A $\beta$  plaques, lipophilicity, and blood-brain barrier permeability in rhesus monkeys.<sup>107</sup> [<sup>18</sup>F]MK-3328 illustrated the best combination of low *in vivo* binding potential in white matter and cortical grey matter, low lipophilicity, and high affinity for A $\beta$  plaques in rhesus monkeys.<sup>107</sup> [<sup>18</sup>F]MK-3328 was subsequently tested in AD patients, showing punctuate, displaceable binding in the cortical grey matter without binding in the cerebellum.<sup>107,131</sup> It was then tested in clinical trials among healthy controls and AD patients, but only fulfilled phase one until its premature termination.<sup>131</sup> NHP models can play a fundamental role in PET tracer development and safety evaluations, paving the road towards clinical trials involving human participants.  $\gamma$ -secretase modulators (GSM) and synthesised [<sup>11</sup>C]SGSM-15606 were developed to visualise the distribution of  $\gamma$ -secretase in one male rhesus monkey (13 years old).<sup>132</sup> This  $\gamma$ -secretase-based PET radioligand demonstrated high selectivity and high brain intake, in the midbrain and anterior cingulate cortex.<sup>132</sup> This study provides the first molecular neuroimaging of  $\gamma$ -secretase, which not only facilitates the investigation of the role of A $\beta$  and  $\gamma$ -secretase in AD pathogenesis, but also helps in drug assessment and development.<sup>133</sup> In addition to the development and validation of novel PET tracers using NHPs, some studies also use NHPs to evaluate the association between different tracers targeting A $\beta$  plaques, glucose metabolism, mitochondrial proteins, and acetylcholine

receptors, aimed at improving our understanding of AD pathogenesis.<sup>134,135</sup>

Beyond molecular neuroimaging of A $\beta$  plaques and A $\beta$ -related proteins, other studies have also evaluated novel PET tracers for neuroimaging of AD-associated proteins or receptors. <sup>11</sup>C-LSN3172176 was synthesised to visualise the M<sub>1</sub> muscarinic acetylcholine receptor (mAChR) in rhesus monkeys.<sup>136</sup> mAChR plays a critical role in learning and memory and is tightly associated with cognitive decline in neurological disorders, including AD.<sup>136</sup> <sup>11</sup>C-LSN3172176 displayed rapid metabolism, fast kinetics, and high uptake in the brains of rhesus monkeys, while its uptake was significantly reduced with pre-treatment with scopolamine and AZD6088.<sup>136</sup> The validity examination of <sup>11</sup>C-LSN3172176 in NHPs suggested that it may be the first optimal radiotracer for mAChR.<sup>137,138</sup> Furthermore, as dysregulation of microtubule is associated with AD, [<sup>11</sup>C]MPC-6827 was developed to image microtubules and assess reproducibility in male cynomolgus monkeys.<sup>139</sup> Soluble epoxide hydrolase is a bifunctional enzyme, and its dysregulation is associated with neuropathologic disorders, including AD.<sup>140</sup> A novel PET tracer for imaging soluble epoxide hydrolase, [18F]FNBP, was first tested in the brains of baboons and demonstrated high and rapid brain uptake.<sup>140</sup> Given the high similarities between NHPs and human, NHPs have become involved in the evaluation of novel AD-associated PET tracers to pave the way towards clinical translation in human subjects. NHP models of AD are more valuable than rodent models of AD in the pre-clinical assessment of neuroimaging biomarkers because they can resolve many concerns, including the safety, kinetics, sensitivity, and specificity of PET tracers, which reduces the cost of unnecessary clinical trials and increases the translational rate of novel PET tracers.

#### **Active immunotherapy (vaccination)**

Active immunotherapy, or preventative immunisation, uses inactivated virus, bacteria, or part of these pathogens to stimulate the patient's immune system to generate antibodies against the pathogen, such as against A $\beta$  in AD. A cocktail of human A $\beta$  peptides were injected into five aged vervet monkeys over 10 months, leading to the generation of plasma anti-A $\beta$  antibodies that could recognise monomeric and oligomeric A $\beta$  instead of full-length APP.<sup>141</sup> Immunisation with human A $\beta$  peptides also resulted in increased plasma levels of A $\beta$ <sub>1-40</sub> at day 300, accompanied by significantly lower levels of CSF A $\beta$ <sub>1-40</sub> and A $\beta$ <sub>1-42</sub> at day 100, suggesting the controversial "peripheral sink hypothesis".<sup>141</sup> Of note, all vervet monkeys recruited in this study already demonstrated severe A $\beta$  plaques and CAA prior to active immunisation, but the authors did not compare parenchymal and vascular A $\beta$  burden pre- and post-immunisation.<sup>141</sup> Active immunisation studies using NHPs should use young, disease-free NHPs to enable researchers to observe the effects of the vaccine. Subsequently, 25 young, disease-free mouse lemurs were used to observe antibody responses after immunisation with A $\beta$ <sub>1-42</sub> and its derivatives, including K6A $\beta$ <sub>1-30</sub>, K6A $\beta$ <sub>1-30</sub>[E<sub>18</sub>E<sub>19</sub>], and A $\beta$ <sub>1-30</sub>[E<sub>18</sub>E<sub>19</sub>].<sup>142</sup> K6A $\beta$ <sub>1-30</sub> resulted in high, stable anti-A $\beta$  IgG responses in multiple mouse lemurs, so researchers chose this derivative for further immunisation in older primates.<sup>142</sup> Cynomolgus monkeys were also immunised with the A $\beta$  vaccine combined with prior immunisation of a diphtheria-tetanus toxoid vaccine.<sup>143</sup> Very recently, optimised ACI-24, a liposome vaccine designed to generate anti-A $\beta$  antibody responses without simultaneous T cell activation, was also tested on young four cynomolgus monkeys in a pre-clinical study.<sup>144</sup> Vaccinated cynomolgus monkeys generated high levels of IgG antibodies

against pyroglutamate A $\beta$ .<sup>144</sup> These studies revealed several roles for NHPs in pre-clinical studies of AD vaccination, including vaccine tolerance, kinetic assessment, and long-term monitoring of side effects, aiding the translational application of AD vaccines in human subjects. Additionally, assessing whether an A $\beta$  vaccine can ameliorate AD-associated pathologies is critical. Multiple species of NHPs, including rhesus monkeys, cynomolgus monkeys, and pigtailed monkeys, were immunised using aggregated A $\beta$ <sub>1-42</sub> admixed with monophosphoryl lipid A as an adjuvant for five consecutive times within 14 weeks, followed by six-months of monitoring.<sup>145</sup> While all animals developed a strong, sustained level of anti-A $\beta$  IgG antibodies in serum, only 80% of the aged NHPs generated detectable antibodies and their immune responses were more delayed and weaker compared with the younger monkeys.<sup>145</sup> Comparing the pre- and post-immunisation levels of CSF A $\beta$  and Tau, slight decreases in CSF A $\beta$ <sub>1-42</sub>, increases in Tau, and differences in Tau/A $\beta$ <sub>1-42</sub> ratio were observed in the aged population.<sup>145</sup> Regarding the A $\beta$  burden at the pre- and post-immunisation stages, this study only compared histopathologic examinations in all immunised NHPs and non-immunised NHPs and they performed A $\beta$  PET scanning at baseline.<sup>145</sup> Overall, compared with rodent models of AD, NHPs are the superior models of AD that can accurately predict how long a vaccine will generate antibodies and how adverse effects will present in pre-clinical studies. The simultaneous use of a rodent model and NHP model are encouraged to obtain robust information prior to clinical trials involving human subjects.<sup>2</sup> In the last two decades, young and disease-free NHP models of AD have been mainly used to evaluate the safety and tolerance of AD vaccines in pre-clinical studies. In future studies, young, disease-free NHPs are expected to be examined by PET neuroimaging of A $\beta$  and Tau pre- and post-immunisation to estimate whether AD vaccines can prevent or post-pone the occurrence of AD pathologies before clinical trials.

#### **Therapeutic development and validation**

##### **Passive immunotherapy (mAb)**

The field has developed advanced techniques to identify patients at the asymptomatic phase for early management, aiming at postponing clinical symptoms or reversing pathogenetic mechanisms, but no DMTs have been granted expecting symptom-modifying treatments. The current symptom-modifying treatments of AD include inhibitors of acetylcholinesterase enzyme (AChE) (donepezil, galantamine, and rivastigmine) and N-methyl-D aspartate (NMDA) receptor antagonists (memantine).<sup>146</sup> Donepezil could ameliorate spatial cognition deficits and protect neurons from senility in an A $\beta$ -induced tree shrew model of AD,<sup>147</sup> while memantine has demonstrated partial effectiveness in resolving spatial memory impairment.<sup>123</sup> Given the improved understanding of AD in recent decades, some researchers advocate that AD may be caused by an impairment of innate immunity, and that it may be treated by tools of adaptive immunity.<sup>148</sup> The administration of anti-A $\beta$  and anti-Tau mAb might be effective passive immunotherapies of AD.<sup>146</sup> NHPs are rarely involved in the pre-clinical testing of mAb therapies. Only one study re-engineered a single chain Fv antibody against A $\beta$  with a fusion protein with mAb against the human insulin receptor to develop mAb-based therapy of AD that can cross the human blood-brain barrier.<sup>149</sup> Given the currently available spontaneous and induced NHP models of AD, essential pre-clinical studies involving NHPs are expected to test the safety, efficiency, and long-term adverse effects of mAb treatments of AD prior to the translation into clinical trials involving human subjects. The field is investigating numerous human resources and financial



investments into the clinical trials of mAb treatments, but its low translational rate is remarkable.<sup>146</sup> One possible explanation is that the human subjects recruited by clinical trials are already too old to be treated by mAb treatments. In addition to rodent models of AD, recruiting NHP models of AD at middle age in pre-clinical studies will contribute to identification of the effects of mAb treatments and selecting the most promising mAb treatments, facilitating further translational work with controlled budgets.

### AD pathogenesis-associated treatments

While anti-A $\beta$  or anti-Tau mAb treatments target the cardinal features of AD, AD is also associated with neuroprotective factors and many receptors that may have therapeutic potential. Pathological alterations in neuronal circuits and synapses may explain the link between AD proteopathies and cognitive impairment.<sup>150</sup> Brain-derived neurotrophic factor (BDNF) is tightly associated with neuronal survival in the entorhinal cortex and maintenance of synaptic plasticity in learning and memory.<sup>150</sup> In adult and aged rhesus monkeys, lentiviral vectors expressing BDNF genes were delivered into their entorhinal cortices.<sup>116</sup> BDNF prevented lesion-induced neuronal death in the entorhinal cortex, reversed neuronal size in the entorhinal cortex, and ameliorated age-related impairments in visuospatial cognition.<sup>116</sup> Based on these preliminary results, the first-in-human clinical trial that test whether AVV2-BDNF gene therapy will slow or prevent neuronal loss in the brains of patients with early AD will start shortly ([www.clinicaltrials.gov/ct2/show/NCT05040217](http://www.clinicaltrials.gov/ct2/show/NCT05040217)). Furthermore, the cholinergic system is also a critical focus of therapeutic development in AD, such as donepezil, one of the granted symptom-modifying treatments of AD. The fourth subtype of mAChR, M4, participates in the actions of acetylcholine and has become a new target to modify behavioural and cognitive alterations in AD.<sup>151</sup> Very recently, the effect of an M4 receptor was characterised in six adult rhesus monkeys.<sup>151</sup> This compound improved cognitive abilities in the object retrieval detour task and the visuospatial paired-associates learning, suggesting its potential in modifying AD symptoms.<sup>151</sup> However, whether this novel compound is superior to the existing AChE inhibitors for AD requires further investigation.

### Drug repurposing

The translation from laboratory discoveries into clinical applications of novel therapeutics takes substantial amounts of time and human resources in addition to being accompanied by a high failure rate. Thus, the repurposing of “old” drugs with approved safety, tolerance, and adverse effects to treat common and rare diseases is becoming a popular.<sup>152</sup> AD has long been associated with diabetes. A high sugar/high fat diet, physical inactivity, and mental stress all lead to hyperglycaemia, which is the main feature of insulin resistance and diabetes, further resulting in cognitive deterioration.<sup>153</sup> The brains of human subjects with AD are characterised by defective insulin signalling and impaired glucose metabolism, indicating that anti-diabetic treatments may be promising DMTs for AD.<sup>154</sup> In 2018, liraglutide, a glucagon-like peptide 1 analog developed to treat type 2 diabetes, was tested in A $\beta$ -induced NHP model of AD.<sup>154</sup> Based on the A $\beta$ -induced NHP protocol established by Forny-Germano’s study, six NHP models of AD, using cynomolgus monkeys, were established via ICV-A $\beta$  injection once every three days consecutively for up to 24 days.<sup>154</sup> Two of the six NHP models received daily subcutaneous injections of liraglutide beginning one week prior to ICV-A $\beta$  injection and lasted until the end of the ICV-A $\beta$  injections.<sup>154</sup> ICV-A $\beta$ -treated monkeys exhibited diffuse A $\beta$  peptides, p-Tau, tangle formation, synapse loss,

and glial activation, which recapitulated many AD features.<sup>154</sup> Reduced levels of insulin receptors were observed in the frontal cortex, hippocampus, and amygdala.<sup>154</sup> Comparing ICV-A $\beta$ -treated and ICV-A $\beta$ /liraglutide-treated monkeys, the administration of liraglutide conferred modest protection against the loss of synaptophysin, reduced density of synapses, and hyperphosphorylation of Tau in the hippocampus, frontal cortex, and amygdala.<sup>154</sup> This study illustrated the possible association between A $\beta$  and insulin dysregulation, further strengthening the theory that glucose hypometabolism and insulin receptor signalling is closely associated with AD. The protective effects of the anti-diabetes treatment, liraglutide, against AD-associated proteopathies and neuronal insulin signalling were also demonstrated, even though full protection was not achieved. Obviously, strengthening synapses and restoring neuronal insulin signalling are insufficient to treat AD, so the combination of anti-diabetic treatments and other therapeutics may be administered concurrently to modify AD progression. Another anti-diabetic drug, pioglitazone, which has an unclear biochemical mechanism of action and may be associated with mitochondria functions and oxidative stress, was also tested on male vervet monkeys to treat neurodegenerative disorders.<sup>155</sup> In the last five years, with increasing awareness of the association between diabetes and AD, the repurposing of anti-diabetic drugs for AD treatment has been launched and NHP models of AD are useful to assess their therapeutic effects prior to clinical trials involving human subjects.

Although the amyloid theory has dominated the AD field for decades, its low clinical translational rate raises concerns that AD may not be fully explained by A $\beta$ . Recent large-scale genome-wide association studies have identified over 130 susceptibility loci associated with AD risks and over half of them implicate a role for the innate immune system.<sup>148</sup> Innate immune responses are altered in both the central and peripheral pool, including microglial activation, astrocyte activation, monocyte alteration, and AD-associated pro-inflammatory profiles.<sup>148,156,157</sup> Consequently, drug repurposing of anti-inflammatory drugs has become a plausible approach to treat AD. Dimebolin (latrepirdine), a non-selective anti-histamine drug, has indicated its effectiveness in modifying dementia symptoms in the initial trials.<sup>158</sup> It was then tested on young adult (11–17 years old) and aged (20–31 years old) rhesus monkeys to evaluate its modulation of cognition.<sup>159</sup> In both young adult and aged rhesus monkeys, dimebolin increased performance on DMTS tasks, manifesting acutely improved working memory and a protracted response for at least 24 hours.<sup>159</sup> In 2015, ibuprofen, a nonsteroidal anti-inflammatory drug, was tested on five to seven conscious cynomolgus monkeys and 16 healthy subjects, and further compared the subsequent A $\beta$  burden levels after the administration of GSM-1.<sup>160</sup> A single dose of GSM-1 significantly reduced the ratio of A $\beta$ <sub>1–42</sub>:A $\beta$ <sub>1–40</sub> in plasma and CSF, but a single high dose of ibuprofen did not modulate the plasma levels of A $\beta$  in cynomolgus monkeys and human subjects.<sup>160</sup> The GSM activity of ibuprofen was not detected in this study, which is consistent with previous conclusions that only long-term administration of ibuprofen would confer moderate protection against AD.<sup>160,161</sup> As indicated by genomic studies, the development of innate immune boosters that can promote innate phagocytosis of A $\beta$  is also expected to resolve AD proteopathies.<sup>148</sup>

### Lifestyle modifications

Given the limited options of DMTs and the restricted applications of early diagnostic tools in AD, effective preventive strategies are highly encouraged to reduce an individual’s exposure to AD-associated risk factors, including dietary interventions,

physical activity, and sleeping improvement.<sup>162</sup> Calorie restriction may prevent A $\beta$  accumulation in rodent models of AD by promoting NAD<sup>+</sup>-dependent SIRT1 mediated deacetylase activity.<sup>163</sup> A 30% calorie restriction in squirrel monkeys reduced the levels of A $\beta$ <sub>1-42</sub> and A $\beta$ <sub>1-40</sub>, and the reduced portion of A $\beta$  peptides were inversely associated with SIRT1 protein in the temporal cortex of squirrel monkeys.<sup>163</sup> Most interestingly, this 30% calorie restriction elevated the activity of  $\alpha$ -secretase but did not alter that of  $\beta$ - or  $\gamma$ -secretase, as supported by decreased ROCK1 protein in the same brain region.<sup>163</sup> This study demonstrated the A $\beta$  modulating ability of calorie restriction for the first time, but the authors did not compare other AD-associated pathologies or the differences in cognitive decline between the treatment and control groups. The 30% calorie restriction also reduced stress responsiveness without affecting orientation and attention behaviour in 44 rhesus monkeys (19–31 years old).<sup>164</sup> Their stress reactivity was associated with brain atrophy in regions responsible for emotional regulation and microstructural tissue density, and this relationship was also reduced by 30% calorie restriction.<sup>164</sup> It is expected that future studies would first construct spontaneous or induced NHP models of AD and then deliver calorie restriction to specifically assess its modulation of AD-associated pathologies and behaviours. To be more specific about diet, the dietary amino acid L-serine in tofu and seaweeds slowed the development of tangles and A $\beta$  plaques in NHPs and human subjects with amyotrophic lateral sclerosis.<sup>165,166</sup> An interesting study compared Western diet, mimicking the diet consumed by American women (40–49 years old), and Mediterranean diet using middle-aged (11–13 years old) female cynomolgus monkeys.<sup>167</sup> The Western diet group presented higher grey matter volume and cortical thickness in the temporoparietal regions, which may confer protection against AD but may also be caused by neuroinflammation.<sup>167</sup> The volume of white matter was reduced in the Western diet group but remained intact in the Mediterranean group, coinciding with early biomarkers of AD neuropathology.<sup>167</sup> The observation of healthy diet and calorie restriction indicates that lifestyle modification can confer protection against AD even though their underlying mechanisms remain inconclusive, and their protective strengths remain low.

### Chinese medicine in tree shrews

In China and other East Asian countries, a wide range of traditional Chinese medical herbs have been used as therapeutic and preventative strategies for numerous disorders for thousands of years. *Panax ginseng* C.A. Mey. (ginseng) is one of the most well-known and valuable traditional medical herbs conferring anti-inflammatory, anti-tumour, and anti-oxidative effects.<sup>168</sup> Ginsenosides, the major pharmacologically active ingredient of ginseng, possess strong AChE inhibitory potential, greatly improving cognitive and memory decline in AD.<sup>168</sup> Ginsenosides play a neuroprotective role in AD by inhibiting A $\beta$  aggregation and Tau hyperphosphorylation, ameliorating inflammation, reducing apoptosis, promoting neurotrophic factors, and improving mitochondrial dysfunctions.<sup>168</sup> In 2020, a cohort of male Chinese tree shrews were administrated intra-hippocampal injections of A $\beta$ <sub>25-35</sub> or control saline (CT group) to establish an induced NHP model of AD.<sup>169</sup> Six groups of the animals subsequently received intraperitoneal intragastric administration of donepezil (DN group), intraperitoneal intragastric administration of Ginsenoside Rg1 (GRg1) with low, middle, or high doses, or control saline solution (AD group) orally for eight weeks.<sup>169</sup> GRg1 oral treatment led to cognitive improvement, as assessed by Morris water maze, and decreased levels of Tau in the hippocampus and cortex in the DN and

GRg1 groups.<sup>169</sup> More specifically, tree shrews in the middle and high-GRg1 groups had significantly lower numbers of Tau<sup>+</sup> cells, compared with the low-GRg1 group and the DN group.<sup>169</sup> The subsequent 16S ribosomal RNA sequencing illustrated different profiles of gut microbiota between the different groups, in which middle and high doses of GRg1 modified the gut microbiota to resemble the CT group.<sup>169</sup> After screening for the optimal dosage of GRg1 for AD modification, another cohort of tree shrew models of AD were established via ventricle injections of A $\beta$ <sub>25-35</sub>, followed by a high dose of GRg1 only.<sup>170</sup> GRg1 inhibited the expression of  $\beta$ -secretase 1 but promoted the expressions of microtubule-associated protein 2 and FOX-3 in the hippocampus of A $\beta$ /GRg1-treated tree shrews compared with the A $\beta$ -treated group.<sup>170</sup> A $\beta$ /GRg1-treated tree shrews also demonstrated lower levels of A $\beta$ , p-Tau, and the pro-apoptotic factor Bax and increased levels of BCL-2 in the hippocampus and cortex, compared with the A $\beta$ -treated group.<sup>170</sup> More recently, GRg1 was shown to increase the antioxidant activities of SOD, CAT, GPx and reduce the inflammatory factors interleukin-1 and IBA-1.<sup>171</sup> The ratio of BCL-2 to Bax was increased in the A $\beta$ /GRg1-treated group, accompanied by reduced expression of Caspase-3, GSK-3 $\beta$ , and  $\beta$ -catenin.<sup>171</sup> In brief, high doses of GRg1 are promising at alleviating oxidative stresses, pro-inflammatory markers, pro-apoptotic activities, AD-associated proteopathies, and cognitive deficits induced by A $\beta$  injections in tree shrews.<sup>170,171</sup> GRg1 oral treatment is also closely associated with gut microbiota AD by altering the abundances of *Bacteroidetes*, *Proteobacteria*, *Verrucomicrobia*, and *Lactobacillaceae*.<sup>169,170</sup> These studies utilized appropriate study design, comprehensive histological assessment, and cognitive examination, forming a theoretical basis for the examination of GRg1 in clinical trials involving human subjects.

### Future directions

It is anticipated that the NHP model of AD will be used in more and more AD drug development projects, to evaluate the drug administration routes, pharmacokinetics, pharmacodynamics, tolerability, safety, and most importantly, the drug efficacy prior to Phase I clinical trials. Thus, great effort is needed to improve the current NHP models of AD, particularly in imaging, laboratory biomarkers and behavioral tests for drug efficacy evaluation. A $\beta$  PET scan with appropriate radioisotope labeled tracers will be applied in the next couple of years, together with novel blood and urine biomarkers. These studies will therefore provide necessary data and solid evidence to facilitate clinical trials in human subjects.

### Conclusions

After the first identification of AD over 100 years ago, the field is still attempting to understand the fundamental aetiology and pathogenesis underlying AD. The application of animal models of AD that fully recapitulate AD-associated pathologies and symptoms can greatly advance our understanding of the molecular, cellular, physiological, and psychological processes along the course of the disease. This review has summarised the spontaneous and induced NHP models of AD and their recent contributions to AD research. Spontaneous NHP models of AD exhibit wide-spread A $\beta$  depositions, CAA, glial activation, and moderate cognitive decline at the elderly age, while NHP models of AD induced by ICV-A $\beta$ , brain homogenates, FA, and ICV-STZ further present with AD-resembling p-Tau, minor NFTs, and brain atrophy. The co-occurrence of all AD-associated pathologies and behavioural changes is

rarely observed in rodent models, but it is reported in several NHP studies due to the close phylogenetic relationship, similar AD-associated genetics, similar neuroanatomy, physiology, neuronal functions, and high-order cognitive, emotional, and social behaviours between NHPs and human subjects. In the last two decades, NHP models of AD are increasingly involved in the development of novel PET tracers, A $\beta$  vaccines, DMTs, and dietary modifications to aid in their translation into clinical trials involving human subjects, aiming at improving the diagnostic criteria, preventative strategies, and therapeutic treatments for AD. However, the investigations into the NHP models of AD are associated with some limitations. Compared with rodent models of AD, the use of NHP models of AD requires higher financial costs, greater genetic manipulation, smaller sample sizes, and more specialised researchers and facilities. There is still an absence of a standardised protocol to establish a broadly accepted NHP model of AD, which may increase the discrepancies across different studies. Based on the studies by Yue and Forny-Germano, the field should generate a guideline which recommends that certain inducers, dosages of inducers, injection frequencies, and inoculation periods should be met to produce reliable NHP models of AD. A good study design that assesses a broad range of AD-associated pathologies and behaviour changes must be incorporated into NHP studies to enable peer researchers to comprehensively interpretate the effects of PET tracers, A $\beta$  vaccines, DMTs, or lifestyle modifications. The establishment of a standardised NHP model of AD and the engagement of a comprehensive assessment of NHPs will greatly accelerate the translation from NHP discoveries into clinical trials involving human subjects, thus greatly speeding up the discoveries of biomarkers and DMTs for AD.

### Acknowledgments

The authors are grateful to the University of Melbourne for providing open access to PubMed for literature review.

### Funding

This work was supported by the Melbourne Research Scholarship provided by the Florey Institute of Neuroscience and Mental Health, the University of Melbourne, and Qianqiang Life Science Melbourne R&D Centre. We sincerely appreciate funding support from the Ministry of Science and Technology of China (program grant No. SQ2018YFC200022 to BG), and the Victorian Government's Operational Infrastructure Support Grant to the Florey Institute.

### Conflict of interest

Ben J. Gu has been an Editor-in-Chief of the *Journal of Exploratory Research in Pharmacology* since June 2021. The authors have no other conflicts of interests to declare.

### Author contributions

Study design (YL and BG), writing (YL and BG), critical revision of the manuscript (YL), supervision (BG).

### References

- [1] Scheltens P, De Strooper B, Kivipelto M, Holstege H, Ch  telat G, Te-

unissen CE, *et al*. Alzheimer's disease. *Lancet* 2021;397(10284):1577–1590. doi:10.1016/S0140-6736(20)32205-4, PMID:33667416.

- [2] Van Dam D, De Deyn PP. Non human primate models for Alzheimer's disease-related research and drug discovery. *Expert Opin Drug Discov* 2017;12(2):187–200. doi:10.1080/17460441.2017.1271320, PMID:27960560.
- [3] DeTure MA, Dickson DW. The neuropathological diagnosis of Alzheimer's disease. *Mol Neurodegener* 2019;14(1):32. doi:10.1186/s13024-019-0333-5, PMID:31375134.
- [4] De Strooper B, Karran E. The Cellular Phase of Alzheimer's Disease. *Cell* 2016;164(4):603–615. doi:10.1016/j.cell.2015.12.056, PMID:26871627.
- [5] Sperling RA, Aisen PS, Beckett LA, Bennett DA, Craft S, Fagan AM, *et al*. Toward defining the preclinical stages of Alzheimer's disease: recommendations from the National Institute on Aging-Alzheimer's Association workgroups on diagnostic guidelines for Alzheimer's disease. *Alzheimers Dement* 2011;7(3):280–292. doi:10.1016/j.jalz.2011.03.003, PMID:21514248.
- [6] McKhann GM, Knopman DS, Chertkow H, Hyman BT, Jack CR Jr, Kawas CH, *et al*. The diagnosis of dementia due to Alzheimer's disease: recommendations from the National Institute on Aging-Alzheimer's Association workgroups on diagnostic guidelines for Alzheimer's disease. *Alzheimers Dement* 2011;7(3):263–269. doi:10.1016/j.jalz.2011.03.005, PMID:21514250.
- [7] Selkoe DJ, Hardy J. The amyloid hypothesis of Alzheimer's disease at 25 years. *EMBO Mol Med* 2016;8(6):595–608. doi:10.15252/emmm.201606210, PMID:27025652.
- [8] Thal DR, R  b U, Orantes M, Braak H. Phases of A beta-deposition in the human brain and its relevance for the development of AD. *Neurology* 2002;58(12):1791–1800. doi:10.1212/wnl.58.12.1791, PMID:12084879.
- [9] Greenberg SM, Bacskai BJ, Hernandez-Guillamon M, Pruzin J, Sperling R, van Veluw SJ. Cerebral amyloid angiopathy and Alzheimer disease - one peptide, two pathways. *Nat Rev Neurol* 2020;16(1):30–42. doi:10.1038/s41582-019-0281-2, PMID:31827267.
- [10] Chang CW, Shao E, Mucke L. Tau: Enabler of diverse brain disorders and target of rapidly evolving therapeutic strategies. *Science* 2021;371:6532. doi:10.1126/science.abb8255, PMID:33632820.
- [11] Medeiros R, Baglietto-Vargas D, LaFerla FM. The role of tau in Alzheimer's disease and related disorders. *CNS Neurosci Ther* 2011;17(5):514–524. doi:10.1111/j.1755-5949.2010.00177.x, PMID:20553310.
- [12] Braak H, Alafuzoff I, Arzberger T, Kretschmar H, Del Tredici K. Staging of Alzheimer disease-associated neurofibrillary pathology using paraffin sections and immunocytochemistry. *Acta Neuropathol* 2006;112(4):389–404. doi:10.1007/s00401-006-0127-z, PMID:16906426.
- [13] Cacace R, Sleegers K, Van Broeckhoven C. Molecular genetics of early-onset Alzheimer's disease revisited. *Alzheimers Dement* 2016;12(6):733–748. doi:10.1016/j.jalz.2016.01.012, PMID:27016693.
- [14] Thinakaran G, Koo EH. Amyloid precursor protein trafficking, processing, and function. *J Biol Chem* 2008;283(44):29615–29619. doi:10.1074/jbc.R800019200, PMID:18650430.
- [15] Poirier J, Davignon J, Bouthillier D, Kogan S, Bertrand P, Gauthier S. Apolipoprotein E polymorphism and Alzheimer's disease. *Lancet* 1993;342(8873):697–699. doi:10.1016/0140-6736(93)91705-q, PMID:8103819.
- [16] Neuner SM, Tcw J, Goate AM. Genetic architecture of Alzheimer's disease. *Neurobiol Dis* 2020;143:104976. doi:10.1016/j.nbd.2020.104976, PMID:32565066.
- [17] Sanchez-Varo R, Mejias-Ortega M, Fernandez-Valenzuela JJ, Nu  ez-D  az C, Caceres-Palomo L, Vegas-Gomez L, *et al*. Transgenic Mouse Models of Alzheimer's Disease: An Integrative Analysis. *Int J Mol Sci* 2022;23(10):5404. doi:10.3390/ijms23105404, PMID:35628216.
- [18] Moss MB, Moore TL, Schettler SP, Killiany R, Rosene D. Successful vs. Unsuccessful Aging in the Rhesus Monkey. In: Riddle DR (ed). *Brain Aging: Models, Methods, and Mechanisms*. Boca Raton (FL): CRC Press/Taylor & Francis; 2007. Chapter 2. Available from: <https://www.ncbi.nlm.nih.gov/books/NBK1833/>.
- [19] Heuer E, Rosen RF, Cintron A, Walker LC. Nonhuman primate models of Alzheimer-like cerebral proteopathy. *Curr Pharm Des* 2012;18(8):1159–1169. doi:10.2174/138161212799315885, PMID:



- 22288403.
- [20] Li HW, Zhang L, Qin C. Current state of research on non-human primate models of Alzheimer's disease. *Animal Model Exp Med* 2019;2(4):227–238. doi:10.1002/ame2.12092, PMID:31942555.
  - [21] Bartus RT, Fleming D, Johnson HR. Aging in the rhesus monkey: debilitating effects on short-term memory. *J Gerontol* 1978;33(6):858–871. doi:10.1093/geronj/33.6.858, PMID:106081.
  - [22] Cowan N. What are the differences between long-term, short-term, and working memory? *Prog Brain Res* 2008;169:323–338. doi:10.1016/s0079-6123(07)00020-9, PMID:18394484.
  - [23] Bartus RT, Dean RL 3rd, Fleming DL. Aging in the rhesus monkey: effects on visual discrimination learning and reversal learning. *J Gerontol* 1979;34(2):209–219. doi:10.1093/geronj/34.2.209, PMID:108323.
  - [24] Wenk GL. A primate model of Alzheimer's disease. *Behav Brain Res* 1993;57(2):117–122. doi:10.1016/0166-4328(93)90127-c, PMID:8117419.
  - [25] Dudkin KN, Chueva IV, Makarov FN, Beach TG, Roher A. Impaired processes of working memory in the monkey model of Alzheimer's disease. *Dokl Biol Sci* 2002;383:106–108. doi:10.1023/a:1015373420424, PMID:12053557.
  - [26] Dudkin KN, Chueva IV, Makarov FN, Bich TG, Roher AE. Impairments in working memory and decision-taking processes in monkeys in a model of Alzheimer's disease. *Neurosci Behav Physiol* 2005;35(3):281–289. doi:10.1007/s11055-005-0057-6, PMID:15875490.
  - [27] Dudkin KN, Chueva IV, Makarov FN, Bich TG, Roher AE. Disorders of learning and memory processes in a monkey model of Alzheimer's disease: the role of the associative area of the cerebral cortex. *Neurosci Behav Physiol* 2006;36(8):789–799. doi:10.1007/s11055-006-0089-6, PMID:16964455.
  - [28] Presty SK, Bachevalier J, Walker LC, Struble RG, Price DL, Mishkin M, *et al*. Age differences in recognition memory of the rhesus monkey (*Macaca mulatta*). *Neurobiol Aging* 1987;8(5):435–440. doi:10.1016/0197-4580(87)90038-8, PMID:3683724.
  - [29] Rapp PR, Amaral DG. Evidence for task-dependent memory dysfunction in the aged monkey. *J Neurosci* 1989;9(10):3568–3576. doi:10.1523/JNEUROSCI.09-10-03568.1989, PMID:2795141.
  - [30] Bachevalier J. Behavioral changes in aged rhesus monkeys. *Neurobiol Aging* 1993;14(6):619–621. doi:10.1016/0197-4580(93)90048-g, PMID:8295665.
  - [31] Moss MB, Killiany RJ, Lai ZC, Rosene DL, Herndon JG. Recognition memory span in rhesus monkeys of advanced age. *Neurobiol Aging* 1997;18(1):13–19. doi:10.1016/s0197-4580(96)00211-4, PMID:8983028.
  - [32] Calhoun ME, Mao Y, Roberts JA, Rapp PR. Reduction in hippocampal cholinergic innervation is unrelated to recognition memory impairment in aged rhesus monkeys. *J Comp Neurol* 2004;475(2):238–246. doi:10.1002/cne.20181, PMID:15211464.
  - [33] Struble RG, Price DL Jr, Cork LC, Price DL. Senile plaques in cortex of aged normal monkeys. *Brain Res* 1985;361(1-2):267–275. doi:10.1016/0006-8993(85)91298-3, PMID:4084799.
  - [34] Selkoe DJ, Bell DS, Podlisny MB, Price DL, Cork LC. Conservation of brain amyloid proteins in aged mammals and humans with Alzheimer's disease. *Science* 1987;235(4791):873–877. doi:10.1126/science.3544219, PMID:3544219.
  - [35] Walker LC, Kitt CA, Schwam E, Buckwald B, Garcia F, Sepinwall J, *et al*. Senile plaques in aged squirrel monkeys. *Neurobiol Aging* 1987;8(4):291–296. doi:10.1016/0197-4580(87)90067-4, PMID:3306432.
  - [36] Cork LC, Masters C, Beyreuther K, Price DL. Development of senile plaques. Relationships of neuronal abnormalities and amyloid deposits. *Am J Pathol* 1990;137(6):1383–1392. PMID:1701963.
  - [37] Heilbroner PL, Kemper TL. The cytoarchitectonic distribution of senile plaques in three aged monkeys. *Acta Neuropathol* 1990;81(1):60–65. doi:10.1007/bf00662638, PMID:1707575.
  - [38] Thal DR, Capetillo-Zarate E, Del Tredici K, Braak H. The development of amyloid beta protein deposits in the aged brain. *Sci Aging Knowledge Environ* 2006;2006(6):re1. doi:10.1126/sageke.2006.6.re1, PMID:16525193.
  - [39] Podlisny MB, Tolan DR, Selkoe DJ. Homology of the amyloid beta protein precursor in monkey and human supports a primate model for beta amyloidosis in Alzheimer's disease. *Am J Pathol* 1991;138(6):1423–1435. PMID:1905108.
  - [40] Nakamura S, Kiatipattanasakul W, Nakayama H, Ono F, Sakakibara I, Yoshikawa Y, *et al*. Immunohistochemical characteristics of the constituents of senile plaques and amyloid angiopathy in aged cynomolgus monkeys. *J Med Primatol* 1996;25(4):294–300. doi:10.1111/j.1600-0684.1996.tb00213.x, PMID:8906609.
  - [41] Gearing M, Tigges J, Mori H, Mirra SS. A beta40 is a major form of beta-amyloid in nonhuman primates. *Neurobiol Aging* 1996;17(6):903–908. doi:10.1016/s0197-4580(96)00164-9, PMID:9363802.
  - [42] Kanemaru K, Iwatsubo T, Ihara Y. Comparable amyloid beta-protein (A beta) 42(43) and A beta 40 deposition in the aged monkey brain. *Neurosci Lett* 1996;214(2-3):196–198. doi:10.1016/0304-3940(96)12893-7, PMID:8878117.
  - [43] Bons N, Mestre N, Petter A. Senile plaques and neurofibrillary changes in the brain of an aged lemurian primate, *Microcebus murinus*. *Neurobiol Aging* 1992;13(1):99–105. doi:10.1016/0197-4580(92)90016-q, PMID:1542387.
  - [44] Bons N, Mestre N, Ritchie K, Petter A, Podlisny M, Selkoe D. Identification of amyloid beta protein in the brain of the small, short-lived lemurian primate *Microcebus murinus*. *Neurobiol Aging* 1994;15(2):215–220. doi:10.1016/0197-4580(94)90115-5, PMID:7838294.
  - [45] Uno H, Alsum PB, Dong S, Richardson R, Zimbric ML, Thieme CS, *et al*. Cerebral amyloid angiopathy and plaques, and visceral amyloidosis in aged macaques. *Neurobiol Aging* 1996;17(2):275–281. doi:10.1016/0197-4580(95)02063-2, PMID:8744409.
  - [46] Bons N, Rieger F, Prudhomme D, Fisher A, Krause KH. *Microcebus murinus*: a useful primate model for human cerebral aging and Alzheimer's disease? *Genes Brain Behav* 2006;5(2):120–130. doi:10.1111/j.1601-183X.2005.00149.x, PMID:16507003.
  - [47] Oikawa N, Kimura N, Yanagisawa K. Alzheimer-type tau pathology in advanced aged nonhuman primate brains harboring substantial amyloid deposition. *Brain Res* 2010;1315:137–149. doi:10.1016/j.brainres.2009.12.005, PMID:20004650.
  - [48] Norvin D, Kim G, Baker-Nigh A, Geula C. Accumulation and age-related elevation of amyloid- $\beta$  within basal forebrain cholinergic neurons in the rhesus monkey. *Neuroscience* 2015;298:102–111. doi:10.1016/j.neuroscience.2015.04.011S0306-4522(15)00342-5, PMID:25869619.
  - [49] Paspalas CD, Carlyle BC, Leslie S, Preuss TM, Crimins JL, Huttner AJ, *et al*. The aged rhesus macaque manifests Braak stage III/IV Alzheimer's-like pathology. *Alzheimers Dement* 2018;14(5):680–691. doi:10.1016/j.jalz.2017.11.005, PMID:29241829.
  - [50] Koinuma S, Shimozaawa N, Yasutomi Y, Kimura N. Aging induces abnormal accumulation of A $\beta$  in extracellular vesicle and/or intraluminal membrane vesicle-rich fractions in nonhuman primate brain. *Neurobiol Aging* 2021;106:268–281. doi:10.1016/j.neurobiolaging.2021.06.022, PMID:34329965.
  - [51] Schmidtke D, Zimmermann E, Trouche SG, Fontès P, Verdier JM, Mestre-Francés N. Linking cognition to age and amyloid- $\beta$  burden in the brain of a nonhuman primate (*Microcebus murinus*). *Neurobiol Aging* 2020;94:207–216. doi:10.1016/j.neurobiolaging.2020.03.025, PMID:32650184.
  - [52] Uchiyama T, Endo K, Kondo H, Okabayashi S, Shimozaawa N, Yasutomi Y, *et al*. Tau pathology in aged cynomolgus monkeys is progressive supranuclear palsy/corticobasal degeneration- but not Alzheimer disease-like -Ultrastructural mapping of tau by EDX. *Acta Neuropathol Commun* 2016;4(1):118. doi:10.1186/s40478-016-0385-5, PMID:27842611.
  - [53] Pawlik M, Fuchs E, Walker LC, Levy E. Primate-like amyloid-beta sequence but no cerebral amyloidosis in aged tree shrews. *Neurobiol Aging* 1999;20(1):47–51. doi:10.1016/s0197-4580(99)00017-2, PMID:10466892.
  - [54] Yamashita A, Fuchs E, Taira M, Hayashi M. Amyloid beta (A $\beta$ ) protein- and amyloid precursor protein (APP)-immunoreactive structures in the brains of aged tree shrews. *Curr Aging Sci* 2010;3(3):230–238. doi:10.2174/1874609811003030230, PMID:20735344.
  - [55] Walker LC, Masters C, Beyreuther K, Price DL. Amyloid in the brains of aged squirrel monkeys. *Acta Neuropathol* 1990;80(4):381–387. doi:10.1007/bf00307691, PMID:2239150.

- [56] Elfenbein HA, Rosen RF, Stephens SL, Switzer RC, Smith Y, Pare J, *et al*. Cerebral beta-amyloid angiopathy in aged squirrel monkeys. *Histol Histopathol* 2007;22(2):155–167. doi:10.14670/hh-22.155, PMID:17149688.
- [57] Mestre-Francés N, Keller E, Calenda A, Barelli H, Checler F, Bons N. Immunohistochemical analysis of cerebral cortical and vascular lesions in the primate *Microcebus murinus* reveal distinct amyloid beta1-42 and beta1-40 immunoreactivity profiles. *Neurobiol Dis* 2000;7(1):1–8. doi:10.1006/nbdi.1999.0270, PMID:10671318.
- [58] Silhol S, Calenda A, Jallageas V, Mestre-Frances N, Bellis M, Bons N. beta-Amyloid protein precursor in *Microcebus murinus*: genotyping and brain localization. *Neurobiol Dis* 1996;3(3):169–182. doi:10.1006/nbdi.1996.0017, PMID:8980017.
- [59] Martin LJ, Sisodia SS, Koo EH, Cork LC, Dellovade TL, Weidemann A, *et al*. Amyloid precursor protein in aged nonhuman primates. *Proc Natl Acad Sci U S A* 1991;88(4):1461–1465. doi:10.1073/pnas.88.4.1461, PMID:1899927.
- [60] Fukumoto H, Rosene DL, Moss MB, Raju S, Hyman BT, Irizarry MC. Beta-secretase activity increases with aging in human, monkey, and mouse brain. *Am J Pathol* 2004;164(2):719–725. doi:10.1016/s0002-9440(10)63159-8, PMID:14742275.
- [61] Fan Y, Luo R, Su LY, Xiang Q, Yu D, Xu L, *et al*. Does the Genetic Feature of the Chinese Tree Shrew (*Tupaia belangeri chinensis*) Support Its Potential as a Viable Model for Alzheimer's Disease Research? *J Alzheimers Dis* 2018;61(3):1015–1028. doi:10.3233/jad-170594, PMID:29332044.
- [62] Fan Y, Ye MS, Zhang JY, Xu L, Yu DD, Gu TL, *et al*. Chromosomal level assembly and population sequencing of the Chinese tree shrew genome. *Zool Res* 2019;40(6):506–521. doi:10.24272/j.issn.2095-8137.2019.063, PMID:31418539.
- [63] Calenda A, Mestre-Francés N, Czech C, Pradier L, Petter A, Bons N, *et al*. Molecular cloning, sequencing, and brain expression of the presenilin 1 gene in *Microcebus murinus*. *Biochem Biophys Res Commun* 1996;228(2):430–439. doi:10.1006/bbrc.1996.1678, PMID:8920931.
- [64] Calenda A, Mestre-Francés N, Czech C, Pradier L, Petter A, Perret M, *et al*. Cloning of the presenilin 2 cDNA and its distribution in brain of the primate, *Microcebus murinus*: coexpression with betaAPP and Tau proteins. *Neurobiol Dis* 1998;5(5):323–333. doi:10.1006/nbdi.1998.0205, PMID:10069575.
- [65] Kimura N, Nakamura SI, Honda T, Takashima A, Nakayama H, Ono F, *et al*. Age-related changes in the localization of presenilin-1 in cynomolgus monkey brain. *Brain Res* 2001;922(1):30–41. doi:10.1016/s0006-8993(01)03146-8, PMID:11730699.
- [66] Kimura N, Nakamura SI, Ono F, Sakakibara I, Ishii Y, Kyuwa S, *et al*. Presenilin-2 in the cynomolgus monkey brain: investigation of age-related changes. *Primates* 2004;45(3):167–175. doi:10.1007/s10329-004-0076-x, PMID:14986149.
- [67] Li MX, Wang WG, Kuang DX, Ruan LY, Li XH, Huang X, *et al*. Identification, characterization and expression profiles of PSEN2 in the Chinese tree shrew (*Tupaia belangeri chinensis*). *J Integr Neurosci* 2020;19(2):249–257. doi:10.31083/j.jin.2020.02.28, PMID:32706189.
- [68] Calenda A, Jallageas V, Silhol S, Bellis M, Bons N. Identification of a unique apolipoprotein E allele in *Microcebus murinus*; ApoE brain distribution and co-localization with beta-amyloid and tau proteins. *Neurobiol Dis* 1995;2(3):169–176. doi:10.1006/nbdi.1995.0018, PMID:9174000.
- [69] Fainman J, Eid MD, Ervin FR, Palmour RM. A primate model for Alzheimer's disease: investigation of the apolipoprotein E profile of the vervet monkey of St. Kitts. *Am J Med Genet B Neuropsychiatr Genet* 2007;144B(6):818–819. doi:10.1002/ajmg.b.30276, PMID:17373728.
- [70] Gearing M, Rebeck GW, Hyman BT, Tigges J, Mirra SS. Neuropathology and apolipoprotein E profile of aged chimpanzees: implications for Alzheimer disease. *Proc Natl Acad Sci U S A* 1994;91(20):9382–9386. doi:10.1073/pnas.91.20.9382, PMID:7937774.
- [71] Härtig W, Klein C, Brauer K, Schüppel KF, Arendt T, Brückner G, *et al*. Abnormally phosphorylated protein tau in the cortex of aged individuals of various mammalian orders. *Acta Neuropathol* 2000;100(3):305–312. doi:10.1007/s004010000183, PMID:10965801.
- [72] Datta D, Leslie SN, Wang M, Morozov YM, Yang S, Mentone S, *et al*. Age-related calcium dysregulation linked with tau pathology and impaired cognition in non-human primates. *Alzheimers Dement* 2021;17(6):920–932. doi:10.1002/alz.12325, PMID:33829643.
- [73] Bons N, Jallageas V, Silhol S, Mestre-Frances N, Petter A, Delacourte A. Immunocytochemical characterization of Tau proteins during cerebral aging of the lemurian primate *Microcebus murinus*. *C R Acad Sci III* 1995;318(1):77–83. PMID:7757807.
- [74] Giannakopoulos P, Silhol S, Jallageas V, Mallet J, Bons N, Bouras C, *et al*. Quantitative analysis of tau protein-immunoreactive accumulations and beta amyloid protein deposits in the cerebral cortex of the mouse lemur, *Microcebus murinus*. *Acta Neuropathol* 1997;94(2):131–139. doi:10.1007/s004010050684, PMID:9255387.
- [75] Latimer CS, Shively CA, Keene CD, Jorgensen MJ, Andrews RN, Register TC, *et al*. A nonhuman primate model of early Alzheimer's disease pathologic change: Implications for disease pathogenesis. *Alzheimers Dement* 2019;15(1):93–105. doi:10.1016/j.jalz.2018.06.3057, PMID:30467082.
- [76] Rodriguez-Callejas JD, Fuchs E, Perez-Cruz C. Evidence of Tau Hyperphosphorylation and Dystrophic Microglia in the Common Marmoset. *Front Aging Neurosci* 2016;8:315. doi:10.3389/fnagi.2016.00315, PMID:28066237.
- [77] Rodriguez-Callejas JD, Fuchs E, Perez-Cruz C. Increased oxidative stress, hyperphosphorylation of tau, and dystrophic microglia in the hippocampus of aged *Tupaia belangeri*. *Glia* 2020;68(9):1775–1793. doi:10.1002/glia.23804, PMID:32096580.
- [78] Gazzaley AH, Thakker MM, Hof PR, Morrison JH. Preserved number of entorhinal cortex layer II neurons in aged macaque monkeys. *Neurobiol Aging* 1997;18(5):549–553. doi:10.1016/s0197-4580(97)00112-7, PMID:9390783.
- [79] Keuter JI, Luiten PG, Fuchs E. Preservation of hippocampal neuron numbers in aged rhesus monkeys. *Neurobiol Aging* 2003;24(1):157–165. doi:10.1016/s0197-4580(02)00062-3, PMID:12493561.
- [80] Edler MK, Munger EL, Meindl RS, Hopkins WD, Ely JJ, Erwin JM, *et al*. Neuron loss associated with age but not Alzheimer's disease pathology in the chimpanzee brain. *Philos Trans R Soc Lond B Biol Sci* 2020;375(1811):20190619. doi:10.1098/rstb.2019.0619, PMID:32951541.
- [81] Frye BM, Craft S, Register TC, Kim J, Whitlow CT, Barcus RA, *et al*. Early Alzheimer's disease-like reductions in gray matter and cognitive function with aging in nonhuman primates. *Alzheimers Dement (N Y)* 2022;8(1):e12284. doi:10.1002/trc2.12284, PMID:35310523.
- [82] Podlisy MB, Stephenson DT, Frosch MP, Tolan DR, Lieberburg I, Clemens JA, *et al*. Microinjection of synthetic amyloid beta-protein in monkey cerebral cortex fails to produce acute neurotoxicity. *Am J Pathol* 1993;142(1):17–24. PMID:8424453.
- [83] McKee AC, Kowall NW, Schumacher JS, Beal MF. The neurotoxicity of amyloid beta protein in aged primates. *Amyloid* 1998;5(1):1–9. doi:10.3109/13506129809007283, PMID:9546999.
- [84] Geula C, Wu CK, Saroff D, Lorenzo A, Yuan M, Yankner BA. Aging renders the brain vulnerable to amyloid beta-protein neurotoxicity. *Nat Med* 1998;4(7):827–831. doi:10.1038/nm0798-827, PMID:9662375.
- [85] Li W, Wu Y, Min F, Li Z, Huang J, Huang R. A nonhuman primate model of Alzheimer's disease generated by intracranial injection of amyloid- $\beta$ 42 and thiorphan. *Metab Brain Dis* 2010;25(3):277–284. doi:10.1007/s11011-010-9207-9, PMID:20838863.
- [86] Beckman D, Ott S, Donis-Cox K, Janssen WG, Bliss-Moreau E, Rudebeck PH, *et al*. Oligomeric A $\beta$  in the monkey brain impacts synaptic integrity and induces accelerated cortical aging. *Proc Natl Acad Sci U S A* 2019;116(52):26239–26246. doi:10.1073/pnas.1902301116, PMID:31871145.
- [87] Beckman D, Morrison JH. Towards developing a rhesus monkey model of early Alzheimer's disease focusing on women's health. *Am J Primatol* 2021;83(11):e23289. doi:10.1002/ajp.23289, PMID:34056733.
- [88] Forny-Germano L, Lyra E Silva NM, Batista AF, Brito-Moreira J, Gralle M, Boehnke SE, *et al*. Alzheimer's disease-like pathology induced by amyloid- $\beta$  oligomers in nonhuman primates. *J Neurosci* 2014;34(41):13629–13643. doi:10.1523/JNEUROSCI.1353-14.2014, PMID:25297091.
- [89] Jebelli JD, Piers TM. Amyloid- $\beta$  oligomers unveil a novel primate model of sporadic Alzheimer's disease. *Front Neurosci* 2015;9:47. doi:10.3389/fnins.2015.00047, PMID:25852450.



- [90] Yue F, Feng S, Lu C, Zhang T, Tao G, Liu J, *et al*. Synthetic amyloid- $\beta$  oligomers drive early pathological progression of Alzheimer's disease in nonhuman primates. *iScience* 2021;24(10):103207. doi:10.1016/j.isci.2021.103207, PMID:34704001.
- [91] Wakeman DR, Weed MR, Perez SE, Cline EN, Viola KL, Wilcox KC, *et al*. Intrathecal amyloid-beta oligomer administration increases tau phosphorylation in the medial temporal lobe in the African green monkey: A nonhuman primate model of Alzheimer's disease. *Neuropathol Appl Neurobiol* 2022;48(4):e12800. doi:10.1111/nan.12800, PMID:35156715.
- [92] Lin N, Xiong LL, Zhang RP, Zheng H, Wang L, Qian ZY, *et al*. Injection of A $\beta$ 1-40 into hippocampus induced cognitive lesion associated with neuronal apoptosis and multiple gene expressions in the tree shrew. *Apoptosis* 2016;21(5):621–640. doi:10.1007/s10495-016-1227-4, PMID:26897171.
- [93] Baker HF, Ridley RM, Duchon LW, Crow TJ, Bruton CJ. Induction of beta (A4)-amyloid in primates by injection of Alzheimer's disease brain homogenate. Comparison with transmission of spongiform encephalopathy. *Mol Neurobiol* 1994;8(1):25–39. doi:10.1007/bf02778005, PMID:8086126.
- [94] Maclean CJ, Baker HF, Ridley RM, Mori H. Naturally occurring and experimentally induced beta-amyloid deposits in the brains of marmosets (*Callithrix jacchus*). *J Neural Transm (Vienna)* 2000;107(7):799–814. doi:10.1007/s007020070060, PMID:11005545.
- [95] Ridley RM, Baker HF, Windle CP, Cummings RM. Very long term studies of the seeding of beta-amyloidosis in primates. *J Neural Transm (Vienna)* 2006;113(9):1243–1251. doi:10.1007/s00702-005-0385-2, PMID:16362635.
- [96] Lam S, Petit F, Hérard AS, Boluda S, Eddarkaoui S, Guillermier M, *et al*. E. B. Neuropathology Network. Transmission of amyloid-beta and tau pathologies is associated with cognitive impairments in a primate. *Acta Neuropathol Commun* 2021;9(1):165. doi:10.1186/s40478-021-01266-8, PMID:34641980.
- [97] Kamat PK. Streptozotocin induced Alzheimer's disease like changes and the underlying neural degeneration and regeneration mechanism. *Neural Regen Res* 2015;10(7):1050–1052. doi:10.4103/1673-5374.160076, PMID:26330820.
- [98] Heo JH, Lee SR, Lee ST, Lee KM, Oh JH, Jang DP, *et al*. Spatial distribution of glucose hypometabolism induced by intracerebroventricular streptozotocin in monkeys. *J Alzheimers Dis* 2011;25(3):517–523. doi:10.3233/JAD-2011-102079, PMID:21471644.
- [99] Lee Y, Kim YH, Park SJ, Huh JW, Kim SH, Kim SU, *et al*. Insulin/IGF signaling-related gene expression in the brain of a sporadic Alzheimer's disease monkey model induced by intracerebroventricular injection of streptozotocin. *J Alzheimers Dis* 2014;38(2):251–267. doi:10.3233/JAD-130776, PMID:23948941.
- [100] Park SJ, Kim YH, Nam GH, Choe SH, Lee SR, Kim SU, *et al*. Quantitative expression analysis of APP pathway and tau phosphorylation-related genes in the ICV STZ-induced non-human primate model of sporadic Alzheimer's disease. *Int J Mol Sci* 2015;16(2):2386–2402. doi:10.3390/ijms16022386, PMID:25622254.
- [101] Yeo HG, Lee Y, Jeon CY, Jeong KJ, Jin YB, Kang P, *et al*. Characterization of Cerebral Damage in a Monkey Model of Alzheimer's Disease Induced by Intracerebroventricular Injection of Streptozotocin. *J Alzheimers Dis* 2015;46(4):989–1005. doi:10.3233/JAD-143222, PMID:25881906.
- [102] Wu J, Basha MR, Brock B, Cox DP, Cardozo-Pelaez F, McPherson CA, *et al*. Alzheimer's disease (AD)-like pathology in aged monkeys after infantile exposure to environmental metal lead (Pb): evidence for a developmental origin and environmental link for AD. *J Neurosci* 2008;28(1):3–9. doi:10.1523/JNEUROSCI.4405-07.200828/1/3, PMID:18171917.
- [103] Wang F, Chen D, Wu P, Klein C, Jin C. Formaldehyde, Epigenetics, and Alzheimer's Disease. *Chem Res Toxicol* 2019;32(5):820–830. doi:10.1021/acs.chemrestox.9b00090, PMID:30964647.
- [104] Yang M, Miao J, Rizak J, Zhai R, Wang Z, Huma T, *et al*. Alzheimer's disease and methanol toxicity (part 2): lessons from four rhesus macaques (*Macaca mulatta*) chronically fed methanol. *J Alzheimers Dis* 2014;41(4):1131–1147. doi:10.3233/JAD-131532, PMID:24787917.
- [105] Zhai R, Rizak J, Zheng N, He X, Li Z, Yin Y, *et al*. Alzheimer's Disease-Like Pathologies and Cognitive Impairments Induced by Formaldehyde in Non-Human Primates. *Curr Alzheimer Res* 2018;15(14):1304–1321. doi:10.2174/1567205015666180904150118, PMID:30182853.
- [106] Rosen RF, Walker LC, Levine H 3rd. PIB binding in aged primate brain: enrichment of high-affinity sites in humans with Alzheimer's disease. *Neurobiol Aging* 2011;32(2):223–234. doi:10.1016/j.neurobiolaging.2009.02.011S0197-4580(09)00046-3, PMID:19329226.
- [107] Hostetler ED, Sanabria-Bohórquez S, Fan H, Zeng Z, Gammage L, Miller P, *et al*. [18F]Fluoroazabenzoxazoles as potential amyloid plaque PET tracers: synthesis and in vivo evaluation in rhesus monkey. *Nucl Med Biol* 2011;38(8):1193–1203. doi:10.1016/j.nucmedbio.2011.04.004, PMID:21741254.
- [108] Hillmer AT, Li S, Zheng MQ, Scheunemann M, Lin SF, Nabulsi N, *et al*. PET imaging of  $\alpha(7)$  nicotinic acetylcholine receptors: a comparative study of [(18)F]ASEM and [(18)F]DBT-10 in nonhuman primates, and further evaluation of [(18)F]ASEM in humans. *Eur J Nucl Med Mol Imaging* 2017;44(6):1042–1050. doi:10.1007/s00259-017-3621-8, PMID:28120003.
- [109] Gary C, Lam S, Hérard AS, Koch JE, Petit F, Gipchtein P, *et al*. Encephalopathy induced by Alzheimer brain inoculation in a non-human primate. *Acta Neuropathol Commun* 2019;7(1):126. doi:10.1186/s40478-019-0771-x, PMID:31481130.
- [110] Heuer E, Jacobs J, Du R, Wang S, Keifer OP, Cintron AF, *et al*. Amyloid-Related Imaging Abnormalities in an Aged Squirrel Monkey with Cerebral Amyloid Angiopathy. *J Alzheimers Dis* 2017;57(2):519–530. doi:10.3233/JAD-160981, PMID:28269776.
- [111] Nakamura T, Dinh TH, Asai M, Nishimaru H, Matsumoto J, Takamura Y, *et al*. Non-invasive electroencephalographical (EEG) recording system in awake monkeys. *Heliyon* 2020;6(5):e04043. doi:10.1016/j.heliyon.2020.e04043, PMID:32490247.
- [112] Chen JA, Fears SC, Jasinska AJ, Huang A, Al-Sharif NB, Scheibel KE, *et al*. Neurodegenerative disease biomarkers A $\beta$ (1-40), A $\beta$ (1-42), tau, and p-tau(181) in the vervet monkey cerebrospinal fluid: Relation to normal aging, genetic influences, and cerebral amyloid angiopathy. *Brain Behav* 2018;8(2):e00903. doi:10.1002/brb3.903, PMID:29484263.
- [113] Li ZH, He XP, Li H, He RQ, Hu XT. Age-associated changes in amyloid- $\beta$  and formaldehyde concentrations in cerebrospinal fluid of rhesus monkeys. *Zool Res* 2020;41(4):444–448. doi:10.24272/j.issn.2095-8137.2020.088, PMID:32543791.
- [114] Souder DC, Dreischmeier IA, Smith AB, Wright S, Martin SA, Sagar MAK, *et al*. Rhesus monkeys as a translational model for late-onset Alzheimer's disease. *Aging Cell* 2021;20(6):e13374. doi:10.1111/ace1.13374, PMID:33951283.
- [115] Batterman KV, Cabrera PE, Moore TL, Rosene DL. T Cells Actively Infiltrate the White Matter of the Aging Monkey Brain in Relation to Increased Microglial Reactivity and Cognitive Decline. *Front Immunol* 2021;12:607691. doi:10.3389/fimmu.2021.607691, PMID:33664743.
- [116] Nagahara AH, Merrill DA, Coppola G, Tsukada S, Schroeder BE, Shaked GM, *et al*. Neuroprotective effects of brain-derived neurotrophic factor in rodent and primate models of Alzheimer's disease. *Nat Med* 2009;15(3):331–337. doi:10.1038/nm.1912, PMID:19198615.
- [117] Eberling JL, Roberts JA, Rapp PR, Tuszyński MH, Jagust WJ. Cerebral glucose metabolism and memory in aged rhesus macaques. *Neurobiol Aging* 1997;18(4):437–443. doi:10.1016/S0197-4580(97)00040-7, PMID:9330976.
- [118] Plagenhoef MR, Callahan PM, Beck WD, Blake DT, Terry AV Jr. Aged rhesus monkeys: Cognitive performance categorizations and preclinical drug testing. *Neuropharmacology* 2021;187:108489. doi:10.1016/j.neuropharm.2021.108489, PMID:33561449.
- [119] Herndon JG, Moss MB, Rosene DL, Killiany RJ. Patterns of cognitive decline in aged rhesus monkeys. *Behav Brain Res* 1997;87(1):25–34. doi:10.1016/S0166-4328(96)02256-5, PMID:9331471.
- [120] Moore TL, Killiany RJ, Herndon JG, Rosene DL, Moss MB. Impairment in abstraction and set shifting in aged rhesus monkeys. *Neurobiol Aging* 2003;24(1):125–134. doi:10.1016/S0197-4580(02)00054-4, PMID:12493558.
- [121] Moore TL, Schettler SP, Killiany RJ, Herndon JG, Luebke JJ, Moss MB, *et al*. Cognitive impairment in aged rhesus monkeys associated with monoamine receptors in the prefrontal cortex. *Behav Brain Res* 2005;160(2):208–221. doi:10.1016/j.bbr.2004.12.003, PMID:15863218.
- [122] Picq JL, Aujard F, Volk A, Dhenain M. Age-related cerebral atrophy in

- nonhuman primates predicts cognitive impairments. *Neurobiol Aging* 2012;33(6):1096–1109. doi:10.1016/j.neurobiolaging.2010.09.009, PMID:20970891.
- [123] Rahman A, Lamberty Y, Schenker E, Cella M, Languille S, Bordet R, *et al*. Effects of acute administration of donepezil or memantine on sleep-deprivation-induced spatial memory deficit in young and aged non-human primate grey mouse lemurs (*Microcebus murinus*). *PLoS One* 2017;12(9):e0184822. doi:10.1371/journal.pone.0184822, PMID:28922421.
- [124] Joly M, Ammersdörfer S, Schmidtke D, Zimmermann E. Touch-screen-based cognitive tasks reveal age-related impairment in a primate aging model, the grey mouse lemur (*Microcebus murinus*). *PLoS One* 2014;9(10):e109393. doi:10.1371/journal.pone.0109393, PMID:25299046.
- [125] Easton A, Parker K, Derrington AM, Parker A. Behaviour of marmoset monkeys in a T-maze: comparison with rats and macaque monkeys on a spatial delayed non-match to sample task. *Exp Brain Res* 2003;150(1):114–116. doi:10.1007/s00221-003-1409-5, PMID:12698223.
- [126] Lai ZC, Moss MB, Killiany RJ, Rosene DL, Herndon JG. Executive system dysfunction in the aged monkey: spatial and object reversal learning. *Neurobiol Aging* 1995;16(6):947–954. doi:10.1016/0197-4580(95)02014-4, PMID:8622786.
- [127] Lyons DM, Lopez JM, Yonutas HM, Haghnazar H, Gash DM, Zhang Z, *et al*. Decreased mitochondrial bioenergetics and calcium buffering capacity in the basal ganglia correlates with motor deficits in a non-human primate model of aging. *Neurobiol Aging* 2015;36(5):1903–1913. doi:10.1016/j.neurobiolaging.2015.01.018, PMID:25726361.
- [130] Shively CA, Willard SL, Register TC, Bennett AJ, Pierre PJ, Laudenslager ML, *et al*. Aging and physical mobility in group-housed Old World monkeys. *Age (Dordr)* 2012;34(5):1123–1131. doi:10.1007/s11357-011-9350-1, PMID:22203457.
- [131] Uzuogunam BC, Librizzi D, Hooshyar Yousefi B. PET Radiopharmaceuticals for Alzheimer's Disease and Parkinson's Disease Diagnosis, the Current and Future Landscape. *Molecules* 2020;25(4):977. doi:10.3390/molecules25040977, PMID:32098280.
- [132] Xu Y, Wang C, Wey HY, Liang Y, Chen Z, Choi SH, *et al*. Molecular imaging of Alzheimer's disease-related gamma-secretase in mice and nonhuman primates. *J Exp Med* 2020;217(12):e20182266. doi:10.1084/jem.20182266, PMID:32936886.
- [133] Ni R. Positron Emission Tomography in Animal Models of Alzheimer's Disease Amyloidosis: Translational Implications. *Pharmaceuticals (Basel)* 2021;14(11):1179. doi:10.3390/ph14111179, PMID:34832961.
- [134] Tsukada H, Nishiyama S, Ohba H, Kanazawa M, Kakiuchi T, Harada N. Comparing amyloid- $\beta$  deposition, neuroinflammation, glucose metabolism, and mitochondrial complex I activity in brain: a PET study in aged monkeys. *Eur J Nucl Med Mol Imaging* 2014;41(11):2127–2136. doi:10.1007/s00259-014-2821-8, PMID:24919653.
- [135] Nishiyama S, Ohba H, Kanazawa M, Kakiuchi T, Tsukada H. Comparing  $\alpha 7$  nicotinic acetylcholine receptor binding, amyloid- $\beta$  deposition, and mitochondria complex-I function in living brain: A PET study in aged monkeys. *Synapse* 2015;69(10):475–483. doi:10.1002/syn.21842, PMID:26234533.
- [136] Nabulsi NB, Holden D, Zheng MQ, Bois F, Lin SF, Najafzadeh S, *et al*. Evaluation of (11)C-LSN3172176 as a Novel PET Tracer for Imaging M(1) Muscarinic Acetylcholine Receptors in Nonhuman Primates. *J Nucl Med* 2019;60(8):1147–1153. doi:10.2967/jnumed.118.222034, PMID:30733324.
- [137] Naganawa M, Nabulsi N, Henry S, Matuskey D, Lin SF, Slieker L, *et al*. First-in-Human Assessment of (11)C-LSN3172176, an M1 Muscarinic Acetylcholine Receptor PET Radiotracer. *J Nucl Med* 2021;62(4):553–560. doi:10.2967/jnumed.120.246967, PMID:32859711.
- [138] Ozenil M, Aronow J, Millard M, Langer T, Wadsak W, Hacker M, *et al*. Update on PET Tracer Development for Muscarinic Acetylcholine Receptors. *Pharmaceuticals (Basel)* 2021;14(6):530. doi:10.3390/ph14060530, PMID:34199622.
- [139] Damuka N, Czoty PW, Davis AT, Nader MA, Nader SH, Craft S, *et al*. PET Imaging of [(11)C]MPC-6827, a Microtubule-Based Radiotracer in Non-Human Primate Brains. *Molecules* 2020;25(10):2289. doi:10.3390/molecules25102289, PMID:32414052.
- [140] Du Y, Minn I, Foss C, Lesniak WG, Hu F, Dannals RF, *et al*. PET imaging of soluble epoxide hydrolase in non-human primate brain with [(18)F]FNDP. *EJNMMI Res* 2020;10(1):67. doi:10.1186/s13550-020-00657-7, PMID:32572592.
- [141] Lemere CA, Beierschmitt A, Iglesias M, Spooner ET, Bloom JK, Leverone JF, *et al*. Alzheimer's disease abeta vaccine reduces central nervous system abeta levels in a non-human primate, the Caribbean vervet. *Am J Pathol* 2004;165(1):283–297. doi:10.1016/S0002-9440(10)63296-8, PMID:15215183.
- [142] Trouche SG, Asuni A, Rouland S, Wisniewski T, Frangione B, Verdier JM, *et al*. Antibody response and plasma Abeta1-40 levels in young *Microcebus murinus* primates immunized with Abeta1-42 and its derivatives. *Vaccine* 2009;27(7):957–964. doi:10.1016/j.vaccine.2008.12.012S0264-410X(08)01724-6, PMID:19114076.
- [143] Yano A, Ito K, Miwa Y, Kanazawa Y, Chiba A, Iigo Y, *et al*. The Peptide Vaccine Combined with Prior Immunization of a Conventional Diphtheria-Tetanus Toxoid Vaccine Induced Amyloid  $\beta$  Binding Antibodies on *Cynomolgus* Monkeys and Guinea Pigs. *J Immunol Res* 2015;2015:786501. doi:10.1155/2015/786501, PMID:26539559.
- [144] Vukicevic M, Fiorini E, Siegert S, Carpintero R, Rincon-Restrepo M, Lopez-Deber P, *et al*. An amyloid beta vaccine that safely drives immunity to a key pathological species in Alzheimer's disease: pyroglutamate amyloid beta. *Brain Commun* 2022;4(1):fcac022. doi:10.1093/braincomms/fcac022, PMID:35479516.
- [145] Kofler J, Lopresti B, Janssen C, Trichel AM, Maslah E, Finn OJ, *et al*. Preventive immunization of aged and juvenile non-human primates to  $\beta$ -amyloid. *J Neuroinflammation* 2012;9:84. doi:10.1186/1742-2094-9-84, PMID:22554253.
- [146] Vaz M, Silvestre S. Alzheimer's disease: Recent treatment strategies. *Eur J Pharmacol* 2020;887:173554. doi:10.1016/j.ejphar.2020.173554, PMID:32941929.
- [147] Zheng H, Niu S, Zhao H, Li S, Jiao J. Donepezil improves the cognitive impairment in a tree shrew model of Alzheimer's disease induced by amyloid- $\beta$ (1-40) via activating the BDNF/TrkB signal pathway. *Metab Brain Dis* 2018;33(6):1961–1974. doi:10.1007/s11011-018-0303-6, PMID:30105614.
- [148] Li Y, Laws SM, Miles LA, Wiley JS, Huang X, Masters CL, *et al*. Genomics of Alzheimer's disease implicates the innate and adaptive immune systems. *Cell Mol Life Sci* 2021;78(23):7397–7426. doi:10.1007/s00018-021-03986-5, PMID:34708251.
- [149] Boado RJ, Lu JZ, Hui EK, Pardridge WM. IgG-single chain Fv fusion protein therapeutic for Alzheimer's disease: Expression in CHO cells and pharmacokinetics and brain delivery in the rhesus monkey. *Biotechnol Bioeng* 2010;105(3):627–635. doi:10.1002/bit.22576, PMID:19816967.
- [150] Gao L, Zhang Y, Sterling K, Song W. Brain-derived neurotrophic factor in Alzheimer's disease and its pharmaceutical potential. *Transl Neurodegener* 2022;11(1):4. doi:10.1186/s40035-022-00279-0, PMID:35090576.
- [151] Lange HS, Vardigan JD, Cannon CE, Puri V, Henze DA, Uslander JM. Effects of a novel M4 muscarinic positive allosteric modulator on behavior and cognitive deficits relevant to Alzheimer's disease and schizophrenia in rhesus monkey. *Neuropharmacology* 2021;197:108754. doi:10.1016/j.neuropharm.2021.108754, PMID:34389398.
- [152] Pushpakom S, Iorio F, Eyers PA, Escott KJ, Hopper S, Wells A, *et al*. Drug repurposing: progress, challenges and recommendations. *Nat Rev Drug Discov* 2019;18(1):41–58. doi:10.1038/nrd.2018.168, PMID:30310233.
- [153] Lee HJ, Seo HI, Cha HY, Yang YJ, Kwon SH, Yang SJ. Diabetes and Alzheimer's Disease: Mechanisms and Nutritional Aspects. *Clin Nutr Res* 2018;7(4):229–240. doi:10.7762/cnr.2018.7.4.229, PMID:30406052.
- [154] Batista AF, Forny-Germano L, Clarke JR, Lyra E Silva NM, Brito-Moreira J, Boehnke SE, *et al*. The diabetes drug liraglutide reverses cognitive impairment in mice and attenuates insulin receptor and


- synaptic pathology in a non-human primate model of Alzheimer's disease. *J Pathol* 2018;245(1):85–100. doi:10.1002/path.5056, PMID: 29435980.
- [155] Blackburn JK, Jamwal S, Wang W, Elsworth JD. Pioglitazone transiently stimulates paraoxonase-2 expression in male nonhuman primate brain: Implications for sex-specific therapeutics in neurodegenerative disorders. *Neurochem Int* 2022;152:105222. doi:10.1016/j.neuint.2021.105222, PMID:34767873.
- [156] Li Y, Huang X, Fowler C, Lim YY, Laws SM, Faux N, *et al*. Identification of Leukocyte Surface P2X7 as a Biomarker Associated with Alzheimer's Disease. *Int J Mol Sci* 2022;23(14):7867. doi:10.3390/ijms23147867, PMID:35887215.
- [157] Huang X, Li Y, Fowler C, Doecke JD, Lim YY, Drysdale C, *et al*. Leukocyte surface biomarkers implicate deficits of innate immunity in sporadic Alzheimer's disease. *Alzheimers Dement* 2022. doi:10.1002/alz.12813, PMID:36349985.
- [158] Sachdeva D, Burns A. Dimebolin in dementia. *CNS Neurosci Ther* 2011;17(3):199–205. doi:10.1111/j.1755-5949.2010.00156.x, PMID: 20553307.
- [159] Webster SJ, Wilson CA, Lee CH, Mohler EG, Terry AV Jr, Buccafusco JJ. The acute effects of dimebolin, a potential Alzheimer's disease treatment, on working memory in rhesus monkeys. *Br J Pharmacol* 2011;164(3):970–978. doi:10.1111/j.1476-5381.2011.01432.x, PMID:21486290.
- [160] Ling IF, Golde TE, Galasko DR, Koo EH. Modulation of A $\beta$ 42 in vivo by  $\gamma$ -secretase modulator in primates and humans. *Alzheimers Res Ther* 2015;7(1):55. doi:10.1186/s13195-015-0137-y137, PMID:26244059.
- [161] Dokmeci D. Ibuprofen and Alzheimer's disease. *Folia Med (Plovdiv)* 2004;46(2):5–10. PMID:15506544.
- [162] Bhatti GK, Reddy AP, Reddy PH, Bhatti JS. Lifestyle Modifications and Nutritional Interventions in Aging-Associated Cognitive Decline and Alzheimer's Disease. *Front Aging Neurosci* 2019;11:369. doi:10.3389/fnagi.2019.00369, PMID:31998117.
- [163] Qin W, Chachich M, Lane M, Roth G, Bryant M, de Cabo R, *et al*. Calorie restriction attenuates Alzheimer's disease type brain amyloidosis in Squirrel monkeys (*Saimiri sciureus*). *J Alzheimers Dis* 2006;10(4):417–422. doi:10.3233/jad-2006-10411, PMID:17183154.
- [164] Willette AA, Coe CL, Colman RJ, Bendlin BB, Kastman EK, Field AS, *et al*. Calorie restriction reduces psychological stress reactivity and its association with brain volume and microstructure in aged rhesus monkeys. *Psychoneuroendocrinology* 2012;37(7):903–916. doi:10.1016/j.psyneuen.2011.10.006, PMID:22119476.
- [165] Cox PA, Davis DA, Mash DC, Metcalf JS, Banack SA. Dietary exposure to an environmental toxin triggers neurofibrillary tangles and amyloid deposits in the brain. *Proc Biol Sci* 2016;283:1823. doi:10.1098/rspb.2015.2397, PMID:26791617.
- [166] Cox PA, Metcalf JS. Traditional Food Items in Ogimi, Okinawa: L-Serine Content and the Potential for Neuroprotection. *Curr Nutr Rep* 2017;6(1):24–31. doi:10.1007/s13668-017-0191-0, PMID:28331770.
- [167] Frye BM, Craft S, Register TC, Andrews RN, Appt SE, Vitolins MZ, *et al*. Diet, psychosocial stress, and Alzheimer's disease-related neuroanatomy in female nonhuman primates. *Alzheimers Dement* 2021;17(5):733–744. doi:10.1002/alz.12232, PMID:33270373.
- [168] Li J, Huang Q, Chen J, Qi H, Liu J, Chen Z, *et al*. Neuroprotective Potentials of Panax Ginseng Against Alzheimer's Disease: A Review of Preclinical and Clinical Evidences. *Front Pharmacol* 2021;12:688490. doi:10.3389/fphar.2021.688490, PMID:34149431.
- [169] Wang L, Lu J, Zeng Y, Guo Y, Wu C, Zhao H, *et al*. Improving Alzheimer's disease by altering gut microbiota in tree shrews with ginsenoside Rg1. *FEMS Microbiol Lett* 2020;367(4):fnaa011. doi:10.1093/femsle/fnaa011, PMID:31950993.
- [170] Guo Y, Wang L, Lu J, Jiao J, Yang Y, Zhao H, *et al*. Ginsenoside Rg1 improves cognitive capability and affects the microbiota of large intestine of tree shrew model for Alzheimer's disease. *Mol Med Rep* 2021;23(4):291. doi:10.3892/mmr.2021.11931, PMID:33649817.
- [171] Yang Y, Wang L, Zhang C, Guo Y, Li J, Wu C, *et al*. Ginsenoside Rg1 improves Alzheimer's disease by regulating oxidative stress, apoptosis, and neuroinflammation through Wnt/GSK-3 $\beta$ / $\beta$ -catenin signaling pathway. *Chem Biol Drug Des* 2022;99(6):884–896. doi:10.1111/cbdd.14041, PMID:35313087.



## Review Article

# Brief Insight on Nanovesicular Liposomes as Drug-delivery Carriers for Medical Applications



Madhavi Pravinkumar Chudasma, Sakshi Alpeshkumar Shah, Mohammad Hamran Nasiruddin Qureshi, Nirav Shah, Devarshi Shah, Riddhi Trivedi and Viral Hareshkumar Shah\* 

Department of Pharmaceutics, Sal Institute of Pharmacy, Ahmedabad, India

Received: November 16, 2022 | Revised: January 09, 2023 | Accepted: February 02, 2023 | Published online: April 27, 2023

### Abstract

Nanotechnology has revolutionized and improved the potential of drug-delivery systems. Lipidic nanovesicles, termed liposomes, offer several benefits as drug-delivery carriers due to their compositional similarity with human biological membranes. Some of the advantages offered by liposomes include targeted drug delivery and improved pharmacokinetics of an entrapped drug substance, leading to enhanced bioavailability. Additionally, the reduction in the drug dose or dosing frequency, reduced drug toxicity or side effects, longer and controlled therapeutic response of a drug essential for the treatment of chronic diseases, and improved patient acceptance margins are some other benefits offered by liposomes. The easily modifiable surface of liposomes makes it an ideal vehicle for targeting a drug to the desired site. The current review provides insight on liposomes as drug-delivery carriers. This review summarizes the classification of compositional constituents of liposomes based on their chemical nature and structure. Morphology-based classification of liposomes along with methods of preparation and characterization for liposomes are also summarized. The current review emphasizes the medical applications of liposomes, specifically as delivery carriers for therapeutic and diagnostic agents. The article features detailed therapeutic applications of liposomes based on routes of administration and specific disease conditions. Diagnostic applications of liposomes for improving the efficiency of available techniques to treat diseases such as cancer are also discussed. Liposomes are thus reviewed as multifaceted nanovesicular carriers with potential therapeutic and diagnostic medical applications. The prospective multifunctional application of combining imaging functionality with therapeutic agents in a single liposome for diagnosis and real-time treatment is anticipated to be the future of liposomal formulations.

### Introduction

The efficacy of a drug substance for the treatment, mitigation, management, or prevention of disease conditions or disorders relies upon its therapeutic efficiency, low exhibition of toxic or side effects at the required therapeutic dose or dosing frequency, and ability to reach the desired target site at the effective concentration as well as to stay at that target site for the desired time length. Due to restrictions in allowed structural modifications of drug substances required to achieve the desired pharmacokinetic properties while maintaining its thera-

peutic action, the role of drug deliverables is prominent and indispensable for achieving the desired therapeutic response of drug substances in low doses, for longer duration, and with reduced side effects. Nanotechnology has revolutionized the potential of drug deliverables in delivering the drug substances at the desired target site in therapeutic doses with improved pharmacokinetic properties of adsorption, distribution, metabolism, and excretion, which ultimately affect the bioavailability of drug substances. Reduction in drug toxicity or side effects by decreasing its dose or dosing frequency, targeting the drug to the desired site, controlling the action of drug substances desired to treat chronic disease or disorders, and improving patients' compliance are some added benefits of nanotechnology. Amongst the nanoparticle drug-delivery carriers, vesicular drug-delivery systems, particularly lipid-based vesicular systems that encapsulate the drug substance in the core or within the matrix of phospholipids, are gaining attention because of several of their advantages, which are compiled and summarized in the current review paper.

The first and most widely explored lipid vesicle-based nanodrug-delivery carrier is popularly known as liposomes. The notion of liposomes, which were initially known to be “bangosomes,” was

**Keywords:** Vesicular drug-delivery system; Nanocarriers; Liposomes; Phospholipids; Therapeutic applications; Diagnostic applications.

**Abbreviations:** BBB, blood-brain barrier; PDI, polydispersity index.

\*Correspondence to: Viral Hareshkumar Shah, Department of Pharmaceutics, Sal Institute of Pharmacy, Ahmedabad 380060, India. ORCID: <https://orcid.org/0000-0003-4740-0856>. Tel: +91-9277202747, Fax: +91-079-67129000, E-mail: [viralshah779@yahoo.com](mailto:viralshah779@yahoo.com)

**How to cite this article:** Chudasma MP, Shah SA, Qureshi MHN, Shah N, Shah D, Trivedi R, et al. Brief Insight on Nanovesicular Liposomes as Drug-delivery Carriers for Medical Applications. *J Explor Res Pharmacol* 2023;8(3):222–236. doi: 10.14218/JERP.2022.00086.



pioneered by Alec D. Bangham between the 1950s and 1960s, and they received recognition as drug-delivery carriers in 1971 by the scientist Gregory Gregoriadis. Liposomes, which are composed of closed bilayers of phospholipids to form a vesicle, exhibit significant structural and compositional similarities to biological membranes prevailing in the human body; thus, liposomes enhance the adsorption rate and bioavailability of drug substances entrapped in their vesicular structure. In addition, the easily modifiable surface properties of liposomes make it a potential drug-delivery vehicle for achieving targeted therapeutic activity of drug substances. Currently, liposomal formulations of antifungal agents and anticancer chemotherapeutic agents for tumor targeting have exhibited considerable benefits over conventional therapies. More recently, mucormycosis, a fatal fungal infection, has been demonstrated to be managed significantly better through liposomal delivery of amphotericin B (antifungal drug substance) in comparison to any other drug-delivery system.<sup>1</sup> The potential of liposomes has been explored and proven in medical as well as in nonmedical fields like catalysts, bioreactors, ecology, cosmetics, etc.<sup>2</sup>

## Composition of liposomes

### Phospholipids

Phospholipids are the building block and basic structural component of liposomes. A bilayer of phospholipids constitutes the shell of vesicular liposomes. Based on the desired properties and applications, different types and classes of phospholipids are used for formulating liposomes.

### Classification of phospholipids based on their internal composition (alcohol active group)

Glycerophospholipids are phospholipids with a glycerol backbone, comprised of glycerol-3-phosphate esterification at the C1 and C2 positions. There are six different subtypes of glycerophospholipids, including phosphatidic acid, lecithin (phosphatidylcholine), cephalin (phosphatidylethanolamine), phosphatidylinositol, phosphatidylserine, and cardiopolin (diphosphatidylglycerol).<sup>3</sup>

Phosphatidic acid is the smallest and most basic glycerol phospholipid. It has a strong anion that provides a negative charge density to the membrane. Phosphatidic acid is a synthetic phospholipid with several possible derivatives (Table 1), which can be synthesized according to the required application.<sup>4</sup>

Lecithin is an egg yolk-derived natural choline-based phospholipid. It is a zwitterionic molecule, consisting of partial positive and negative charges. This phospholipid has a major influence on membrane properties such as “fluidity.” There are two types of lecithin: dipalmitoyl lecithin and lysolecithin. The structures and chemical names of several lecithin derivatives synthesized according to their applications are depicted in Table 1.

The naming of cephalins was derived from the word cephalic, meaning “related to the head.” The polar head group of cephalins is highly reactive and small in size; therefore, this type of compound has a low hydration rate. Cephalins are synthesized by adding cytidine diphosphate ethanolamine to diglyceride. Cephalins can be treated with ethanolamine, which consists of a reactive nitrogen base, to further synthesize several other derivatives for varied applications. Several derivatives of cephalins are as follows: 1,2-dierucoyl-*sn*-glycero-3-phosphoethanolamine, 1,2-dilauroyl-*sn*-glycero-3-phosphoethanolamine, 1,2-dimyristoyl-*sn*-glycero-3-phosphoethanolamine, 1,2-dipalmitoyl-*sn*-glycero-3-phosphoethanolamine, 1,2-distearoyl-*sn*-glycero-3-phosphoethanolamine,

1,2-dioleoyl-*sn*-glycero-3-phosphoethanolamine, and 1-palmitoyl-2-oleoyl-*sn*-glycero-3-phosphoethanolamine.

Phosphatidylinositol is synthesized by the reaction between the isomeric form of myo-inositol and phosphatidic acid. Inositol is present in all types of tissues as well as in cells and has a saturated fatty acid chain. Phosphatidylinositol is anionic in nature.

Phosphatidylserine is a synthetic phospholipid. Serine is anionic in nature, and derivatives of phosphatidylserine include the following: 1,2-dilauroyl-*sn*-glycero-3-phosphoserine, 1,2-dimyristoyl-*sn*-glycero-3-phosphoserine, 1,2-dioleoyl-*sn*-glycero-3-phosphoserine, 1,2-dipalmitoyl-*sn*-glycero-3-phosphoserine, and 1,2-distearoyl-*sn*-glycero-3-phosphoserine.

Cardiolipin contains two molecules of phosphatidic glycerol. It consists of two optically active carbons and also has a number of unsaturated fatty acid chains. Several derivatives of cardiolipin are as follow: 1,2-dierucoyl-*sn*-glycero-3 [phospho-rac-(1-glycerol)], 1,2-dilauroyl-*sn*-glycero-3 [phospho-rac-(1-glycerol)], 1,2-dilauroyl-*sn*-glycero-3 [phospho-rac-(1-glycerol)] (ammonium salt), 1,2-dimyristoyl-*sn*-glycero-3 [phospho-rac-(1-glycerol)], 1,2-dimyristoyl-*sn*-glycero-3 [phospho-rac-(1-glycerol)] (ammonium salt), 1,2-dioleoyl-*sn*-glycero-3 [phospho-rac-(1-glycerol)], 1,2-dipalmitoyl-*sn*-glycero-3 [phospho-rac-(1-glycerol)], 1,2-dipalmitoyl-*sn*-glycero-3 [phospho-rac-(1-glycerol)] (ammonium salt), 1,2-distearoyl-*sn*-glycero-3 [phospho-rac-(1-glycerol)], 1,2-distearoyl-*sn*-glycero-3 [phospho-rac-(1-glycerol)] (ammonium salt), and 1-palmitoyl-2-oleoyl-*sn*-glycero-3 [phospho-rac-(1-glycerol)].

Chemically, sphingomyelins are *N*-acyl sphingosine-1-phosphatidylcholine. The backbone of sphingomyelins is sphingosine. Each molecule of sphingomyelin consists of an acyl chain. Generally, naturally obtained sphingosines contain 20 or more acyl groups. Therefore, the structure of sphingomyelin molecules is asymmetric. The phase-transition temperature of sphingomyelins ranges from 30°C to 45°C.

### Classification of phospholipids based on surface charges

Anionic phospholipids are negatively charged phospholipids that resemble the biological membrane proteins. Phosphatidic acid, phosphatidylinositol, and phosphatidylserine are some examples of anionic phospholipids.

Cationic phospholipids are positively charged phospholipids that help to deliver negatively charged nucleic acids like DNA, mRNA, and siRNA by ionic interactions. Dioleoyl phosphatidylethanolamine and 1,2-dioleoyl-3-trimethylammonium propane are two examples of cationic phospholipids.

### Classification of phospholipids based on its origin source

Natural phospholipids are obtained from natural sources like wheat germ, flax seed, sunflower, soybeans, egg yolk, and milk. Meanwhile, synthetic or semisynthetic phospholipids are tailor made, chemically synthesised phospholipids. Some examples of synthetic phospholipids are 1,2-dimyristoyl-*sn*-glycero-3-phosphate, 1,2-dipalmitoyl-*sn*-glycero-3-phosphate, dipalmitoylphosphatidylcholine, 1,2-dilauroyl-*sn*-glycero-3-phosphocholine, dimyristoylphosphatidylglycerol, 1,2-dipalmitoyl-*sn*-glycero-3-phosphoglycerol, sodium salt, etc.

### Classification of phospholipids based on the fatty acid chain saturation

Saturated chain fatty acids exhibit comparatively more chemical stability against oxidation and hydrolysis. Some examples of saturated fatty acids include 1,2-dimyristoyl-*sn*-glycero-3-phosphate,



**Table 1. Phospholipids used in liposomal formulations along with the chemical name and structure<sup>4</sup>**

Phospholipid	Structure and chemical name	
Phosphatidic acid	1,2-Dioleoyl- <i>sn</i> -glycero-3-phosphate (DOPA)	1,2-Dilauroyl- <i>sn</i> -glycero-3-phosphate (DLPA)
	1,2-Dimyristoyl- <i>sn</i> -glycero-3-phosphate (DMPA)	1,2-Distearoyl- <i>sn</i> -glycero-3-phosphate (DSPA)
	1,2-Dipalmitoyl- <i>sn</i> -glycero-3-phosphate (DPPA)	
Lecithin	1,2-Didecanoyl- <i>sn</i> -glycero-3-phosphocholine (DDPC)	1,2-Dierucoyl- <i>sn</i> -glycero-3-phosphocholine (DEPC)
	1,2-Dilinoleoyl- <i>sn</i> -glycero-3-phosphocholine (DLOPC)	1,2-Dilauroyl- <i>sn</i> -glycero-3-phosphocholine (DLPC)
	1,2-Dimyristoyl- <i>sn</i> -glycero-3-phosphocholine (DMPC)	1,2-Dioleoyl- <i>sn</i> -glycero-3-phosphocholine (DOPC)
	1,2-Dipalmitoyl- <i>sn</i> -glycero-3-phosphocholine (DPPC)	1,2-Distearoyl- <i>sn</i> -glycero-3-phosphocholine (DSPC)
	1-Palmitoyl-2-oleoyl- <i>sn</i> -glycero-3-phosphocholine (POPC)	1,2-Dierucoyl- <i>sn</i> -glycero-3-phosphocholine (DEPC)
Cephalin (phosphatidyl ethanolamine)	1,2-Dilauroyl- <i>sn</i> -glycero-3-phosphoethanolamine (DLPE)	1,2-Dimyristoyl- <i>sn</i> -glycero-3-phosphoethanolamine (DMPE)
	1,2-Dipalmitoyl- <i>sn</i> -glycero-3-phosphoethanolamine (DPPE)	1,2-Dioleoyl- <i>sn</i> -glycero-3-phosphoethanolamine (DOPE)
	1-Palmitoyl-2-oleoyl- <i>sn</i> -glycero-3-phosphoethanolamine (POPE)	1,2-Dierucoyl- <i>sn</i> -glycero-3-phosphoethanolamine (DEPE)
	1,2-Distearoyl- <i>sn</i> -glycero-3-phosphoethanolamine (DSPE)	
Cardiolipin	1,2-Dierucoyl- <i>sn</i> -glycero-3[phospho-rac-(1-glycerol) (DEPG)	1,2-Dilauroyl- <i>sn</i> -glycero-3[phospho-rac-(1-glycerol) (ammonium salt) (DLPG-NH <sub>4</sub> )
	1,2-Dimyristoyl- <i>sn</i> -glycero-3[phospho-rac-(1-glycerol) (DMPG)	1,2-Dioleoyl- <i>sn</i> -glycero-3[phospho-rac-(1-glycerol) (DOPG)
	1,2-Dipalmitoyl- <i>sn</i> -glycero-3[phospho-rac-(1-glycerol) (ammonium salt) (DPPG-NH <sub>4</sub> )	1,2-Distearoyl- <i>sn</i> -glycero-3[phospho-rac-(1-glycerol) (ammonium salt) (DSPG-NH <sub>4</sub> )
	1-Palmitoyl-2-oleoyl- <i>sn</i> -glycero-3[phospho-rac-(1-glycerol) (POPG)	
Phosphatidyl serine (PS)	1,2-Dilauroyl- <i>sn</i> -glycero-3-phosphoserine (DLPS)	1,2-Dimyristoyl- <i>sn</i> -glycero-3-phosphoserine (DMPS)
	1,2-Dioleoyl- <i>sn</i> -glycero-3-phosphoserine (DOPS)	1,2-Dipalmitoyl- <i>sn</i> -glycero-3-phosphoserine (DPPS)
	1,2-Distearoyl- <i>sn</i> -glycero-3-phosphoserine (DSPS)	

1,2-dipalmitoyl-*sn*-glycero-3-phosphate, 1,2-distearoyl-*sn*-glycero-3-phosphate, 1,2-dilauroyl-*sn*-glycero-3-phosphocholine, and 1,2-dilauroyl-*sn*-glycero-3-phosphoethanolamine, etc.

Unsaturated chain fatty acids are more prone to oxidation and hydrolysis. Some examples of unsaturated fatty acids are; 1,2-dierucoyl-*sn*-glycero-3-phosphocholine, 1,2-dilinoleoyl-*sn*-glycero-3-phosphocholine, 1,2-dioleoyl-*sn*-glycero-3-phosphocholine, 1,2-dierucoyl-*sn*-glycero-3-phosphocholine, etc.

#### Classification of phospholipids based on morphology (shape)

Phospholipids can be classified based on their morphology as follows: conical shaped, e.g., lysophosphatidylcholine and lysophosphatidic acid; straight chain, e.g., phosphatidylcholine; and inverted conical shaped, e.g., phosphatidic acid and phosphatidylethanolamine.

#### Cholesterol

Along with phospholipids, cholesterol is an important component

of liposomes. It plays an important role in holding the tight vesicular structure of liposomes thereby maintaining vesicular integrity and stability. Due to its structural composition, cholesterol occupies the gaps between phospholipids in the vesicles, thereby preventing diffusion and leakage of entrapped components. Additionally, cholesterol can also increase the loading efficacy of both hydrophilic and lipophilic materials to be incorporated in liposomes.

#### Types of liposomes

Liposomes are categorized into different types mainly based on parameters like size of the vesicle, lamellarity, and composition of vesicles (Table 2).

#### Lamellarity-based classification

The number of bilayers present in liposomes determines the lamellarity of the vesicles. It is an important parameter that affects the

**Table 2. Classification of liposomes based on size, lamellarity, and composition**

Parameter	Size	Lipid bilayer
Size and lamellarity		
Small lamellar vesicles	20–100 nm	Single
Medium lamellar vesicles	>100 nm	Single
Large lamellar vesicles)	>100 nm	Single
Oligo lamellar vesicles	0.1–1 nm	5 lipid bilayers
Multilamellar vesicles	>0.5 $\mu$ m	5–25 lipid bilayers
Multivesicular vesicles	>1 mm	multi compartment (honeycomb like)
Application and composition		
Conventional liposomes		
Charged liposome		
Stealth stabilized liposomes		
Stimuli-responsive liposomes		
Actively-targeted liposomes		

encapsulation efficiency of liposomes. Based on lamellarity, the vesicles are classified as unilamellar vesicles (consisting of one phospholipid bilayer), oligolamellar vesicles (consisting of five phospholipid bilayers), and multilamellar vesicles (consisting of 5–25 phospholipid bilayers).

#### Size-based classification

The vesicle dimension is an acute parameter affecting the circulation half-life of liposomes in the human body. Based on the size of the liposomes, they are classified as small vesicles (with a vesicular diameter between 20 nm and 100 nm), medium vesicles (with a vesicular diameter >100 nm), or giant vesicles (with a vesicular diameter of 1  $\mu$ m).<sup>5</sup>

Liposomes are often classified based on a mixture of size and lamellarity parameters as follows: small unilamellar vesicles, with a diameter of 20–100 nm and one lipid bilayer; medium unilamellar vesicles, with a diameter of >100 nm and containing one lipid bilayer; giant unilamellar vesicles, with a diameter of 1  $\mu$ m and containing one lipid bilayer; oligolamellar vesicles, with a diameter of 0.1–1 nm and containing approximately five lipid bilayers; multilamellar large vesicles, with a diameter of >0.5  $\mu$ m and containing 5–25 lipid bilayers; and multivesicular vesicles, liposomes with a diameter of >1 mm and containing a multicompartiment (like a honeycomb) of lipid bilayers, e.g., vesicles within vesicles.<sup>5</sup>

#### Application- and composition-based classification

Conventional liposomes are liposomes that are usually composed of solely phospholipids and/or cholesterol. They are vesicular structures with lipid bilayers surrounding an aqueous core; they exhibit a brief blood circulation time due to the speedy uptake by the mononuclear phagocyte system, which in turn helps in macrophage-targeting and vaccination purposes.<sup>6</sup>

Charged liposomes are physically stabilized liposomes as the surface charges on the liposomes repel each other and decrease the aggregation rate and extent. Positively charged cationic liposomes avert their passive diffusion into cells; therefore, they are broadly used in delivering macromolecules for gene therapy, tumor-targeted therapy, and brain-targeted therapy by crossing the blood-brain barrier (BBB). Anionic liposomes are negatively charged and are

commonly utilized for transdermal drug transport due to their greater permeation rate across the stratum corneum.<sup>4</sup>

Stealth liposomes are surface-modified liposomes with a polymeric, specific ligand and polyethylene glycol (PEG) that are made for specific applications like targeting, stabilization, or an increased residence time in the human body.

Stimuli-responsive liposomes are liposomes that are activated by physicochemical or biochemical stimuli for targeting a specific site or for achieving a desired encapsulated drug release. Stimuli-responsive liposomes have two induction sources: external induction sources (like heat, magnetic field, light, electric field, and ultrasound) and internal induction sources (like pH, redox potential, and enzymes).

Actively-targeted liposomes are liposomes that are useful for the site-specific delivery of drugs through receptor targeting, monoclonal antibodies, or large or small protein-based targeting or peptide-based targeting molecules.

#### Mechanism of action of liposomes

##### Endocytosis

The liposome is engulfed by the cell membrane after binding to the cell surface through a receptor, ligand, or antibody. Liposomes release the entrapped drug after cellular engulfment; thus, first-pass metabolism of the drug is prevented.

##### Content transfer

Liposomes have a similar structure to human cell membranes, so the phospholipids of liposomes transfer their contents (drug substance) across the cell membrane after interacting with the cell membrane lipids.

##### Fusion

In this mechanism, the phospholipids of liposomes fuse with the phospholipids of the cell membrane, and during this fusion mechanism, the cell membrane and liposome lipids coalesce together in a single membrane, resulting in drug content transfer from the liposomes to the cells.

### Adsorption

In this process, liposomes adhere to the surface of the cell membrane through attractive forces between the liposomes and the cell membrane, followed by the release of drug from the liposomes and the uptake of unchanged drug by the cells.

#### Methods for preparing liposomes

For liposomal formulation preparation, the following generic steps are followed:<sup>4-8</sup> (1) lipids are dissolved in an organic solvent; (2) drug loading (active or passive); (3) evaporation of the organic solvent of the lipidic solution; (4) hydration of the lipid; (5) downsizing the vesicles; (6) post formulation process (purification, sterilization); (7) liposome characterization.

The most widely used techniques for liposome preparation are summarized below.

#### Bangham method (lipid film hydration)

The phospholipid components are dissolved in an organic solvent, and the organic solvent is gradually evaporated under a vacuum to obtain a uniform, thin lipid film of stacked phospholipid bilayers. The formed film is finally hydrated with water or an aqueous buffer to obtain liposomes.<sup>4</sup>

#### Solvent injection method

Phospholipids are dissolved in ethanol and injected into preheated aqueous buffer or distilled water. In a preheated aqueous phase, ethanol is evaporated and the dispersed phospholipids self-assemble to form closed vesicles called liposomes. Alternatively, phospholipids can be dissolved in ether, which is a more volatile organic solvent, and then the ether can be evaporated more effectively to form concentrated liposomes with a high entrapment efficiency.<sup>8</sup>

#### Reverse-phase evaporation method

The reverse-phase evaporation method is based on the principle of inverted micelle formation through reverse-phase evaporation. In this technique, phospholipids are dissolved in an organic phase, and aqueous components of liposomes are dissolved in a water phase. The formation of inverted micelles is the foundation of reverse-phase evaporation. Both the phases are then macerated together at a high temperature, leading to evaporation of the organic solvent and the formation of liposomes.<sup>8</sup>

#### Detergent removal method

Phospholipids are solubilized at their critical micelle concentrations with the aid of detergents to form micelles. The formed micelles acquire themselves into closed vesicles as the detergent is removed through dialysis using detergent-free buffers or through gel permeation chromatography. In this technique, when detergent and phospholipids are added to an aqueous phase, the micellar size and polydispersity increase significantly, and dilution of the system beyond the micellar phase boundary transit the polydisperse micelles to more uniform vesicles.

Once the liposomal vesicles are obtained by utilizing any of the abovementioned techniques, the desired size and lamellarity of the liposomes can be obtained using downsizing techniques such as sonication (probe or bath), extrusion (membrane or French cell), freeze thawing, etc.<sup>8</sup>

### Physical characterization of liposomes

The quality, efficiency, and stability of liposomes as a drug-delivery formulation can be assessed through several characterization

tests, as mentioned below:

#### Particle size, polydispersity index (PDI), lamellarity, and zeta potential

The particle size, lamellarity, and zeta potential properties depend on the composition components of the liposomes and the preparation method. The particle size, zeta potential, and PDI are important characterization parameters that have an impact on the physicochemical stability, entrapment efficiency, *in-vivo* performance, and heterogeneity of the liposomal formulation. The particle size, PDI, and zeta potential of liposomes can be determined by dynamic light-scattering techniques and laser Doppler velocimetry. Electron microscopy (e.g., scanning electron microscopy and transmission electron microscopy), fluorescence microscopy, and atomic force microscopy-based techniques can be used to assess the lamellarity and morphology of liposomes.<sup>9</sup> Liposomal formulations with PDI values less than 0.5 and a zeta potential of around  $+30 \pm 5$  mV and  $-30 \pm 5$  mV are considered as monodispersed liposomes with a good physicochemical stability.

#### Entrapment efficiency

The maximum amount of drug that can be encapsulated in a liposomal vesicle is termed as its entrapment efficiency. The entrapment efficiency of liposomes is determined by disruption of the phospholipid bilayer using methanol, ethanol, or triton X-100, followed by centrifugation and decantation of the entrapped drug in pellet form. The entrapped drug pellets are then solubilized in a suitable solvent and quantified using spectrophotometric or chromatographic techniques.

#### Drug release

The composition, method of preparation, lamellarity, and surface modifications of liposomes may alter the release rate of an entrapped drug substance from liposomes. The dialysis technique is frequently used to assess the *in-vitro* release rate of a drug substance from a liposomal formulation. Prewetted dialysis bags with specific molecular weight cut-off values that can retain the liposomes while allowing the drug released from the liposomes to cross the membrane and enter the receptor solvent medium are used. At predetermined time points, aliquots from the receptor solvent medium are withdrawn and quantified using spectrophotometric or chromatographic techniques to determine the release rate of drug from the liposomal formulation.

#### Physicochemical stability

Phospholipids are susceptible to a number of chemical reactions like peroxidation, hydrolysis, and photolysis, leading to their deterioration and thereby impacting their chemical stability. The ability of liposomes to retain their particle size and PDI is termed as its physical stability. Inappropriate particle sizes and surface charges may lead to liposome aggregation, thereby reducing their physical stability, which can significantly impact their performance. In the presence of serum proteins or other biological substances, the ability of liposomes to retain their integrity is referred to as biological stability. The physicochemical stability of liposomes can be assessed as per the International Council for Harmonisation of Technical Requirements for Registration of Pharmaceuticals for Human Use guidelines.

In addition to the abovementioned tests, liposomes are assessed for other parameters like pH, osmolality, pyrogenicity, sterility, toxicity, pharmacokinetics, and other evaluation parameters depending on the final dosage form into which liposomes are dispersed.

## Applications of liposomes

### *Therapeutic applications as drug-delivery carriers*

Liposomes are drug-delivery vesicles with varied applications due to the advantages offered by them. Liposomes can increase the efficacy of a drug substance by improving its pharmacokinetic parameters. Liposomes, due to their morphology, composition, and flexibility in terms of surface modifications can offer several benefits for delivering the entrapped drug substance effectively via various drug-delivery routes. Liposomes are beneficial drug-delivery carriers specifically for drugs with a narrow therapeutic index because they aid drug distribution and increase drug safety and efficacy. Treatment strategies are experiencing a paradigm shift from synthetic drug molecules to biologically derived therapeutics.<sup>10</sup> Liposomes also have been widely investigated as potential delivery carriers for therapeutic biologics, e.g., antisense oligonucleotides, cloned genes, recombinant proteins, therapeutic peptides (hormones), nucleic acids (siRNA, mRNA, pDNA), CRISPR/Cas9, and vaccines.

### *Application of liposomes as drug-delivery carriers administered via different routes*

Liposomes have the potential to improve the efficacy of routes like ocular, nasal, inhalation, oral, transdermal, and rectal as portals to enable the drug substance to reach the systemic circulation or target sites (Table 3).<sup>11-33</sup>

#### **Ocular route**

Various drugs used in ophthalmic disorders that are meant to be delivered to the systemic circulation through the ocular route suffer the limitation of a low effectiveness when delivered through conventional ophthalmic formulations like eye drops.<sup>34</sup> The low residence time of a drug in the eye due to rapid drainage through the lacrimal fluid as well as the low permeability of most drugs result in very low ophthalmic bioavailability. Liposomes, due to their composition, increase the drug substance permeation rate and extent across the ocular surface, resulting in an improved ophthalmic bioavailability and thereby therapeutic efficiency of the drug substance. Additionally, drug-loaded liposomes entrapped or dispersed in ocular lenses can prolong the residence time of drugs in the ophthalmic cavity. Charged liposomes administered as an ophthalmic spray or as a hydrogel have the ability to adhere with mucin present on the corneal surface through electrostatic bond formation, thereby increasing the residence time of drug in the ophthalmic cavity; moreover, charged liposomes can also control the release rate of entrapped drug for a prolonged therapeutic response.<sup>35</sup> Liposomes adsorb to the corneal layer and transfer the drug molecules to the corneal epithelial cell membrane. Liposomes can also travel by liposomal endocytosis. Liposomes consisting of a hydrogel or spray exhibit a higher penetration than conventional ophthalmic formulations.<sup>36</sup>

#### **Intranasal route**

The intranasal route is one of the most prominent routes for the delivery of drugs that cannot be administered through the oral route due to limitations like first-pass metabolism, instability of biological conditions of the human gastrointestinal tract, the local action of the drug is needed in the nasal cavity, or targeting the drug to the brain.<sup>37</sup> Liposomes are considered as biocompatible drug-delivery carriers, which enhance the absorption of drugs across the nasal mucosa. Additionally, liposomes offer added advantages like the ability to encapsulate both small and large drug molecule with a

broad range of hydrophobicity levels and pKa values, thus providing controlled and targeted drug release profiles. Several successful liposomal formulations for enhancing the nasal penetration and absorption of drug molecules like calcitonin, insulin, and influenza vaccine are approved by the US Federal Drug Administration and commercially available in the global market. Liposome-loaded nasal hydrogel or mucoadhesive gel formulations can increase the nasal drug penetration rate because of the longer duration of residence time of the drug substance at the absorption site. Liposomal nasal hydrogels can also control the release of the drug to achieve an efficient prolonged therapeutic response. The intranasal route is also considered as a promising route for rapid drug absorption into the brain via the systemic circulation.<sup>38,39</sup> Nasal cavities can also transport a drug substance to the brain through olfactory neurons or the geminal nerve. Two major barriers for transporting drug substances to the brain are the cerebrospinal fluid barrier and the BBB. Rapid mucociliary clearance in the central nervous system decreases the drug absorption. The liposomal drug-delivery system would not only overcome the mentioned barriers, but it would also increase the absorption rate of the drug substance through the nasal cavity due to its phospholipid composition.<sup>40</sup>

#### **Inhalation route**

Chronic and acute respiratory infections are difficult to treat through conventional inhalation-based antibiotic treatment therapy. The low tissue/cell penetration rate of antibiotics delivered through the conventional inhalation route in the form of dry powder inhalers requires high doses of antibiotics, leading to dose-related drug toxicity or antibiotic resistance. Inhaled liposomes are a novel approach for treating respiratory infections. Liposomal inhalation preparations are biocompatible, nontoxic, biodegradable, and stable in the inhibitory barrier of the sputum. Additionally, inhalable drug-loaded liposomes can increase the therapeutic index, drug absorption and penetration rates, and retention time of the drug at targeted sites, thereby maximizing the therapeutic efficacy and minimizing the drug side effects. Conventional inhalation antibiotics exhibit a short half-life in alveoli, so three or more daily administrations of drug are required.<sup>41</sup> The liposomal inhalation drug formulation can release the drug in a slow and controlled manner to achieve prolonged drug action, which in turn would decrease the dosing frequency of the drug substance by maintaining the concentration of the drug in the lungs above the minimum effective concentration.

#### **Oral route**

Liposomes were conventionally designed for parenteral drug administration, but they were then modified and investigated to increase the oral bioavailability of macromolecules like insulin by increasing the absorption rate of insulin through the gastrointestinal tract, resulting in destruction of the phospholipid bilayers and leading to leakage of the entrapped drug substance.<sup>42</sup> The hurdles of the oral administration of liposomes can be combated through surface modification or surface coating of liposomes and by substitution of phospholipids with hydrogenated phospholipids. Coating liposomes with large-chain polymers like chitosan can impart stability to liposomes in a gastric environment. Matrix modifications of liposomes by adding bile salts also improve the stability of liposomes in the gastrointestinal tract.<sup>43</sup> Colon targeting of a drug-delivery substance through the oral route is essential to reduce the toxicity and to enhance the efficacy of therapeutic agents used for the treatment of local colonic diseases or disorders like colon cancer, inflammatory bowel disease, and colonic infection.<sup>44</sup>



Table 3. Representative illustrations of investigated liposomal drug formulations administered through various routes<sup>11-33</sup>

Route of drug administration	Liposomal composition	Therapeutic agent	Application
<b>Ocular</b>	Phosphatidylcholine, cholesterol	Acyclovir	Increased absorption and controlled release of the drug
	1,2-Dimyristoyl- <i>sn</i> -glycero-3-phosphocholine (DMPC), cholesterol	Lidocaine	Controlled and prolonged release of the drug for 8 days
	Phosphatidylcholine, cholesterol	Ciprofloxacin	Liposomal hydrogel increases ocular availability of the drug, enhances the therapeutic efficacy, and prolongs the release of the drug
<b>Nasal</b>	L-phosphatidylcholine, cholesterol	Acetazolamide	Multilamellar liposomes provide a significant decrease in the intraocular pressure for a prolonged duration
	Egg phosphatidylcholine, cholesterol	Pilocarpine nitrate	Increased drug bioavailability
	L- $\alpha$ -Dipalmitoylphosphocholine (DPPC), cholesterol	Acyclovir	Enhanced nasal penetration and drug bioavailability
	L-alpha-Phosphatidyl choline, cholesterol	Ovalbumin (OVA)	Increased stability, bioavailability, and therapeutic efficacy of ovalbumin
	1,2-Dioleoyl-3-trimethylammonium-propane (DOTAP), 1,2-distearoyl- <i>sn</i> -glycero-3-phosphoethanolamine- <i>N</i> -[methoxy (polyethyleneglycol)-2000 (DSPE-PEG-2000) and cholesterol	Protamine	Improved and potent immunotherapeutic effect against cancer
<b>Inhalation</b>	1,2-ditetradecanoyl- <i>sn</i> -glycero-3-phosphocholine, cholesterol	Fexofenadine	Increased drug bioavailability and prolonged drug exposure
	Soybean phosphatidylcholine, cholesterol	Valproic acid	Increased permeation of valproic acid across the blood-brain barrier, sustained release of drug, reduced drug side effects, and improved patient compliance
	1, 2-Dipalmitoyl- <i>sn</i> -glycero-3-phosphoglycerol-sodium salt (DPPG)/1, 2-dipalmitoyl- <i>sn</i> -glycero-3-phosphocholine (DPPC)/1, 2-distearoyl- <i>sn</i> -glycero-3-phosphoglycerol, sodium salt (DSPG)/1,2-dipalmitoyl- <i>sn</i> -glycero-3-phosphoethanolamine- <i>N</i> -(lissamine rhodamine B sulfonyl) (DPPE), cholesterol	N-acetylcysteine	Coated liposomes resulted in the prolonged release of drug, good deposition and retention of coated liposomes in the lungs
	1,2-Dipalmitoyl- <i>sn</i> -glycero-3-phosphocholine (DPPC)/1,2-dipalmitoyl- <i>sn</i> -glycero-3-phosphoethanolamine- <i>N</i> -[4-( <i>p</i> -maleimidomethyl) cyclohexane-carboxamide] (DPPE-MCC)/fluorescence labelled phospholipid 1,2-dioleoyl- <i>sn</i> -glycero-3-phosphoethanolamine- <i>N</i> -(lissamine rhodamine B sulfonyl) (DOPE-Liss.Rhod.)	Salmon calcitonin	Improved oral bioavailability and stability of the drug substance
	Dipalmitoyl phosphatidylcholine, phosphatidylinositol	Insulin	Improved oral bioavailability and stability of the drug substance
<b>Oral</b>	Phosphatidylcholine, cholesterol	Paclitaxel	Increased drug uptake by the gastrointestinal mucosa and improved drug intestinal absorption
	L-a-Dipalmitoylphosphatidyl choline (DPPC), cholesterol	Cyclosporine A (CSA)	Improved bioavailability of CSA
	1,2-Dipalmitoyl- <i>sn</i> -glycero-3-phosphocholine (DPPC)	Tamoxifen citrate and Raloxifene hydrochloride	Enhanced oral absorption of both drug substances with increased tumor targeting and anti-cancer properties of the drug substances

(continued)

Table 3. (continued)

Route of drug administration	Liposomal composition	Therapeutic agent	Application
Transdermal	1,2-Dimyristoyl- <i>sn</i> -glycero-3-phosphocholine (DMPC), cholesterol	Indocyanine green (ICG)	Chitosan coating of liposomes stabilized the encapsulated unstable photosensitizer, ICG. In addition, positively-charged chitosan coating of liposomes facilitated the cellular uptake and permeation of ICG
	Soya phosphatidylcholine (PC), 1,2-dihexadecanoyl- <i>sn</i> -glycero-3-phosphoethanolamine	Methotrexate (MTX)	Enhanced transdermal flux, targeting of drug to the epidermal and dermal sites, controlled release of MTX
	Soyaphosphatidylcholine (PC), cholesterol	Propranolol hydrochloride	Improved transdermal flux and bioavailability of the drug substance
	Hydrogenated soya phosphatidyl choline (HSPC), cholesterol	Acyclovir sodium	Improved systemic bioavailability of the drug substance
	Soya phosphatidylcholine (soya PC)	Indinavir	Improved entrapment efficiency, enhanced transdermal flux, and improved systemic bioavailability of Indinavir
Rectal	1,2-Distearoyl- <i>sn</i> -glycero-3-phosphocholine (DSPC), 1,2-dipalmitoyl- <i>sn</i> -glycero-3-phosphocholine (DPPC), 1,2-distearoyl- <i>sn</i> -glycero-3-phosphoethanolamine- <i>N</i> -[methoxy(polyethylene glycol)-2000] (DSPE-PEG2000)	Doxorubicin (Dox)	Improved anticancer efficacy and reduced side effects of Dox
	Phosphatidylcholine (PC) phosphatidylethanolamine, cholesterol	Ferritin	Increased immunization efficacy of ferritin against sexually transmitted infections such as HIV

A surface-modified coated liposomal formulation can also be useful for targeting the drug substance to a specific colonic tumor site to increase the therapeutic efficacy and to reduce the associated side effects of drug substances.

### Transdermal route

The stratum corneum layer of the skin acts as a major barrier towards permeation of a drug substance to the underlying epidermal, dermal, or subcutaneous regions or to the systemic circulation via the skin. High-molecular-weight and hydrophilic drug substances have a very poor permeation rate and a low systemic bioavailability when delivered through the transdermal route. Due to their structural and compositional similarities to the cell membranes and skin layers, liposomal drug-delivery systems can easily permeate across the stratum corneum barrier layer of the skin along with the encapsulated drug substance.<sup>45</sup> Thus, liposomes can increase the permeation rate and therefore the bioavailability of drugs delivered through the transdermal route.

### Rectal route

The rectal administration of a drug is considered in medical practice for drug substances against a local disease or disorder as well as for increasing the systemic bioavailability of therapeutic agents that are metabolized or are unstable when delivered through oral or other routes. The major limitations associated with delivering a drug substance through the rectal route are as follows: low mucosal permeation rate of the drug substance and degradation of the drug substance by enzymes present in the microflora of the rectal cavity. Liposomes are stable in the mucosa and can increase the permeation rate of the drug substance across the rectal mucosa and also protect the encapsulated drug against enzymatic degradation, thereby increasing the systemic bioavailability of drug substances delivered through the rectal route.

### Parenteral route

Liposomes are used as formulations for delivering drugs through the parenteral route to accomplish therapeutic goals like improving the therapeutic efficiency, reducing the toxicity, and sustaining or controlling the release rate of a drug substance for a prolonged duration by creating a depot system. Liposomes offer several benefits such as adaptability towards the delivery of macromolecules, capability of encapsulating both hydrophilic and lipophilic drug substances, targeted delivery to a desired site, and adaptability towards surface modification, enabling an increase in its residence time in systemic circulation.<sup>46</sup> Thus, liposomes can serve as potential formulations for delivering a drug through the parenteral route.

## Disease-specific applications of liposomes

### Skin disorders

Mostly, skin disorders arise superficially on the surface of the human body. Based on the involvement and location of the disorder, liposomal formulations offer site-specific drug delivery and can deliver the drug to different layers of the skin, ranging from the topical surface, epidermis, dermis, or deep down in blood vessels beneath the skin.<sup>11</sup> Topical liposomal formulations avoid the first-pass metabolism of the drug and provide site-specific drug delivery (Table 4).<sup>12,47-51</sup>

### Acne

Visible nodules on the face can be termed as acne vulgaris. Come-

**Table 4. Representative illustrations of investigated liposomal drug formulations used to treat skin disorders<sup>47–51</sup>**

Disease	Liposome composition	Therapeutic agent	Application
Acne	Cholesterol HSPC	Adapalene	Topical adapalene liposome delivery enhanced drug permeation and reduced adapalene side effects
Skin burns	Lipoid S 100	Mupirocin	Liposomal formulation dispersed in hydrogel showed sustained drug release and improved antimicrobial activity of drug
Vitiligo	Cholesterol, DC-cholesterol, sodium deoxycholate	Psoralen	Psoralen loaded deformable liposomal vesicles showed high penetration rate of drug and reduced the pigmentation process
Psoriasis	Phosphatidyl choline, oleic acid	Methotrexate	Methotrexate loaded liposomes exhibited higher skin permeability
Leishmaniasis	Cholesterol, DPPC, DPPS	Lupane	Lupane-loaded liposomes efficiently diminished parasite abundance affecting certain cytokines

DC, dimethylaminoethane-carbamoyl; DPPC, dipalmitoylphosphatidylcholine; DPPS, dipalmitoylphosphatidylserine; HSPC, hydrogenated soy phosphatidylcholine.

done, seborrhoea, lifeless pores due to plugged hair follicles filled with oil are common causes of acne. Retinoids, antibiotics, and several herbal agents are used to treat acne.<sup>13</sup> Liposomal formulations can increase the penetration rate of the drug substance in the superficial layers of the skin or to the systemic circulation through blood vessels located deep down in the skin as desired according to the mechanism of action of the drug substance, thereby improving its therapeutic efficiency.<sup>14</sup>

#### Skin burns

Skin burns may occur due to various causes such as chemical exposure, electric shock, and exposure to heat or radiation. According to the depth of the wound and the area of the injury, a skin burn can be characterized as one of four different degrees.<sup>15</sup> Liposomal formulations encapsulating growth factors essential for tissue regeneration enhance the wound healing process.<sup>16</sup>

#### Vitiligo

Visible white patches on the skin due to melanocyte loss is termed as vitiligo. Phototherapy, surgical methods, and topical and systemic drug treatments are the preferred methods to treat vitiligo.<sup>17</sup> A topical liposomal formulation with an encapsulated drug substance has been demonstrated to increase the efficacy of a drug substance by increasing or enhancing the repigmentation process.<sup>18,19</sup>

#### Psoriasis

A chronic autoimmune skin disorder associated with epidermal hyperproliferation, abnormal differentiation of keratinocytes, leu-

kocyte infiltration, and endothelial vascular changes is termed as psoriasis. According to the severity of disease, the treatment strategy is chosen.<sup>20,21</sup> A liposomal formulation can increase the therapeutic efficiency of drugs like cyclosporine used to treat psoriasis by improving its permeation rate across the skin layers, thereby increasing the therapeutic drug concentration at the desired site.<sup>22</sup>

#### Leishmaniasis

Leishmaniasis is a parasitic disease that can be treated through local or systemic chemotherapy based on the severity of the disease.<sup>23</sup> Conventional drug therapy includes antimonials, amphotericin B, pentamidine, paromomycin, and miltefosine, which are less effective and exhibit high toxicity as well as several adverse reactions.<sup>20–23</sup> Drug-loaded liposome-based therapy enhances the drug permeation rate and can sustain the release of drug for a prolonged therapeutic effect.<sup>24</sup> Liposomal formulations can decrease the dose or dosing frequency of a drug substance due to the increased therapeutic concentration of the drug reaching the target site, thereby decreasing the dose- and dosing frequency-related side effects and adverse reactions.

#### Autoimmune disorders

Autoimmune disorders are chronic conditions caused due to genetic, environmental, or physiological factors.<sup>25–27</sup> A liposome-based nanovesicle drug-delivery approach is noninvasive, can increase the therapeutic efficiency of a drug substance, can increase patient compliance, can be delivered site-specifically, and hence is beneficial for the effective treatment of autoimmune disorders (Table 5).<sup>28–30,52–54</sup>

**Table 5. Representative illustrations of investigated liposomal drug formulations used to treat autoimmune disorders<sup>52–54</sup>**

Disease	Liposome composition	Therapeutic agent	Results
Type 1 diabetes	Cholesterol, SPC, DSPE-biotin	Insulin	Improved insulin oral bioavailability and accelerated cellular uptake
Multiple sclerosis	EPC, ManDOGa (targeting ligand)	Immunodominant peptides of MBP	MBP delivered through liposomes efficiently suppressed autoimmune encephalomyelitis in Dark Agouti rats, lowering the severity of the attack
Rheumatoid arthritis	Cholesteryl hemisuccinate, DPPE, DPPE-HA	Prednisolone	Liposomes increased the cellular uptake and cytostatic activity of entrapped prednisolone

DSPE, 1,2-distearoyl-*sn*-glycero-3-phosphorylethanolamine; DPPE, dipalmitoylphosphatidylethanolamine; HA, hyaluronic acid; EPC, egg phosphatidylcholine; ManDOG, mono-mannosyl dioleoyl glycerol; MBP, myelin basic protein; SPC, soybean phosphatidylcholine.

**Table 6. Representative illustrations of investigated liposomal drug formulations used to treat respiratory disorders<sup>57–60</sup>**

Disease	Liposome composition	Therapeutic agent	Results
Asthma	Cholesterol, DOPS	rSLPI	rSLPI-loaded liposomes enhanced the drug stability and its residence time in the lungs
Pneumonia	Cholesterol, HSPC, DSPE-PEG	Daptomycin, Clarithromycin	The combined drug-liposomal formulation exhibited more effective antibacterial activity in comparison to conventional formulations
Pneumonia	Cholesterol, DPPC	Polymyxin B	The liposomal formulation increased drug uptake by macrophages and delivered polymyxin B into the epithelial lining fluid, ensuring a greater drug effect at the target site
Tuberculosis	Cholesterol, lecithin	Rifampicin	The rifampicin-loaded liposomal formulation reduced the drug toxicity, enhanced the drug bioavailability, and released the drug in a controlled manner

DOPS, dioleoyl[phospho-L-serine]; DPPC, dipalmitoylphosphatidylcholine; DSPE-PEG, distearoylphosphoethanolamine-*N*-poly(ethylene glycol) 2000; DPPC, dipalmitoylphosphatidylcholine; HSPC, hydrogenated soy phosphatidylcholine; rSLPI, recombinant secretory leukocyte protease inhibitor.

### Type 1 diabetes

Type 1 diabetes is a metabolic disease in which pancreatic insulin-secreting  $\beta$ -cells are permanently demolished.<sup>31,32</sup> Therapy for this disease includes insulin injected daily; however, patient compliance is often poor.<sup>33,47,48</sup> The oral route is not viable due to the poor bioavailability of insulin.<sup>49–51,55</sup> Liposomal formulations can increase the stability and therefore the bioavailability of insulin delivered through the oral route, leading to the effective treatment of type 1 diabetes.

### Multiple sclerosis

Multiple sclerosis is an inflammatory neurological condition. This disease is characterized by demyelinated axons and oxidative stress. In the treatment of multiple sclerosis, the major challenge is for the drug to cross the BBB and reach the target site. Liposomal formulations can improve the biodistribution and pharmacokinetics of the drug, leading to an enhanced permeation rate of drug across the BBB.

### Rheumatoid arthritis

Rheumatoid arthritis is a chronic autoimmune disease condition of the bone joint with cartilage destruction, leading to pain and tissue dysfunction. Rheumatoid arthritis therapy includes treatment through nonsteroidal anti-inflammatory drugs, biologics, corticosteroids, and disease-modifying antirheumatic drugs. However, the drugs exhibit a poor systemic bioavailability and a rapid clearance rate, leading to high doses or dosing frequency, several side effects, and poor patient compliance.<sup>56</sup> Liposomal delivery can enhance the systemic bioavailability of drugs due to an increased permeation rate, leading to a reduced dose and/or dosing frequency as well as fewer drug-related side effects.

### Respiratory disease

A liposome-based nanovesicular drug-delivery system can provide enhanced therapeutic efficacy in the treatment of respiratory disease due to the higher site specificity and enhanced dose accuracy at the target sites, thus reducing systemic toxicity and irritation in the lungs (Table 6).<sup>52,53,57–60</sup>

### Asthma

Asthma is mainly an allergic response and a chronic condition leading to airway inflammation and blockage.  $\beta_2$  agonists, corticosteroids, anticholinergics, and oxygen therapy are used for the

management and treatment of asthma. Liposomes can increase the residence time of drugs in the lungs and therefore increase the therapeutic efficacy of the drug substances.<sup>56</sup>

### Pneumonia

Pneumonia is an infection of the air sac in a single lung or both lungs caused by fluid or pus deposition. Antibiotics are prescribed for the treatment and management of pneumonia. Liposomes can increase the residence time of drugs in the lungs as well as the lung tissue concentration of the drug substance, thus increasing the therapeutic efficacy.<sup>57–59</sup>

### Tuberculosis

Tuberculosis is an airborne pulmonary infection. Antituberculosis agents like isoniazid, ethambutol, rifampin, and pyrazinamide are used for the treatment and management of tuberculosis. A liposomal formulation of antituberculosis agents may enhance the pulmonary drug concentration, leading to a reduction in the dose and dosing frequency as well as resulting in a reduced incidence of drug resistance.<sup>60</sup>

### Neurological disorders

The BBB offers a major challenge to drug delivery to the brain in neurological disorders as it is highly lipophilic in nature and has a high expression of efflux pump proteins like P-glycoprotein, which decreases the penetration rate of drug substances across the BBB. Due to the lipophilic nature of liposomes, they can prove effective in transporting drugs to the brain by overcoming the BBB (Table 7).<sup>63–67</sup>

### Alzheimer's disease

Alzheimer's disease is a neurodegenerative disease state caused by the formation of  $\beta$ -amyloid plaques. Alzheimer's disease leads to memory loss and brain atrophy. Surface-modified novel liposomal formulations can easily transport the drug across the BBB to the target site, thus increasing the therapeutic efficiency of a drug substance in Alzheimer's disease patients.<sup>61</sup>

### Seizures

A central nervous system disease caused by unusual neuronal signals in the brain leads to seizures. The lipophilic nature of a liposomal formulation efficiently delivers the drug to the target location, leading to rapid and effective seizure management.



**Table 7. Representative illustrations of investigated liposomal drug formulations used to treat neurological disorders<sup>63–67</sup>**

Disease	Liposome composition	Therapeutic agent	Results
Alzheimer's disease	Cholesterol, DSPC, DSPE-PEG, transferrin	$\alpha$ -Mangostin	Surface modified liposomes with transferrin resulted in enhanced BBB penetration and brain-targeting drug delivery
Seizure	Cholesterol, SPC	Nimodipine	Nimodipine-loaded liposomal formulation increased the bioavailability of drug and reduced the pilocarpine-induced seizure attack in mice model
PD	Cholesterol, PC, chitosan	Levodopa	Chitosan-coated levodopa liposomes diminished levodopa-induced dyskinesia and increased the therapeutic efficiency of levodopa
Migraine	Soya lecithin	Rizatriptan benzoate	improved drug permeation, higher flux across nasal mucosa, no damage to epithelial layer, improvement in bioavailability
CI	DPPC, DSPE-PEG	Tacrolimus	Liposome formulation lowered brain injury and increased the therapeutic efficacy of tacrolimus

BBB, blood-brain barrier; DSPC, distearoylphosphocholine; DSPE-PEG, distearoylphosphoethanolamine-*N*-poly(ethylene glycol) 2000; DPPC, dipalmitoylphosphocholine; PC, phosphatidylcholine.

### Parkinson's disease

Parkinson's disease is a neuron deterioration disease condition caused by the absence of dopamine in the basal ganglia and also by the loss of dopaminergic neurons. A liposomal formulation can target the delivery of a drug that is essential in the treatment of Parkinson's disease to the brain, thus leading to less neuronal loss.<sup>62</sup>

### Cerebral infarction

Cerebral infarction is a brain tissue disease caused by the reduction of blood flow as well as the depletion of nutrients and oxygen supply to the brain tissues, and it eventually leads to brain cell death. The early management and effective treatment of cerebral infarction reduce the risk of brain hemorrhage. Liposomes can increase the bioavailability and therapeutic efficiency of drugs used for the effective management and rapid treatment of cerebral infarction.

### Cardiac disorders

Nanoliposomal formulations enhance the plasma residence time and drug accumulation at the target site, thus increasing the therapeutic efficiency of drug substances used to treat cardiac disorders. Additionally, the surface modification of liposomes can aid targeted drug delivery and control the release of drug substances used to treat cardiac disorders (Table 8).<sup>69–71</sup>

### Atherosclerosis

Atherosclerosis is caused by lipid accumulation, which in turn results in narrowing blood vessels and a poor blood flow in the artery, leading to myocardial infarction, stroke, and angina.<sup>68</sup>

Surface-modified liposomal vesicles with encapsulated antiatherosclerotic agents can enhance the targeted action of a drug at the plaque formation site, thereby increasing the therapeutic effect of the drug.<sup>69</sup>

### Myocardial infarction

Myocardial infarction is caused by a poor blood supply in the heart muscles. A liposomal formulation can target the drug substance to the heart and result in its accumulation in the infarcted region, inflicting fewer myocardial infarctions and cardiac fibrosis areas, thus improving the drug substance efficiency and reducing its side effects.<sup>70</sup>

### Restenosis

Restenosis is a condition in which there is the narrowing of arteries, leading to a restricted blood flow. A liposomal formulation can control the release of the drug, leading to the prolonged therapeutic response of the drug substance, which is desired in restenosis.<sup>71</sup>

### Cancer

Abnormal and uncontrolled multiplication of cells leading to tumor formation is termed as cancer. The treatment and management of cancer is done mainly through surgery or chemotherapy, which is very painful due to biodistribution and the effect of anticancer agents not only to tumor cells but also to healthy cells. Anticancer chemotherapy lacks specificity towards the target site, has a low plasma retention time, exhibits severe toxic side effects, and is not very stable or permeable.<sup>72</sup> Anticancer drug-loaded liposomes can

**Table 8. Representative illustrations of investigated liposomal drug formulations used to treat cardiac disorders<sup>69–71</sup>**

Disease	Liposome composition	Loaded drug	Results
Atherosclerosis	Cholesterol, DPPC, DSPE-PEG-E-selectin binding peptide	Atorvastatin	Atorvastatin and curcumin-loaded liposomes with pegylation reduced drug toxicity and inflammatory reactions of drug; also, pegylation of liposomes with selectin binding peptide resulted in enhanced cellular uptake of drug-loaded liposomes
Myocardial infarction	Cholesterol, lecithin, sodium deoxycholate	$\alpha$ -tocopherol	$\alpha$ -Tocopherol-loaded liposomal hydrogel increased the stability and therapeutic efficacy of $\alpha$ -tocopherol
Restenosis	EPC, DOTAP, DSPE-PEG	Estradiol	Liposomal formulations resulted in the controlled release and increased therapeutic efficacy of estradiol

DOTAP, dioleoyltrimethylammoniumpropane; DPPC, dipalmitoylphosphocholine; DSPE-PEG, distearoylphosphoethanolamine-*N*-poly(ethylene glycol) 2000; EPC, egg phosphatidylcholine.

**Table 9.** Representative illustrations of investigated liposomal drug formulations used to treat cancer<sup>72-74</sup>

Disease	Liposome composition	Loaded drug	Results
AIDS-related Kaposi's sarcoma	Cholesterol, PEGylated phospholipids	Doxorubicin	Surface modified liposomes prolonged the half-life and anticancer efficiency of doxorubicin
Lung cancer	Cholesterol, PEGylated phospholipids	Etoposide	Liposomal formulation enhanced cell apoptosis induction, increased cell cycle arrest and exhibited enhanced antiproliferative effect
Pancreatic cancer	Cholesterol, PEGylated phospholipids	Azobenzene derivatives	Liposomal formulation diminished the nonspecific biodistribution of anticancer drugs along with controlled release drug delivery and reduced the multidrug resistance of drug

be targeted specifically to tumor sites through proper surface modifications, reducing the impact of chemotherapy on healthy cells and thereby reducing the associated pain. Additionally, liposomes have the ability to enhance permeability, impart biocompatibility, reduce immunogenicity, and increase the retention of drug at the target site; thus, they act as a potential carrier for chemotherapeutic agents (Table 9).<sup>72-74</sup>

### Infectious disease

#### Fungal and viral infections

Recently, in 2021, people worldwide were affected by the COVID-19 pandemic. A current study has illustrated the effective creation of a remdesivir dosage form that is nebulized and scalable for self-medication against COVID-19. AL-Rem (aerosolized remdesivir) is practical for large-scale manufacturing thanks to the use of Federal Drug Administration-approved phospholipids and a modified hydration technique with a widely utilized particle size reduction technology.<sup>75</sup> Some COVID-19 patients also were infected by black fungi, leading to the infectious disease termed as mucormycosis. Amphotericin B is used as the first-line treatment for mucormycosis. Amphotericin B in its free form has a poor penetration rate at the target location, leading to its decreased efficiency and increased dose or dosing frequency and thus resulting in dose-related side effects like ionosphere toxicity and neurotoxicity.<sup>76</sup> A liposomal amphotericin B formulation demonstrated an improved drug penetration rate and uptake at the target site, resulting in an increased therapeutic efficiency, a reduced drug dose, fewer dose-related side effects, and less drug toxicity.<sup>77</sup> A liposomal formulation of amphotericin B also has been reported to reduce the incidence of drug resistance.<sup>1</sup>

#### Parasitic and bacterial infections

Malaria is endemic in several nations worldwide, and the major limitations of antimalarial drug substances are treatment failure due to *Plasmodium* species resistance as well as limited bioavailability due to poor water solubility, biostability, and permeability. A drug-delivery platform using liposomes can overcome the limitations of antimalarial therapy as liposomes, due to their dual hydrophilic as well as hydrophobic nature, can deliver water-soluble and lipid-soluble antimalarial drugs together to reduce the incidence of *Plasmodium* species resistance. Liposomes additionally offer the benefits of biodegradability, biocompatibility, and low toxicity, making them a potential vehicle for delivering antimalarial drug substances. Liposomes serve as an excellent drug-delivery carrier in parasitic infections like Leishmaniasis. Liposomes can offer targeted therapy to specific and targeted sites desired in parasitic infections, thereby increasing the therapeutic efficacy and reducing the toxicity of drug substances as well as the incidence of drug resistance.

### Diagnostic applications of liposomes

In addition to their wide therapeutic applications, liposomes also have been investigated and exploited as carriers of chemical substances used for diagnostic purposes. Due to the inherent photoimaging properties of the components utilized in liposomal formulations, they can be utilized in various bioimaging techniques such as photoacoustic imaging and fluorescence.<sup>78</sup> Additionally, since the lipid components of liposomes can interchange with serum lipoproteins, the serum lipoproteins have a decreased ability to absorb imaging agents. Also, liposomes can improve the solubility and bioavailability of encapsulated imaging agents, thereby improving their imaging performance.<sup>79</sup> Furthermore, liposomes have the ability to increase the sensitivity of detection as they can bind to specific cells through receptor-mediated endocytosis due to the low-density lipoproteins that migrate within the liposomes.

In cardiovascular disorders, liposomes have been explored to improve the sensitivity and specificity of ultrasonography and echocardiography for investigating thrombosis diagnosis and for thrombolytic therapy monitoring.<sup>80</sup>

Liposome lipids conjugated with fluorescent labels have been demonstrated to be a useful technique to visualize the physical positions of antigens and to understand the mechanics of the major histocompatibility complex pathway in phagocytic antigen-presenting cells, which would be helpful for successful and effective vaccine development.<sup>81</sup> Thus, liposomes can serve as a potential delivery carrier for increasing the diagnostic efficiency of available imaging techniques. Also, several research investigations have explored the multifunctional potential of liposomes by combining their imaging functionality with therapeutic agents in a single liposome for diagnosis and real-time treatment.<sup>82</sup> Representative illustrations of commercialized Federal Drug Administration-approved therapeutic liposomal formulations are depicted in Table 10.

### Future perspectives

Liposomes are multifaceted nanovesicular drug-delivery carriers with potential therapeutic and diagnostic medical applications. Liposomes are drug-delivery vehicles that have the potential to increase the therapeutic efficiency of a drug substance by offering benefits like targeted delivery at the desired site, enhanced bioavailability, and reduced dose/dosing frequency. The prospective multifunctional application of combining imaging functionality with therapeutic agents in a single liposome for diagnosis and real-time treatment is anticipated to be the future of liposomal formulations.

### Conclusions

Liposomes as nanosized lipidic vesicular carriers have been used in a broad range of medical applications. The potential of li-

**Table 10. Representative illustrations of commercialized Federal Drug Administration-approved therapeutic liposomal formulations**

Brand name	Active pharmaceutical ingredient	Indication	Company
Doxil®	Doxorubicin	AIDS-related Kaposi's sarcoma	Baxter Healthcare Corp.
AmBisome®	Amphotericin B	Febrile fungal infection, leishmaniasis, candida, and cryptococcus infection	Galen Pharma
DepoCyt®	Cytarabine	Lymphomatous meningitis	Pacira Pharmaceuticals
DaunoXome®	Daunorubicin	HIV-related Kaposi sarcoma	Galen Pharma
DepoDur®	Morphine	Pain management	Pacira Pharmaceuticals
Exparel®	Bupivacaine	Postsurgical analgesia	Pacira Pharmaceuticals
Marqibo®	Vincristine	Acute lymphoblastic leukemia	Acrotech Biopharma
Onivyde®	Irinotecan	Adenocarcinoma of the pancreas	IpSEN Inc.
Inflexal®	Inactivated hemagglutinin of influenza virus strain A and B	Influenza	Janssen vaccines

posomes as drug-delivery carriers for a broad range of therapeutic substances, ranging from biologicals to synthetic drugs, is promising as they increase the therapeutic efficiency of drugs. Liposomes offer benefits such as targeted drug delivery to the disease location, improved pharmacokinetic parameters and bioavailability of the drug substance, reduced toxicity and side effects of the drug substance, and increased circulation residence time of the entrapped drug in the blood. Due to the inherent photoimaging properties of the components utilized in the liposomal formulation, they exhibit diagnostic applications in various bioimaging techniques like photoacoustic imaging and fluorescence. Liposomes can improve the solubility and bioavailability of encapsulated imaging agents, thereby improving the imaging performance of several diagnostic techniques. Liposomes also have been investigated for multifunctional applications by combining their imaging functionality with therapeutic agents in a single liposome for diagnosis and real-time treatment. Thus, liposomes have been proven as lipid vesicular carriers with potential in a wide range of medical applications, and future investigations and developments will broaden their scope as delivery vesicles in multifaceted areas.

### Funding

The authors received no funding for completing this review.

### Conflict of interest

The authors have no conflict of interests related to this publication.

### Author contributions

Contributed to study concept and design, supervision, and critical revision of the manuscript (VHS), drafting (MPC, SAS, MHNQ), supervision (NS, DS, RT).

### References

- [1] Fisher EW, Toma A, Fisher PH, Cheesman AD. Rhinocerebral mucormycosis: use of liposomal amphotericin B. *J Laryngol Otol* 1991;105(7):575–577. doi:10.1017/s0022215100116652, PMID:1875144.
- [2] Liu P, Chen G, Zhang J. A Review of Liposomes as a Drug Delivery System: Current Status of Approved Products, Regulatory Environments, and Future Perspectives. *Molecules* 2022;27(4):1372. doi:10.3390/molecules27041372, PMID:35209162.
- [3] Shah V, Jobanputra A, Saxena B, Nivsarkar M. Development and Characterization of Saturated Fatty Acid-Engineered, Silica-Coated Lipid Vesicular System for Effective Oral Delivery of Alfa-Choriogonadotropin. *AAPS PharmSciTech* 2021;22(3):118. doi:10.1208/s12249-021-01985-0, PMID:33782790.
- [4] Nsairat H, Khater D, Sayed U, Odeh F, Al Bawab A, Alshaer W. Liposomes: structure, composition, types, and clinical applications. *Heliyon* 2022;8(5):e09394. doi:10.1016/j.heliyon.2022.e09394, PMID:35600452.
- [5] Dymek M, Sikora E. Liposomes as biocompatible and smart delivery systems - the current state. *Adv Colloid Interface Sci* 2022;309:102757. doi:10.1016/j.cis.2022.102757, PMID:36152374.
- [6] Lee MK. Liposomes for Enhanced Bioavailability of Water-Insoluble Drugs: In Vivo Evidence and Recent Approaches. *Pharmaceutics* 2020;12(3):264. doi:10.3390/pharmaceutics12030264, PMID:32183185.
- [7] Lee W, Im HJ. Theranostics Based on Liposome: Looking Back and Forward. *Nucl Med Mol Imaging* 2019;53(4):242–246. doi:10.1007/s13139-019-00603-z, PMID:31456856.
- [8] Akbarzadeh A, Rezaei-Sadabady R, Davaran S, Joo SW, Zarghami N, Hanifepour Y, *et al*. Liposome: classification, preparation, and applications. *Nanoscale Res Lett* 2013;8(1):102. doi:10.1186/1556-276X-8-102, PMID:23432972.
- [9] Kanasova M, Nesmerak K. Systematic review of liposomes' characterization methods. *J Monatsh Chem* 2017;148:1581–1593. doi:10.1007/s00706-017-1994-9.
- [10] Kim EM, Jeong HJ. Liposomes: Biomedical Applications. *Chonnam Med J* 2021;57(1):27–35. doi:10.4068/cmj.2021.57.1.27, PMID:33537216.
- [11] Law SL, Huang KJ, Chiang CH. Acyclovir-containing liposomes for potential ocular delivery. Corneal penetration and absorption. *J Control Release* 2000;63(1-2):135–140. doi:10.1016/s0168-3659(99)00192-3, PMID:10640587.
- [12] Gulsen D, Li CC, Chauhan A. Dispersion of DMPC liposomes in contact lenses for ophthalmic drug delivery. *Curr Eye Res* 2005;30(12):1071–1080. doi:10.1080/02713680500346633, PMID:16354620.
- [13] Hosny KM. Ciprofloxacin as ocular liposomal hydrogel. *AAPS PharmSciTech* 2010;11(1):241–246. doi:10.1208/s12249-009-9373-4, PMID:20151337.
- [14] Durrani AM, Davies NM, Thomas M, Kellaway IW. Pilocarpine bioavailability from a mucoadhesive liposomal ophthalmic drug delivery system. *J Int Pharmaceutics* 1992;88(1-3):409–415. doi:10.1016/0378-5173(92)90340-8.
- [15] Alsarra IA, Hamed AY, Alanazi FK. Acyclovir liposomes for intranasal systemic delivery: development and pharmacokinetics evaluation. *Drug Deliv* 2008;15(5):313–321. doi:10.1080/10717540802035251, PMID:18763162.
- [16] Kaplan M, Demiröz FT, Vural I, Çelebi N. Development and characterization of gels and liposomes containing ovalbumin for nasal delivery.

- J Drug Delivery 2018;44:108–117. doi:10.1016/j.jddst.2017.12.006.
- [17] Mai Y, Guo J, Zhao Y, Ma S, Hou Y, Yang J. Intranasal delivery of cationic liposome-protamine complex mRNA vaccine elicits effective anti-tumor immunity. *Cell Immunol* 2020;354:104143. doi:10.1016/j.cellimm.2020.104143, PMID:32563850.
  - [18] Jufri M, Yuwanda A, Surini S, Harahap Y. Study of valproic acid liposomes for delivery into the brain through an intranasal route. *Heliyon* 2022;8(3):e09030. doi:10.1016/j.heliyon.2022.e09030, PMID:35284670.
  - [19] Hamedinasab H, Rezayan AH, Mellat M, Mashreghi M, Jaafari MR. Development of chitosan-coated liposome for pulmonary delivery of N-acetylcysteine. *Int J Biol Macromol* 2020;156:1455–1463. doi:10.1016/j.ijbiomac.2019.11.190, PMID:31770553.
  - [20] Hathout RM, Mansour S, Mortada ND, Guinedi AS. Liposomes as an ocular delivery system for acetazolamide: in vitro and in vivo studies. *AAPS PharmSciTech* 2007;8(1):1. doi:10.1208/pt0801001, PMID:17408209.
  - [21] Qiang F, Shin HJ, Lee BJ, Han HK. Enhanced systemic exposure of fexofenadine via the intranasal administration of chitosan-coated liposome. *Int J Pharm* 2012;430(1-2):161–166. doi:10.1016/j.ijpharm.2012.04.007, PMID:22525082.
  - [22] Gradauer K, Barthelmes J, Vonach C, Almer G, Mangge H, Teubl B, *et al.* Liposomes coated with thiolated chitosan enhance oral peptide delivery to rats. *J Control Release* 2013;172(3):872–878. doi:10.1016/j.jconrel.2013.10.011, PMID:24140721.
  - [23] Kisel MA, Kulik LN, Tsybovsky IS, Vlasov AP, Vorob'yov MS, Kholodova EA, *et al.* Liposomes with phosphatidylethanol as a carrier for oral delivery of insulin: studies in the rat. *Int J Pharm* 2001;216(1-2):105–114. doi:10.1016/S0378-5173(01)00579-8, PMID:11274812.
  - [24] Liu Y, Yang T, Wei S, Zhou C, Lan Y, Cao A, *et al.* Mucus adhesion- and penetration-enhanced liposomes for paclitaxel oral delivery. *J Int J Pharm* 2018;537(1-2):245–256. doi:10.1016/j.ijpharm.2017.12.044.
  - [25] Meshal MAA, Khidr SH, Bayomi MA, Angary AAA. Oral administration of liposomes containing cyclosporine: a pharmacokinetic study. *J Int Pharmaceutics* 1998;168(2):163–168. doi:10.1016/S0378-5173(98)00066-0.
  - [26] Mutlu Ağardana NBM, Değimb Z, Yilmaz S, Altıntaş L, Topale T. Tamoxifen/raloxifene loaded liposomes for oral treatment of breast cancer. *J Drug Deliv Sci Technol* 2020;57:101–112. doi:10.1016/j.jddst.2020.101612.
  - [27] Lee EH, Lim SJ, Lee MK. Chitosan-coated liposomes to stabilize and enhance transdermal delivery of indocyanine green for photodynamic therapy of melanoma. *Carbohydr Polym* 2019;224:115143. doi:10.1016/j.carbpol.2019.115143, PMID:31472877.
  - [28] Dubey V, Mishra D, Dutta T, Nahar M, Saraf DK, Jain NK. Dermal and transdermal delivery of an anti-psoriatic agent via ethanolic liposomes. *J Control Release* 2007;123(2):148–154. doi:10.1016/j.jconrel.2007.08.005, PMID:17884226.
  - [29] Mishra D, Garg M, Dubey V, Jain S, Jain NK. Elastic liposomes mediated transdermal delivery of an anti-hypertensive agent: propranolol hydrochloride. *J Pharm Sci* 2007;96(1):145–155. doi:10.1002/jps.20737, PMID:16960826.
  - [30] Jain SK, Gupta Y, Jain A, Rai K. Enhanced transdermal delivery of acyclovir sodium via elastic liposomes. *Drug Deliv* 2008;15(3):141–147. doi:10.1080/10717540801952407, PMID:18379926.
  - [31] Dubey V, Mishra D, Nahar M, Jain V, Jain NK. Enhanced transdermal delivery of an anti-HIV agent via ethanolic liposomes. *Nanomedicine* 2010;6(4):590–596. doi:10.1016/j.nano.2010.01.002, PMID:20093197.
  - [32] Lokerse WJM, Kneepkens ECM, Hagen TLMT, Eggermont AMM, Grull H, Koning GA, *et al.* In depth study on thermosensitive liposomes: Optimizing formulations for tumor specific therapy and in vitro to in vivo relations. *Biomaterials* 2016;82:138–150. doi:10.1016/j.biomaterials.2015.12.023, PMID:26761778.
  - [33] Zhou F, Kraehenbuhl JP, Neutra MR. Mucosal IgA response to rectally administered antigen formulated in IgA-coated liposomes. *Vaccine* 1995;13(7):637–644. doi:10.1016/0264-610X(94)00029-M, PMID:7668033.
  - [34] Daraee H, Etemadi A, Kouhi M, Alimirzalu S, Akbarzadeh A. Application of liposomes in medicine and drug delivery. *Artif Cells Nanomed Biotechnol* 2016;44(1):381–391. doi:10.3109/21691401.2014.953633, PMID:25222036.
  - [35] Craig JP, Purslow C, Murphy PJ, Wolffsohn JS. Effect of a liposomal spray on the pre-ocular tear film. *Cont Lens Anterior Eye* 2010;33(2):83–87. doi:10.1016/j.clae.2009.12.007, PMID:20096622.
  - [36] Achouri D, Alhanout K, Piccerelle P, Andrieu V. Recent advances in ocular drug delivery. *Drug Dev Ind Pharm* 2013;39(11):1599–1617. doi:10.3109/03639045.2012.736515, PMID:23153114.
  - [37] Pallagi E, Jójárt-Laczkovich O, Németh Z, Szabó-Révész P, Csóka I. Application of the QbD-based approach in the early development of liposomes for nasal administration. *Int J Pharm* 2019;562:11–22. doi:10.1016/j.ijpharm.2019.03.021, PMID:30877028.
  - [38] Vyas SP, Goswami SK, Singh R. Liposomes based nasal delivery system of nifedipine: Development and characterization. *J Int Pharmaceutics* 1995;118(1):23–30. doi:10.1016/0378-5173(94)00296-H.
  - [39] Salade L, Wauthoz N, Vermeersch M, Amighi K, Goole J. Chitosan-coated liposome dry-powder formulations loaded with ghrelin for nose-to-brain delivery. *Eur J Pharm Biopharm* 2018;129:257–266. doi:10.1016/j.ejpb.2018.06.011, PMID:29902517.
  - [40] Narayan R, Singh M, Ranjan O, Nayak Y, Garg S, Shavi GV, *et al.* Development of risperidone liposomes for brain targeting through intranasal route. *Life Sci* 2016;163:38–45. doi:10.1016/j.lfs.2016.08.033, PMID:27593571.
  - [41] Bassetti M, Vena A, Russo A, Peghin M. Inhaled Liposomal Antimicrobial Delivery in Lung Infections. *Drugs* 2020;80(13):1309–1318. doi:10.1007/s40265-020-01359-z, PMID:32691293.
  - [42] Wu W, Lu Y, Qi J. Oral delivery of liposomes. *Ther Deliv* 2015;6(11):1239–1241. doi:10.4155/tde.15.69, PMID:26584253.
  - [43] Pantze SF, Parmentier J, Hofhaus G, Fricker G. Matrix liposomes: A solid liposomal formulation for oral administration. *Eur J Lipid Sci Technol* 2014;116:1145–1154. doi:10.1002/ejlt.201300409.
  - [44] Hua S. Orally administered liposomal formulations for colon targeted drug delivery. *Front Pharmacol* 2014;5:138. doi:10.3389/fphar.2014.00138, PMID:24959147.
  - [45] Patel H, Shah C, Shah V, Upadhyay U. Factorial designing, development and in-vitro evaluation of liposomal gel for topical delivery of quetiapine. *J AAPS* 2012;7(4):290–302.
  - [46] Wang Y, Grainger DW. Lyophilized liposome-based parenteral drug development: Reviewing complex product design strategies and current regulatory environments. *Adv Drug Deliv Rev* 2019;151:152:56–71. doi:10.1016/j.addr.2019.03.003, PMID:30898571.
  - [47] Kumar V, Banga AK. Intradermal and follicular delivery of adapalene liposomes. *Drug Dev Ind Pharm* 2016;42(6):871–879. doi:10.3109/03639045.2015.1082580, PMID:27031916.
  - [48] Hurler J, Berg OA, Skar M, Conradi AH, Johnsen PJ, Skalko-Basnet N. Improved burns therapy: liposomes-in-hydrogel delivery system for mupirocin. *J Pharm Sci* 2012;101(10):3906–3915. doi:10.1002/jps.23260, PMID:22777770.
  - [49] Doppalapudi S, Mahira S, Khan W. Development and in vitro assessment of psoralen and resveratrol co-loaded ultradeformable liposomes for the treatment of vitiligo. *J Photochem Photobiol B* 2017;174:44–57. doi:10.1016/j.jphotobiol.2017.07.007, PMID:28753523.
  - [50] Srisuk P, Thongnopnua P, Raktanonchai U, Kanokpanont S. Physicochemical characteristics of methotrexate-entrapped oleic acid-containing deformable liposomes for in vitro transepidermal delivery targeting psoriasis treatment. *Int J Pharm* 2012;427(2):426–434. doi:10.1016/j.ijpharm.2012.01.045, PMID:22310459.
  - [51] Barros NB, Migliaccio V, Facundo VA, Ciancaglini P, Stábéli RG, Nicolette R, *et al.* Liposomal-lupane system as alternative chemotherapy against cutaneous leishmaniasis: macrophage as target cell. *Exp Parasitol* 2013;135(2):337–343. doi:10.1016/j.exppara.2013.07.022, PMID:23933281.
  - [52] Zhang X, Qi J, Lu Y, He W, Li X, Wu W. Biotinylated liposomes as potential carriers for the oral delivery of insulin. *Nanomedicine* 2014;10(1):167–176. doi:10.1016/j.nano.2013.07.011, PMID:23891617.
  - [53] Belogurov AA Jr, Stepanov AV, Smirnov IV, Melamed D, Bacon A, Mamedov AE, *et al.* Liposome-encapsulated peptides protect against experimental allergic encephalitis. *FASEB J* 2013;27(1):222–231. doi:10.1096/fj.12-213975, PMID:23047895.
  - [54] Gouveia VM, Lopes-de-Araújo J, Costa Lima SA, Nunes C, Reis S. Hyaluronic acid-conjugated pH-sensitive liposomes for targeted delivery



- of prednisolone on rheumatoid arthritis therapy. *Nanomedicine (Lond)* 2018;13(9):1037–1049. doi:10.1016/j.jconrel.2011.12.024, PMID:29790395.
- [55] Wong CY, Al-Salami H, Dass CR. Recent advancements in oral administration of insulin-loaded liposomal drug delivery systems for diabetes mellitus. *Int J Pharm* 2018;549(1-2):201–217. doi:10.1016/j.ijpharm.2018.07.041, PMID:30071309.
- [56] Zeb A, Qureshi OS, Yu CH, Akram M, Kim HS, Kim MS, *et al*. Enhanced anti-rheumatic activity of methotrexate-entrapped ultradeformable liposomal gel in adjuvant-induced arthritis rat model. *Int J Pharm* 2017;525(1):92–100. doi:10.1016/j.ijpharm.2017.04.032, PMID:28428089.
- [57] Gibbons A, Padilla-Carlín D, Kelly C, Hickey AJ, Taggart C, McElvaney NG, *et al*. The effect of liposome encapsulation on the pharmacokinetics of recombinant secretory leukocyte protease inhibitor (rSLPI) therapy after local delivery to a guinea pig asthma model. *Pharm Res* 2011;28(9):2233–2245. doi:10.1007/s11095-011-0454-1, PMID:21647791.
- [58] Li Y, Su T, Zhang Y, Huang X, Li J, Li C. Liposomal co-delivery of daptomycin and clarithromycin at an optimized ratio for treatment of methicillin-resistant *Staphylococcus aureus* infection. *Drug Deliv* 2015;22(5):627–637. doi:10.3109/10717544.2014.880756, PMID:24471983.
- [59] He J, Abdelraouf K, Ledesma KR, Chow DS, Tam VH. Pharmacokinetics and efficacy of liposomal polymyxin B in a murine pneumonia model. *Int J Antimicrob Agents* 2013;42(6):559–564. doi:10.1016/j.ijantimicag.2013.07.009, PMID:24016799.
- [60] Patil JS, Devi VK, Devi K, Sarasija S. A novel approach for lung delivery of rifampicin-loaded liposomes in dry powder form for the treatment of tuberculosis. *Lung India* 2015;32(4):331–338. doi:10.4103/0970-2113.159559, PMID:26180381.
- [61] Papadia K, Markoutsas E, Mourtas S, Giannou AD, La Ferla B, Nicotra F, *et al*. Multifunctional LUV liposomes decorated for BBB and amyloid targeting. A. *In vitro* proof-of-concept. *Eur J Pharm Sci* 2017;101:140–148. doi:10.1016/j.ejps.2017.02.019, PMID:28193538.
- [62] Xiang Y, Wu Q, Liang L, Wang X, Wang J, Zhang X, *et al*. Chlorotoxin-modified stealth liposomes encapsulating levodopa for the targeting delivery against Parkinson's disease in the MPTP-induced mice model. *J Drug Target* 2012;20(1):67–75. doi:10.3109/1061186X.2011.595490, PMID:22149216.
- [63] Chen ZL, Huang M, Wang XR, Fu J, Han M, Shen YQ, *et al*. Transferrin-modified liposome promotes  $\alpha$ -mangostin to penetrate the blood-brain barrier. *Nanomedicine* 2016;12(2):421–430. doi:10.1016/j.nano.2015.10.02, PMID:26711963.
- [64] Moreno LC, Cavalcanti IM, Satyal P, Santos-Magalhães NS, Rolim HM, Freitas RM. Acute toxicity and anticonvulsant activity of liposomes containing nimodipine on pilocarpine-induced seizures in mice. *Neurosci Lett* 2015;585:38–42. doi:10.1016/j.neulet.2014.11.025, PMID:25445375.
- [65] Cao X, Hou D, Wang L, Li S, Sun S, Ping Q, *et al*. Effects and molecular mechanism of chitosan-coated levodopa nanoliposomes on behavior of dyskinesia rats. *Biol Res* 2016;49(1):32. doi:10.1186/s40659-016-0093-4, PMID:27378167.
- [66] Kempwade AA, Taranalli AD, Hiremath RD, Joshi SA. Formulation and Evaluation of Flexible Liposome Embedded *In Situ* Thermoreversible Intranasal Gel of Rizatriptan Benzoate. *Indian J Pharm Sci* 2022;84(4):863–873. doi:10.36468/pharmaceutical-sciences.981.
- [67] Fukuta T, Ishii T, Asai T, Sato A, Kikuchi T, Shimizu K, *et al*. Treatment of stroke with liposomal neuroprotective agents under cerebral ischemia conditions. *Eur J Pharm Biopharm* 2015;97(Pt A):1–7. doi:10.1016/j.ejpb.2015.09.020, PMID:26455340.
- [68] Benne N, van Duijn J, Lozano Vigario F, Lebourg RJT, van Veelen P, Kuiper J, *et al*. Anionic 1,2-distearoyl-sn-glycero-3-phosphoglycerol (DSPG) liposomes induce antigen-specific regulatory T cells and prevent atherosclerosis in mice. *J Control Release* 2018;291:135–146. doi:10.1016/j.jconrel.2018.10.028, PMID:30365993.
- [69] Li X, Xiao H, Lin C, Sun W, Wu T, Wang J, *et al*. Synergistic effects of liposomes encapsulating atorvastatin calcium and curcumin and targeting dysfunctional endothelial cells in reducing atherosclerosis. *Int J Nanomedicine* 2019;14:649–665. doi:10.2147/IJN.S189819, PMID:30697048.
- [70] Qu Y, Tang J, Liu L, Song L, Chen S, Gao Y.  $\alpha$ -Tocopherol liposome loaded chitosan hydrogel to suppress oxidative stress injury in cardiomyocytes. *Int J Biol Macromol* 2019;125:1192–1202. doi:10.1016/j.ijbiomac.2018.09.092, PMID:30227207.
- [71] Haeri A, Sadeghian S, Rabbani S, Anvari MS, Erfan M, Dadashzadeh S. PEGylated estradiol benzoate liposomes as a potential local vascular delivery system for treatment of restenosis. *J Microencapsul* 2012;29(1):83–94. doi:10.3109/02652048.2011.630107, PMID:22047547.
- [72] Zare Kazemabadi F, Heydarinasab A, Akbarzadeh A, Ardjmand M. Preparation, characterization and *in vitro* evaluation of PEGylated nanoliposomal containing etoposide on lung cancer. *Artif Cells Nanomed Biotechnol* 2019;47(1):3222–3230. doi:10.1080/21691401.2019.1646265, PMID:31373225.
- [73] Elbayoumi TA, Torchilin VP. Enhanced cytotoxicity of monoclonal anti-cancer antibody 2C5-modified doxorubicin-loaded PEGylated liposomes against various tumor cell lines. *Eur J Pharm Sci* 2007;32(3):159–168. doi:10.1016/j.ejps.2007.05.113, PMID:17707615.
- [74] Yao C, Wang P, Li X, Hu X, Hou J, Wang L, *et al*. Near-Infrared-Triggered Azobenzene-Liposome/Upconversion Nanoparticle Hybrid Vesicles for Remotely Controlled Drug Delivery to Overcome Cancer Multi-drug Resistance. *Adv Mater* 2016;28(42):9341–9348. doi:10.1002/adma.201503799, PMID:27578301.
- [75] Vartak R, Patil SM, Saraswat A, Patki M, Kunda NK, Patel K. Aerosolized nanoliposomal carrier of remdesivir: an effective alternative for COVID-19 treatment *in vitro*. *Nanomedicine (Lond)* 2021;16(14):1187–1202. doi:10.2217/nnm-2020-0475, PMID:33982600.
- [76] Shah VH, Jobanputra A. Enhanced Ungual Permeation of Terbinafine HCl Delivered Through Liposome-Loaded Nail Lacquer Formulation Optimized by QbD Approach. *AAPS PharmSciTech* 2018;19(1):213–224. doi:10.1208/s12249-017-0831-0, PMID:28681334.
- [77] Spellberg B, Walsh TJ, Kontoyiannis DP, McDermis J Jr, Ibrahim AS. Recent advances in the management of mucormycosis: from bench to bedside. *Clin Infect Dis* 2009;48(12):1743–1751. doi:10.1086/599105, PMID:19435437.
- [78] De Leo V, Milano F, Agostiano A, Catucci L. Recent Advancements in Polymer/Liposome Assembly for Drug Delivery: From Surface Modifications to Hybrid Vesicles. *Polymers (Basel)* 2021;13(7):1027. doi:10.3390/polym13071027, PMID:33810273.
- [79] Ning B, Huang Z, Youngquist BM, Scott JW, Niu A, Bojanowski CM, *et al*. Liposome-mediated detection of SARS-CoV-2 RNA-positive extracellular vesicles in plasma. *Nat Nanotechnol* 2021;16(9):1039–1044. doi:10.1038/s41565-021-00939-8, PMID:34294909.
- [80] Sercombe L, Veerati T, Moheimi F, Wu SY, Sood AK, Hua S. Advances and Challenges of Liposome Assisted Drug Delivery. *Front Pharmacol* 2015;6:286. doi:10.3389/fphar.2015.00286, PMID:26648870.
- [81] Levchenko TS, Hartner WC, Torchilin VP. Liposomes in diagnosis and treatment of cardiovascular disorders. *Methodist Debakey Cardiovasc J* 2012;8(1):36–41. doi:10.14797/mdcj-8-1-36, PMID:22891109.
- [82] Lin C, Gao H, Ouyang L. Advance cardiac nanomedicine by targeting the pathophysiological characteristics of heart failure. *J Control Release* 2021;337:494–504. doi:10.1016/j.jconrel.2021.08.002, PMID:34358590.



## Review Article

# Flavin-containing Monooxygenases in the Brain and their Involvement in Neurodegeneration and Aging



Boyu Li and Zhuoling An\*

Department of Pharmacy, Beijing Chao-Yang Hospital, Capital Medical University, Beijing, China

Received: August 15, 2022 | Revised: December 27, 2022 | Accepted: March 17, 2023 | Published online: April 28, 2023

## Abstract

Flavin-containing monooxygenases (FMOs) catalyze the oxygenation of a diverse range of sulfur or nitrogen-containing xenobiotics. Recently accumulated evidence has demonstrated the roles of FMOs in physiological and pathological conditions, including neurodegeneration and aging. However, the mechanisms underlying their functions are poorly understood. In this review, we summarize the expression and localization of FMOs in the brain, the endogenous chemicals and xenobiotics metabolized by FMOs, and the consequences of FMO deficiency. The understanding of FMOs activity in the brain is important for fully elucidating the roles of FMOs in pathological mechanisms.

## Introduction

Flavin-containing monooxygenases (FMOs) constitute a family of microsomal enzymes catalyzing the oxidation of nucleophilic heteroatom-containing xenobiotics.<sup>1</sup> They oxygenate the sulfur or nitrogen atoms in chemicals with soft nucleophiles.<sup>2</sup> FMOs are involved in the pathogenic process of trimethylaminuria, atherosclerosis, cardiovascular disease, diabetes, and metabolic disorders.<sup>3–6</sup> In recent years, the involvement of FMOs in neurodegeneration and aging has emerged,<sup>7</sup> but the underlying mechanisms have not been elucidated. In this review, we summarize the expression and localization of FMOs in the brain, the endogenous chemicals and xenobiotics metabolized by FMOs in the brain, and the consequences of FMO deficiency.

## FMO

FMO (EC 1.14.13.8) was first described by Ziegler *et al.*<sup>8,9</sup> Humans possess five functional FMO genes, designated *FMO1–5*. *FMO1–4* are clustered on chromosome 1 q24.3, and *FMO5* is lo-

cated at 1q21.1.<sup>10,11</sup> Numerous allelic variants, including approximately 20 of human *FMO1*, have been reported.<sup>12</sup>

Mammalian FMOs are NADPH- and oxygen-dependent microsomal monooxygenases that usually metabolize nitrogen- and sulfur-containing compounds.<sup>1,13,14</sup> The catalytic mechanism involves a first step in which FAD undergoes a 2-electron reduction by NADPH. The reduced flavin then reacts rapidly with molecular oxygen to form peroxyflavin. This nucleophilic attack by the substrate on FADOOH results in the transfer of one atom of molecular oxygen to the substrate with another contributing to the formation of water.

Trimethylaminuria is a currently confirmed rare inherited metabolic disorder associated with abnormal amounts of dietary-derived trimethylamine and is caused by the mutations in *FMO3*.<sup>15,16</sup>

## Emerging roles of FMOs in neurodegeneration and aging

### Amyotrophic lateral sclerosis

Association between FMOs and amyotrophic lateral sclerosis (ALS) has been widely reported although some reports are contradictory. Malaspina *et al.*<sup>17</sup> reported an 80% reduction in *FMO1* mRNA levels in the spinal cord of sporadic ALS patients. In contrast, Gagliardi *et al.*<sup>18</sup> observed greater *FMO1* expression in the spinal cord and brain stem of ALS patients compared with that in healthy controls. Gagliardi *et al.*<sup>19</sup> found that the mRNA levels of all FMOs except for *FMO3* were up-regulated in the brain of SOD1-mutated (G93A) ALS mice compared with control mice, with the highest increase in *FMO1* in the spinal cord and brainstem. Cereda *et al.*<sup>12</sup> found a significantly elevated frequency of *FMO1* single nucleotide polymorphisms in female sporadic ALS patients, further indicating that specific allelic variants of *FMO1* might be associated with ALS development.

**Keywords:** Flavin-containing monooxygenases (FMOs); Brain; Expression; Location; Substrates; Deficiency; Neurodegeneration and aging.

**Abbreviations:** ALS, amyotrophic lateral sclerosis; CYP, cytochrome P450; FMOs, flavin-containing monooxygenases; MPP<sup>+</sup>, 1-methyl-4-phenylpyridinium; MPTP, 1-methyl-4-phenyl-1,2,3,6-tetrahydropyridine; PD, Parkinson's disease; PTP, 4-phenyl-1,2,3,6-tetrahydropyridine; TMAO, trimethylamine N-oxide; NADPH, nicotinamide adenine dinucleotide phosphate oxidase; FAD, flavin adenine dinucleotide.

\*Correspondence to: Zhuoling An, Department of Pharmacy, Beijing Chao-yang Hospital, Capital Medical University, Beijing 100020, China. ORCID: <https://orcid.org/0000-0002-7996-5002>. Tel: +86 010 85231362, Fax: +86 010-8523-1362, E-mail: [anzhuoling@163.com](mailto:anzhuoling@163.com)

**How to cite this article:** Li B, An Z. Flavin-containing Monooxygenases in the Brain and their Involvement in Neurodegeneration and Aging. *J Explor Res Pharmacol* 2023;8(3):237–241. doi: 10.14218/JERP.2022.00067.

### Parkinsonism

Accumulating evidence indicates a relationship between FMOs and parkinsonism. The FMO gene cluster is associated with the volume of the lentiform nucleus, which is a physiological marker associated with Parkinson's disease (PD). Nicotine can be N-oxidized by FMOs and can reduce oxidative stress and neuro-inflammation in the brain and improve synaptic plasticity and neuronal survival of dopaminergic (DA) neurons, thereby benefiting PD patients.<sup>20,21</sup> MPTP (1-methyl-4-phenyl-1,2,3,6-tetrahydropyridine) is a neurotoxin and its toxic metabolite 1-methyl-4-phenylpyridinium (MPP<sup>+</sup>) can kill DA neurons and elicit parkinsonism. MPTP can be deactivated by FMOs into a harmless metabolite in the brain (discussed in detail in the section, *Endogenous Substances and Xenobiotics Oxygenated by FMOs in the Brain*). In addition, we have shown that FMO1 deficiency promotes neuroinflammation that affects the survival of DA neurons in mice. The levels of *FMO1* mRNA transcripts decreased in a rotenone model of parkinsonism, accompanied by decreasing levels of *parkin* mRNA transcripts and increased Caspase-3 activation.<sup>22,23</sup>

### Aging

*FMO1–5* have all been reported to be transcriptionally activated in classical mouse models of longevity, including calorie restriction, growth hormone/insulin-like growth factor 1 signaling disruption, and rapamycin treatment.<sup>7</sup> The expression of *FMO3* is up-regulated in the liver of a variety of longevity mouse models.<sup>24–27</sup> However, up-regulation of *FMO3* expression in hepatocytes of murine models has recently been shown to prevent or reverse hepatic aging. This mimicked calorie restriction and the associated mechanism is probably attributed to the promotion of autophagy.<sup>28</sup> Furthermore, feeding with a normal diet significantly down-regulated *FMO1* mRNA transcripts in mice in an age-dependent manner,<sup>29</sup> indicating that reduced *FMO1* expression contributes to the progression of aging. However, the specific mechanism underlying its role is still unknown.

### The expression and localization of FMOs in the brain

The mRNAs of mammalian FMO isoforms can be detected in different organs, including the liver, kidney, lung, and brain.<sup>30</sup> FMOs are active in human, rat, mouse, rabbit, hamster, and guinea pig brains.<sup>31–37</sup> Here we mainly review FMO activity in mouse and human brains.

#### Mouse brain

In an adult mouse brain, *FMO1* and 5 are the most abundant FMOs, as detected using isoform-specific antisense RNA probes.<sup>30</sup> *FMO1* mRNA transcripts are observed in neurons of the cerebrum and the choroid plexus while *FMO5* mRNA transcripts are only detected in neurons of the cerebrum. FMO expression in astrocytes remains controversial. Janmohamed *et al.*<sup>30</sup> reported no detectable FMO activity *in vivo*, while Di Monte *et al.*<sup>38</sup> detected FMO activity in primary cultures of mouse astrocytes.

In the neonatal brain, the most abundant FMO mRNA transcripts are *FMO1*, and their level drops by approximately 80% at 8 weeks of age. The levels of *FMO5* mRNA transcripts are 70% of *FMO1* in neonates and are similar to that of *FMO1* in 3-, 5- and 8-week-old mouse brains. *FMO2*, 3, and 4 mRNA transcripts are present at relatively low levels; approximately <1 molecule/cell.

#### Human brain

Zhang *et al.*<sup>34</sup> examined the developmental expression of FMOs in

60 human brain samples detecting all *FMO1–5* mRNA transcripts. FMO mRNA levels in the brain were much lower than that in other tissues, about less than 1% compared with the most abundant tissues observed (i.e., *FMO1* in the kidney, *FMO2* in the lung, and *FMO3* and 5 in the liver). *FMO1* is the only subtype to be down-regulated in adult human brains, while the amounts of other FMO mRNA transcripts in human brains remain similar among different age groups. Few studies have reported the expression of FMOs in human brains. Cashman *et al.*<sup>39</sup> found that *FMO3* was selectively expressed in the substantia nigra of human brains by immunohistochemistry.

### Endogenous substances and xenobiotics oxygenated by FMOs in the brain

#### Endogenous substances

FMO catalyzes the N- and S-oxygenation of several endogenous substances, including phenethylamine, tyramine, amphetamine, and trimethylamine that can be converted by FMO in the brain with clinical significance.<sup>40</sup> S-oxygenation of hypotaurine by FMO1 contributes to the production of taurine in the brain, which possesses neurotransmitter, antioxidant, and anti-inflammatory functions.<sup>41</sup>

#### Xenobiotics

FMO oxidizes particular xenobiotics in the brain. Nicotine, which is abundant in tobacco smoke and can diminish oxidative stress and neuroinflammation in the brain, is hydroxylated by CYP2A6 and undergoes glucuronidation by UDP-glucuronosyl transferases and oxidation by FMO.<sup>21,42,43</sup> Several psychoactive drugs, *e.g.* imipramine, chlorpromazine, and fluoxetine, are N- or S-oxygenated by FMO in both rat and human brains.<sup>31,32,44</sup> Imipramine causes greater sedation in wild-type animals compared with *FMO1*-null mice, probably because imipramine N-oxide is produced in the wild-type brain and a higher concentration of desipramine is produced in the *FMO1*-null brain.<sup>45</sup>

A typical xenobiotic oxidized by FMO is the pro-neurotoxin, MPTP, which can lead to DA neuron degeneration and parkinsonism in humans.<sup>46–48</sup> MPTP in the brain is rapidly converted to the toxic MPP<sup>+</sup><sup>49,50</sup> by monoamine oxidase B<sup>51,52</sup> or CYP (marmoset CYP2D6 and human CYP1A2).<sup>47,49,53</sup> However, MPTP can be deactivated to 4-phenyl-1,2,3,6-tetrahydropyridine (PTP) and MPTP N-oxide that is non-neurotoxic, by CYP2D6 and FMO (Fig. 1).<sup>53–55</sup> The concentrations of MPP<sup>+</sup> in *Suncus* brains after a single intraperitoneal administration of MPTP were markedly higher than that in rats, probably because of the lack of FMO activity in *Suncus* brains.<sup>56</sup> *FMO1* and 3 may contribute to this detoxification. MPTP N-oxygenation in human brain microsomes was consistently catalyzed by human *FMO1* and 3.<sup>53</sup>

### What are the consequences of FMO deficiency?

Genetic deficiency of FMOs has several consequences. *FMO1* deficiency promotes neuroinflammation that affects the survival of DA neurons in C57BL/6N mice.<sup>23</sup> Mice with *FMO1*, 2, and 4 deficiency exhibit a lean phenotype and enhanced resting energy expenditure, those with *FMO1* deficiency most likely underlying the metabolic phenotype.<sup>57</sup> *FMO3* is a target of insulin and knock-down of *FMO3* expression in insulin-resistant mice improves glucose tolerance.<sup>6</sup> Knockdown of *FMO3* expression in the liver of low-density lipoprotein receptor-knockout mice leads to decreased

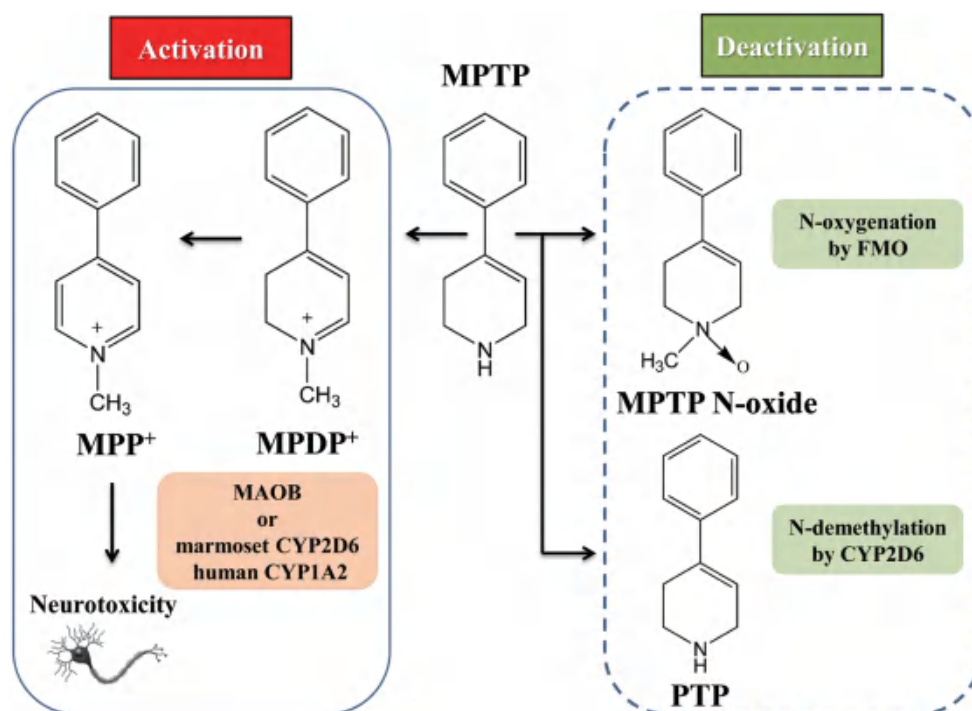


**Fig. 1. Metabolic activation and deactivation of MPTP.** Activation: MPTP was rapidly converted to the toxic metabolite MPP<sup>+</sup> through the intermediate MPDP<sup>+</sup> once in the brain mediated by monoamine oxidase B or CYP (marmoset CYP2D6 and human CYP1A2). Deactivation: MPTP N-oxygenation was efficiently mediated by FMOs in marmoset liver and brain microsomes. PTP formation was efficiently mediated by CYP2D6 in marmoset liver microsomes. FMOs, flavin-containing monooxygenases; MPTP, 1-methyl-4-phenyl-1,2,3,6-tetrahydropyridine; MPP<sup>+</sup>, 1-methyl-4-phenylpyridinium; PTP, 4-phenyl-1,2,3,6-tetrahydropyridine; CYP, cytochrome P450.

circulating trimethylamine N-oxide (TMAO) levels (an independent risk factor for cardiovascular disease) and atherosclerosis.<sup>4,5</sup> *Fmo5*<sup>-/-</sup> mice exhibit a lean phenotype and are resistant to age-related changes in glucose homeostasis compared with wild-type mice, indicating that FMO5 is a regulator of metabolic aging.<sup>58</sup> *Fmo5*<sup>-/-</sup> mice also possess metabolic characteristics similar to those of germ-free mice, indicating that FMO5 is crucial for sensing or responding to gut bacteria.<sup>59</sup> However, conditional knock-down of brain FMOs has not been reported.

### Further directions

The precise roles of FMOs in pathological processes remain to be determined. In-depth knowledge of FMO gene expression and protein localization and identification of substrates in the brain that are oxidized by FMOs may help in understanding the mechanisms of action of FMOs and their importance in the pathogenesis of neuronal degeneration and aging.

### Conclusions

The potential involvement of FMOs in neurodegeneration and aging has been demonstrated in recent years. FMOs play important roles in metabolizing certain endogenous chemicals and xenobiotics in the brain, which participate in physiological and pathological processes. Knowledge of the expression and localization of FMOs in the brain, the endogenous chemicals and xenobiotics metabolized by FMOs, and the consequences of FMO deficiency can help us understand their involvement in neurodegeneration and aging.

### Acknowledgments

We thank Dr. Shifeng Chu for his helpful advice and Jinglin Wang, Bingqing Ren, Linxi Zhang for their involvement in discussions.

### Funding

This work was supported by (1) The National Natural Science Foundation of China (Grant no. 81803500), (2) The Beijing Hospitals Authority Innovation Studio of Young Staff Funding Support (code 202108), and (3) The Undergraduate Scientific Research Training Program (XSKY2022).

### Conflict of interest

The authors declare no conflict of interests.

### Author contributions

Writing of the original draft (BL); supervision (ZA).

### References

- [1] Phillips IR, Shephard EA. Drug metabolism by flavin-containing monooxygenases of human and mouse. *Expert Opin Drug Metab Toxicol* 2017;13(2):167–181. doi:10.1080/17425255.2017.1239718, PMID:27678284.
- [2] Cashman JR. Role of flavin-containing monooxygenase in drug development. *Expert Opin Drug Metab Toxicol* 2008;4(12):1507–1521. doi:10.1517/17425250802522188, PMID:19040327.



- [3] Fennema D, Phillips IR, Shephard EA. Trimethylamine and Trimethylamine N-Oxide, a Flavin-Containing Monooxygenase 3 (FMO3)-Mediated Host-Microbiome Metabolic Axis Implicated in Health and Disease. *Drug Metab Dispos* 2016;44(11):1839–1850. doi:10.1124/dmd.116.070615, PMID:27190056.
- [4] Shih DM, Wang Z, Lee R, Meng Y, Che N, Charugundla S, *et al*. Flavin containing monooxygenase 3 exerts broad effects on glucose and lipid metabolism and atherosclerosis. *J Lipid Res* 2015;56(1):22–37. doi:10.1194/jlr.M051680, PMID:25378658.
- [5] Shih DM, Zhu W, Schugar RC, Meng Y, Jia X, Miikeda A, *et al*. Genetic Deficiency of Flavin-Containing Monooxygenase 3 (Fmo3) Protects Against Thrombosis but Has Only a Minor Effect on Plasma Lipid Levels–Brief Report. *Arterioscler Thromb Vasc Biol* 2019;39(6):1045–1054. doi:10.1161/ATVBAHA.119.312592, PMID:31070450.
- [6] Miao J, Ling AV, Manthena PV, Gearing ME, Graham MJ, Crooke RM, *et al*. Flavin-containing monooxygenase 3 as a potential player in diabetes-associated atherosclerosis. *Nat Commun* 2015;6:6498. doi:10.1038/ncomms7498, PMID:25849138.
- [7] Rossner R, Kaeberlein M, Leiser SF. Flavin-containing monooxygenases in aging and disease: Emerging roles for ancient enzymes. *J Biol Chem* 2017;292(27):11138–11146. doi:10.1074/jbc.R117.779678, PMID:28515321.
- [8] Ziegler DM. Flavin-containing monooxygenases: catalytic mechanism and substrate specificities. *Drug Metab Rev* 1988;19(1):1–32. doi:10.3109/03602538809049617, PMID:3293953.
- [9] Poulsen LL, Ziegler DM. Multisubstrate flavin-containing monooxygenases: applications of mechanism to specificity. *Chem Biol Interact* 1995;96(1):57–73. doi:10.1016/0009-2797(94)03583-t, PMID:7720105.
- [10] Phillips IR, Dolphin CT, Clair P, Hadley MR, Hutt AJ, McCombie RR, *et al*. The molecular biology of the flavin-containing monooxygenases of man. *Chem Biol Interact* 1995;96(1):17–32. doi:10.1016/0009-2797(94)03580-2, PMID:7720101.
- [11] Hernandez D, Janmohamed A, Chandan P, Phillips IR, Shephard EA. Organization and evolution of the flavin-containing monooxygenase genes of human and mouse: identification of novel gene and pseudogene clusters. *Pharmacogenetics* 2004;14(2):117–130. doi:10.1097/00008571-200402000-00006, PMID:15077013.
- [12] Cereda C, Gabanti E, Corato M, de Silvestri A, Alimonti D, Cova E, *et al*. Increased incidence of FMO1 gene single nucleotide polymorphisms in sporadic amyotrophic lateral sclerosis. *Amyotroph Lateral Scler* 2006;7(4):227–234. doi:10.1080/17482960600864413, PMID:17127561.
- [13] Krueger SK, Williams DE. Mammalian flavin-containing monooxygenases: structure/function, genetic polymorphisms and role in drug metabolism. *Pharmacol Ther* 2005;106(3):357–387. doi:10.1016/j.pharmthera.2005.01.001, PMID:15922018.
- [14] Cashman JR. Structural and catalytic properties of the mammalian flavin-containing monooxygenase. *Chem Res Toxicol* 1995;8(2):166–181. doi:10.1021/tx00044a001, PMID:7766799.
- [15] Treacy EP, Akerman BR, Chow LM, Youil R, Bibeau C, Lin J, *et al*. Mutations of the flavin-containing monooxygenase gene (FMO3) cause trimethylaminuria, a defect in detoxication. *Hum Mol Genet* 1998;7(5):839–845. doi:10.1093/hmg/7.5.839, PMID:9536088.
- [16] Cashman JR, Camp K, Fakharzadeh SS, Fennessey PV, Hines RN, Mamer OA, *et al*. Biochemical and clinical aspects of the human flavin-containing monooxygenase form 3 (FMO3) related to trimethylaminuria. *Curr Drug Metab* 2003;4(2):151–170. doi:10.2174/1389200033489505, PMID:12678693.
- [17] Malaspina A, Kaushik N, de Belleruche J. Differential expression of 14 genes in amyotrophic lateral sclerosis spinal cord detected using gridded cDNA arrays. *J Neurochem* 2001;77(1):132–145. doi:10.1046/j.1471-4159.2001.t01-1-00231.x, PMID:11279269.
- [18] Gagliardi S, Abel K, Bianchi M, Milani P, Bernuzzi S, Corato M, *et al*. Regulation of FMO and PON detoxication systems in ALS human tissues. *Neurotox Res* 2013;23(4):370–377. doi:10.1007/s12640-012-9356-1, PMID:23073612.
- [19] Gagliardi S, Ogliari P, Davin A, Corato M, Cova E, Abel K, *et al*. Flavin-containing monooxygenase mRNA levels are up-regulated in als brain areas in SOD1-mutant mice. *Neurotox Res* 2011;20(2):150–158. doi:10.1007/s12640-010-9230-y, PMID:21082301.
- [20] Barreto GE, Iarkov A, Moran VE. Beneficial effects of nicotine, cotinine and its metabolites as potential agents for Parkinson's disease. *Front Aging Neurosci* 2014;6:340. doi:10.3389/fnagi.2014.00340, PMID:25620929.
- [21] Perez-Paramo YX, Chen G, Ashmore JH, Watson CJW, Nasrin S, Adams-Haduch J, *et al*. Nicotine-N'-Oxidation by Flavin Monooxygenase Enzymes. *Cancer Epidemiol Biomarkers Prev* 2019;28(2):311–320. doi:10.1158/1055-9965.EPI-18-0669, PMID:30381441.
- [22] Li B, Yuan Y, Zhang W, He W, Hu J, Chen N. Flavin-containing monooxygenase, a new clue of pathological proteins in the rotenone model of parkinsonism. *Neurosci Lett* 2014;566:11–16. doi:10.1016/j.neulet.2013.11.036, PMID:24440618.
- [23] Li B, Yang S, Ye J, Chu S, Chen N, An Z. Flavin-containing monooxygenase 1 deficiency promotes neuroinflammation in dopaminergic neurons in mice. *Neurosci Lett* 2021;764:136222. doi:10.1016/j.neulet.2021.136222, PMID:34500002.
- [24] Swindell WR. Genes and gene expression modules associated with caloric restriction and aging in the laboratory mouse. *BMC Genomics* 2009;10:585. doi:10.1186/1471-2164-10-585, PMID:19968875.
- [25] Steinbaugh MJ, Sun LY, Bartke A, Miller RA. Activation of genes involved in xenobiotic metabolism is a shared signature of mouse models with extended lifespan. *Am J Physiol Endocrinol Metab* 2012;303(4):E488–E495. doi:10.1152/ajpendo.00110.2012, PMID:22693205.
- [26] Schirra HJ, Anderson CG, Wilson WJ, Kerr L, Craik DJ, Waters MJ, *et al*. Altered metabolism of growth hormone receptor mutant mice: a combined NMR metabolomics and microarray study. *PLoS One* 2008;3(7):e2764. doi:10.1371/journal.pone.0002764, PMID:18648510.
- [27] Swindell WR. Gene expression profiling of long-lived dwarf mice: longevity-associated genes and relationships with diet, gender and aging. *BMC Genomics* 2007;8:353. doi:10.1186/1471-2164-8-353, PMID:17915019.
- [28] Guo D, Shen Y, Li W, Li Q, Miao Y, Zhong Y. Upregulation of flavin-containing monooxygenase 3 mimics calorie restriction to retard liver aging by inducing autophagy. *Aging (Albany NY)* 2020;12(1):931–944. doi:10.18632/aging.102666, PMID:31927537.
- [29] Bhagwat SV, Bhamre S, Boyd MR, Ravindranath V. Cerebral metabolism of imipramine and a purified flavin-containing monooxygenase from human brain. *Neuropsychopharmacology* 1996;15(2):133–142. doi:10.1016/0893-133X(95)00175-D, PMID:8840349.
- [30] Janmohamed A, Hernandez D, Phillips IR, Shephard EA. Cell-, tissue-, sex- and developmental stage-specific expression of mouse flavin-containing monooxygenases (Fmos). *Biochem Pharmacol* 2004;68(1):73–83. doi:10.1016/j.bcp.2004.02.036, PMID:15183119.
- [31] Bhamre S, Bhagwat SV, Shankar SK, Williams DE, Ravindranath V. Cerebral flavin-containing monooxygenase-mediated metabolism of antidepressants in brain: immunochemical properties and immunocytochemical localization. *J Pharmacol Exp Ther* 1993;267(1):555–559. PMID:8229786.
- [32] Bhamre S, Bhagwat SV, Shankar SK, Boyd MR, Ravindranath V. Flavin-containing monooxygenase mediated metabolism of psychoactive drugs by human brain microsomes. *Brain Res* 1995;672(1-2):276–280. doi:10.1016/0006-8993(94)01135-5, PMID:7749747.
- [33] Zane NR, Chen Y, Wang MZ, Thakker DR. Cytochrome P450 and flavin-containing monooxygenase families: age-dependent differences in expression and functional activity. *Pediatr Res* 2018;83(2):527–535. doi:10.1038/pr.2017.226, PMID:28922349.
- [34] Zhang J, Cashman JR. Quantitative analysis of FMO gene mRNA levels in human tissues. *Drug Metab Dispos* 2006;34(1):19–26. doi:10.1124/dmd.105.006171, PMID:16183778.
- [35] Bhagwat SV, Bhamre S, Boyd MR, Ravindranath V. Further characterization of rat brain flavin-containing monooxygenase. Metabolism of imipramine to its N-oxide. *Biochem Pharmacol* 1996;51(11):1469–1475. doi:10.1016/0006-2952(96)00088-3, PMID:8630088.
- [36] Blake BL, Philpot RM, Levi PE, Hodgson E. Xenobiotic biotransforming enzymes in the central nervous system: an isoform of flavin-containing monooxygenase (FMO4) is expressed in rabbit brain. *Chem Biol Interact* 1996;99(1-3):253–261. doi:10.1016/0009-2797(95)03679-2, PMID:8620573.
- [37] Kawaji A, Isobe M, Takabatake E. Differences in enzymatic properties of flavin-containing monooxygenase in brain microsomes

- of rat, mouse, hamster, guinea pig and rabbit. *Biol Pharm Bull* 1997;20(8):917–919. doi:10.1248/bpb.20.917, PMID:9300142.
- [38] Di Monte DA, Wu EY, Irwin I, Delanney LE, Langston JW. Biotransformation of 1-methyl-4-phenyl-1,2,3,6-tetrahydropyridine in primary cultures of mouse astrocytes. *J Pharmacol Exp Ther* 1991;258(2):594–600. PMID:1907660.
- [39] Cashman JR, Zhang J. Interindividual differences of human flavin-containing monooxygenase 3: genetic polymorphisms and functional variation. *Drug Metab Dispos* 2002;30(10):1043–1052. doi:10.1124/dmd.30.10.1043, PMID:12228178.
- [40] Lin J, Cashman JR. Detoxication of tyramine by the flavin-containing monooxygenase: stereoselective formation of the trans oxime. *Chem Res Toxicol* 1997;10(8):842–852. doi:10.1021/tx970030o, PMID:9282832.
- [41] Veeravalli S, Phillips IR, Freire RT, Varshavi D, Everett JR, Shephard EA. Flavin-Containing Monooxygenase 1 Catalyzes the Production of Taurine from Hypotaurine. *Drug Metab Dispos* 2020;48(5):378–385. doi:10.1124/dmd.119.089995, PMID:32156684.
- [42] Hukkanen J, Jacob P 3rd, Benowitz NL. Metabolism and disposition kinetics of nicotine. *Pharmacol Rev* 2005;57(1):79–115. doi:10.1124/pr.57.1.3, PMID:15734728.
- [43] von Weymarn LB, Brown KM, Murphy SE. Inactivation of CYP2A6 and CYP2A13 during nicotine metabolism. *J Pharmacol Exp Ther* 2006;316(1):295–303. doi:10.1124/jpet.105.091306, PMID:16188955.
- [44] Ravindranath V, Boyd MR. Xenobiotic metabolism in brain. *Drug Metab Rev* 1995;27(3):419–448. doi:10.3109/03602539508998330, PMID:8521749.
- [45] Hernandez D, Janmohamed A, Chandan P, Omar BA, Phillips IR, Shephard EA. Deletion of the mouse *Fmo1* gene results in enhanced pharmacological behavioural responses to imipramine. *Pharmacogenet Genomics* 2009;19(4):289–299. doi:10.1097/FPC.0b013e328328d507, PMID:19262426.
- [46] Langston JW, Ballard PA Jr. Parkinson's disease in a chemist working with 1-methyl-4-phenyl-1,2,5,6-tetrahydropyridine. *N Engl J Med* 1983;309(5):310. doi:10.1056/nejm198308043090511, PMID:6602944.
- [47] Ballard PA, Tetrad JW, Langston JW. Permanent human parkinsonism due to 1-methyl-4-phenyl-1,2,3,6-tetrahydropyridine (MPTP): seven cases. *Neurology* 1985;35(7):949–956. doi:10.1212/wnl.35.7.949, PMID:3874373.
- [48] Davis KD, Taub E, Houle S, Lang AE, Dostrovsky JO, Tasker RR, *et al*. Globus pallidus stimulation activates the cortical motor system during alleviation of parkinsonian symptoms. *Nat Med* 1997;3(6):671–674. doi:10.1038/nm0697-671, PMID:9176495.
- [49] Langston JW. The MPTP Story. *J Parkinsons Dis* 2017;7(s1):S11–S19. doi:10.3233/JPD-179006, PMID:28282815.
- [50] Langston JW, Irwin I, Langston EB, Forno LS. 1-Methyl-4-phenylpyridinium ion (MPP<sup>+</sup>): identification of a metabolite of MPTP, a toxin selective to the substantia nigra. *Neurosci Lett* 1984;48(1):87–92. doi:10.1016/0304-3940(84)90293-3, PMID:6332288.
- [51] Chiba K, Trevor A, Castagnoli N Jr. Metabolism of the neurotoxic tertiary amine, MPTP, by brain monoamine oxidase. *Biochem Biophys Res Commun* 1984;120(2):574–578. doi:10.1016/0006-291x(84)91293-2, PMID:6428396.
- [52] Heikkila RE, Manzino L, Cabbat FS, Duvoisin RC. Protection against the dopaminergic neurotoxicity of 1-methyl-4-phenyl-1,2,5,6-tetrahydropyridine by monoamine oxidase inhibitors. *Nature* 1984;311(5985):467–469. doi:10.1038/311467a0, PMID:6332989.
- [53] Uehara S, Uno Y, Inoue T, Murayama N, Shimizu M, Sasaki E, *et al*. Activation and deactivation of 1-methyl-4-phenyl-1,2,3,6-tetrahydropyridine by cytochrome P450 enzymes and flavin-containing monooxygenases in common marmosets (*Callithrix jacchus*). *Drug Metab Dispos* 2015;43(5):735–742. doi:10.1124/dmd.115.063594, PMID:25735838.
- [54] Bajpai P, Sangar MC, Singh S, Tang W, Bansal S, Chowdhury G, *et al*. Metabolism of 1-methyl-4-phenyl-1,2,3,6-tetrahydropyridine by mitochondrion-targeted cytochrome P450 2D6: implications in Parkinson disease. *J Biol Chem* 2013;288(6):4436–4451. doi:10.1074/jbc.M112.402123, PMID:23258538.
- [55] Herraiz T, Guillén H, Galisteo J. Metabolite profile resulting from the activation/inactivation of 1-methyl-4-phenyl-1,2,3,6-tetrahydropyridine and 2-methyltetrahydro- $\beta$ -carboline by oxidative enzymes. *Biomed Res Int* 2013;2013:248608. doi:10.1155/2013/248608, PMID:23984327.
- [56] Mushiroda T, Ariyoshi N, Yokoi T, Takahara E, Nagata O, Kato H, *et al*. Accumulation of the 1-methyl-4-phenylpyridinium ion in suncus (*Suncus murinus*) brain: implication for flavin-containing monooxygenase activity in brain microvessels. *Chem Res Toxicol* 2001;14(2):228–232. doi:10.1021/tx0001225, PMID:11258972.
- [57] Veeravalli S, Omar BA, Houseman L, Hancock M, Gonzalez Malagon SG, Scott F, *et al*. The phenotype of a flavin-containing monooxygenase knockout mouse implicates the drug-metabolizing enzyme FMO1 as a novel regulator of energy balance. *Biochem Pharmacol* 2014;90(1):88–95. doi:10.1016/j.bcp.2014.04.007, PMID:24792439.
- [58] Gonzalez Malagon SG, Melidoni AN, Hernandez D, Omar BA, Houseman L, Veeravalli S, *et al*. The phenotype of a knockout mouse identifies flavin-containing monooxygenase 5 (FMO5) as a regulator of metabolic ageing. *Biochem Pharmacol* 2015;96(3):267–277. doi:10.1016/j.bcp.2015.05.013, PMID:26049045.
- [59] Scott F, Gonzalez Malagon SG, O'Brien BA, Fennema D, Veeravalli S, Coveney CR, *et al*. Identification of Flavin-Containing Monooxygenase 5 (FMO5) as a Regulator of Glucose Homeostasis and a Potential Sensor of Gut Bacteria. *Drug Metab Dispos* 2017;45(9):982–989. doi:10.1124/dmd.117.076612, PMID:28646079.



## Review Article

# Ferroptosis: Opportunities and Challenges in Cancer



Ying-Jie Jia<sup>1</sup>, Yu Zhang<sup>1</sup>, Xu-Bin Ma<sup>1</sup>, Yang Wang<sup>1</sup>, Ying-Qi Tian<sup>1</sup>, Peng-Xing He<sup>1,2\*</sup> and Yi-Chao Xu<sup>1,2\*</sup>

<sup>1</sup>Key Laboratory of Advanced Drug Preparation Technologies, Ministry of Education, Institute of Pharmaceutical Sciences, Institute of Pharmaceutical Sciences, School of Pharmaceutical Sciences, Zhengzhou University, Zhengzhou, China; <sup>2</sup>The First Affiliated Hospital of Zhengzhou University, Zhengzhou University, Zhengzhou, China

Received: January 11, 2023 | Revised: March 30, 2023 | Accepted: April 17, 2023 | Published online: May 23, 2023

## Abstract

Ferroptosis is a programmed cell death mainly manifested as accumulation of ferrous ions and cell lipid peroxidation. Ferroptosis is well regulated by multiple signaling pathways, of which SLC7A11/GPX4 axis is the key pathway negatively regulating ferroptosis by eliminating lipid peroxidation. While disorder of iron homeostasis catalyzes the lipid peroxidation by supplying ferrous iron. Lipid metabolism participates in ferroptosis by offering lipid substrates. In addition, transsulfuration pathway and FSP1/CoQ10 also involve in ferroptosis. Evading ferroptosis is one strategy that cancer bypasses cell death and develops resistance to chemotherapy or radiotherapy, making ferroptosis inducers the potential treatment for cancer. The objective of this review is to summarize the ferroptosis signaling pathways and ferroptosis inducers, thus exploring the opportunities and challenges of inducing ferroptosis in cancer.

## Introduction

In 2012, Dixon *et al.* proposed a type of unique programmed cell death type, ferroptosis, which is mainly characterized by high intracellular lipid peroxidation and iron disorders.<sup>1</sup> Morphologically, ferroptosis is mainly manifested by decreased mitochondrial volume or disappeared mitochondrial crest, increased mitochondrial membrane potential and membrane density.<sup>2</sup> In terms of biochemistry, it

is mainly involved the increase of reactive oxygen species (ROS), decreased activity of glutathione peroxidase 4 (GPX4), iron disorder and accumulation of lipid peroxidation.<sup>3</sup> Ferroptosis is a newly discovered programmed cell death, many signaling pathways and proteins involved in ferroptosis are continuously discovered and reported (Fig. 1). It is well known that Solute Carrier Family 7 Member 11 (SLC7A11)/GPX4 inhibits ferroptosis by eliminating the ROS and lipid peroxidation. While iron metabolism and lipid metabolism participate in ferroptosis by supplying ferrous iron and unsaturated lipid.<sup>4,5</sup> In addition, ferroptosis can also be regulated by transsulfuration pathway and mevalonate pathway through regulating cysteine level and coenzyme Q10 (CoQ10) content, respectively.<sup>6,7</sup>

Ferroptosis is associated with various diseases, including (neuro)degenerative diseases, ischemia-reperfusion injury, acute kidney injury, and cancer.<sup>8</sup> Evading ferroptosis is one of manners that tumor cells bypass cell death, inhibiting different key molecules of ferroptosis can re-sensitive tumor cells to ferroptosis. In addition, the higher the level of ferroptosis in cancer patients receiving radiotherapy, the better the radiation response and the longer the survival of patient.<sup>9</sup> Evading ferroptosis plays key role in resistance of cancer to chemotherapy or radiotherapy, inducing ferroptosis might overcome chemotherapy or radiotherapy resistance.<sup>10</sup> Recently reported ferroptosis inducers can be divided into four categories according to their mechanisms. The first and second categories are the ferroptosis inducers that directly targeting SLC7A11 and GPX4, respectively.<sup>11–13</sup> The third type of ferroptosis inducers is ferroptosis inducing 56 (FIN56) inducers that consume CoQ10 by activating squalene synthase, promoting cellular lipid peroxidation, and ultimately inducing ferroptosis.<sup>7,12</sup> The fourth type is 1,2-dioxolane FINO2 inducers that indirectly inhibit GPX4 and directly oxidize iron to induce lipid peroxidation.<sup>14</sup>

**Keywords:** Ferroptosis; SLC7A11; Iron metabolism; Lipid metabolism; Ferroptosis inducer.

**Abbreviations:** AA, arachidonic acid; AACT, acetoacetyl-CoA thiolase; ACSL4, Acyl-CoA synthase long chain member 4; AdA, adrenal acid; AHCYL1, adenosine homocysteine 1; CARS, cysteinyl- tRNA synthetase; CBS, cystathionine-β-synthase; CTH, cystathionine c-lyase; DMT1, divalent metal transporter 1; FPN1, ferroportin 1; FPP, farnesyl pyrophosphate; FSP1, ferroptosis suppressor protein 1; GPX4, glutathione peroxidase 4; GR, glutathione reductase; GSH, glutathione; HMG-CoA, 3-hydroxy-3-methylglutaryl CoA; HMGR, hydroxymethylglutaryl CoA reductase; HMGS, 3-hydroxy-3-methylglutaryl CoA synthase; IPP, isopentenyl pyrophosphate; LOXs, lipoxygenases; LPCAT3, lysophosphatidylcholine transferase 3; MAT1A/MAT2A, methionine adenosine transferase 1a/1a; MS, methionine synthetase; MTs, methyltransferase; MVA, mevalonic acid; NCOA4, nuclear receptor coactivator 4; PC, phosphatidylcholine; PE, phosphatidylethanolamine; PUFA, polyunsaturated fatty acid; ROS, reactive oxygen species; SAH, s-adenosine homocysteine; SAHH, S-adenosine homocysteine hydrolase; SAM, S-adenosine methionine; STEAP3, six-transmembrane epithelial antigen of prostate 3; Tf, transferrin; TFR1, transferrin receptor 1.

\*Correspondence to: Yi-Chao Xu and Peng-Xing He, Key Laboratory of Advanced Drug Preparation Technologies, Ministry of Education, Institute of Pharmaceutical Sciences, School of Pharmaceutical Sciences, Zhengzhou University, Zhengzhou 450001, China. ORCID: <https://orcid.org/0000-0002-4558-0518> (YCX) and <https://orcid.org/0000-0003-2679-127X> (PXH). Tel: +0086-0371-67781907 (YCX) and +0086-0371-67781907 (PXH), E-mail: xuyc2017@zzu.edu.cn (YCX) and hepengxing@zzu.edu.cn (PXH)

**How to cite this article:** Jia YJ, Zhang Y, Ma XB, Wang Y, Tian YQ, He PX, *et al.* Ferroptosis: Opportunities and Challenges in Cancer. *J Explor Res Pharmacol* 2023;8(3):242–252. doi: 10.14218/JERP.2023.00003.



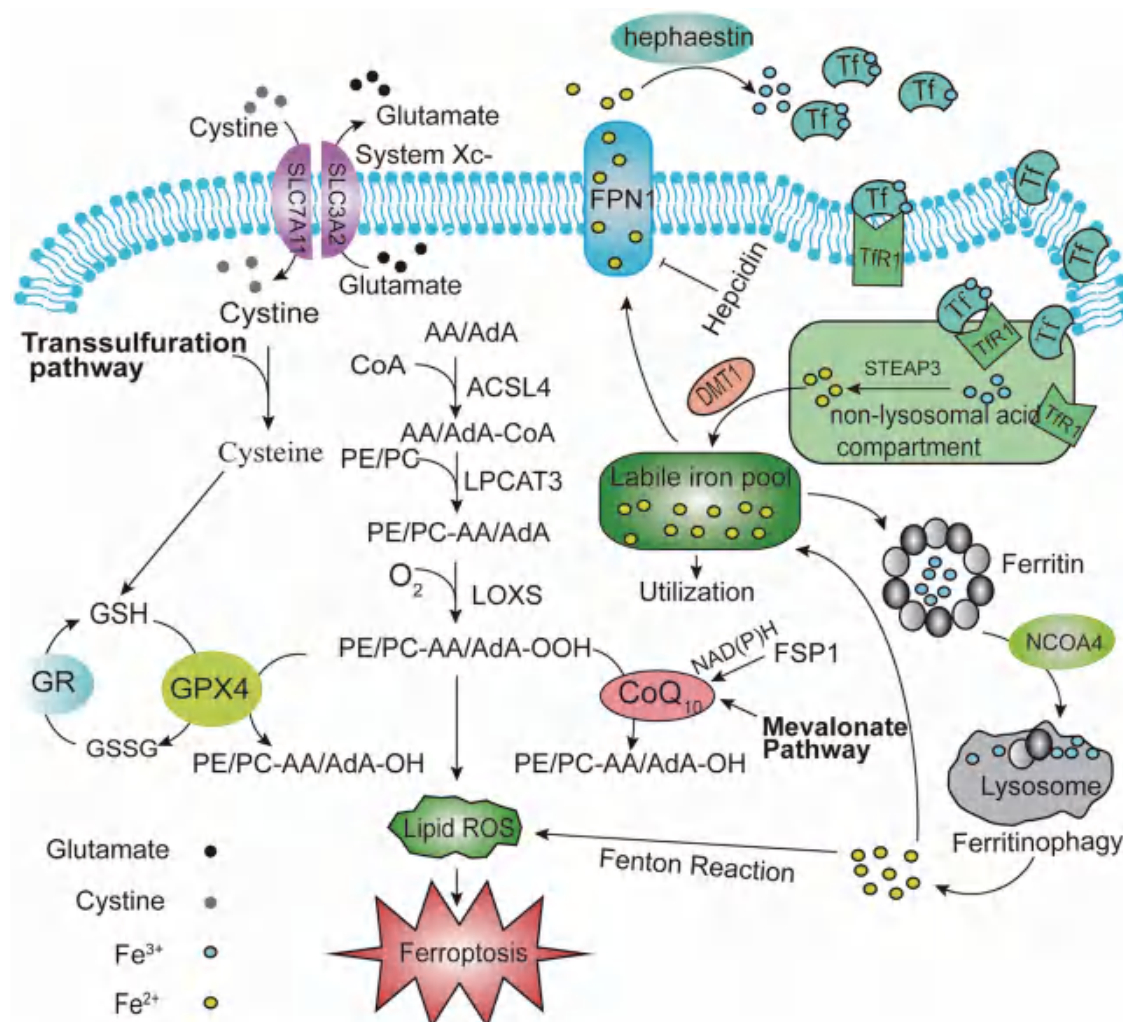


**Fig. 1. Ferroptosis signaling pathways.** AA, arachidonic acid; ACSL4, Acyl-CoA synthase long chain member 4; AdA, adrenic acid; CoA, coenzyme A; CoQ10, Coenzyme Q10; DMT1, divalent metal transporter 1; FPN1, ferroportin 1; FSP1, ferroptosis suppressor protein 1; GPX4, glutathione peroxidase 4; GR, glutathione reductase; GSH, glutathione; GSSG, oxidized; LOXS, lipoxygenases; LPCAT3, lysophosphatidylcholine transferase 3; NADH, reduced form of nicotinamide adenine dinucleotide; NADPH, reduced form of nicotinamide adenine dinucleotide phosphate; NCOA4, nuclear receptor coactivator 4.; PC, phosphatidylcholine; PE, phosphatidylethanolamine; ROS, reactive oxygen species; SLC3A2, solute carrier family 3 member 2; SLC7A11, solute carrier family 7, member 11; STEAP3, six-transmembrane epithelial antigen of prostate 3; Tf, transferrin; TfR1, transferrin receptor 1.

## Ferroptosis signaling pathways

### SLC7A11/GPX4 axis

SLC7A11, also known as xCT, together with heavy chain subunit Solute Carrier Family 3 Member 2 (SLC3A2) form cystine-glutamate acid reverse transporter (System Xc<sup>-</sup>), mediating the exchange of intracellular glutamate with extracellular cystine at 1:1. Once transported into the cell, cystine is rapidly converted into cysteine (L-cysteine), which is then utilized to synthesize glutathione (GSH).<sup>15</sup> In the heterodimer of System Xc<sup>-</sup>, SLC7A11 executes the function of transporting amino acids, while SLC3A2 is required for the stability and trafficking of SLC7A11 to the cell membrane.<sup>16</sup> mTORC2, as a growth factor integrating variety of signaling pathway, phosphorylates the 26th serine of SLC7A11 to reduce its activity, thereby inhibiting cystine intake and glutathione metabolism.<sup>17</sup> The regulation of SLC7A11 has been well reviewed by Boyi Gan group.<sup>18</sup> GPX4 plays a pivotal role in ferroptosis by

reducing lipid hydroperoxides to lipid alcohols.<sup>19</sup> GPX4, as a selenase, requires the participation of GSH acts as a cofactor.<sup>20,21</sup> Inhibition of SLC7A11 or GPX4 activity can induce the production of lipid ROS, which in turn induces ferroptosis.<sup>19,22</sup>

### Transsulfuration pathway

Transsulfuration pathway, as the backup supply of cysteine, plays important role in the growth of cancer cells. Transsulfuration pathway negatively regulates ferroptosis by de novo synthesizing cysteine (Fig. 2), which is a rate-limiting precursor for the synthesis of GSH.<sup>23</sup> Intracellular cysteine is indirectly supplied with cysteine by System Xc<sup>-</sup> or directly produced by the transsulfuration pathway.<sup>15</sup> Once intracellular cysteine is deficient, the cell will initiate transsulfuration pathway to synthesize cysteine from methionine.<sup>6</sup> In transsulfuration pathway, methionine reacts with ATP to form S-adenosine methionine (SAM) under the catalysis of methionine adenosine transferase Ia/IIa (MAT1A/MAT2A).<sup>24,25</sup> Then



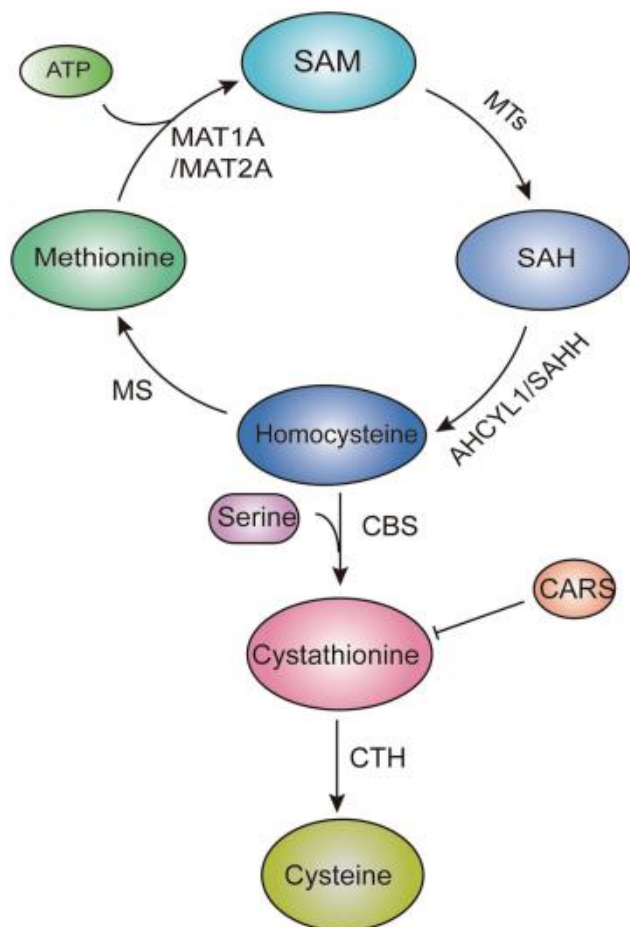


**Fig. 2. Transsulfuration pathway.** AHCYL1, adenosine homocysteine 1; ATP, adenosine triphosphate; CARS, cysteinyl- tRNA synthetase; CBS, cystathionine- $\beta$ -synthase; CTH, cystathionine c-lyase; MAT1A/MAT2A, methionine adenosine transferase 1 $\alpha$ /1 $\alpha$ ; MS, methionine synthetase; MTs, methyltransferase; SAH, s-adenosine homocysteine; SAHH, S-adenosine homocysteine hydrolase; SAM, S-adenosine methionine.

SAM is converted to s-adenosine homocysteine (SAH) by losing a methyl group in the presence of methyltransferase (MTs).<sup>25</sup> SAH is then hydrolyzed to form homocysteine in the presence of adenosine homocysteine 1 (AHCYL1) or S-adenosine homocysteine hydrolase (SAHH).<sup>25,26</sup> Finally, Under the action of the enzyme cystathionine- $\beta$ -synthase (CBS), serine is coupled into homocysteine to form cystathionine, which can then be cleaved by cystathionine c-lyase (CTH) to release cysteine.<sup>6,27</sup>

Several investigations have reported that upregulation of transsulfuration pathway prevented ferroptosis induced by SLC7A11 inhibition. Knockdown of cysteinyl- tRNA synthetase (CARS) could upregulate the transsulfuration pathway by accumulation of cystathionine, thus suppressing erastin induced ferroptosis.<sup>28</sup> It has been reported that transformation of SAM to SAH determined the transsulfuration pathway activity, inducible of which contributed to cellular cysteine pool and promoted cancer cell growth upon cysteine restriction.<sup>27</sup> Depletion of parkinsonism-associated deglycase DJ-1, an oncogene located at 1P36.12-13 of human genome, reduced the activity of SAHH, thus leading to inhibition of transsulfuration pathway, enhancing the sensitivity of cancer cells to SLC7A11 inhibitor.<sup>29,30</sup>

### Iron metabolism

Iron is an indispensable trace element in the human body and is widely involved in metabolism and biology process as a cofactor or component of the enzymes.<sup>31</sup> Excess irons will damage cells by catalyzing Fenton reaction, thus inducing ferroptosis.<sup>32-35</sup> Normally, absorbed irons in blood vessel are ferric irons ( $\text{Fe}^{3+}$ ) bound by transferrin (Tf). Tf containing one or two ferric ions binds to transferrin receptor 1 (TfR1), forming a complex that enters the cell via receptor-mediated endocytosis and then enters the non-lysosomal acid compartment.<sup>36</sup> Ferric ions are then released from the transferrin complex by endosomal acidification and reduced to ferrous ions ( $\text{Fe}^{2+}$ ) by six-transmembrane epithelial antigen of prostate 3 (STEAP3), Tf will separate from its receptor TfR1 and re-enter the bloodstream to capture ferric ions.<sup>37,38</sup> Meanwhile, divalent metal transporter protein 1 (DMT1) accounts for the transfer of ferrous ions to the labile iron pool, in which ferrous ions are easily transported to different cell machinery to participate in the synthesis of DNA synthase, heme and iron-sulfur cluster enzymes.<sup>38,39</sup> The excess ferrous ions are then stored in ferritin as the type of ferric irons.<sup>39</sup> Nuclear receptor coactivator 4 (NCOA4), as the selective cargo receptor of ferritin, participating in the autophagy of ferritin, thus releasing the stored ferrous irons.<sup>40</sup> Ferroportin 1 (FPN1) is a transmembrane protein responsible for iron output and iron balance in cells, degradation of which is regulated by hepcidin, a circulatory regulatory hormone peptide produced by liver cells.<sup>41,42</sup>

Accumulation of ferrous irons in tumor cells affected by various factors will induce ferroptosis by participating in the production of lipid ROS. Knock-down of NCOA4 could abolish degradation of ferritin and reduce the intracellular  $\text{Fe}^{2+}$  level, thus inhibiting ferroptosis induced by erastin.<sup>43</sup> New studies have shown that upregulated FPN1 can also inhibit ferroptosis, while silencing or downregulating FPN1 enhances the sensitivity of tumor cells to ferroptosis inducer.<sup>44,45</sup>

IRE (iron response element) /IRP (iron regulatory protein) axis plays critical role in maintaining iron homeostasis through post-transcriptional regulation of iron-related genes. IRP1 and IRP2 specifically recognize the IREs and regulate cell iron homeostasis by blocking or promoting the translation of target mRNAs bound by IRE, which contains conserved stem-loop.<sup>46,47</sup> Binding of IREs with IRPs is well regulated by iron concentration.<sup>48</sup> When intracellular irons are deficient, IRP1 binds to the IRE of TfR1 and ferritin, thus increasing the iron uptake and reducing iron storage.<sup>49</sup> On the contrary, high iron content in cells will reduce iron intake and increase iron storage by releasing of IRP1/2 from IRE of TfR1 and ferritin.<sup>38,50</sup> It has been found dihydroartemisinin made cells sensitive to ferroptosis by impinging IRP-IRE system and lysosomal mediated ferritin degradation, both of which increased the intracellular free iron content.<sup>51</sup>

### Lipid metabolism pathway

Lipid peroxidation is an important manifestation of ferroptosis and unsaturated fatty acids are the substrates of lipid peroxidation, thus disorder of lipid metabolism is closely related with ferroptosis. Identifying the lipid substances and pivotal enzymes for lipid peroxidation will supply more information for ferroptosis. Among the various lipids, phospholipid-related polyunsaturated fatty acids (PUFAs) such as phosphatidylethanolamine (PE) and phosphatidylcholine (PC) play key role in ferroptosis as the substrates for lipid peroxidation.<sup>52</sup> Genome-wide CRISPR-based genetic screen uncovers that Acyl-CoA synthase long chain member 4 (ACSL4) is essential for ferroptosis execution.<sup>53</sup> ACSL4 connects CoA to arachidonic acid (AA) and adrenal acid (AdA) to form fatty acyl-

coA esters.<sup>53</sup> Then, under the catalysis of lysophosphatidylcholine transferase 3 (LPCAT3), AA-CoA and AdA-CoA react with PC or PE to form PE-AA and PE-AdA.<sup>54</sup> Lipoxygenases (LOXs) are dioxygenases that catalyze the peroxidation of PUFAs to produce various lipid peroxides and bioactive lipids in the presence of molecular oxygen.<sup>55,56</sup> Genetic or pharmacological inhibition of ACSL4 inhibited ferroptosis by preventing the esterification of AA or AdA into PE, which was the only lipid oxidized in endoplasmic-reticulum-associated compartments during ferroptosis.<sup>57</sup> Arachidonate 12-Lipoxygenase (ALOX12) was indispensable for p53 induced ferroptosis and dispensable for erastin induced ferroptosis.<sup>58</sup> In addition, Genome-wide CRISPR/Cas9-mediated screen uncovered that cytochrome P450 oxidoreductase promoted ferroptosis across a wide range of lineages and cell-states by peroxidation of membrane polyunsaturated phospholipids.<sup>59</sup> The relationship between ferroptosis and lipid metabolism is complex, and its specific mechanism still needs to be further explored.

### Mevalonate pathway

The mevalonate pathway occurs in the cytoplasm, where Acetoacetyl-CoA thiolase (AACT) produces acetoacetyl-CoA by condensation of two units of acetyl-coA, and then 3-hydroxy-3-methylglutaryl CoA synthase (HMGS) condensates acetoacetyl-CoA and acetyl-CoA to form 3-hydroxy-3-methylglutaryl CoA (HMG-CoA), which is then catalyzed by hydroxymethylglutaryl-CoA reductase (HMGR) to generate mevalonic acid (MVA).<sup>60</sup> MVA is then phosphorylated by MVA kinase and converted to isopentenyl pyrophosphate (IPP), which contributes to the synthesis of farnesyl pyrophosphate (FPP). FPP is converted to squalene, and finally squalene is converted to cholesterol.<sup>61</sup> In addition, FPP can also participate in the production of CoQ10.<sup>62</sup> Thus, the mevalonate pathway finally leads to the production of CoQ10, cholesterol, and IPP (Fig. 3).<sup>7,52,63</sup> CoQ10 is a fat-soluble antioxidant with the function of scavenging oxygen free radicals, protecting lipids in golgi and plasma membranes from oxidation.<sup>7,64</sup> Ferroptosis suppressor protein 1 (FSP1) with myristic acylation is recruited to the plasma membrane to reduce CoQ10 by using NAD(P)H, preventing the reproduction of lipid peroxides, thus inhibiting ferroptosis.<sup>65–68</sup> FSP1-CoQ10-NAD(P)H pathway is the stand-alone parallel system with GSH-GPX4 pathway to inhibit phospholipid peroxidation and ferroptosis.<sup>69</sup>

In addition, the mevalonate pathway participates in ferroptosis by supplying IPP for production of selenoproteins, including GPX4. As an intermediate product of the mevalonate pathway, IPP is required for isoprenylation of selenocysteine tRNA, which is indispensable for synthesizing selenoprotein GPX4.<sup>70</sup> HMGR inhibitor statins reduced GPX4 expression in cancer cells, leading to elevated lipid peroxides and making cancer cells sensitive to ferroptosis.<sup>71</sup>

### p53

p53 is a well-known tumor suppressor that induces cell cycle arrest and cell apoptosis. Recently, it has been reported that p53 induces ferroptosis through pleiotropic effect.<sup>72</sup> Mutant p53<sup>3KR</sup>, which is defective for the conventional p53 functions, still be able to repress SLC7A11 and induce ferroptosis upon ROS-induced stress.<sup>73,74</sup> In addition, p53 induced ferroptosis required enzymatic activity of ALOX12, which is inhibited by SLC7A11, but independent of GPX4.<sup>58</sup> Recently, scientists found that p53-driven ferroptosis under ROS stress can also be suppressed by calcium-independent phospholipase iPLA2 $\beta$ , which mediated detoxification of peroxidized lipids.<sup>75</sup>

Moreover, p53 induced ferroptosis by directly activating its target gene spermidine/spermine N1-acetyltransferase 1 (SAT1), which induced lipid peroxidation.<sup>76</sup> p53 suppresses tumor through regulating its target gene, glutamine synthase 2 (GLS2), which exerts antioxidant defense function.<sup>77</sup> Another article reported that GLS2 knockdown inhibits ferroptosis in mouse embryonic fibroblasts.<sup>78</sup> Therefore, whether p53 induces ferroptosis by promoting GLS2 expression is worth further investigation.

However, wild-type p53 could delay induction of ferroptosis by regulating its transcriptional target CDKN1A (encoding p21).<sup>79</sup> p53 can also inhibit ferroptosis in a transcription-independent manner. For example, the deletion of p53 prevents the nuclear accumulation of dipeptidyl peptidase-4 (DPP4), thus facilitates plasma-membrane-associated DPP4-dependent lipid peroxidation, which finally results in ferroptosis.<sup>80</sup>

### Targeting ferroptosis in cancer

In recent years, more and more researchers are committed to discovering the development process of cancer, and found that ferroptosis is closely related to the occurrence and development of cancers. The ferroptosis inducers are attracting increasing attention in cancer treatment. In addition, ferroptosis inducers can enhance the effect of chemotherapy by inducing ferroptosis and reducing chemotherapy resistance, thereby improving the treatment effect. In this part, we elucidate the rational of targeting ferroptosis and the reported ferroptosis inducers (Table 1).<sup>1,7,13,22,81–115</sup>

#### SLC7A11 inhibitors

SLC7A11 mediates uptake of extracellular cystine, which guarantees glutathione synthesis and maintains GPX4 enzyme activity to inhibit ferroptosis.<sup>15,20</sup> SLC7A11 overexpression has been observed in hepatocellular carcinoma and is associated with poor prognosis.<sup>116,117</sup> SLC7A11 is regulated by multiple enzymes and pathways. It has been reported that mutant p53 fail to induce cell cycle arrest and cell apoptosis, but still be able to repress SLC7A11 and induce ferroptosis upon ROS-induced stress.<sup>73,74</sup> Tumor suppressor BRCA1-associated protein 1 (BAP1) frequently mutated or deleted in sporadic human cancers, inactivation of BAP1 inhibited ferroptosis by releasing SLC7A11 inhibition, thus BAP1 mutated cancer cells were sensitive to SLC7A11 inhibitor erastin.<sup>118</sup> OTUB1 is overexpressed in a variety of human cancers, and it can inhibit ferroptosis by stabilizing SLC7A11.<sup>119</sup> In short, SLC7A11 is an important target for the treatment of cancer and more and more SLC7A11 inhibitors have been discovered and reported.

In 2012, researchers firstly proposed that erastin induced ferroptosis by inhibiting System Xc<sup>-</sup> activity.<sup>1</sup> Later, more reports proved that erastin induce ferroptosis by inhibiting SLC7A11 activity in variety of cancer cells.<sup>81,120</sup> Given the fact that poor water solubility and unstability of erastin, a metabolically stable erastin analogue, imidazole ketone erastin (IKE), has been developed.<sup>22,82</sup> Sorafenib, as a multi-target kinase inhibitor, is clinically used for the treatment of unresectable hepatocellular carcinoma.<sup>121</sup> In 2014, it was firstly reported that sorafenib can induce ferroptosis by inhibiting System Xc<sup>-</sup>.<sup>122</sup> However, it was recently reported that Sorafenib could not induce ferroptosis by inhibiting System Xc<sup>-</sup>, thus it might not be a true ferroptosis inducer.<sup>123</sup> Sulfasalazine is clinically used for treating ulcerative colitis.<sup>124</sup> Recent study found that sulfasalazine is also a novel potent inhibitor of the System Xc<sup>-</sup>.<sup>83</sup> However, all SLC7A11 inhibitors currently identified, including sulfasalazine and erastin, have off-target effects, which limits their clinical use as SLC7A11 specific inhibitors.<sup>125</sup>

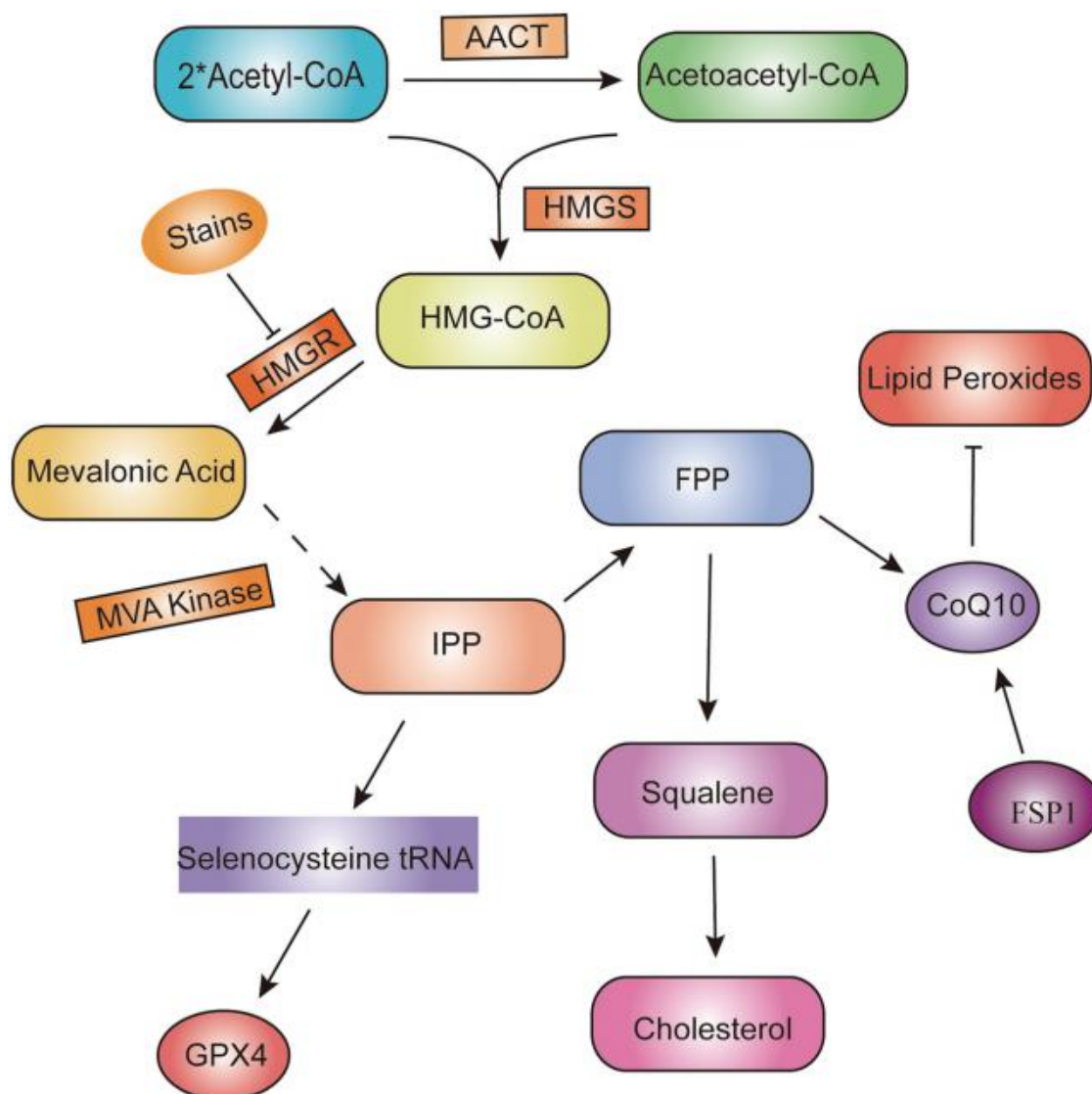


**Fig. 3. Mevalonate pathway.** AACT, acetoacetyl-CoA thiolase; HMGS, 3-hydroxy-3-methylglutaryl-CoA synthase; HMG-CoA, 3-hydroxy-3-methylglutaryl CoA; HMGR, hydroxymethylglutaryl CoA reductase; MVA, mevalonic acid; IPP, isopentenyl pyrophosphate; FPP, farnesyl pyrophosphate; CoQ10, Coenzyme Q10; FSP1, ferroptosis suppressor protein 1; GPX4, glutathione peroxidase 4.

In addition, a variety of compounds have been reported to be able to indirectly inhibit SLC7A11, such as the newly discovered small molecule compound 6-Thioguanine,<sup>84</sup> the drug Tirapazamine,<sup>85</sup> and T-2 Toxin.<sup>86</sup> The oral anti-diabetic drug metformin can also reduce the stability of SLC7A11 by inhibiting UFMylation of SLC7A11, and its combination with sulfasalazine can synergistically induce ferroptosis in breast cancer cells.<sup>87</sup> Some natural products, including Talaroconvolutin A,<sup>88</sup> Tanshinone IIA,<sup>89</sup> Actinidia chinensis Planch and Capsaicin,<sup>90,91</sup> can also induce ferroptosis by partially inhibiting SLC7A11.

#### GPX4 inhibitors

GPX4 is a selenase that utilizes GSH as a cofactor to reduce membrane phospholipid peroxide to maintain cellular redox homeostasis, thus negatively regulating ferroptosis.<sup>20</sup> Pharmacological inhibition or genetic absence of GPX4 induce ferroptosis in

mouse tumor xenografts.<sup>19</sup> Analyzing the data from TCGA, scientists found that GPX4 expression in various cancer tissues is higher than that in normal tissues, and it is negatively correlated with the prognosis of cancer patients.<sup>126</sup> High expression of GPX4 promotes tumor recurrence in melanoma xenograft mice models.<sup>71</sup> In addition, GPX4 plays important role in the survival of drug resistant cancer cells.<sup>127</sup> Therefore, GPX4 serves as the potential target to treat cancer by inducing ferroptosis.

The first reported GPX4 inhibitor RSL3 covalently interacts with selenocysteine, the active site of GPX4, to inhibit enzymatic activity of GPX4, thus inducing ferroptosis.<sup>13</sup> Poor pharmacokinetic property of RSL3 restricted its application in vivo. Recent studies reported that small-molecule compound QD394 and compound 26a induce ferroptosis by directly targeting GPX4.<sup>92,93</sup> In addition, many small-molecule compounds induce ferroptosis mainly through GPX4 inhibition, including Jiyuan oridonin A

**Table 1. Ferroptosis inducers**

Ferroptosis inducers	Target	Basic mechanism	Tumor type	Reference
Erastin, IKE, Sorafenib, Sulfasalazine, 6-Thioguanine	SLC7A11	Inhibit System Xc <sup>-</sup>	Fibrosarcoma, Colorectal cancer, Diffuse large B cell lymphoma, Astrocytoma, Lung carcinoma cancer, Lymphoma, Non-Hodgkin's Lymphoma, Gastric cancer	1,86,22,82,83,84
Tirapazamine, T-2 Toxin, Tanshinone IIA, Talaroconvolutin A	SLC7A11	Inhibit the expression of SLC7A11	Osteosarcoma, Lung cancer, Gastric cancer, Colorectal cancer	85,86,88,89
Metformin	SLC7A11	Reduces the protein stability of SLC7A11	Breast cancer	87
Actinidia chinensis Planch, Capsaicin	SLC7A11	Inhibit the expression of SLC7A11 and GPX4	Gastric cancer, Non-small cell lung cancer	90,91
RSL3, QD394, Compound 26a, Honokiol, FINO2,	GPX4	Inhibit GPX4 enzymatic activity	Renal carcinoma, Colon cancer, B-lymphoblastic cell leukemia line, Pancreatic cancer, Breast cancer, Breast adenocarcinoma, Fibrosarcoma	13,92,93,103,110
Jiyuan oridonin A derivative a2 Compound 21, Tetrahydro citrate, Bufotaline, Dihydroisotanshinone I Solasonine, Cucurbitin B, Gambogenic acid, Thiostrepton, Red ginseng polysaccharide, Apatinib, Simvastatin, Atorvastatin	GPX4	Downregulate GPX4 expression	Gastric cancer, Hepatocellular carcinoma, Nasopharyngeal carcinoma, Melanoma, Human cardiomyocytes, Murine skeletal muscle cells, Breast cancer, Non-small cell lung cancer, Lung cancer, Gastric cancer, Triple-negative breast cancer, Pancreatic cancer	94–109,102,104–109
DMOCPTL, FIN56	GPX4	Promote degradation of GPX4,	Triple-negative breast cancer, Fibrosarcoma	7,101
Curcumin analogues EF24, Cadmium	HMOX1	Directly up-regulating HMOX1 expression	Osteosarcoma, Hepatic stellate cells	111,112
Artesunate, Saponin Formosanin C	Ferritin	Promote ferritin phagocytosis	Hepatic stellate cells, Hepatocellular carcinoma	113,114
Baicalin	Ferritin	Down-regulate ferritin	Bladder cancer	115

DMOCPTL, derivative of natural product parthenolide; EF24, 3,5-bis (2-fluorobenzylidene)-4-piperidone; FIN56, ferroptosis inducing 56; FINO2, 1,2-dioxolane; HMOX1, heme-oxygenase 1; IKE, imidazole ketone erastin; QD394, quinazolinone reactive oxygen species inducer; RSL3, RAS-selective lethal 3; SLC7A11, solute carrier family 7 member 11.

derivative a2,<sup>94</sup> compound 21,<sup>95</sup> tetrahydrocitrate,<sup>96</sup> and Bufotaline.<sup>97</sup> It has long been reported that many natural products inhibited cancer cells through multiple targets. Accompany with the report of ferroptosis, researchers found that many natural compounds, including dihydroisotanshinone I,<sup>98,99</sup> solasonine,<sup>100</sup> DMOCPTL,<sup>101</sup> cucurbitin B,<sup>102</sup> and honokiol<sup>103</sup> could induce ferroptosis by inhibiting GPX4 activity or reducing GPX4 protein level. Natural products gambogenic acid,<sup>104</sup> thiostrepton,<sup>105</sup> and red ginseng polysaccharide<sup>106</sup> could suppress GPX4 expression by regulating upstream transcriptional factors, thus inducing ferroptosis. In addition, small molecule compounds atorvastatin, apatinib, and simvastatin induce ferroptosis by indirectly downregulating GPX4.<sup>107–109</sup> The discovery of GPX4 inhibitors also supplies the information for the regulation of GPX4 in cancer cells.

### FIN56

As a type 3 ferroptosis inducer, FIN56 induces ferroptosis by promoting GPX4 degradation.<sup>7</sup> Except degrading GPX4, FIN56 can

also reduce intracellular antioxidants (like CoQ10) by activating squalene synthase, thus promoting cellular lipid peroxidation and ferroptosis.<sup>7</sup> In addition, FIN56-induced ferroptosis is related to autophagy, and inhibition of autophagy at different stages could weaken FIN56-induced lipid peroxidation and GPX4 degradation.<sup>128</sup>

### FINO2

FINO2 triggers ferroptosis through mechanisms different from that of SLC7A11 inhibitors or GPX4 inhibitors.<sup>14</sup> FINO2, serves as an endoperoxide, induces ferroptosis by directly oxidizing iron and indirectly inhibiting GPX4, which effect can be reversed by iron chelating agents.<sup>110</sup>

### Others ferroptosis inducers

In addition to above mentioned ferroptosis inducers, researchers have developed many ferroptosis inducers by targeting other key ferroptosis regulators, like heme oxygenase-1 (HMOX1), ferrous ions or ACSL4 etc. HMOX1 protects cell through its byproduct



bilirubin, and its overexpression reduces ROS levels and lipid peroxidation.<sup>129</sup> Combination of lapatinib and cilacine co-induces ferroptosis by reducing heme oxygenase-1 protein expression.<sup>129</sup> However, it has also been reported that HMOX1 can induce cell death by promoting intracellular ferrous accumulation.<sup>130</sup> Newly discovered ferroptosis inducers such as curcumin analogues EF24<sup>111</sup> and heavy metal cadmium<sup>112</sup> can induce ferroptosis by directly up-regulating HMOX1 expression.

Triggering ferritin phagocytosis, a lysosome-mediated autophagy process that degrading ferritin and inducing ferroptosis, is a new strategy to induce ferroptosis.<sup>131</sup> It had been reported that natural compounds Artesunate,<sup>113</sup> Saponin Formosanin C,<sup>114</sup> and Arsenite<sup>132</sup> can induce ferroptosis by promoting ferritin phagocytosis. The natural product Baicalin can also induce ferroptosis by down-regulating ferritin heavy chain 1.<sup>115</sup>

In addition, Yiqi Huayu Decoction, created by Professor Liu Shenlin, can cause ferroptosis through multiple targets, such as reducing the content of GSH in cells and up-regulating the expression of ACSL4.<sup>133</sup>

### Future directions

Ferroptosis, as a newly discovered programmed cell death, plays important role in cancer. The biology functions of SLC7A11 and GPX4 in ferroptosis have been well investigated. Relationship of ferroptosis with iron and lipid metabolisms are complicated, and are gradually investigated. Ferroptosis also co-occur with autophagy and apoptosis, but the mechanism is still unclear. In addition, diversity of cancer makes ferroptosis executing differently in different cancer types. Thus, it is still a challenge to totally understand the ferroptosis in cancer. Like the other anti-tumor drugs or molecules, ferroptosis inducers also face the problems of selectivity, sensitivity and pharmacokinetics. There is an urgent need to develop high selective ferroptosis inducer to reduce toxicity.

### Conclusions

Ferroptosis has been discovered for 10 years, we have known many knowledge of ferroptosis, but the mechanism of ferroptosis, especially the lipid metabolism in ferroptosis, is still unclear. Given the role of ferroptosis in cancer, many ferroptosis inducers have been discovered and reported, and the ferroptosis inducers also help the investigation of ferroptosis. This paper reviews the research progress of ferroptosis signaling pathways and ferroptosis inducers. Although great progress has been made in ferroptosis-related research in recent years, specific regulatory mechanisms and targets of ferroptosis inducers have yet to be explored.

### Acknowledgments

None.

### Funding

This work was supported by grants from Key Science Project of University in Henan (23A350007 for YCX), and National Natural Science Foundation of China (No. U2004101 for PXH).

### Conflict of interest

The authors have no conflict of interests related to this publication.

### Author contributions

Conceptualization and supervision (YCX), drafting of the manuscript (YJJ), critical revision of the manuscript (PXH), review and editing (YZ, XBM, YW and YQT). All authors have made a significant contribution to this study and have approved the final manuscript.

### References

- [1] Dixon SJ, Lemberg KM, Lamprecht MR, Skouta R, Zaitsev EM, Gleason CE, *et al*. Ferroptosis: an iron-dependent form of nonapoptotic cell death. *Cell* 2012;149(5):1060–1072. doi:10.1016/j.cell.2012.03.042, PMID:22632970.
- [2] Xie Y, Hou W, Song X, Yu Y, Huang J, Sun X, *et al*. Ferroptosis: process and function. *Cell Death Differ* 2016;23(3):369–379. doi:10.1038/cdd.2015.158, PMID:26794443.
- [3] Stockwell BR, Friedmann Angeli JP, Bayir H, Bush AI, Conrad M, Dixon SJ, *et al*. Ferroptosis: A Regulated Cell Death Nexus Linking Metabolism, Redox Biology, and Disease. *Cell* 2017;171(2):273–285. doi:10.1016/j.cell.2017.09.021, PMID:28985560.
- [4] Bai Y, Meng L, Han L, Jia Y, Zhao Y, Gao H, *et al*. Lipid storage and lipophagy regulates ferroptosis. *Biochem Biophys Res Commun* 2019;508(4):997–1003. doi:10.1016/j.bbrc.2018.12.039, PMID:30545638.
- [5] Nakamura T, Naguro I, Ichijo H. Iron homeostasis and iron-regulated ROS in cell death, senescence and human diseases. *Biochim Biophys Acta Gen Subj* 2019;1863(9):1398–1409. doi:10.1016/j.bbagen.2019.06.010, PMID:31229492.
- [6] McBean GJ. The transsulfuration pathway: a source of cysteine for glutathione in astrocytes. *Amino Acids* 2012;42(1):199–205. doi:10.1007/s00726-011-0864-8, PMID:21369939.
- [7] Shimada K, Skouta R, Kaplan A, Yang WS, Hayano M, Dixon SJ, *et al*. Global survey of cell death mechanisms reveals metabolic regulation of ferroptosis. *Nat Chem Biol* 2016;12(7):497–503. doi:10.1038/nchembio.2079, PMID:27159577.
- [8] Li J, Cao F, Yin HL, Huang ZJ, Lin ZT, Mao N, *et al*. Ferroptosis: past, present and future. *Cell Death Dis* 2020;11(2):88. doi:10.1038/s41419-020-2298-2, PMID:32015325.
- [9] Lei G, Zhang Y, Koppula P, Liu X, Zhang J, Lin SH, *et al*. The role of ferroptosis in ionizing radiation-induced cell death and tumor suppression. *Cell Res* 2020;30(2):146–162. doi:10.1038/s41422-019-0263-3, PMID:31949285.
- [10] Wang Y, Wu X, Ren Z, Li Y, Zou W, Chen J, *et al*. Overcoming cancer chemotherapy resistance by the induction of ferroptosis. *Drug Resist Updat* 2023;66:100916. doi:10.1016/j.drug.2022.100916, PMID:36610291.
- [11] Yang WS, Stockwell BR. Ferroptosis: Death by Lipid Peroxidation. *Trends Cell Biol* 2016;26(3):165–176. doi:10.1016/j.tcb.2015.10.014, PMID:26653790.
- [12] Feng H, Stockwell BR. Unsolved mysteries: How does lipid peroxidation cause ferroptosis? *PLoS Biol* 2018;16(5):e2006203. doi:10.1371/journal.pbio.2006203, PMID:29795546.
- [13] Yang WS, Kim KJ, Gaschler MM, Patel M, Shchepinov MS, Stockwell BR. Peroxidation of polyunsaturated fatty acids by lipoxygenases drives ferroptosis. *Proc Natl Acad Sci U S A* 2016;113(34):E4966–E4975. doi:10.1073/pnas.1603244113, PMID:27506793.
- [14] Gaschler MM, Andia AA, Liu H, Csuka JM, Hurlocker B, Vaiana CA, *et al*. FINO<sub>2</sub> initiates ferroptosis through GPX4 inactivation and iron oxidation. *Nat Chem Biol* 2018;14(5):507–515. doi:10.1038/s41589-018-0031-6, PMID:29610484.
- [15] Ji X, Qian J, Rahman SMJ, Siska PJ, Zou Y, Harris BK, *et al*. xCT (SLC7A11)-mediated metabolic reprogramming promotes non-small cell lung cancer progression. *Oncogene* 2018;37(36):5007–5019. doi:10.1038/s41388-018-0307-z, PMID:29789716.
- [16] Nakamura E, Sato M, Yang H, Miyagawa F, Harasaki M, Tomita K, *et al*. 4F2 (CD98) heavy chain is associated covalently with an amino acid transporter and controls intracellular trafficking and membrane topology of 4F2 heterodimer. *J Biol Chem* 1999;274(5):3009–3016. doi:10.1074/jbc.274.5.3009, PMID:9915839.

- [17] Gu Y, Albuquerque CP, Braas D, Zhang W, Villa GR, Bi J, *et al.* mTORC2 Regulates Amino Acid Metabolism in Cancer by Phosphorylation of the Cystine-Glutamate Antiporter xCT. *Mol Cell* 2017;67(1):128–138. e7. doi:10.1016/j.molcel.2017.05.030, PMID:28648777.
- [18] Koppula P, Zhuang L, Gan B. Cystine transporter SLC7A11/xCT in cancer: ferroptosis, nutrient dependency, and cancer therapy. *Protein Cell* 2021;12(8):599–620. doi:10.1007/s13238-020-00789-5, PMID:33000412.
- [19] Yang WS, SriRamaratnam R, Welsch ME, Shimada K, Skouta R, Viswanathan VS, *et al.* Regulation of ferroptotic cancer cell death by GPX4. *Cell* 2014;156(1-2):317–331. doi:10.1016/j.cell.2013.12.010, PMID:24439385.
- [20] Seiler A, Schneider M, Förster H, Roth S, Wirth EK, Culmsee C, *et al.* Glutathione peroxidase 4 senses and translates oxidative stress into 12/15-lipoxygenase dependent- and AIF-mediated cell death. *Cell Metab* 2008;8(3):237–248. doi:10.1016/j.cmet.2008.07.005, PMID:18762024.
- [21] Ingold I, Berndt C, Schmitt S, Doll S, Poschmann G, Buday K, *et al.* Selenium Utilization by GPX4 Is Required to Prevent Hydroperoxide-Induced Ferroptosis. *Cell* 2018;172(3):409–422.e21. doi:10.1016/j.cell.2017.11.048, PMID:29290465.
- [22] Zhang Y, Tan H, Daniels JD, Zandkarimi F, Liu H, Brown LM, *et al.* Imidazole Ketone Erastin Induces Ferroptosis and Slows Tumor Growth in a Mouse Lymphoma Model. *Cell Chem Biol* 2019;26(5):623–633. e9. doi:10.1016/j.chembiol.2019.01.008, PMID:30799221.
- [23] Armstrong JS, Steinauer KK, Hornung B, Irish JM, Lecane P, Birrell GW, *et al.* Role of glutathione depletion and reactive oxygen species generation in apoptotic signaling in a human B lymphoma cell line. *Cell Death Differ* 2002;9(3):252–263. doi:10.1038/sj.cdd.4400959, PMID:11859408.
- [24] Yudkoff M. Chapter 42 - Disorders of Amino Acid Metabolism. In: *Basic Neurochemistry*. 8th ed. Elsevier; 2012:737–754. doi:10.1016/B978-0-12-374947-5.00042-0.
- [25] Mota-Martorell N, Jové M, Borrás C, Berdún R, Obis E, Sol J, *et al.* Methionine transsulfuration pathway is upregulated in long-lived humans. *Free Radic Biol Med* 2021;162:38–52. doi:10.1016/j.freeradbiomed.2020.11.026, PMID:33271279.
- [26] Liang Q, Ou M, Ren Y, Yao Z, Hu R, Li J, *et al.* Molecular cloning, characterization and expression analysis of S-adenosyl-L-homocysteine hydrolase (SAHH) during the pathogenic infection of *Litopenaeus vannamei* by *Vibrio alginolyticus*. *Fish Shellfish Immunol* 2019;88:284–292. doi:10.1016/j.fsi.2019.02.058, PMID:30849500.
- [27] Zhu J, Berisa M, Schwörer S, Qin W, Cross JR, Thompson CB. Transsulfuration Activity Can Support Cell Growth upon Extracellular Cysteine Limitation. *Cell Metab* 2019;30(5):865–876.e5. doi:10.1016/j.cmet.2019.09.009, PMID:31607565.
- [28] Hayano M, Yang WS, Corn CK, Pagano NC, Stockwell BR. Loss of cysteinyl-tRNA synthetase (CARS) induces the transsulfuration pathway and inhibits ferroptosis induced by cystine deprivation. *Cell Death Differ* 2016;23(2):270–278. doi:10.1038/cdd.2015.93, PMID:26184909.
- [29] Takahashi-Niki K, Niki T, Iguchi-Ariga SMM, Ariga H. Transcriptional Regulation of DJ-1. *Adv Exp Med Biol* 2017;1037:89–95. doi:10.1007/978-981-10-6583-5\_7, PMID:29147905.
- [30] Cao J, Chen X, Jiang L, Lu B, Yuan M, Zhu D, *et al.* DJ-1 suppresses ferroptosis through preserving the activity of S-adenosyl homocysteine hydrolase. *Nat Commun* 2020;11(1):1251. doi:10.1038/s41467-020-15109-y, PMID:32144268.
- [31] Gao G, Li J, Zhang Y, Chang YZ. Cellular Iron Metabolism and Regulation. *Adv Exp Med Biol* 2019;1173:21–32. doi:10.1007/978-981-13-9589-5\_2, PMID:31456203.
- [32] Galaris D, Pantopoulos K. Oxidative stress and iron homeostasis: mechanistic and health aspects. *Crit Rev Clin Lab Sci* 2008;45(1):1–23. doi:10.1080/10408360701713104, PMID:18293179.
- [33] Puntarulo S. Iron, oxidative stress and human health. *Mol Aspects Med* 2005;26(4-5):299–312. doi:10.1016/j.mam.2005.07.001, PMID:16102805.
- [34] Huang LL, Liao XH, Sun H, Jiang X, Liu Q, Zhang L. Augmenter of liver regeneration protects the kidney from ischaemia-reperfusion injury in ferroptosis. *J Cell Mol Med* 2019;23(6):4153–4164. doi:10.1111/jcmm.14302, PMID:30993878.
- [35] Zhao Z. Iron and oxidizing species in oxidative stress and Alzheimer's disease. *Aging Med (Milton)* 2019;2(2):82–87. doi:10.1002/agm2.12074, PMID:31942516.
- [36] van Renswoude J, Bridges KR, Harford JB, Klausner RD. Receptor-mediated endocytosis of transferrin and the uptake of Fe in K562 cells: identification of a nonlysosomal acidic compartment. *Proc Natl Acad Sci U S A* 1982;79(20):6186–6190. doi:10.1073/pnas.79.20.6186, PMID:6292894.
- [37] Dautry-Varsat A, Ciechanover A, Lodish HF. pH and the recycling of transferrin during receptor-mediated endocytosis. *Proc Natl Acad Sci U S A* 1983;80(8):2258–2262. doi:10.1073/pnas.80.8.2258, PMID:6300903.
- [38] Wang J, Pantopoulos K. Regulation of cellular iron metabolism. *Biochem J* 2011;434(3):365–381. doi:10.1042/BJ20101825, PMID:21348856.
- [39] Torti SV, Torti FM. Iron and cancer: more ore to be mined. *Nat Rev Cancer* 2013;13(5):342–355. doi:10.1038/nrc3495, PMID:23594855.
- [40] Mancias JD, Pontano Vaites L, Nissim S, Biancur DE, Kim AJ, Wang X, *et al.* Ferritinophagy via NCOA4 is required for erythropoiesis and is regulated by iron dependent HERC2-mediated proteolysis. *Elife* 2015;4:e10308. doi:10.7554/eLife.10308, PMID:26436293.
- [41] Ramey G, Deschemin JC, Durel B, Canonne-Hergaux F, Nicolas G, Vaulont S. Heparin targets ferroportin for degradation in hepatocytes. *Haematologica* 2010;95(3):501–504. doi:10.3324/haematol.2009.014399, PMID:19773263.
- [42] Nemeth E, Tuttle MS, Powelson J, Vaughn MB, Donovan A, Ward DM, *et al.* Heparin regulates cellular iron efflux by binding to ferroportin and inducing its internalization. *Science* 2004;306(5704):2090–2093. doi:10.1126/science.1104742, PMID:15514116.
- [43] Gryzik M, Asperti M, Denardo A, Arosio P, Poli M. NCOA4-mediated ferritinophagy promotes ferroptosis induced by erastin, but not by RSL3 in HeLa cells. *Biochim Biophys Acta Mol Cell Res* 2021;1868(2):118913. doi:10.1016/j.bbamcr.2020.118913, PMID:33245979.
- [44] Geng N, Shi BJ, Li SL, Zhong ZY, Li YC, Xua WL, *et al.* Knockdown of ferroportin accelerates erastin-induced ferroptosis in neuroblastoma cells. *Eur Rev Med Pharmacol Sci* 2018;22(12):3826–3836. doi:10.26355/eurev\_201806\_15267, PMID:29949159.
- [45] Ma S, Henson ES, Chen Y, Gibson SB. Ferroptosis is induced following siramesine and lapatinib treatment of breast cancer cells. *Cell Death Dis* 2016;7(7):e2307. doi:10.1038/cddis.2016.208, PMID:27441659.
- [46] Maio N, Zhang DL, Ghosh MC, Jain A, SantaMaria AM, Rouault TA. Mechanisms of cellular iron sensing, regulation of erythropoiesis and mitochondrial iron utilization. *Semin Hematol* 2021;58(3):161–174. doi:10.1053/j.seminhematol.2021.06.001, PMID:34389108.
- [47] Volz K. Conservation in the Iron Responsive Element Family. *Genes (Basel)* 2021;12(9):1365. doi:10.3390/genes12091365, PMID:34573347.
- [48] Zhou ZD, Tan EK. Iron regulatory protein (IRP)-iron responsive element (IRE) signaling pathway in human neurodegenerative diseases. *Mol Neurodegener* 2017;12(1):75. doi:10.1186/s13024-017-0218-4, PMID:29061112.
- [49] Anderson GJ, Frazer DM. Current understanding of iron homeostasis. *Am J Clin Nutr* 2017;106(Suppl 6):1559S–1566S. doi:10.3945/ajcn.117.155804, PMID:29070551.
- [50] Nemeth E, Ganz T. Heparin-Ferroportin Interaction Controls Systemic Iron Homeostasis. *Int J Mol Sci* 2021;22(12):6493. doi:10.3390/ijms22126493, PMID:34204327.
- [51] Chen GQ, Benthani FA, Wu J, Liang D, Bian ZX, Jiang X. Artemisinin compounds sensitize cancer cells to ferroptosis by regulating iron homeostasis. *Cell Death Differ* 2020;27(1):242–254. doi:10.1038/s41418-019-0352-3, PMID:31114026.
- [52] Lee JY, Kim WK, Bae KH, Lee SC, Lee EW. Lipid Metabolism and Ferroptosis. *Biology (Basel)* 2021;10(3):184. doi:10.3390/biology10030184, PMID:33801564.
- [53] Doll S, Proneth B, Tyurina YY, Panzilius E, Kobayashi S, Ingold I, *et al.* ACSL4 dictates ferroptosis sensitivity by shaping cellular lipid composition. *Nat Chem Biol* 2017;13(1):91–98. doi:10.1038/nchembio.2239, PMID:27842070.
- [54] Hishikawa D, Shindou H, Kobayashi S, Nakanishi H, Taguchi R, Shimizu T. Discovery of a lysophospholipid acyltransferase family essential for membrane asymmetry and diversity. *Proc Natl Acad Sci U S A* 2008;105(8):2830–2835. doi:10.1073/pnas.0712245105, PMID:18287005.
- [55] Pidgeon GP, Lysaght J, Krishnamoorthy S, Reynolds JV, O'Byrne K, Nie

- D, *et al*. Lipoxygenase metabolism: roles in tumor progression and survival. *Cancer Metastasis Rev* 2007;26(3-4):503–524. doi:10.1007/s10555-007-9098-3, PMID:17943411.
- [56] Merchant N, Bhaskar LVKS, Momin S, Sujatha P, Reddy ABM, Nagaraju GP. 5-Lipoxygenase: Its involvement in gastrointestinal malignancies. *Crit Rev Oncol Hematol* 2018;127:50–55. doi:10.1016/j.critrevonc.2018.05.012, PMID:29891111.
- [57] Kagan VE, Mao G, Qu F, Angeli JP, Doll S, Croix CS, *et al*. Oxidized arachidonic and adrenic PEs navigate cells to ferroptosis. *Nat Chem Biol* 2017;13(1):81–90. doi:10.1038/nchembio.2238, PMID:27842066.
- [58] Chu B, Kon N, Chen D, Li T, Liu T, Jiang L, *et al*. ALOX12 is required for p53-mediated tumour suppression through a distinct ferroptosis pathway. *Nat Cell Biol* 2019;21(5):579–591. doi:10.1038/s41556-019-0305-6, PMID:30962574.
- [59] Zou Y, Li H, Graham ET, Deik AA, Eaton JK, Wang W, *et al*. Cytochrome P450 oxidoreductase contributes to phospholipid peroxidation in ferroptosis. *Nat Chem Biol* 2020;16(3):302–309. doi:10.1038/s41589-020-0472-6, PMID:32080622.
- [60] Liao P, Hemmerlin A, Bach TJ, Chye ML. The potential of the mevalonate pathway for enhanced isoprenoid production. *Biotechnol Adv* 2016;34(5):697–713. doi:10.1016/j.biotechadv.2016.03.005, PMID:26995109.
- [61] Guerra B, Recio C, Aranda-Tavió H, Guerra-Rodríguez M, García-Castellano JM, Fernández-Pérez L. The Mevalonate Pathway, a Metabolic Target in Cancer Therapy. *Front Oncol* 2021;11:626971. doi:10.3389/fonc.2021.626971, PMID:33718197.
- [62] Zaleski AL, Taylor BA, Thompson PD. Coenzyme Q10 as Treatment for Statin-Associated Muscle Symptoms-A Good Idea, but.... *Adv Nutr* 2018;9(4):519S–523S. doi:10.1093/advances/nmy010, PMID:30032220.
- [63] Zheng J, Conrad M. The Metabolic Underpinnings of Ferroptosis. *Cell Metab* 2020;32(6):920–937. doi:10.1016/j.cmet.2020.10.011, PMID:33217331.
- [64] Turunen M, Olsson J, Dallner G. Metabolism and function of coenzyme Q. *Biochim Biophys Acta* 2004;1660(1-2):171–199. doi:10.1016/j.bbame.2003.11.012, PMID:14757233.
- [65] Frei B, Kim MC, Ames BN. Ubiquinol-10 is an effective lipid-soluble antioxidant at physiological concentrations. *Proc Natl Acad Sci U S A* 1990;87(12):4879–4883. doi:10.1073/pnas.87.12.4879, PMID:2352956.
- [66] Bersuker K, Hendricks JM, Li Z, Magtanong L, Ford B, Tang PH, *et al*. The CoQ oxidoreductase FSP1 acts parallel to GPX4 to inhibit ferroptosis. *Nature* 2019;575(7784):688–692. doi:10.1038/s41586-019-1705-2, PMID:31634900.
- [67] Doll S, Freitas FP, Shah R, Aldrovandi M, da Silva MC, Ingold I, *et al*. FSP1 is a glutathione-independent ferroptosis suppressor. *Nature* 2019;575(7784):693–698. doi:10.1038/s41586-019-1707-0, PMID:31634899.
- [68] Tang D, Chen X, Kang R, Kroemer G. Ferroptosis: molecular mechanisms and health implications. *Cell Res* 2021;31(2):107–125. doi:10.1038/s41422-020-00441-1, PMID:33268902.
- [69] Hadian K. Ferroptosis Suppressor Protein 1 (FSP1) and Coenzyme Q(10) Cooperatively Suppress Ferroptosis. *Biochemistry* 2020;59(5):637–638. doi:10.1021/acs.biochem.0c00030, PMID:32003211.
- [70] Warner GJ, Berry MJ, Moustafa ME, Carlson BA, Hatfield DL, Faust JR. Inhibition of selenoprotein synthesis by selenocysteine tRNA[Ser] Sec lacking isopentenyladenosine. *J Biol Chem* 2000;275(36):28110–28119. doi:10.1074/jbc.M001280200, PMID:10821829.
- [71] Viswanathan VS, Ryan MJ, Dhruv HD, Gill S, Eichhoff OM, Seashore-Ludlow B, *et al*. Dependency of a therapy-resistant state of cancer cells on a lipid peroxidase pathway. *Nature* 2017;547(7664):453–457. doi:10.1038/nature23007, PMID:28678785.
- [72] Jiang L, Hickman JH, Wang SJ, Gu W. Dynamic roles of p53-mediated metabolic activities in ROS-induced stress responses. *Cell Cycle* 2015;14(18):2881–2885. doi:10.1080/15384101.2015.1068479, PMID:26218928.
- [73] Jiang L, Kon N, Li T, Wang SJ, Su T, Hibshoosh H, *et al*. Ferroptosis as a p53-mediated activity during tumour suppression. *Nature* 2015;520(7545):57–62. doi:10.1038/nature14344, PMID:25799988.
- [74] Kang R, Kroemer G, Tang D. The tumor suppressor protein p53 and the ferroptosis network. *Free Radic Biol Med* 2019;133:162–168. doi:10.1016/j.freeradbiomed.2018.05.074, PMID:29800655.
- [75] Chen D, Chu B, Yang X, Liu Z, Jin Y, Kon N, *et al*. iPLA2 $\beta$ -mediated lipid detoxification controls p53-driven ferroptosis independent of GPX4. *Nat Commun* 2021;12(1):3644. doi:10.1038/s41467-021-23902-6, PMID:34131139.
- [76] Ou Y, Wang SJ, Li D, Chu B, Gu W. Activation of SAT1 engages polyamine metabolism with p53-mediated ferroptotic responses. *Proc Natl Acad Sci U S A* 2016;113(44):E6806–E6812. doi:10.1073/pnas.1607152113, PMID:27698118.
- [77] Hu W, Zhang C, Wu R, Sun Y, Levine A, Feng Z. Glutaminase 2, a novel p53 target gene regulating energy metabolism and antioxidant function. *Proc Natl Acad Sci U S A* 2010;107(16):7455–7460. doi:10.1073/pnas.1001006107, PMID:20378837.
- [78] Gao M, Monian P, Quadri N, Ramasamy R, Jiang X. Glutaminolysis and Transferrin Regulate Ferroptosis. *Mol Cell* 2015;59(2):298–308. doi:10.1016/j.molcel.2015.06.011, PMID:26166707.
- [79] Tarangelo A, Magtanong L, Bieging-Rolett KT, Li Y, Ye J, Attardi LD, *et al*. p53 Suppresses Metabolic Stress-Induced Ferroptosis in Cancer Cells. *Cell Rep* 2018;22(3):569–575. doi:10.1016/j.celrep.2017.12.077, PMID:29346757.
- [80] Xie Y, Zhu S, Song X, Sun X, Fan Y, Liu J, *et al*. The Tumor Suppressor p53 Limits Ferroptosis by Blocking DPP4 Activity. *Cell Rep* 2017;20(7):1692–1704. doi:10.1016/j.celrep.2017.07.055, PMID:28813679.
- [81] Xu X, Zhang X, Wei C, Zheng D, Lu X, Yang Y, *et al*. Targeting SLC7A11 specifically suppresses the progression of colorectal cancer stem cells via inducing ferroptosis. *Eur J Pharm Sci* 2020;152:105450. doi:10.1016/j.ejps.2020.105450, PMID:32621966.
- [82] Larraufie MH, Yang WS, Jiang E, Thomas AG, Slusher BS, Stockwell BR. Incorporation of metabolically stable ketones into a small molecule probe to increase potency and water solubility. *Bioorg Med Chem Lett* 2015;25(21):4787–4792. doi:10.1016/j.bmcl.2015.07.018, PMID:26231156.
- [83] Gout PW, Buckley AR, Simms CR, Bruchovsky N. Sulfasalazine, a potent suppressor of lymphoma growth by inhibition of the x(c)-cystine transporter: a new action for an old drug. *Leukemia* 2001;15(10):1633–1640. doi:10.1038/sj.leu.2402238, PMID:11587223.
- [84] Zhang J, Gao M, Niu Y, Sun J. From DNMT1 degrader to ferroptosis promoter: Drug repositioning of 6-Thioguanine as a ferroptosis inducer in gastric cancer. *Biochem Biophys Res Commun* 2022;603:75–81. doi:10.1016/j.bbrc.2022.03.026, PMID:35278883.
- [85] Shi Y, Gong M, Deng Z, Liu H, Chang Y, Yang Z, *et al*. Tirapazamine suppress osteosarcoma cells in part through SLC7A11 mediated ferroptosis. *Biochem Biophys Res Commun* 2021;567:118–124. doi:10.1016/j.bbrc.2021.06.036, PMID:34147710.
- [86] Wang G, Qin S, Zheng Y, Xia C, Zhang P, Zhang L, *et al*. T-2 Toxin Induces Ferroptosis by Increasing Lipid Reactive Oxygen Species (ROS) and Downregulating Solute Carrier Family 7 Member 11 (SLC7A11). *J Agric Food Chem* 2021;69(51):15716–15727. doi:10.1021/acs.jafc.1c05393, PMID:34918923.
- [87] Yang J, Zhou Y, Xie S, Wang J, Li Z, Chen L, *et al*. Metformin induces Ferroptosis by inhibiting UFMylation of SLC7A11 in breast cancer. *J Exp Clin Cancer Res* 2021;40(1):206. doi:10.1186/s13046-021-02012-7, PMID:34162423.
- [88] Xia Y, Liu S, Li C, Ai Z, Shen W, Ren W, *et al*. Discovery of a novel ferroptosis inducer-talaroconvolutin A-killing colorectal cancer cells in vitro and in vivo. *Cell Death Dis* 2020;11(11):988. doi:10.1038/s41419-020-03194-2, PMID:33203867.
- [89] Guan Z, Chen J, Li X, Dong N. Tanshinone IIA induces ferroptosis in gastric cancer cells through p53-mediated SLC7A11 down-regulation. *Biosci Rep* 2020;40(8):BSR20201807. doi:10.1042/bsr20201807, PMID:32776119.
- [90] Gao Z, Deng G, Li Y, Huang H, Sun X, Shi H, *et al*. Actinidia chinensis Planch prevents proliferation and migration of gastric cancer associated with apoptosis, ferroptosis activation and mesenchymal phenotype suppression. *Biomed Pharmacother* 2020;126:110092. doi:10.1016/j.biopha.2020.110092, PMID:32203890.
- [91] Liu XY, Wei DG, Li RS. Capsaicin induces ferroptosis of NSCLC by regulating SLC7A11/GPX4 signaling in vitro. *Sci Rep* 2022;12(1):11996. doi:10.1038/s41598-022-16372-3, PMID:35835852.
- [92] Hu S, Sechi M, Singh PK, Dai L, McCann S, Sun D, *et al*. A Novel Redox Modulator Induces a GPX4-Mediated Cell Death That Is Dependent



- on Iron and Reactive Oxygen Species. *J Med Chem* 2020;63(17):9838–9855. doi:10.1021/acs.jmedchem.0c01016, PMID:32809827.
- [93] Xu C, Xiao Z, Wang J, Lai H, Zhang T, Guan Z, *et al.* Discovery of a Potent Glutathione Peroxidase 4 Inhibitor as a Selective Ferroptosis Inducer. *J Med Chem* 2021;64(18):13312–13326. doi:10.1021/acs.jmedchem.1c00569, PMID:34506134.
- [94] Liu Y, Song Z, Liu Y, Ma X, Wang W, Ke Y, *et al.* Identification of ferroptosis as a novel mechanism for antitumor activity of natural product derivative a2 in gastric cancer. *Acta Pharm Sin B* 2021;11(6):1513–1525. doi:10.1016/j.apsb.2021.05.006, PMID:34221865.
- [95] Wang H, Wu D, Gao C, Teng H, Zhao Y, He Z, *et al.* Seco-Lupane Triterpene Derivatives Induce Ferroptosis through GPX4/ACSL4 Axis and Target Cyclin D1 to Block the Cell Cycle. *J Med Chem* 2022;65(14):10014–10044. doi:10.1021/acs.jmedchem.2c00664, PMID:35801495.
- [96] Yin J, Lin Y, Fang W, Zhang X, Wei J, Hu G, *et al.* Tetrandrine Citrate Suppresses Breast Cancer via Depletion of Glutathione Peroxidase 4 and Activation of Nuclear Receptor Coactivator 4-Mediated Ferritinophagy. *Front Pharmacol* 2022;13:820593. doi:10.3389/fphar.2022.820593, PMID:35614944.
- [97] Zhang W, Jiang B, Liu Y, Xu L, Wan M. Bufotalin induces ferroptosis in non-small cell lung cancer cells by facilitating the ubiquitination and degradation of GPX4. *Free Radic Biol Med* 2022;180:75–84. doi:10.1016/j.freeradbiomed.2022.01.009, PMID:35038550.
- [98] Lin YS, Shen YC, Wu CY, Tsai YY, Yang YH, Lin YY, *et al.* Danshen Improves Survival of Patients With Breast Cancer and Dihydroisotanshinone I Induces Ferroptosis and Apoptosis of Breast Cancer Cells. *Front Pharmacol* 2019;10:1226. doi:10.3389/fphar.2019.01226, PMID:31736748.
- [99] Wu CY, Yang YH, Lin YS, Chang GH, Tsai MS, Hsu CM, *et al.* Dihydroisotanshinone I induced ferroptosis and apoptosis of lung cancer cells. *Biomed Pharmacother* 2021;139:111585. doi:10.1016/j.biopha.2021.111585, PMID:33862493.
- [100] Jin M, Shi C, Li T, Wu Y, Hu C, Huang G. Solasonine promotes ferroptosis of hepatoma carcinoma cells via glutathione peroxidase 4-induced destruction of the glutathione redox system. *Biomed Pharmacother* 2020;129:110282. doi:10.1016/j.biopha.2020.110282, PMID:32531676.
- [101] Ding Y, Chen X, Liu C, Ge W, Wang Q, Hao X, *et al.* Identification of a small molecule as inducer of ferroptosis and apoptosis through ubiquitination of GPX4 in triple negative breast cancer cells. *J Hematol Oncol* 2021;14(1):19. doi:10.1186/s13045-020-01016-8, PMID:33472669.
- [102] Huang S, Cao B, Zhang J, Feng Y, Wang L, Chen X, *et al.* Induction of ferroptosis in human nasopharyngeal cancer cells by cucurbitacin B: molecular mechanism and therapeutic potential. *Cell Death Dis* 2021;12(3):237. doi:10.1038/s41419-021-03516-y, PMID:33664249.
- [103] Guo C, Liu P, Deng G, Han Y, Chen Y, Cai C, *et al.* Honokiol induces ferroptosis in colon cancer cells by regulating GPX4 activity. *Am J Cancer Res* 2021;11(6):3039–3054. PMID:34249443.
- [104] Wang M, Li S, Wang Y, Cheng H, Su J, Li Q. Gambogic acid induces ferroptosis in melanoma cells undergoing epithelial-to-mesenchymal transition. *Toxicol Appl Pharmacol* 2020;401:115110. doi:10.1016/j.taap.2020.115110, PMID:32533954.
- [105] Zhang W, Gong M, Zhang W, Mo J, Zhang S, Zhu Z, *et al.* Thiostrepton induces ferroptosis in pancreatic cancer cells through STAT3/GPX4 signalling. *Cell Death Dis* 2022;13(7):630. doi:10.1038/s41419-022-05082-3, PMID:35859150.
- [106] Zhai FG, Liang QC, Wu YY, Liu JQ, Liu JW. Red ginseng polysaccharide exhibits anticancer activity through GPX4 downregulation-induced ferroptosis. *Pharm Biol* 2022;60(1):909–914. doi:10.1080/13880209.2022.2066139, PMID:35575436.
- [107] Zhao L, Peng Y, He S, Li R, Wang Z, Huang J, *et al.* Apatinib induced ferroptosis by lipid peroxidation in gastric cancer. *Gastric Cancer* 2021;24(3):642–654. doi:10.1007/s10120-021-01159-8, PMID:33544270.
- [108] Yao X, Xie R, Cao Y, Tang J, Men Y, Peng H, *et al.* Simvastatin induced ferroptosis for triple-negative breast cancer therapy. *J Nanobiotechnology* 2021;19(1):311. doi:10.1186/s12951-021-01058-1, PMID:34627266.
- [109] Zhang Q, Qu H, Chen Y, Luo X, Chen C, Xiao B, *et al.* Atorvastatin Induces Mitochondria-Dependent Ferroptosis via the Modulation of Nrf2-xCT/GPx4 Axis. *Front Cell Dev Biol* 2022;10:806081. doi:10.3389/fcell.2022.806081, PMID:35309902.
- [110] Abrams RP, Carroll WL, Woerpel KA. Five-Membered Ring Peroxide Selectively Initiates Ferroptosis in Cancer Cells. *ACS Chem Biol* 2016;11(5):1305–1312. doi:10.1021/acscchembio.5b00900, PMID:26797166.
- [111] Lin H, Chen X, Zhang C, Yang T, Deng Z, Song Y, *et al.* EF24 induces ferroptosis in osteosarcoma cells through HMOX1. *Biomed Pharmacother* 2021;136:111202. doi:10.1016/j.biopha.2020.111202, PMID:33453607.
- [112] Zeng L, Zhou J, Wang X, Zhang Y, Wang M, Su P. Cadmium attenuates testosterone synthesis by promoting ferroptosis and blocking autophagosome-lysosome fusion. *Free Radic Biol Med* 2021;176:176–188. doi:10.1016/j.freeradbiomed.2021.09.028, PMID:34610361.
- [113] Kong Z, Liu R, Cheng Y. Artesunate alleviates liver fibrosis by regulating ferroptosis signaling pathway. *Biomed Pharmacother* 2019;109:2043–2053. doi:10.1016/j.biopha.2018.11.030, PMID:30551460.
- [114] Lin PL, Tang HH, Wu SY, Shaw NS, Su CL. Saponin Formosanin C-induced Ferritinophagy and Ferroptosis in Human Hepatocellular Carcinoma Cells. *Antioxidants (Basel)* 2020;9(8):E682. doi:10.3390/antiox9080682, PMID:32751249.
- [115] Kong N, Chen X, Feng J, Duan T, Liu S, Sun X, *et al.* Baicalin induces ferroptosis in bladder cancer cells by downregulating FTH1. *Acta Pharm Sin B* 2021;11(12):4045–4054. doi:10.1016/j.apsb.2021.03.036, PMID:35024325.
- [116] Huang Y, Dai Z, Barbacioru C, Sadée W. Cystine-glutamate transporter SLC7A11 in cancer chemosensitivity and chemoresistance. *Cancer Res* 2005;65(16):7446–7454. doi:10.1158/0008-5472.CAN-04-4267, PMID:16103098.
- [117] Guo W, Zhao Y, Zhang Z, Tan N, Zhao F, Ge C, *et al.* Disruption of xCT inhibits cell growth via the ROS/autophagy pathway in hepatocellular carcinoma. *Cancer Lett* 2011;312(1):55–61. doi:10.1016/j.canlet.2011.07.024, PMID:21906871.
- [118] Zhang Y, Shi J, Liu X, Feng L, Gong Z, Koppula P, *et al.* BAP1 links metabolic regulation of ferroptosis to tumour suppression. *Nat Cell Biol* 2018;20(10):1181–1192. doi:10.1038/s41556-018-0178-0, PMID:30202049.
- [119] Liu T, Jiang L, Tavana O, Gu W. The Deubiquitylase OTUB1 Mediates Ferroptosis via Stabilization of SLC7A11. *Cancer Res* 2019;79(8):1913–1924. doi:10.1158/0008-5472.CAN-18-3037, PMID:30709928.
- [120] Song X, Zhu S, Chen P, Hou W, Wen Q, Liu J, *et al.* AMPK-Mediated BECN1 Phosphorylation Promotes Ferroptosis by Directly Blocking System X(c)(-) Activity. *Curr Biol* 2018;28(15):2388–2399.e5. doi:10.1016/j.cub.2018.05.094, PMID:30057310.
- [121] Wilhelm SM, Adnane L, Newell P, Villanueva A, Llovet JM, Lynch M. Preclinical overview of sorafenib, a multikinase inhibitor that targets both Raf and VEGF and PDGF receptor tyrosine kinase signaling. *Mol Cancer Ther* 2008;7(10):3129–3140. doi:10.1158/1535-7163.MCT-08-0013, PMID:18852116.
- [122] Dixon SJ, Patel DN, Welsch M, Skouta R, Lee ED, Hayano M, *et al.* Pharmacological inhibition of cystine-glutamate exchange induces endoplasmic reticulum stress and ferroptosis. *Elife* 2014;3:e02523. doi:10.7554/eLife.02523, PMID:24844246.
- [123] Zheng J, Sato M, Mishima E, Sato H, Proneth B, Conrad M. Sorafenib fails to trigger ferroptosis across a wide range of cancer cell lines. *Cell Death Dis* 2021;12(7):698. doi:10.1038/s41419-021-03998-w, PMID:34257282.
- [124] Northfield TC. Ulcerative colitis and Crohn's colitis: differential diagnosis and treatment. *Drugs* 1977;14(3):198–206. doi:10.2165/00003495-197714030-00003, PMID:332482.
- [125] Koppula P, Zhang Y, Zhuang L, Gan B. Amino acid transporter SLC7A11/xCT at the crossroads of regulating redox homeostasis and nutrient dependency of cancer. *Cancer Commun (Lond)* 2018;38(1):12. doi:10.1186/s40880-018-0288-x, PMID:29764521.
- [126] Zhang X, Sui S, Wang L, Li H, Zhang L, Xu S, *et al.* Inhibition of tumor propellant glutathione peroxidase 4 induces ferroptosis in cancer cells and enhances anticancer effect of cisplatin. *J Cell Physiol* 2020;235(4):3425–3437. doi:10.1002/jcp.29232, PMID:31556117.
- [127] Hangauer MJ, Viswanathan VS, Ryan MJ, Bole D, Eaton JK, Matov A, *et al.* Drug-tolerant persister cancer cells are vulnerable to GPX4 inhibition. *Nature* 2017;551(7679):247–250. doi:10.1038/nature24297, PMID:29088702.



- [128] Sun YD, Berleth N, Wu WX, Schlutermann D, Deitersen J, Stuhldreier F, *et al*. Fin56-induced ferroptosis is supported by autophagy-mediated GPX4 degradation and functions synergistically with mTOR inhibition to kill bladder cancer cells. *Cell Death Dis* 2021;12(11):1028. doi:10.1038/s41419-021-04306-2, PMID:34716292.
- [129] Villalpando-Rodriguez GE, Blankstein AR, Konzelman C, Gibson SB. Lysosomal Destabilizing Drug Siramesine and the Dual Tyrosine Kinase Inhibitor Lapatinib Induce a Synergistic Ferroptosis through Reduced Heme Oxygenase-1 (HO-1) Levels. *Oxid Med Cell Longev* 2019;2019:9561281. doi:10.1155/2019/9561281, PMID:31636810.
- [130] Chang LC, Chiang SK, Chen SE, Yu YL, Chou RH, Chang WC. Heme oxygenase-1 mediates BAY 11-7085 induced ferroptosis. *Cancer Lett* 2018;416:124–137. doi:10.1016/j.canlet.2017.12.025, PMID:29274359.
- [131] Masaldan S, Clatworthy SAS, Gamell C, Meggyesy PM, Rigopoulos AT, Haupt S, *et al*. Iron accumulation in senescent cells is coupled with impaired ferritinophagy and inhibition of ferroptosis. *Redox Biol* 2018;14:100–115. doi:10.1016/j.redox.2017.08.015, PMID:28888202.
- [132] Xiao J, Zhang S, Tu B, Jiang X, Cheng S, Tang Q, *et al*. Arsenite induces ferroptosis in the neuronal cells via activation of ferritinophagy. *Food Chem Toxicol* 2021;151:112114. doi:10.1016/j.fct.2021.112114, PMID:33722599.
- [133] Song S, Wen F, Gu S, Gu P, Huang W, Ruan S, *et al*. Network Pharmacology Study and Experimental Validation of Yiqi Huayu Decoction Inducing Ferroptosis in Gastric Cancer. *Front Oncol* 2022;12:820059. doi:10.3389/fonc.2022.820059, PMID:35237519.



## Review Article

# Nanotechnology-based Therapeutic Strategies for Dry Eye Disease



Anil K. Philip\*

School of Pharmacy, University of Nizwa, Birkat Al Mouz, Oman

Received: April 19, 2023 | Revised: May 22, 2023 | Accepted: May 24, 2023 | Published online: July 04, 2023

### Abstract

Dry eye disease (DED) is a prevalent ocular condition affecting a significant proportion of the global population. Characterized by disruption of tear film homeostasis, DED results in dryness, discomfort, impaired visual clarity, and potential corneal damage. Despite its severe consequences, consistently effective treatments for DED remain elusive, leaving the majority of patients with persistent symptoms. This review aims to examine recent advancements in DED therapy, emphasizing the role of nanotechnology-based delivery systems in the development of novel treatments. By harnessing the potential of cutting-edge nanotechnology, we aspire to unveil innovative therapeutic strategies that address the unmet needs of patients with DED. Furthermore, we will discuss the current challenges, limitations, and future associated with these novel nanotechnology-based therapies for managing DED.

### Introduction

DED, a general ocular condition, disrupts tear film homeostasis and affects the ocular surface, leading to desiccation, discomfort, impaired visual acuity, and potential corneal deterioration.<sup>1</sup> Contemporary treatments for DED include ocular lubricants, anti-inflammatory medications, and punctal occlusion (closure of tear ducts).<sup>2</sup> Additionally, lifestyle adjustments and environmental modifications can be employed as therapeutic strategies to mitigate the risk of tear film destabilization.<sup>3</sup>

A strong association has been established between the onset of DED and an increased propensity for depressive symptoms, which were prevalent in 50–82% of the examined cases.<sup>4,5</sup> Supporting evidence from other studies also suggests that depression and anxiety frequently coexist in patients with DED.<sup>6</sup> These findings indicate that addressing depressive symptoms is a crucial and often-overlooked aspect of DED management, warranting comprehensive attention to achieve satisfactory outcomes. Moreover, the co-occurrence of anxiety may further aggravate DED symptoms, underscoring the need for a holistic approach to treatment that considers both ocular and psychological factors.

Dry eye has been postulated to be a localized autoimmune disease, as evidenced by various sources. This claim is supported by studies involving a mouse model of dry eye induced by environmental stress.<sup>7</sup> Further evidence includes clinical and biological markers observed in non-Sjögren's dry eye patients,<sup>8</sup> as well as the characterization of dry eye as a localized autoimmune disease.<sup>9</sup> Research findings further corroborate the theory that dry eye syndrome arises because of a disproportion between the protective immunoregulatory and pro-inflammatory pathways of the ocular surface, thus strengthening its autoimmune character.<sup>10</sup> Nonetheless, it is crucial to acknowledge the involvement of other factors in DED pathogenesis, such as environmental and hormonal influences,<sup>8</sup> mucosal tolerance disruption,<sup>9</sup> and toll-like receptor subtype TLR4.<sup>11</sup> Moreover, some limitations of this hypothesis have been highlighted.<sup>12</sup>

An intriguing association has been identified between the peptide LL37 and DED through a research investigation focusing on ocular fatigue-related phenomena.<sup>13</sup> Scientific investigations have observed LL-37's interaction with extracellular DNA, a potential contributor to inflammation in DED, which facilitates its translocation into ocular surface cells. This process activates the TLR9-MyD88 signalling pathway, subsequently eliciting a type 1 interferon response and triggering the adaptive immune response,<sup>14</sup> thereby implicating it in the pathogenesis of DED. However, it is important to note that the study investigating the correlation between LL37, and DED involved a small sample size of patients.<sup>13</sup> Consequently, further research with larger sample sizes is warranted to confirm the role of LL37 in the development of DED.

The tear film (Fig. 1) consists of three separate layers (mucus, aqueous, and lipid layers).<sup>15</sup> Each layer, in its unique way, plays an

**Keywords:** Dry eye disease; Nanoformulations; Tear film; Cubosomes; Niosomes.  
**Abbreviations:** DED, dry eye disease; HA, hyaluronic acid; HSP, heat shock protein; MGD, meibomian gland dysfunction; PG-HPG, Propylene Glycol and Hydroxypropyl Guar; SH, sodium hyaluronate; TBUT, tear film break-up time.

\*Correspondence to: Anil K. Philip, School of Pharmacy, University of Nizwa, Birkat Al Mouz-616, Oman. ORCID: <https://orcid.org/0000-0003-2960-330X>. Tel: +968-97671371, Fax: +968-25446389, E-mail: [philip@unizwa.edu.om](mailto:philip@unizwa.edu.om)

**How to cite this article:** Philip AK. Nanotechnology-based Therapeutic Strategies for Dry Eye Disease. *J Explor Res Pharmacol* 2023;8(3):253–262. doi: 10.14218/JERP.2023.00034.

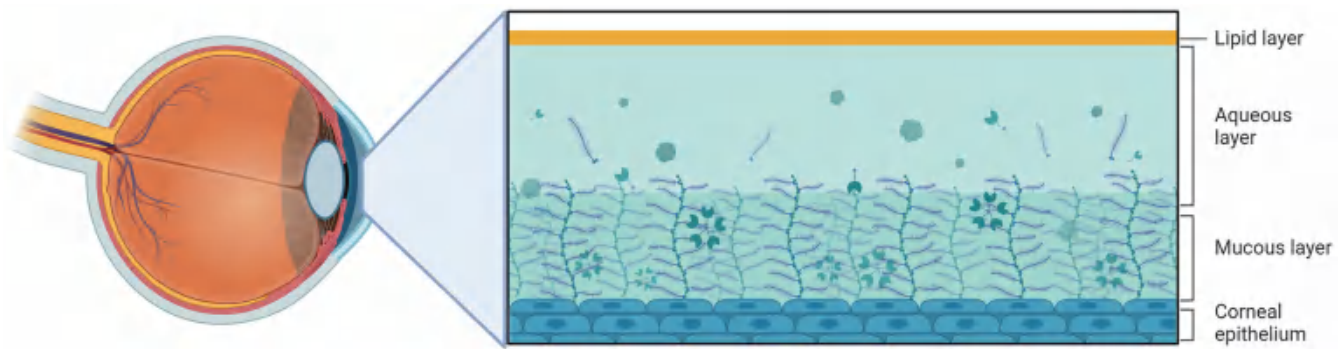


**Fig. 1. The three distinct layers of the tear film: The outer lipid layer, the middle aqueous layer and the inner mucin layer.**

important role in maintaining the integrity and stability of the tear film. Factors such as tear film production, evaporation, absorption, and drainage continuously influence the tear film.<sup>16</sup> Overall, the three layers work in tandem to protect and provide essential eye lubrication, which helps to prevent dryness and irritation of the eye. The thin inner mucin layer secreted by the lacrimal gland and conjunctiva goblet cells contains proteins, growth hormones, and antimicrobials. These contents help stick the tear film to the surface of the eye. The middle aqueous layer (7–8  $\mu\text{m}$  thick) is composed of water, electrolytes, and various substances secreted by the lacrimal gland. The secreted components provide moisture and nutrients to the cornea and the conjunctiva. The outer lipid layer (0.1  $\mu\text{m}$  thick) is composed of meibomian oil secreted by the meibomian glands. The layer reduces the tear surface tension and acts as a barrier to tear evaporation (reduced evaporation up to 95%).<sup>17</sup> A retrospective study found that 86% of patients with DED had meibomian gland dysfunction (MGD).<sup>18</sup> This relationship was supported by other studies,<sup>19–21</sup> whereas DED and MGD were reported to be prevalent among type 2 diabetes, with a prevalence of 72.3% and 55.3%, respectively.<sup>22</sup> However, one potential bias in this study is that only included confirmed a small population type 2 diabetes patients, which may not be representative of all diabetes patients in Ghana. The current consensus in scientific literature is that MGD plays a significant role in the etiology of DED. The pathophysiology of MGD involves a reduction in the secretion of meibum from the meibomian gland, which is the primary causative factor behind the functional abnormalities observed in MGD.<sup>23,24</sup>

For treating the mucin, aqueous, and/or lipid tear film inadequacies, along with the damage to ocular surface linked with DED, various novel therapeutic approaches have been proposed.<sup>25</sup> Studies on patients with Sjögren's syndrome have compared dry eye evaluation tests and presented major treatment conclusions.<sup>26</sup> Another study has shown that hyaluronic acid (HA) can hinder the dehydration of human corneal epithelial cells both in vitro and in vivo.<sup>27</sup> This discovery has the potential to speed up the advancement of more effective treatments for DED. On the other hand, a research has indicated that HA may lead to the counterintuitive outcome of causing the formation of haze and a reduction in the thickness of the epithelium.<sup>28</sup>

DED can be caused by a number of factors, such as medication (both systemic and topical), skin conditions, eye surgeries, exposure to chemicals or heat, prolonged device usage, vitamin A deficiency, wearing contact lenses, environmental elements, and more. Diagnosing DED requires a combination of symptoms and indicators such as tear volume, meniscus evaluation, tear film break-up time (TBUT), Schirmer test, fluorescein staining, phe-

nol red test, tear film osmolarity, lissamine green staining, matrix metalloproteinases, and eyelid examination.<sup>29</sup> Research has also demonstrated that DED may be caused by genetic factors, such as those related to immune response, tear film stability and corneal sensitivity. Recent genetic studies have identified new genetic regions associated with DED, further emphasizing its complex genetic makeup.<sup>30</sup> A study shows that Human Leukocyte Antigen-C1 alleles group is strongly associated with 108.30% increase in the odds of having DED.<sup>31</sup> A study on twins carried out by Vehof *et al.*, discovered that the heritability of DED was around 30% for symptoms and 40% for diagnosis, and there was a range of heritability of 25% to 80% for selected signs.<sup>32</sup> The findings suggested that identifying specific genes associated with DED could lead to better treatments and prevention strategies. Other studies have also indicated that genetic factors could contribute to the onset of DED, alongside environmental influences.<sup>33</sup>

In the US, DED occurs in approximately 6.8% of adults (16 million individuals aged 18 or older). Unfortunately, its incidence increases with age and women are more likely to be affected than men.<sup>34</sup> A study focusing on men (50 years and older) estimated that 4.34% had DED (approximately 1.68 million men). Furthermore, it was predicted that the number of patients with this condition will exceed 2.79 million by 2030.<sup>35</sup> One potential bias is that the study only included male physicians, which may not be representative of the general population. Additionally, the study relied on self-reported data, which may be subject to recall bias or social desirability bias. A cross-sectional study conducted in 16 towns in the Northern West Bank of Palestine to assess the prevalence of DED and potential associated risk factors found that the prevalence of DED was 64% in the study population, with older age and female gender being associated risk factors for its development.<sup>36</sup> However, a limitation of the study is the sampling method. The authors used a multistage sampling method based on the Palestinian central bureau of statistics sampling frame to identify the Palestinian towns participating in the study. While this approach may have helped ensure that a representative sample was obtained, it is possible that some groups were underrepresented or excluded from the study. Similarly, Germany saw an increase in DED prevalence from 20.24 per 1,000 patients in 2008 to 23.13 per 1,000 in 2014. Cataracts were the most frequent ocular comorbidity. The study concluded that these individuals used more healthcare resources and associated costs than their normal cohort.<sup>37</sup> One limitation of the study was that it relied on administrative claims data, which may not accurately reflect actual patient outcomes or treatment patterns. Overall, DED is a common ocular condition affecting a significant portion of the global population, with women and older

individuals being at higher risk. The incidence of DED is predicted to increase in the coming years, leading to increased healthcare resource utilization and associated costs. However, studies assessing the prevalence of DED and associated risk factors may be subject to limitations, such as sampling bias and reliance on self-reported or administrative claims data. Therefore, further research is needed to accurately assess the burden of DED and its risk factors in diverse populations to inform effective prevention and management strategies.

### Diagnosis and management of DED

Generally, the DED diagnostic evaluation includes a thorough patient history, a detailed slit-lamp examination, and additional tests as deemed necessary.<sup>38</sup> Moreover, patient-reported outcomes (PRO) questionnaires are often utilized to measure the severity of DED symptoms. However, it is important to note that not all PRO questionnaires have been validated and, thus, should be utilized with caution.<sup>39</sup> Ultimately, a precise diagnosis of DED requires a combination of tests and PRO questionnaires while ruling out other potential ocular surface conditions such as allergies and infections. The International Dry Eye Workshop (DEWS) report has furnished a comprehensive guide for diagnosing DED. However, with recent advances in diagnostic techniques, certain aspects of the DEWS findings and recommendations require reevaluation.<sup>40</sup> The diagnostic criteria for DED remain a matter of contention, and there is a lack of agreement on disease classification and interpretation of diagnostic tests. Therefore, standardization of disease terminology and diagnostic tools is necessary to enhance the utility of epidemiological and clinical research on DED. Further research and consensus-building efforts are essential to improve our understanding and management of DED.<sup>41</sup>

The identification of DED involves utilizing both subjective and objective assessments. Patients' self-reported symptoms are taken into consideration as a subjective measure, while objective tests entail examining tear film stability through methods like TBUT and fluorescence staining (FTBUT) using a slit-lamp microscope. Although tear film instability tests involve a variety of procedures, some of which may be intrusive, not easily reproducible, and less precise.<sup>19</sup> TBUT has been reported to be associated with a 1,200% increase in the odds of severe DED.<sup>42</sup> The corner fluorescent staining was introduced after suggestions by the Tear Film & Ocular Surface Society Dry Eye Workshop II (TFOS DEWS II) for DED diagnostic procedures. In situations where there is a disagreement between the patient's reported symptoms and the clinical signs, further assessment using additional diagnostic criteria was advised.<sup>43</sup> Back in 2006, a group of experts in the field of DED reached a consensus using the Delphi approach. They suggested the use of the term "dysfunctional tear syndrome" instead of DED in their report.<sup>44</sup> The ODISSEY scoring algorithm serves as a straightforward tool for evaluating ocular surface damage in cases of severe DED, making the diagnosis process more accessible.<sup>43</sup> In DEWS II, a wide range of diagnostic procedures were identified, which included questionnaires, tests for tear film stability, abnormalities in the epithelium, and other methods. Although specific diagnostic criteria were not proposed in the report, it did suggest the most effective tests for diagnosing and tracking DED.<sup>44</sup> Some new techniques for diagnosing dry eye disease involve developing devices that rely on visual acuity to monitor patients' symptoms.<sup>45</sup> Reduced FTBUT (tear film instability) is another means of diagnosing DED,<sup>46</sup> although there is a weak association between dry eye tests and a lack of agreement between subjective symptoms

and clinical signs.<sup>47</sup>

To treat DED, the patient must receive proper education, and management techniques such as using ocular lubricants, modifying the environment (i.e., adding moisture), maintaining good hygiene of the eyelids, employing autologous tears, and tear preservation are recommended.<sup>48</sup> To manage the disease, palliative treatments such as antimicrobial and anti-inflammatory therapy, along with warm compresses, are also utilized.<sup>49</sup> Healthcare providers and patients typically opt for topical ocular preparations to help alleviate the symptoms of DED.<sup>50</sup> Previous investigations had delved into examining the viability of P2Y (purinergic) family receptor agonists as a prospective treatment for DED.<sup>51</sup> Recent studies have revealed that P2Y family receptor agonists show potential as a prospective treatment for DED by increasing tear and mucin production.<sup>52</sup> Diquafosol, a topical P2Y<sub>2</sub> agonist, is already being used as a drug to treat the disease.<sup>53,54</sup> Moreover, antagonists of P2Y<sub>12</sub> receptors, and potentially P2Y<sub>1</sub> receptors, are being tested as anti-thrombotic agents, while a P2Y<sub>2</sub>/P2Y<sub>4</sub> receptor agonist has been found to be effective in treating DED symptoms. Furthermore, TRPM8 receptor agonists such as cryosim-3 are also being studied for their potential to act as a viable treatment for DED.<sup>55–58</sup> A summary of important findings from the development and clinical trials of diquafosol, another P2Y<sub>2</sub> receptor activator, revealed its effectiveness in treating DED in short-term studies.<sup>59</sup> Dinucleoside polyphosphates, created by combining two nucleotides with varying numbers of phosphates, have been suggested as a potential DED treatment. However, the FDA has not approved oral pilocarpine and cevimeline, which activate the muscarinic acetylcholine receptor, for the treatment of DED.<sup>60</sup> P2Y<sub>2</sub> receptors may also be a target for future trials aimed at treating tumors,<sup>61</sup> and therapies targeting P2Y<sub>1</sub> have been proposed as a new approach to treating drug-resistant status epilepticus.<sup>62</sup> Despite the development of many treatments, some patients seek more straightforward or efficient remedies.<sup>63</sup> Currently, no specific curative measures for DED are mentioned in modern medicine.<sup>64</sup> Nonetheless, essential fatty acids are being suggested as a new treatment method for patients with dry eye syndrome.<sup>65</sup> In addition, the use of novel eye drops that contain n-3 eicosapentaenoic and docosahexaenoic acids has been shown to effectively manage mild cases of DED.<sup>66,67</sup> Other recently developed eye drops such as Trimix eye drops,<sup>68</sup> cord blood serum eye drops,<sup>69</sup> HA and trehalose ophthalmic solution (Thealoz® Duo),<sup>70</sup> corticosteroids, MC2-03 0.18% sodium hyaluronate (SH) eye drops,<sup>71</sup> propylene glycol/hydroxypropylguar (PG-HPG) nanoemulsion-based eye drops,<sup>72</sup> and SH/chondroitin sulfate, preservative-free, ophthalmic solution, have demonstrated efficacy in managing mild cases of DED.<sup>73</sup> Trimix eye drops, a combination of viscosity-enhancing HA trehalose, and cationic liposomes comprising stearylamine and phospholipids, showed promising results in improving objective signs and subjective symptoms in patients with DED.<sup>74</sup> However, potential biases and limitations exist. The study for Trimix eye drops was conducted by a single center with a small sample size (25 patients), which limits its generalizability. Also, there was no control group or comparison to other available tear substitutes. Although the article mentions a shift towards complex multi-action combined formulas for DED, it provides no evidence to support this claim, raising questions about their effectiveness.

Additionally, randomized clinical trials have shown that water-based eye drops containing SH, carboxymethylcellulose, or carbomers can also alleviate symptoms associated with DED. Moreover, the new-generation Intense Pulsed Light has been found to be safe and effective in relieving symptoms and signs of MGD-



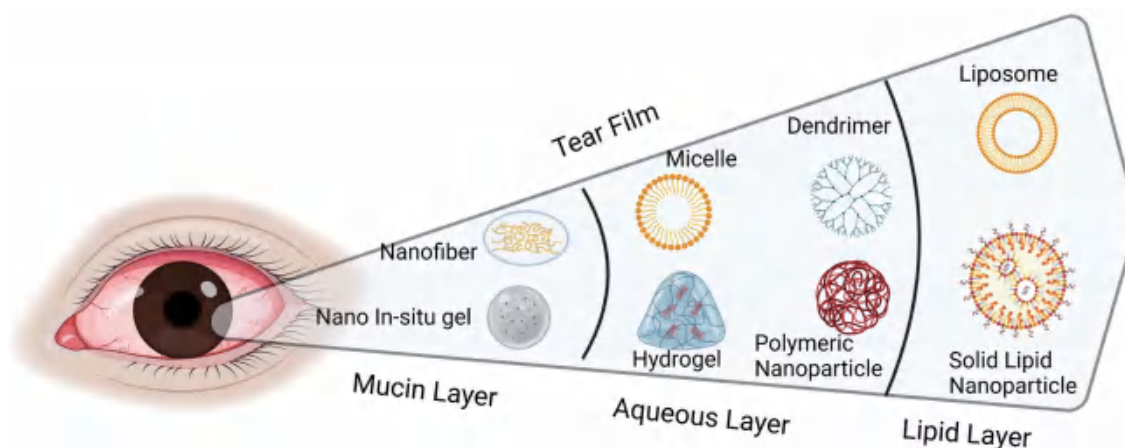


**Fig. 2. Different nanotechnology drug delivery systems applied to the three distinct layers of the tear film.** Certain formulations will have the best bioavailability if they are placed in the right tear film.

related dry eye.<sup>75,76</sup> Automation of diagnostic methods for DED can improve accuracy and ease of acquisition, with semi-automated and fully automated methods showing promise in quantifying DED characteristics.<sup>19</sup> An example of an effective approach to enhance diagnostic accuracy is the utilization of 3D ultrasound, which facilitates evaluation in three orthogonal planes and enables scrutiny of the external appearance of facial features.<sup>77</sup> Additionally, cross-checking may heighten diagnostic accuracy by allowing human experts to apply their information processing heuristics, reasoning methods, and pattern recognition techniques, which automated systems may not possess.<sup>78</sup> Therefore, the implementation of automated noninvasive workup is a promising instrument for the accurate diagnosis of DED.<sup>74</sup>

### Nanotechnology: a cutting-edge approach to DED drug delivery

The burgeoning field of nanotechnology has been making waves in the realm of DED therapy, offering a multitude of innovative possibilities (Fig. 2). By harnessing the power of nanoparticles, researchers have successfully crafted drug carriers that can efficiently penetrate and enhance bioavailability within the anterior segment of the eye.<sup>79</sup> Despite the myriad of promising applications for nanoparticles in ophthalmology, their potential toxicity to ocular tissues, including the cornea, conjunctiva, and retina, under specific conditions warrants careful consideration. As such, elucidating the ocular toxicity of nanoparticles is of paramount importance to ensure the safety and efficacy of these innovative treatments. Further, although there is a strong interest in the use of nanoformulations for delivering phytochemicals to the eye, but this technology has been reported to be a hindrance to the clinical translation of new products due to scalability issues.<sup>80</sup>

To address this challenge, researchers have turned to advanced in vitro cell culture techniques that can closely simulate the human organism. One such technique involves the use of human organoids, which are three-dimensional, self-organizing cell structures derived from pluripotent stem cells. Organoids can accurately mimic the complexities of human tissues and have been employed in various fields of study, including toxicology.<sup>81</sup> Another groundbreaking approach in this domain involves the utilization of nanotechnology to create novel drug delivery systems, such as inhalation-based modalities. Central to the development of these

inhalable powders is the art and science of particle engineering, a pivotal aspect that ensures the successful delivery of drugs with augmented therapeutic effects and precision targeting. By tailoring particle size, morphology, and surface properties, researchers can optimize the performance of inhalable formulations and maximize their clinical benefits.<sup>82</sup> However, potential toxicity issues still remain largely unanswered.

This pioneering area of nano-ophthalmology is currently in its infancy, but it holds immense promise in overcoming the ocular barriers that have long hindered effective drug delivery.<sup>83</sup> The advent of sophisticated nanotechnology-based delivery methods holds the potential to fundamentally transform the landscape of DED management. By providing heightened efficacy and pinpoint accuracy, these techniques promise to elevate therapeutic outcomes and improve patient experiences. Moreover, the dual-capability of nanotechnology to transport both pharmaceutical agents and antigens has piqued the interest of researchers, who are diligently investigating its diverse applications. As the development of this versatile technology advances, the scientific community eagerly awaits the emergence of novel treatment modalities and their potential impact on DED therapy.<sup>84,85</sup>

### Liposomes

The management of DED is witnessing a paradigm shift with the advent of liposome-based therapies (Fig. 3). These innovative strategies offer new hope for the effective treatment of this prevalent ocular ailment. The development of liposome eye spray, for instance, has been heralded as a big advancement.<sup>86</sup> Utilizing vitamin A-coupled liposomes (VA-lip) containing heat shock protein 47 (HSP47) for a formulation (VA-lip HSP47), researchers have identified a novel antifibrotic topical therapy for DED. The liposome has been shown to be effective in DED in a mouse model of chronic graft-versus-host disease (GVHD). In GVHD, the HSP47 has been identified to play a role and DED is the most common manifestation. The ocular instillation of VA-lip HSP47 distributed to the lacrimal glands, knocked down HSP47 expression in fibroblasts, reduced collagen deposition, and restored tear secretion after allogeneic stem cell transplantation. Additionally, ocular instillation of VA-lip HSP47 also ameliorated established lacrimal gland fibrosis and DED.<sup>87</sup> However, studies in humans still need to establish the above claims. Similarly, the potential of thymoquinone loaded liposomes as a therapeutic agent in DED has been

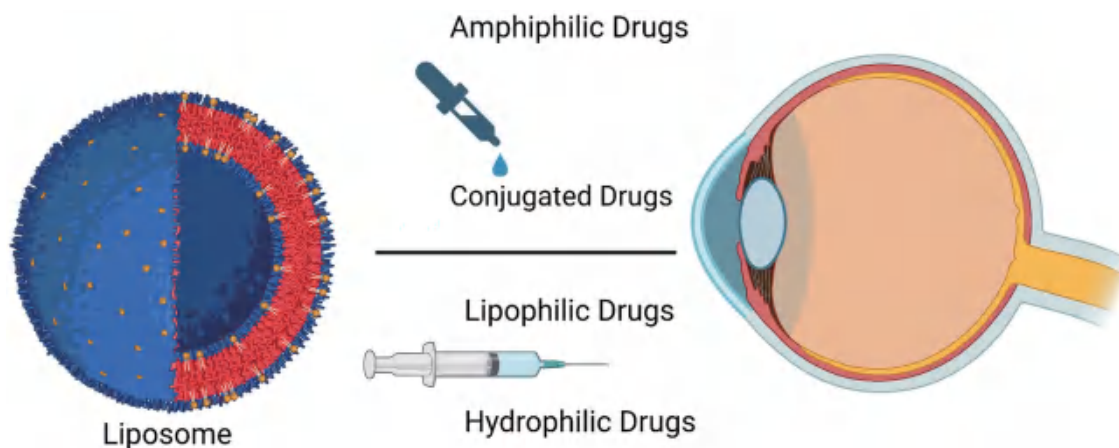


**Fig. 3. Liposome delivery to the eye.** Different properties of the drug which can be formulated as a liposome for the best action are depicted in the figure. Some of them can be given as eye drops, and some as injections.

identified. This effect may be attributed to the anti-inflammatory properties of the encapsulated vitamins and the protective barrier formed by liposomes.<sup>88</sup> Another promising approach involves the use of liposomes loaded with 1-bromoheptadecafluorooctane and tetrandrine, which exert anti-inflammatory effects without substantially impacting intraocular pressure, offering an alternative therapeutic strategy for DED.<sup>89</sup>

### Niosomes

Niosomes are a novel drug delivery system that can be used to treat a variety of ocular diseases, including DED. Studies have shown that niosomes have a high encapsulation efficiency and prolonged drug-release rate for drugs such as doxycycline hyclate and gentamycin sulfate, making them an effective and promising treatment option. Compared to liposomes, niosomes have several advantages, such as their ability to entrap both lipophilic and hydrophilic drugs, their improved drug permeation in corneal cells, their small size which allows for better drug retention on the ocular surface, and their cost effectiveness for production in the pharmaceutical industry. Furthermore, niosomes are more convenient for handling and storage than liposomes. As such, due to their advantageous properties, niosomes offer a promising drug delivery system for treating DED.<sup>90</sup>

According to a preclinical study conducted by Durak *et al.* niosomes loaded with timolol maleate demonstrated high encapsulation efficiency and were found to be more effective at reducing eye pressure compared to other delivery systems.<sup>91</sup> This finding suggests that niosomes loaded with timolol maleate could be used as an effective treatment option for glaucoma, a condition that causes damage to the optic nerve and can lead to vision loss if left untreated. Moreover, a study by Cvenkel *et al.* found that the reduction in intraocular pressure achieved by niosomes loaded with timolol maleate was comparable to other commonly used glaucoma medications such as latanoprost and bimatoprost.<sup>92</sup> There have been studies that demonstrate the successful use of niosomes as ocular drug delivery carriers, which significantly improve the ocular bioavailability of various drugs. For example, one study reported 2.5 times increase in the ocular bioavailability of timolol maleate (a water soluble drug) encapsulated in niosomes compared to a timolol maleate solution. Niosomes are preferred over other vesicular systems for ocular drug delivery due to their chemical stability, low toxicity, biodegradability, biocompatibility,

and non-immunogenicity. Surfactants used in niosomes can act as penetration enhancers to improve the performance and availability of the drug.<sup>93</sup> It is important to note that the success of niosomes as ocular drug delivery carriers may depend on factors such as the specific drug being encapsulated, the formulation and composition of the niosomes, and patient-specific factors.

### Graphene nanocomposites

A recent study focuses on a new antioxidant nanocomposite created from pterostilbene and carboxyl-chitosan modified graphene to control oxidative stress of human corneal epithelial cells. Pterostilbene (PS), found in blueberries, is an antioxidant with potential for medical applications. However, poor hydrophobicity, poor cellular permeability and retention limit its use. Carboxyl-chitosan functionalized graphene (CG) was used to address these limitations as it has good hydrophilicity and ocular biocompatibility. The resulting nanocomposite, PS-CG, had a good antioxidant effect due to its synergistic effects. The activation of the Keap1-Nrf2-ARE signalling pathway enhances the expression of various antioxidative enzymes and detoxification enzymes, preventing oxidative stress that causes dry eye. The synthesis process involved a ball milling method followed by the centrifugation and dialysis process to obtain CG. PS was covalently linked to CG via a  $\pi$ - $\pi$  stacking interaction, resulting in a PS-CG dispersion that can be used to treat dry eye caused by oxidative stress.<sup>94</sup>

### Micelles

Micelles are a type of colloidal drug delivery system that emerges when the concentration of polymer/surfactant exceeds the critical micellar concentration. This solution is commonly used to enhance the drug's solubility and bioavailability, thereby improving its therapeutic efficacy.<sup>95</sup> Micelles are formed by the spontaneous self-assembly of amphiphilic surfactants or diblock polymers at a specific concentration or temperature in a solution, and they can have varied shapes like spheres, cylinders, or star shapes with dimensions that range from 10–200 nm.<sup>96</sup> The morphology of the micelles can have increased circulation time.<sup>97</sup> Other studies also support the claim with their measurement of polymeric micelles in the blood to have a retention at 24 h above 20 % ID/g, which indicates that a large percentage of the micelles are still in circulation.<sup>98</sup>

Micelles are useful in transporting hydrophobic drugs in wa-

ter, with normal micelles being the carriers of choice, while hydrophilic drugs can be delivered using reversed micelles.<sup>99</sup> This makes them ideal for targeting ocular tissue and increasing corneal permeability when applied topically. Micelles, despite their challenges in drug loading, scalability, and potential toxicity from surfactant use, offer notable benefits for DED treatment. Cyclosporin A, a hydrophobic and potent immunosuppressive agent, is used to address DED and prevent corneal transplant rejection. To improve its solubility and ocular bioavailability, researchers have explored nanoparticulate drug delivery systems for cyclosporine A. Polymeric micelles were successfully created utilizing a diblock polymer, specifically Methoxypoly(ethylene glycol)-poly(lactic acid), which was loaded with cyclosporine A via a thin film dispersion method. This micellar approach boosted the drug's retention on the precorneal surface by 4.5 times and decreased its elimination compared to a cyclosporine emulsion. These results highlight the potential of cyclosporine A micelles to enhance the drug's effectiveness in treating DED.<sup>80</sup>

In a study, nanomicelles were formed, which were small, self-assembling particles that can have the potential to improve the bioavailability of drugs by protecting them from precorneal elimination and promoting drug uptake into the eye. These nanomicelles have a better activity than those produced with Ikervis, and their stability and acceptability in patients are improved. Clinical studies will be necessary to identify the effective dose in the treatment of ocular pathologies such as DED.<sup>100</sup>

Among all the discussed nanoformulations, nanomicelles have shown promise in treating DED. This is because of their ability to improve the solubility and stability of drugs, prolong their release, and enhance their penetration into the target tissues. By encapsulating the therapeutic agents within nanomicelles, their bioavailability and efficacy can be increased, leading to improved treatment outcomes for DED.

### Nanoemulsions

Dry eye symptoms have been effectively addressed using a nanoemulsion eye lubricant comprising Propylene Glycol and Hydroxypropyl Guar (PG-HPG). This innovative formulation serves to enhance tear film stability, increase lipid layer density, alleviate dryness and discomfort associated with contact lens use, and provide preventive benefits for maintaining ocular moisture in arid environments. Demonstrating sustained efficacy and tolerability, PG-HPG eye drops have become a widely adopted treatment for DED, and show potential for application in other ocular conditions as well.<sup>2</sup>

Both preclinical and clinical investigations have confirmed the effectiveness of PG-HPG nanoemulsion lubricants in mitigating DED symptoms.<sup>101</sup> The HPG nanoscale droplets promote the optimal distribution of phospholipids within the tear film, thereby contributing to its stability. Results from studies comparing lipid and non-lipid-based aqueous drops have consistently reported sustained relief from dry eye symptoms, reduced severity of superior lid wiper epitheliopathy, and improved tear film consistency and ocular surface properties. These findings have been corroborated by Phase IV clinical trial data, emphasizing the utility of PG-HPG nanoemulsion in the management of DED.<sup>72</sup>

Despite these promising results, there remains a need for more comprehensive clinical trials to establish robust evidence supporting the effectiveness of PG-HPG nanoemulsion lubricants in addressing DED symptoms.<sup>74</sup> Future research should focus on further elucidating the therapeutic potential and efficacy of this novel formulation.

### Cubosomes

Cubosomes, a distinct class of lipid-based nanostructured carriers with dimensions ranging from 100 to 300 nm, offer an expansive surface area and minimal viscosity, rendering them suitable candidates for various drug delivery systems.<sup>102–104</sup> These versatile carriers encapsulate hydrophilic, lipophilic, and amphiphilic drugs, thereby demonstrating a promising potential for diverse administration routes, including oral, ocular, and transdermal applications. Notably, drug absorption is generally facilitated through the transcellular pathway.<sup>105</sup>

An in vivo study investigating the anti-inflammatory effects of fexofenadine hydrochloride in rabbits substantiated the superiority of a cubosomal carrier over an aqueous drug dispersion.<sup>105</sup> Huang *et al.* reported the successful implementation of a cubosome-based drug delivery system for glaucoma treatment using timolol maleate (TM). Ex vivo corneal permeability experiments revealed an elevated penetration of TM cubosomes compared to commercially available eye drops, indicating an enhancement in corneal permeability, increased retention time, and improved bioavailability of ocular drugs for ocular disease treatment.<sup>106</sup>

Moreover, numerous investigations have posited the promise of cubosomes as drug delivery systems for ocular disease therapy, including DED. Eldeeb *et al.* discovered that brimonidine tartrate-loaded cubosomes exhibited augmented corneal permeability and sustained release patterns, culminating in a heightened intraocular pressure-lowering effect relative to commercial eye drops.<sup>107</sup> Nasr *et al.* demonstrated that fluconazole-loaded cubosomes enhanced antifungal activity in the treatment of keratomycosis in rats.<sup>108</sup>

Despite these promising findings, no study has yet directly investigated the efficacy of cubosomes in treating DED. Additionally, the large-scale production of cubosomes presents a significant challenge.<sup>109</sup> Consequently, further research is warranted to explore the potential of cubosomes as a therapeutic strategy for DED and address the obstacles related to their large-scale manufacturing.

### Mucoadhesive nanoparticles

Mucoadhesive nanoparticles are promising drug delivery systems for treating DED. They have been shown to effectively target and deliver drugs to the ocular surface with prolonged retention, resulting in enhanced therapeutic efficacy.<sup>110</sup> The use of phenylboronic acid-modified mucoadhesive nanoparticles has facilitated weekly treatment of experimentally-induced dry eye syndrome, providing a potential solution for patients suffering from this chronic condition.<sup>111</sup> Furthermore, Cyclosporin A, a widely used immunosuppressant drug for treating DED and preventing corneal transplant rejection, can be delivered using mucoadhesive nanoparticle eye drop formulations, increasing the drug's ocular retention and reducing dosage frequency.<sup>80</sup> Chitosan mucoadhesive nanoparticles have the potential to improve ocular drug delivery due to their ability to promote mucoadhesion and enhance corneal penetration, therefore, providing a promising alternative for treating ocular diseases such as dry eye syndrome. However, safety concerns still persist regarding the cross-linked chitosan formulations.<sup>112</sup>

### Future directions

The diagnosis and treatment of DED pose significant challenges due to the multifactorial etiology, lack of consensus on diagnostic criteria, and limitations in current therapeutic approaches.<sup>113</sup> The



inadequacy of commonly used clinical signs and symptoms for diagnosis, along with the challenge of determining disease severity using biomarkers, surrogates, or outcomes, further complicates the management of DED.<sup>114</sup> Addressing the low bioavailability of drugs and the risk of systemic side effects is crucial for enhancing the efficacy of existing treatments, such as topical administration of eye drops, surgery, and contact lens use.

Future studies should focus on the development of reliable diagnostic criteria and the identification of new biomarkers for DED, which will enable more accurate disease classification and monitoring. Additionally, research should continue to explore the potential of nanotechnology-based delivery systems, with particular attention to overcoming the current limitations and paving the way for their successful clinical translation. Ultimately, such advancements will lead to improved management and treatment of DED, enhancing the quality of life for millions of patients worldwide.

## Conclusions

Nanotechnology-based delivery systems have emerged as a promising alternative to conventional ocular delivery systems for the treatment of anterior segment diseases, including DED. These systems have the potential to overcome the challenges associated with current treatment modalities by increasing drug bioavailability, reducing side effects, and enabling targeted drug delivery. However, before these novel delivery systems can be translated into clinical use, further research is needed to address the existing challenges, optimize their performance, and establish their safety and efficacy profiles.

## Acknowledgments

None.

## Funding

None.

## Conflict of interest

The author has no conflict of interests related to this publication.

## Author contributions

Anil K. Philip is the sole author of this work.

## References

- [1] Yang CC, Chien JY, Chou YY, Ciou JW, Huang SP. The Effects of Lycium chinense, Cuscuta chinensis, Senna tora, Ophiopogon japonicus, and Dendrobium nobile Decoction on a Dry Eye Mouse Model. *Medicina (Kaunas)* 2022;58(8):1134. doi:10.3390/medicina58081134, PMID:36013601.
- [2] Srinivasan S, Williams R. Propylene Glycol and Hydroxypropyl Guar Nanoemulsion - Safe and Effective Lubricant Eye Drops in the Management of Dry Eye Disease. *Clin Ophthalmol* 2022;16:3311–3326. doi:10.2147/OPTH.S377960, PMID:36237486.
- [3] Wang MTM, Muntz A, Mamidi B, Wolffsohn JS, Craig JP. Modifiable lifestyle risk factors for dry eye disease. *Cont Lens Anterior Eye* 2021;44(6):101409. doi:10.1016/j.clae.2021.01.004, PMID:33485806.
- [4] Gonzales JA, Chou A, Rose-Nussbaumer JR, Bunya VY, Criswell LA, Shiboski CH, et al. How Are Ocular Signs and Symptoms of Dry Eye Associated With Depression in Women With and Without Sjögren Syndrome? *Am J Ophthalmol* 2018;191:42–48. doi:10.1016/j.ajo.2018.04.004, PMID:29655640.
- [5] Um SB, Yeom H, Kim NH, Kim HC, Lee HK, Suh I. Association between dry eye symptoms and suicidal ideation in a Korean adult population. *PLoS One* 2018;13(6):e0199131. doi:10.1371/journal.pone.0199131, PMID:29924835.
- [6] Senra H, Hernandez-Moreno L, Moreno N, Macedo AF. Anxiety levels moderate the association between visual acuity and health-related quality of life in chronic eye disease patients. *Sci Rep* 2022;12(1):2313. doi:10.1038/s41598-022-06252-1, PMID:35145163.
- [7] Stern ME, Schaumburg CS, Dana R, Calonge M, Niederkorn JY, Pflugfelder SC. Autoimmunity at the ocular surface: pathogenesis and regulation. *Mucosal Immunol* 2010;3(5):425–442. doi:10.1038/mi.2010.26, PMID:20485329.
- [8] Kurtul BE, Sav Aydinli M, Altıaylık Özer P. The Relationship Between Vitamin D Deficiency and Ocular Surface Clinical Parameters in Patients with Non-Sjögren Dry Eye. *Türkiye Klinikleri J Ophthalmol* 2015;24:35–40. doi:10.5336/ophthal.2014-41735.
- [9] Tavakoli A, Markoulli M, Papas E, Flanagan J. The Impact of Probiotics and Prebiotics on Dry Eye Disease Signs and Symptoms. *J Clin Med* 2022;11(16):4889. doi:10.3390/jcm11164889, PMID:36013128.
- [10] Stern ME, Schaumburg CS, Pflugfelder SC. Dry eye as a mucosal autoimmune disease. *Int Rev Immunol* 2013;32(1):19–41. doi:10.3109/08830185.2012.748052, PMID:23360156.
- [11] Simmons KT, Xiao Y, Pflugfelder SC, de Paiva CS. Inflammatory Response to Lipopolysaccharide on the Ocular Surface in a Murine Dry Eye Model. *Invest Ophthalmol Vis Sci* 2016;57(6):2443–2451. doi:10.1167/iovs.15-18396, PMID:27136463.
- [12] Tauber J, Schechter BA, Bacharach J, Toyos MM, Smyth-Medina R, Weiss SL, et al. A Phase II/III, randomized, double-masked, vehicle-controlled, dose-ranging study of the safety and efficacy of OTX-101 in the treatment of dry eye disease. *Clin Ophthalmol* 2018;12:1921–1929. doi:10.2147/OPTH.S175065, PMID:30323548.
- [13] McIntosh RS, Cade JE, Al-Abed M, Shanmuganathan V, Gupta R, Bhan A, et al. The spectrum of antimicrobial peptide expression at the ocular surface. *Invest Ophthalmol Vis Sci* 2005;46(4):1379–1385. doi:10.1167/iovs.04-0607, PMID:15790905.
- [14] McDermott AM. New insight into dry eye inflammation. *Invest Ophthalmol Vis Sci* 2012;53(13):8264. doi:10.1167/iovs.12-11386, PMID:23248237.
- [15] Nagai N, Otake H. Novel drug delivery systems for the management of dry eye. *Adv Drug Deliv Rev* 2022;191:114582. doi:10.1016/j.addr.2022.114582, PMID:36283491.
- [16] Kopacz D, Niezgoda Ł, Fudalej E, Nowak A, Maciejewicz P. Tear Film – Physiology and Disturbances in Various Diseases and Disorders. In: Kopacz D (ed). *Ocular Surface Diseases - Some Current Date on Tear Film Problem and Keratoconic Diagnosis*. IntechOpen; 2021. doi:10.5772/intechopen.94142.
- [17] Chang AY, Purt B. Biochemistry, Tear Film. [Updated 2022 Jun 11]. StatPearls [Internet]. Treasure Island (FL): StatPearls Publishing; 2023. Available from: <https://www.ncbi.nlm.nih.gov/books/NBK572136/>.
- [18] Inoue T, Ideta R, Mera R, Umeki K, Ueno A, Matsui T aki, et al. Additional Instruction by a Nurse Enhanced the Effect of Eyelid Warming on Subjective Symptoms in Patients with Meibomian Gland Dysfunction. *J Healthc Commun* 2018;3(2):29. doi:10.4172/2472-1654.100139.
- [19] Brahim I, Lamard M, Benyoussef AA, Quéllec G. Automation of dry eye disease quantitative assessment: A review. *Clin Exp Ophthalmol* 2022;50(6):653–666. doi:10.1111/ceo.14119, PMID:35656580.
- [20] Zhmud TM, Malachkova NV, Andrushkova OO, Hrizhymalska KY. Meibomian Gland dysfunction and dry eye disease symptoms in patients with type 2 Diabetes Mellitus. *Rep of Morph* 2019;25(4):51–55. doi:10.31393/morphology-journal-2019-25(4)-08.
- [21] Ahuja AS, Bowden FW 3rd, Robben JL. A Novel Treatment for Neurotrophic Corneal Ulcer Using Topical Cenegegermin (OXERVATE™) Containing Recombinant Human Nerve Growth Factor. *Cureus* 2020;12(11):e11724. doi:10.7759/cureus.11724, PMID:33391953.
- [22] Abu EK, Ofori AO, Boadi-Kusi SB, Ocansey S, Yankah RK, Kyei S, et al. Dry eye disease and meibomian gland dysfunction among a clinical sample of type 2 diabetes patients in Ghana. *Afr Health Sci* 2022;22(1):293–302. doi:10.4314/ahs.v22i1.36, PMID:36032480.



- [23] Shukla R, Thool A. Meibomian Gland Dysfunction Causing Dry Eye Syndrome in Computer Users. *Journal of Pharmaceutical Research International* 2021;33(60B):486–493. doi:10.9734/jpri/2021/v33i60B34644.
- [24] Tchegnon E, Liao CP, Ghotbi E, Shipman T, Wang Y, McKay RM, *et al.* Epithelial stem cell homeostasis in Meibomian gland development, dysfunction, and dry eye disease. *JCI Insight* 2021;6(20):e151078. doi:10.1172/jci.insight.151078, PMID:34499624.
- [25] Sullivan D. New therapeutic approaches and challenges for the treatment of dry eye disease. *Acta Ophthalmologica* 2014;92(s253). doi:10.1111/j.1755-3768.2014.3311.x.
- [26] Valim V, Trevisani VF, de Sousa JM, Vilela VS, Belfort R Jr. Current Approach to Dry Eye Disease. *Clin Rev Allergy Immunol* 2015;49(3):288–297. doi:10.1007/s12016-014-8438-7, PMID:25081064.
- [27] Rangarajan R, Kraybill B, Ogundele A, Ketelson HA. Effects of a Hyaluronic Acid/Hydroxypropyl Guar Artificial Tear Solution on Protection, Recovery, and Lubricity in Models of Corneal Epithelium. *J Ocul Pharmacol Ther* 2015;31(8):491–497. doi:10.1089/jop.2014.0164, PMID:26067908.
- [28] Szentmáry N, Seitz B, Langenbucher A, Schlötzer-Schrehardt U, Hofmann-Rummelt C, Naumann GO. Histologic and ultrastructural changes in corneas with granular and macular dystrophy after excimer laser phototherapeutic keratectomy. *Cornea* 2006;25(3):257–263. doi:10.1097/01.icc.0000176603.87376.d8, PMID:16633022.
- [29] Golden MI, Meyer JJ, Patel BC. Dry Eye Syndrome. [Updated 2023 Apr 3]. StatPearls [Internet]. Treasure Island (FL): StatPearls Publishing; 2023. Available from: <https://www.ncbi.nlm.nih.gov/books/NBK470411/>.
- [30] Alves M, Novaes P, Morraye Mde A, Reinach PS, Rocha EM. Is dry eye an environmental disease? *Arq Bras Oftalmol* 2014;77(3):193–200. doi:10.5935/0004-2749.20140050, PMID:25295911.
- [31] Ren G, Shao T, Zhuang Y, Hu H, Zhang X, Huang J, *et al.* Association of killer cell immunoglobulin-like receptor and human leukocyte antigen-C genotype with dry eye disease in a Chinese Han population. *Genet Test Mol Biomarkers* 2012;16(8):910–914. doi:10.1089/gtmb.2011.0355, PMID:22509813.
- [32] Adams MK. Twin study implicates genetic factors in dry eye disease. *Invest Ophthalmol Vis Sci* 2014;55(11):7284. doi:10.1167/iovs.14-15745, PMID:25395545.
- [33] Abdulmannan DM, Naser AY, Ibrahim OK, Mahmood AS, Alyoussef Alkrad J, Sweiss K, *et al.* Visual health and prevalence of dry eye syndrome among university students in Iraq and Jordan. *BMC Ophthalmol* 2022;22(1):265. doi:10.1186/s12886-022-02485-w, PMID:35698109.
- [34] Farrand KF, Fridman M, Stillman IO, Schaumberg DA. Prevalence of Diagnosed Dry Eye Disease in the United States Among Adults Aged 18 Years and Older. *Am J Ophthalmol* 2017;182:90–98. doi:10.1016/j.ajo.2017.06.033, PMID:28705660.
- [35] Schaumberg DA, Dana R, Buring JE, Sullivan DA. Prevalence of dry eye disease among US men: estimates from the Physicians' Health Studies. *Arch Ophthalmol* 2009;127(6):763–768. doi:10.1001/archophthalmol.2009.103, PMID:19506195.
- [36] Shanti Y, Shehadeh R, Bakkar MM, Qaddumi J. Prevalence and associated risk factors of dry eye disease in 16 northern West bank towns in Palestine: a cross-sectional study. *BMC Ophthalmol* 2020;20(1):26. doi:10.1186/s12886-019-1290-z, PMID:31931756.
- [37] Siffel C, Hennies N, Joseph C, Lascano V, Horvat P, Scheider M, *et al.* Burden of dry eye disease in Germany: a retrospective observational study using German claims data. *Acta Ophthalmol* 2020;98(4):e504–e512. doi:10.1111/aos.14300, PMID:31736282.
- [38] Messmer EM. The pathophysiology, diagnosis, and treatment of dry eye disease. *Dtsch Arztebl Int* 2015;112(5):71–81. doi:10.3238/arztebl.2015.0071, PMID:25686388.
- [39] Uchino M, Nishiwaki Y, Michikawa T, Shirakawa K, Kuwahara E, Yamada M, *et al.* Prevalence and risk factors of dry eye disease in Japan: Koumi study. *Ophthalmology* 2011;118(12):2361–2367. doi:10.1016/j.opthta.2011.05.029, PMID:21889799.
- [40] Bron AJ, Tomlinson A, Foulks GN, Pepose JS, Baudouin C, Geerling G, *et al.* Rethinking dry eye disease: a perspective on clinical implications. *Ocul Surf* 2014;12(2 Suppl):S1–S31. doi:10.1016/j.jtos.2014.02.002, PMID:24725379.
- [41] Brewitt H, Sistani F. Dry eye disease: the scale of the problem. *Surv Ophthalmol* 2001;45(Suppl 2):S199–S202. doi:10.1016/s0039-6257(00)00202-2, PMID:11587143.
- [42] Rashid MA, Teo CHY, Mamun S, Ong HS, Tong L. Prevalence and Risk Factors of Severe Dry Eye in Bangladesh-Based Factory Garment Workers. *Diagnostics (Basel)* 2020;10(9):634. doi:10.3390/diagnostics10090634, PMID:32859000.
- [43] Baudouin C, Aragona P, Van Setten G, Rolando M, Irkeç M, Benítez del Castillo J, *et al.* Diagnosing the severity of dry eye: a clear and practical algorithm. *Br J Ophthalmol* 2014;98(9):1168–1176. doi:10.1136/bjophthalmol-2013-304619, PMID:24627252.
- [44] Shimazaki J. Definition and Diagnostic Criteria of Dry Eye Disease: Historical Overview and Future Directions. *Invest Ophthalmol Vis Sci* 2018;59(14):DES7–DES12. doi:10.1167/iovs.17-23475, PMID:30481800.
- [45] Elhusseiny AM, Khalil AA, El Sheikh RH, Bakr MA, Eissa MG, El Sayed YM. New approaches for diagnosis of dry eye disease. *Int J Ophthalmol* 2019;12(10):1618–1628. doi:10.18240/ijo.2019.10.15, PMID:31637199.
- [46] Inomata T, Iwagami M, Hiratsuka Y, Fujimoto K, Okumura Y, Shiang T, *et al.* Maximum blink interval is associated with tear film breakup time: A new simple, screening test for dry eye disease. *Sci Rep* 2018;8(1):13443. doi:10.1038/s41598-018-31814-7, PMID:30194447.
- [47] García-Resúa C, Pena-Verdeal H, Remeseiro B, Giraldez MJ, Yebra-Pimentel E. Correlation between tear osmolality and tear meniscus. *Optom Vis Sci* 2014;91(12):1419–1429. doi:10.1097/OPX.0000000000000412, PMID:25259761.
- [48] Donshik P. Management of Dry Eye. *The Sjögren's Book*. Oxford: Oxford University Press; 2022:235–248. doi:10.1093/oso/9780197502112.003.0023.
- [49] Jester JV, Brown DJ. Wakayama Symposium: Peroxisome proliferator-activated receptor-gamma (PPARγ) and meibomian gland dysfunction. *Ocul Surf* 2012;10(4):224–229. doi:10.1016/j.jtos.2012.07.001, PMID:23084144.
- [50] Walsh K, Jones L. The use of preservatives in dry eye drops. *Clin Ophthalmol* 2019;13:1409–1425. doi:10.2147/OPTH.S211611, PMID:31447543.
- [51] Xu P, Wang H, Shen P, Peng P, Tu Y, Sun Y, *et al.* Practical and Efficient Approach to the Preparation of Diquafosol Tetrasodium. *Org Process Res Dev* 2020;24:1477–1483. doi:10.1021/acs.oprd.0c00209.
- [52] Wang JN, Fan H, Song JT. Targeting purinergic receptors to attenuate inflammation of dry eye. *Purinergic Signal* 2023;19(1):199–206. doi:10.1007/s11302-022-09851-9, PMID:35218451.
- [53] Lau OC, Samarawickrama C, Skalicky SE. P2Y2 receptor agonists for the treatment of dry eye disease: a review. *Clin Ophthalmol* 2014;8:327–334. doi:10.2147/OPTH.S39699, PMID:24511227.
- [54] Yang S, Wu Y, Wang C, Jin X. Ocular Surface Ion-Channels Are Closely Related to Dry Eye: Key Research Focus on Innovative Drugs for Dry Eye. *Front Med (Lausanne)* 2022;9:830853. doi:10.3389/fmed.2022.830853, PMID:35308542.
- [55] Hirabayashi T, Shibato J, Kimura A, Yamashita M, Takenoya F, Shioda S. Potential Therapeutic Role of Pituitary Adenylate Cyclase-Activating Polypeptide for Dry Eye Disease. *Int J Mol Sci* 2022;23(2):664. doi:10.3390/ijms23020664, PMID:35054857.
- [56] Lovász M, Branco Haas C, Antoniolli L, Pacher P, Haskó G. The role of P2Y receptors in regulating immunity and metabolism. *Biochem Pharmacol* 2021;187:114419. doi:10.1016/j.bcp.2021.114419, PMID:33460626.
- [57] Jacobson KA, Delicado EG, Gachet C, Kennedy C, von Kügelgen I, Li B, *et al.* Update of P2Y receptor pharmacology: IUPHAR Review 27. *Br J Pharmacol* 2020;177(11):2413–2433. doi:10.1111/bph.15005, PMID:32037507.
- [58] Zarrinmayeh H, Territo PR. Purinergic Receptors of the Central Nervous System: Biology, PET Ligands, and Their Applications. *Mol Imaging* 2020;19:1536012120927609. doi:10.1177/1536012120927609, PMID:32539522.
- [59] Nichols KK, Yerra B, Kellerman DJ. Diquafosol tetrasodium: a novel dry eye therapy. *Expert Opin Investig Drugs* 2004;13(1):47–54. doi:10.1517/13543784.13.1.47, PMID:14680452.
- [60] Nau J, Wyatt DJ, Rollema H, Crean CS. A Phase I, Open-label, Randomized, 2-Way Crossover Study to Evaluate the Relative Bioavailability of Intranasal and Oral Varenicline. *Clin Ther* 2021;43(9):1595–

1607. doi:10.1016/j.clinthera.2021.07.020, PMID:34456060.
- [61] Örcen A, Yilmaz V, Giriş M, Akcan U, Tüzün E, Erten G. Viability of SH-SY5Y cells is associated with purinergic P2 receptor expression alterations. *Acta Biol Hung* 2017;68(1):22–34. doi:10.1556/018.68.2017.1.3, PMID:28322086.
- [62] Alves M, Smith J, Engel T. Differential Expression of the Metabotropic P2Y Receptor Family in the Cortex Following Status Epilepticus and Neuroprotection via P2Y(1) Antagonism in Mice. *Front Pharmacol* 2019;10:1558. doi:10.3389/fphar.2019.01558, PMID:32009961.
- [63] Faulkner WJ, Granat S. Intranasal Neurostimulation for Dry Eye: First Impressions. *CTOY* 2019;2(1):123–125. doi:10.18314/ctoy.v2i1.1638.
- [64] Bansod RR, Deshmukh A, Bargal R, Jori R. A comparative clinical study of Shatavari Ghrita aschyotana and Carboxy methyl cellulose 0.5% eye drop in the management of dry eyes with special reference to smartphone users. *International Journal of Ayurvedic Medicine* 2023;13(4):1048–1053. doi:10.47552/ijam.v13i4.3034.
- [65] Rand AL, Asbell PA. Nutritional supplements for dry eye syndrome. *Curr Opin Ophthalmol* 2011;22(4):279–282. doi:10.1097/ICU.0b013e3283477d23, PMID:21597374.
- [66] Dry Eye Assessment and Management Study Research Group, Asbell PA, Maguire MG, Pistilli M, Ying GS, Szczotka-Flynn LB, *et al.* n-3 Fatty Acid Supplementation for the Treatment of Dry Eye Disease. *N Engl J Med* 2018;378(18):1681–1690. doi:10.1056/NEJMoa1709691, PMID:29652551.
- [67] Aragona P, Giannaccare G, Mencucci R, Rubino P, Cantera E, Rolando M. Modern approach to the treatment of dry eye, a complex multifactorial disease: a P.I.C.A.S.S.O. board review. *Br J Ophthalmol* 2021;105(4):446–453. doi:10.1136/bjophthalmol-2019-315747, PMID:32703782.
- [68] Carpena-Torres C, Pintor J, Huete-Toral F, Martín-Gil A, Rodríguez-Pomar C, Martínez-Águila A, *et al.* Efficacy of Artificial Tears Based on an Extract of *Artemia salina* Containing Dinucleotides in a Rabbit Dry Eye Model. *Int J Mol Sci* 2021;22(21):11999. doi:10.3390/ijms222111999, PMID:34769429.
- [69] Buzzi M, Versura P. Abstract 11 Outcome of Patients Treated with Umbilical Cord Blood and Homologous Serum Eye Drops. *Stem Cells Transl Med* 2022(Suppl 1):S13. doi:10.1093/stcltm/szac057.011.
- [70] Mencucci R, Favuzza E, Decandia G, Cennamo M, Giansanti F. Hyaluronic Acid/Trehalose Ophthalmic Solution in Reducing Post-Cataract Surgery Dry Eye Signs and Symptoms: A Prospective, Interventional, Randomized, Open-Label Study. *J Clin Med* 2021;10(20):4699. doi:10.3390/jcm10204699, PMID:34682824.
- [71] Lee HS, Ji YS, Yoon KC. Efficacy of hypotonic 0.18% sodium hyaluronate eye drops in patients with dry eye disease. *Cornea* 2014;33(9):946–951. doi:10.1097/ICO.0000000000000165, PMID:24915018.
- [72] Yeu E, Silverstein S, Guillon M, Schulze MM, Galarreta D, Srinivasan S, *et al.* Efficacy and Safety of Phospholipid Nanoemulsion-Based Ocular Lubricant for the Management of Various Subtypes of Dry Eye Disease: A Phase IV, Multicenter Trial. *Clin Ophthalmol* 2020;14:2561–2570. doi:10.2147/OPTH.S261318, PMID:32943837.
- [73] Jun I, Choi S, Lee GY, Choi YJ, Lee HK, Kim EK, *et al.* Effects of Preservative-free 3% Diquafosol in Patients with Pre-existing Dry Eye Disease after Cataract Surgery: A Randomized Clinical Trial. *Sci Rep* 2019;9(1):12659. doi:10.1038/s41598-019-49159-0, PMID:31477748.
- [74] Vigo L, Senni C, Pellegrini M, Vagge A, Ferro Desideri L, Carones F, *et al.* Effects of a New Formulation of Multiple-Action Tear Substitute on Objective Ocular Surface Parameters and Ocular Discomfort Symptoms in Patients with Dry Eye Disease. *Ophthalmol Ther* 2022;11(4):1441–1447. doi:10.1007/s40123-022-00518-7, PMID:35567735.
- [75] Jiang X, Yuan H, Zhang M, Lv H, Chou Y, Yang J, *et al.* The Efficacy and Safety of New-Generation Intense Pulsed Light in the Treatment of Meibomian Gland Dysfunction-Related Dry Eye: A Multicenter, Randomized, Patients-Blind, Parallel-Control, Non-Inferiority Clinical Trial. *Ophthalmol Ther* 2022;11(5):1895–1912. doi:10.1007/s40123-022-00556-1, PMID:35974296.
- [76] Bzovey B, Ngo W. Eyelid Warming Devices: Safety, Efficacy, and Place in Therapy. *Clin Optim (Auckl)* 2022;14:133–147. doi:10.2147/OPTO.S350186, PMID:35959466.
- [77] Barros JG, Reis I, Graça LM. Acute misoprostol toxicity during the first trimester of pregnancy. *Int J Gynaecol Obstet* 2011;113(2):157–158. doi:10.1016/j.ijgo.2010.12.006, PMID:21333990.
- [78] Ong J, Remolina E, Breeden D, Stroozas B, Mohammed J. “Intelligent Data Visualization for Cross-Checking Spacecraft System Diagnoses,” AIAA 2012-2557. Infotech@Aerospace 2012. June 2012.
- [79] Janagam DR, Wu L, Lowe TL. Nanoparticles for drug delivery to the anterior segment of the eye. *Adv Drug Deliv Rev* 2017;122:31–64. doi:10.1016/j.addr.2017.04.001, PMID:28392306.
- [80] Onugwu AL, Nwagwu CS, Onugwu OS, Echezona AC, Agbo CP, Ihim SA, *et al.* Nanotechnology based drug delivery systems for the treatment of anterior segment eye diseases. *J Control Release* 2023;354:465–488. doi:10.1016/j.jconrel.2023.01.018, PMID:36642250.
- [81] Yang C, Yang J, Lu A, Gong J, Yang Y, Lin X, *et al.* Nanoparticles in ocular applications and their potential toxicity. *Front Mol Biosci* 2022;9:931759. doi:10.3389/fmolb.2022.931759, PMID:35911959.
- [82] Muralidharan P, Malapit M, Mallory E, Hayes D Jr, Mansour HM. Inhalable nanoparticulate powders for respiratory delivery. *Nano-medicine* 2015;11(5):1189–1199. doi:10.1016/j.nano.2015.01.007, PMID:25659645.
- [83] Sharma OP, Patel V, Mehta T. Nanocrystal for ocular drug delivery: hope or hype. *Drug Deliv Transl Res* 2016;6(4):399–413. doi:10.1007/s13346-016-0292-0, PMID:27165145.
- [84] Foldvari M. Noninvasive ocular drug delivery: potential transcorneal and other alternative delivery routes for therapeutic molecules in glaucoma. *J Glaucoma* 2014;23(8 Suppl 1):S80–S82. doi:10.1097/IJG.0000000000000122, PMID:25275915.
- [85] Raju HB, Goldberg JL. Nanotechnology for ocular therapeutics and tissue repair. *Expert Review of Ophthalmology* 2008;3(4):431–436. doi:10.1586/17469899.3.4.431.
- [86] Downie LE, Craig JP. Tear film evaluation and management in soft contact lens wear: a systematic approach. *Clin Exp Optom* 2017;100(5):438–458. doi:10.1111/cxo.12597, PMID:28940531.
- [87] Ohigashi H, Hashimoto D, Hayase E, Takahashi S, Ara T, Yamakawa T, *et al.* Ocular instillation of vitamin A-coupled liposomes containing HSP47 siRNA ameliorates dry eye syndrome in chronic GVHD. *Blood Adv* 2019;3(7):1003–1010. doi:10.1182/bloodadvances.2018028431, PMID:30940635.
- [88] Landucci E, Bonomolo F, De Stefani C, Mazzantini C, Pellegrini-Giampietro DE, Bilia AR, *et al.* Preparation of Liposomal Formulations for Ocular Delivery of Thymoquinone: In Vitro Evaluation in HCEC-2 e HConEC Cells. *Pharmaceutics* 2021;13(12):2093. doi:10.3390/pharmaceutics13122093, PMID:34959374.
- [89] Huang L, Gao H, Wang Z, Zhong Y, Hao L, Du Z. Combination Nanotherapeutics for Dry Eye Disease Treatment in a Rabbit Model. *Int J Nanomedicine* 2021;16:3613–3631. doi:10.2147/IJN.S301717, PMID:34079253.
- [90] Khiev D, Mohamed ZA, Vichare R, Paulson R, Bhatia S, Mohapatra S, *et al.* Emerging Nano-Formulations and Nanomedicines Applications for Ocular Drug Delivery. *Nanomaterials (Basel)* 2021;11(1):173. doi:10.3390/nano11010173, PMID:33445545.
- [91] Durak S, Esmaili Rad M, Alp Yetisgin A, Eda Sutova H, Kutlu O, Cetinel S, *et al.* Niosomal Drug Delivery Systems for Ocular Disease-Recent Advances and Future Prospects. *Nanomaterials (Basel)* 2020;10(6):1191. doi:10.3390/nano10061191, PMID:32570885.
- [92] Cvenkel B, Kolko M. Devices and Treatments to Address Low Adherence in Glaucoma Patients: A Narrative Review. *J Clin Med* 2022;12(1):151. doi:10.3390/jcm12010151, PMID:36614952.
- [93] Abdelbary G, El-Gendy N. Niosome-encapsulated gentamicin for ophthalmic controlled delivery. *AAPS PharmSciTech* 2008;9(3):740–747. doi:10.1208/s12249-008-9105-1, PMID:18563578.
- [94] Lin M, Sun X, Ye S, Chen Y, Gao J, Yuan F, *et al.* A new antioxidant made from a pterostilbene functionalized graphene nanocomposite as an efficient treatment for dry eye disease. *Front Chem* 2022;10:942578. doi:10.3389/fchem.2022.942578, PMID:36092674.
- [95] Agrawal RD, Tatode AA, Rarokar NR, Umekar MJ. Polymeric micelle as a nanocarrier for delivery of therapeutic agents: A comprehensive review. *J Drug Delivery Ther* 2020;10:191–5. doi:10.22270/jddt.v10i1-s.3850.
- [96] Santos MS, Tavares FW, Biscaia Jr EC. Molecular Thermodynamics of Micellization: Micelle Size Distributions and Geometry Transitions. *Braz J Chem Eng* 2016;33(3):515–523. doi:10.1590/0104-6632.20160333s20150129.
- [97] Laan AC, Santini C, Jennings L, de Jong M, Bernsen MR, Denkova AG. Radiolabeling polymeric micelles for in vivo evaluation: a novel, fast,

- and facile method. *EJNMMI Res* 2016;6(1):12. doi:10.1186/s13550-016-0167-x, PMID:26860294.
- [98] Jensen AI, Binderup T, Kumar EK P, Kjær A, Rasmussen PH, Andresen TL. Positron emission tomography based analysis of long-circulating cross-linked triblock polymeric micelles in a U87MG mouse xenograft model and comparison of DOTA and CB-TE2A as chelators of copper-64. *Biomacromolecules* 2014;15(5):1625–1633. doi:10.1021/bm401871w, PMID:24645913.
- [99] Guo C, Zhang Y, Yuan H, Zhang Y, Yin T, He H, *et al.* Improved Core Viscosity Achieved by PDLLA(10k)Co-Incorporation Promoted Drug Loading and Stability of mPEG(2k)-b-PDLLA(2.4k) Micelles. *Pharm Res* 2022;39(2):369–379. doi:10.1007/s11095-022-03174-5, PMID:35118566.
- [100] Terreni E, Chetoni P, Tampucci S, Burgalassi S, Al-Kinani AA, Alany RG, *et al.* Assembling Surfactants-Mucoadhesive Polymer Nanomicelles (ASMP-Nano) for Ocular Delivery of Cyclosporine-A. *Pharmaceutics* 2020;12(3):253. doi:10.3390/pharmaceutics12030253, PMID:32168973.
- [101] Agarwal P, Craig JP, Rupenthal ID. Formulation Considerations for the Management of Dry Eye Disease. *Pharmaceutics* 2021;13(2):207. doi:10.3390/pharmaceutics13020207, PMID:33546193.
- [102] Saber MM, Al-Mahallawi AM, Nassar NN, Stork B, Shouman SA. Targeting colorectal cancer cell metabolism through development of cisplatin and metformin nano-cubosomes. *BMC Cancer* 2018;18(1):822. doi:10.1186/s12885-018-4727-5, PMID:30111296.
- [103] Rizwan SB, McBurney WT, Young K, Hanley T, Boyd BJ, Rades T, *et al.* Cubosomes containing the adjuvants imiquimod and monophosphoryl lipid A stimulate robust cellular and humoral immune responses. *J Control Release* 2013;165(1):16–21. doi:10.1016/j.jconrel.2012.10.020, PMID:23142776.
- [104] Abourehab MAS, Ansari MJ, Singh A, Hassan A, Abdelgawad MA, Shrivastav P, *et al.* Cubosomes as an emerging platform for drug delivery: a review of the state of the art. *J Mater Chem B* 2022;10(15):2781–2819. doi:10.1039/d2tb00031h, PMID:35315858.
- [105] Sultan AA, El Nashar NF, Ashmawy SM, El Maghraby GM. Cubosomes for Enhancing Intestinal Absorption of Fexofenadine Hydrochloride: In situ and in vivo Investigation. *Int J Nanomedicine* 2022;17:3543–3560. doi:10.2147/IJN.S370235, PMID:35983479.
- [106] Huang J, Peng T, Li Y, Zhan Z, Zeng Y, Huang Y, *et al.* Ocular Cubosome Drug Delivery System for Timolol Maleate: Preparation, Characterization, Cytotoxicity, Ex Vivo, and In Vivo Evaluation. *AAPS PharmSciTech* 2017;18(8):2919–2926. doi:10.1208/s12249-017-0763-8, PMID:28429294.
- [107] Eldeeb AE, Salah S, Ghorab M. Formulation and evaluation of cubosomes drug delivery system for treatment of glaucoma: Ex-vivo permeation and in-vivo pharmacodynamic study. *Journal of Drug Delivery Science and Technology* 2019;52:236–247. doi:10.1016/j.jddst.2019.04.036.
- [108] Nasr M, Teiama M, Ismail A, Ebada A, Saber S. In vitro and in vivo evaluation of cubosomal nanoparticles as an ocular delivery system for fluconazole in treatment of keratomycosis. *Drug Deliv Transl Res* 2020;10(6):1841–1852. doi:10.1007/s13346-020-00830-4, PMID:32779112.
- [109] Gaballa S, El Garhy O, Abdelkader H. Cubosomes: composition, preparation, and drug delivery applications. *Journal of Advanced Biomedical and Pharmaceutical Sciences* 2020;3(1):1–9. doi:10.21608/JABPS.2019.16887.1057.
- [110] Liu S, Dozois MD, Chang CN, Ahmad A, Ng DL, Hileeto D, *et al.* Prolonged Ocular Retention of Mucoadhesive Nanoparticle Eye Drop Formulation Enables Treatment of Eye Diseases Using Significantly Reduced Dosage. *Mol Pharm* 2016;13(9):2897–2905. doi:10.1021/acs.molpharmaceut.6b00445, PMID:27482595.
- [111] Liu S, Chang CN, Verma MS, Hileeto D, Muntz A, Stahl U, *et al.* Phenylboronic acid modified mucoadhesive nanoparticle drug carriers facilitate weekly treatment of experimentally induced dry eye syndrome. *Nano Res* 2015;8:621–635. doi:10.1007/s12274-014-0547-3.
- [112] Lai JY, Li YT, Wang TP. In vitro response of retinal pigment epithelial cells exposed to chitosan materials prepared with different cross-linkers. *Int J Mol Sci* 2010;11(12):5256–5272. doi:10.3390/ijms11125256, PMID:21614206.
- [113] Li Q, Cao Y, Wang P. Recent Advances in Hydrogels for the Diagnosis and Treatment of Dry Eye Disease. *Gels* 2022;8(12):816. doi:10.3390/gels8120816, PMID:36547340.
- [114] Lemp MA, Sullivan BD, Crews LA. Biomarkers in Dry Eye Disease. *European Ophthalmic Review* 2012;6(3):157–163. doi:10.17925/EOR.2012.06.03.157.



## Case Report

# New Topical Treatment for Psoriasis: A Case Report



Jose Miguel Ingelmo Calvo<sup>1</sup>, José Ruiz Cobo<sup>2</sup> and Mohamed Farouk Allam<sup>3\*</sup>

<sup>1</sup>Department of Plastic Surgery, Hospital HM Malaga, Malaga, Spain; <sup>2</sup>Distrto Sanitario Costa del Sol, SUAP Torremolinos, Malaga, Spain; <sup>3</sup>Department of Family Medicine, Faculty of Medicine, Ain Shams University, Cairo, Egypt

Received: March 07, 2023 | Revised: April 18, 2023 | Accepted: May 01, 2023 | Published online: July 04, 2023

## Abstract

Topical corticosteroids, alone or in combination with calcipotriol, a topical vitamin D analog, have proved effective in treating mild to moderate psoriasis. Topical corticosteroids, like clobetasol propionate, have a vasoconstrictor effect on the peripheral dermal vessels, and this explains skin atrophy in psoriatic patients applying topical corticosteroids regularly for long periods. However, a new topical treatment for psoriasis has been developed and patented. The new treatment is prepared as a lotion and is composed of clobetasol, papaverine hydrochloride, spironolactone, milk-peptide-complex, and propylene glycol. A 47-year-old male presented with extensive psoriasis lesions in the elbows and back. The patient had an irrelevant past medical history and was complaining mainly of severe itching in the psoriatic lesions. The patient was advised to use our newly patented lotion once daily for one week. After 7 days of local application of the new lotion, the patient was examined in the outpatient clinic. The patient reported significant improvement in the itching sensations and remission of the scaled lesions. Comparing the lesions before and after the application of the local treatment for 7 days, it was observed that the psoriasis area severity index score had improved from 20.9 to 1.8. Further studies with larger sample sizes and longer follow-up periods are required to confirm the findings of our case report.

## Introduction

Psoriasis is a worldwide chronic inflammatory skin disease, affecting both genders and any age. It usually leads to significant deterioration of the quality of life of affected patients.<sup>1</sup>

Being a chronic relapsing disease, Psoriasis often needs long-term therapy. Mild to moderate psoriasis can be treated with topical creams of steroid and vitamin D analogs, together with phototherapy. Moderate to severe psoriasis almost always needs systemic treatment.<sup>2</sup>

Topical corticosteroids, alone or in combination with calcipotriol, a topical vitamin D analog, have proven to be effective in treating mild to moderate psoriasis.<sup>3</sup>

Clobetasol propionate is the most effective topical corticosteroids used for the treatment of psoriasis. However, it is usually accompanied by local and systemic adverse effects, like skin atrophy and hypothalamic-pituitary-adrenal axis suppression.<sup>4</sup>

Topical corticosteroids, like clobetasol propionate, have a vasoconstrictor effect on the peripheral dermal vessels, and this ex-

plains skin atrophy in psoriatic patients applying topical corticosteroids regularly for long periods.<sup>3,5</sup>

A new topical treatment for psoriasis was developed and patented by the Spanish Ministry of Industry, Trade, and Tourism (Invention patent reference number 202030824). The new treatment is prepared as a lotion and is composed of clobetasol, papaverine hydrochloride, spironolactone, milk-peptide-complex, and propylene glycol.

We report a case of moderate psoriasis treated with our new patented lotion “Psorisbye”.

## Case report

A 47-year-old male presented with extensive psoriasis lesions in the elbows and back. The patient had an irrelevant past medical history and was complaining mainly of severe itching in the psoriatic lesions.

On examination, multiple plaque lesions in the chin, retroauricular area, forearm and elbow, back, and popliteal regions were observed. In addition, a few erythrodermic psoriatic lesions were observed mainly in the back.

The patient was diagnosed 13 years ago and had been treated with a combination of steroid creams, moisturizers for dry skin, and calcipotriol and betamethasone cutaneous foam (Enstilar®). He had previously used clobetasol ointments and creams (Decloban® and Clovate®) without significant improvement. The patient did not accept the offer of a session of PUVA (psoralen

**Keywords:** Psoriasis; Topical treatment; Psoriasis area severity index; Malaga.

**Abbreviations:** PASI, psoriasis area severity index.

\*Correspondence to: Mohamed Farouk Allam, Department of Family Medicine, Faculty of Medicine, Ain Shams University, Abbasia 11566, Cairo, Egypt. ORCID: <https://orcid.org/0000-0001-5954-8909>. Tel: + (2) 011 43559946, Fax: + (202) 24346888, E-mail: [farouk.allam@med.asu.edu.eg](mailto:farouk.allam@med.asu.edu.eg)

**How to cite this article:** Calvo JMI, Cobo JR, Allam MF. New Topical Treatment for Psoriasis. *J Explor Res Pharmacol* 2023;8(3):263–265. doi: 10.14218/JERP.2023.00015.





**Fig. 1. Elbow of the patient before and after the application of “Psorisbye” with 1 week between images.**

and ultraviolet light A). No immunosuppressive drugs like cyclosporine or methotrexate had been previously used by the patient.

The patient was advised to use our newly patented lotion “Psorisbye” once daily for 1 week and a total of 120ml of “Psorisbye” was used over 1 week. The patient did not receive antihistamine treatment with the lotion during that week.

On the 8<sup>th</sup> day, after 7 days of local application of “Psorisbye”, the patient was examined in the outpatient clinic. The patient reported important improvement in the itching sensations and remission of the scaled lesions.

The gold standard for the assessment of psoriasis is the psoriasis area severity index (PASI). The PASI is a measure of the average redness, thickness, and scaliness of the lesions (each graded on a 0–4 scale), weighted by the area of involvement.<sup>6</sup>

Comparing the lesions before and after the application of the local treatment for 7 days, it was observed that the PASI score improved from 20.9 to 1.8.

Figure 1 shows the elbow of the patient before and after the application of “Psorisbye” with 1 week between the images.

## Discussion

We have herein presented a case of moderate psoriasis that was successfully managed via our new lotion. This case shows an important improvement after only one week of local application of “Psorisbye”.

The excellent results obtained in this case can be explained by the combined effects and equilibrated dosages of the drugs included in “Psorisbye”:

- Clobetasol is a corticosteroid widely used for the treatment of this type of lesion that acts by reducing the proliferation of keratinocytes and eliminating the typical crust that occurs;
- Papaverine hydrochloride acts as a vasodilator agent producing a greater supply of blood flow to the lesion, which facilitates better penetration and access to the dermal lesion;
- Spironolactone is a diuretic that topically acts by reducing the seborrheic hyperproduction that occurs in this type of lesion;
- Milk-peptide-complex reactivates skin cells inducing the pro-

duction of collagen, hyaluronic acid, and fibronectin that improves and softens the structure of the skin;

- Propylene glycol is an alcohol that acts by helping the skin to better absorb hydration by inducing suppleness;
- Excipients: hydroalcoholic solution in the appropriate proportions to obtain the best solubility and stability of the formula.

The potential interactions between the different molecules of the new topical treatment, in particular between spironolactone and papaverine hydrochloride, were carefully monitored in the studied patient. No adverse reactions or interactions were observed. A recent study evaluated the effectiveness of combining topical papaverine hydrochloride and topical spironolactone in the treatment of androgenetic alopecia (AGA). The results of the study showed that the combination of the two agents was better in AGA treatment, with no side effects or adverse interactions.<sup>7</sup>

A recent review reported the photosensitizing potential of 393 different drugs or drug compounds, including topical spironolactone. The level of evidence regarding the abilities of these agents to induce photosensitive reactions varied markedly.<sup>8</sup>

Kemp and co-workers (2019) in their histochemical and molecular biology study reported no evidence that human subjects receiving spironolactone are at particular risk of photosensitivity.<sup>9</sup> Moreover, no photosensitive reaction was observed after applying the new topical lotion.

## Conclusions

The new topical treatment proved to bring significant improvement as indicated by the disappearance of the itching sensation and comparing the pre- and post-PASI score assessment.

Although the results of “Psorisbye” in this case are promising, further studies with larger sample sizes and longer follow-up periods are required to confirm the findings of our case report.

## Acknowledgments

None.

### Funding

None.

### Conflict of interest

JIC, JRC and MFA own the new patent “Psorisbye”, which is patented by the Spanish Ministry of Industry, Trade, and Tourism (Invention patent reference number 202030824). The authors have no other conflict of interests related to this publication.

### Author contributions

Study design (JIC, JRC, MFA), analysis and interpretation of data (JIC, JRC), manuscript writing (JRC, MFA), collection of data (JIC, JRC), critical revision (JRC, MFA).

### Ethical statement

Written informed consent was obtained from the patient for the treatment and publication of this case report and the accompanying image.

### References

- [1] Griffiths CEM, Armstrong AW, Gudjonsson JE, Barker JNWN. Psoriasis. *Lancet* 2021;397(10281):1301–1315. doi:10.1016/S0140-6736(20)32549-6, PMID:33812489.
- [2] Rendon A, Schäkel K. Psoriasis Pathogenesis and Treatment. *Int J Mol Sci* 2019;20(6):E1475. doi:10.3390/ijms20061475, PMID:30909615.
- [3] Feldman SR, Yentzer BA. Topical clobetasol propionate in the treatment of psoriasis: a review of newer formulations. *Am J Clin Dermatol* 2009;10(6):397–406. doi:10.2165/11311020-000000000-00000, PMID:19824740.
- [4] Pels R, Sterry W, Lademann J. Clobetasol propionate—where, when, why? *Drugs Today (Barc)* 2008;44(7):547–557. doi:10.1358/dot.2008.44.7.1122221, PMID:18806904.
- [5] Goldsmith P, Bunker C, Leslie T, Foreman J, Dowd PM. The effect of topical steroid on the actions of vasoconstrictor and vasodilator peptides in human skin. *Skin Pharmacol* 1996;9(5):289–297. doi:10.1159/000211427, PMID:8990503.
- [6] Feldman SR, Krueger GG. Psoriasis assessment tools in clinical trials. *Ann Rheum Dis* 2005;64:ii65–ii68. doi:10.1136/ard.2004.031237, PMID:15708941.
- [7] Abdel-Raouf H, Aly UF, Medhat W, Ahmed SS, Abdel-Aziz RTA. A novel topical combination of minoxidil and spironolactone for androgenetic alopecia: Clinical, histopathological, and physicochemical study. *Dermatol Ther* 2021;34(1):e14678. doi:10.1111/dth.14678, PMID:33320406.
- [8] Hofmann GA, Weber B. Drug-induced photosensitivity: culprit drugs, potential mechanisms and clinical consequences. *J Dtsch Dermatol Ges* 2021;19(1):19–29. doi:10.1111/ddg.14314, PMID:33491908.
- [9] Kemp MG, Krishnamurthy S, Kent MN, Schumacher DL, Sharma P, Excoffon KJDA, *et al*. Spironolactone Depletes the XPB Protein and Inhibits DNA Damage Responses in UVB-Irradiated Human Skin. *J Invest Dermatol* 2019;139(2):448–454. doi:10.1016/j.jid.2018.07.039, PMID:30227140.



Published by Xia & He Publishing Inc.

14090 Southwest Freeway, Suite 300, Sugar Land, Texas, 77478, USA

Telephone: +1-409-420-2868

E-mail: [service@xiahepublishing.com](mailto:service@xiahepublishing.com)

Website: [www.xiahepublishing.com](http://www.xiahepublishing.com)

